Investigation of post-mortem lipids in textiles associated with decomposing remains

by Sharni Collins

Thesis submitted in fulfilment of the requirements for the degree of

Doctor of Philosophy

under the supervision of Dr Maiken Ueland, Dr Luca Maestrini and Associate Professor Barbara Stuart

University of Technology Sydney

Faculty of Science,

School of Mathematical and Physical Sciences,

Centre for Forensic Science

June 2023

Certificate of Authorship and Originality

I, *Sharni Collins*, declare that the work in this thesis is submitted in fulfilment of the requirements of the award of *Doctor of Philosophy*, in the *Faculty of Science* here at the University of Technology Sydney.

This thesis is wholly my own work unless otherwise referenced or acknowledged. In addition, I certify that all information sources and literature used are indicated in the thesis.

This document has not been submitted for qualifications at any other academic institution.

This research is supported by the Australian Government Research Training Program.

Signature: Production Note:
Signature removed prior to publication.

Date: 1st February 2024

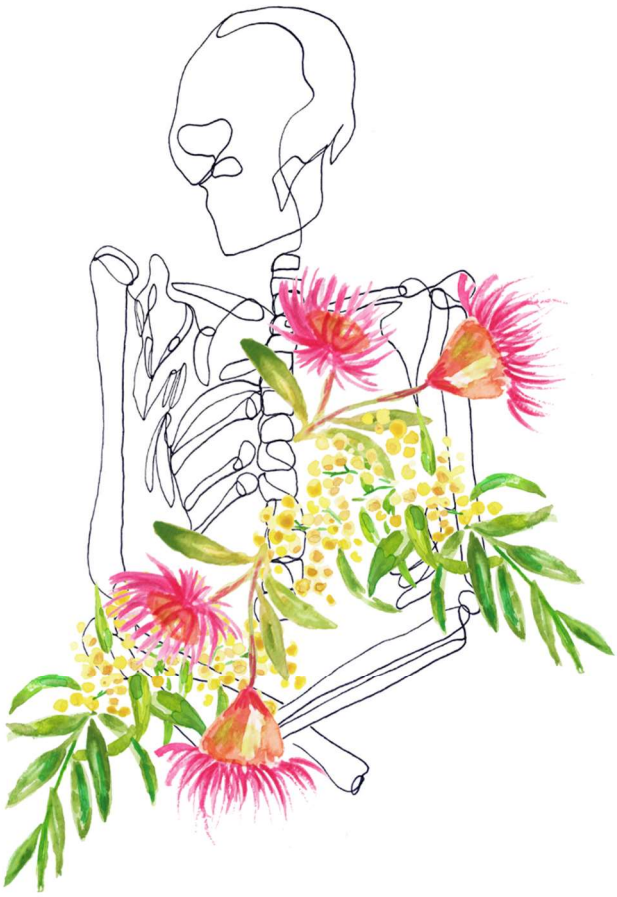

Acknowledgements

I would like to begin by extending my gratitude to my forensic supervisors Dr. Maiken Ueland and Associate Professor Barbara Stuart. Four years ago, you both took me on as your undergraduate Honours student, at a time where I honestly had no idea what I wanted to do or where I wanted to go in my career. From our very first meeting, on July 25th, 2018, you have been incredibly supportive in a personal and academic capacity. Maiken, it has truly been a pleasure to watch your career flourish over the years that I have been lucky enough to work with you. When I first came onto this team, Shari had only recently left, and you had found yourself in a relatively new position as head of the group. It has been inspiring to watch you evolve, giving so much of yourself to your students, whilst still excelling in your own career. I cannot wait to see what is on the horizons for you.

Barb, you have been such a solid foundation and wealth of knowledge from the very beginning. Your academic career and personal example are something to inspire generations of young men and women in forensic science. Thank you both for teaching me and mentoring me with such passion.

Luca, I cannot even begin to express my appreciation for the relationship that we have built over the years. I count my lucky stars that it was you that I got paired with at that *Stats Hour* meeting all those years ago, where I came to you as a truly useless statistics student. I believe it is difficult to measure how much I have learnt over the course of my candidature, but I am still astounded at my capability to independently write, understand and troubleshoot code. The fact that I literally could not even write a simple line of code to open a folder on my desktop, while I have now been able to

dabble in the complexities of Bayesian multilevel models or generalized linear mixed models, is incredible. And you have provided me with the tools to do so. Without our consistent meetings nearly every single week for the better part of the last three years, I truly think I would have gone insane. We met right before the world plummeted into the pandemic and *work from home* orders were enforced. And during that time, your head on that Zoom panel was the thread that anchored me and the helm that steered the ship at times where I really wanted to just give it all up. Your generosity, time and patience are something that I will never find the words to thank you for, but please know that it has not gone unnoticed. It has been a pleasure to be your colleague, student and friend. I look forward to never talking about science or statistics with you in the future, and instead, sharing recipes about pasta and bread.

My time as a PhD candidate has been something for the ages. It began at a time where Australia was literally on fire, with some of the worst bushfires in history. A time where the smoke was so thick and pungent that you could not escape it. I remember sitting in that small office at my desk, staring out the window and not being able to see the building across the street. I recall the discomfort and annoyance of wearing dust masks just so that we could breathe while crossing the streets of the city. Oh, how little we knew about what was to come with masks… I remember the time that Maiken called me on an emergency evacuation trip to AFTER to gather all of the expensive (and important) equipment from the field site, in anticipation that the place would soon be engulfed in flames. Thankfully it never was, but it was truly a time to be alive.

And then came my trip to Japan in early 2020. I distinctly remember visiting my Mum for the last time before I went away and her mentioning to me about this virus that had just broken out in China... We barely made it back into Australia before the

world shut down. The COVID-19 pandemic was in full swing. Lockdowns, masks, deserted streets. It was like something from the movies. I was living in Lewisham at the time of the first lockdown and I am so lucky that I was, because I was just a stone throw away from one of my dearest friends and colleagues.

Ciara, thank you for always being such a stable and constant person in my life, in both a professional and personal capacity. All of those WFH dates, with toasted sandwiches for lunch, or *socially distanced* walks, soccer juggling, coffee breaks or wine nights, were the best parts of that year. Thank you for always being so lovely, kind and caring. Friends like you do not come around often. I am so grateful to have you in my life. I am also so very proud of you. It has been such a pleasure to watch you grow in life, love and work. Oh, and how freaking cool that we got to travel to Europe together.

Jade, I am so grateful to have someone like you to call my best friend. It truly is a rare thing to have friends like you in this world – 24 years of friendship and still going strong. You are the sister that I never had. Thank you for putting up with me and supporting me through Honor's and now my PhD! Those years living with you were some of the best of my life!

To the UTS crew: Alisha, Amber, Bridget, Blake, Caleb, Helen, Minh, John, Liam, Sarah, Samara, Zac, thank you for always making the dark days lighter. Despite the trials and tribulations, we all faced during the wild time that was the last few years, your steadfastness was very much appreciated (and needed). It is truly a beautiful thing to find solace in those with shared experiences. And PhD candidature is one of those uniquely complex experiences which make it difficult to seek comfort from

muggle peoples, no matter how loving and supporting they may be. It is one thing to provide support from the outside, and it is another to be in the depths of despair right there with you. And to all of us who made it out alive, I say *well done*. We did it. All of those long days and sleepless nights. Look at us now.

To Dr. Jen Raymond, Dr. Scott Chadwick, Dr. Georgina Meakin, Dr. Nicole Cattarossi and Dr. Susan Luong, you each have offered me with your unique and invaluable perspectives about life and career over the years. So, I would like to thank you for your advice and support.

I would like to extend my thanks to all of the lovely and selfless technical staff in the labs and in field. You are the cogs that keep the machine going and us researchers would be nothing without you. To our donors and their families – thank you for your gift. Without your generosity, there would be no research.

To my Aunty Mel, Uncle James, Aunty Jen, Mum, Nan, Rach and Claire – without fail, you have been a solid network for me to return to whenever in need. Your generosity, love and support are something that I will forever be in your debt.

And last, but most definitely not least, to my beautiful husband Gabe. You have been my rock. Thank you for putting up with me on the good days, but most importantly, for supporting and loving me through the bad ones. Thank you for understanding me without the need for any words. Thank you for feeding me on the days where I was so hyper fixated on a task that I would forget to eat. Thank you for never failing to me laugh on the days where I barely even smiled. Thank you for always reminding me of my worth and for centering me whenever I would stray from who I wanted to be. Thank you for always keeping my grounded and humble.

This PhD candidature has literally taken me around the world. An opportunity and experience that I will never take for granted. We are but a culmination of the people we meet, the places we visit, and the experiences we have. And for better or for worse, each shape us into the unique individuals that we all are.

Statement and List of Publications

This *thesis by compilation* originates from the published, accepted and submitted works.

Publications included in this thesis:

1. **Collins, S.**, Maestrini, L., Ueland, M., Stuart, B.H. (2022). A preliminary investigation to determine the suitability of pigs as human analogues for post-mortem lipid analysis. Talanta Open, 5, 100100. (Chapter 2).

2. **Collins, S.**, Stuart, B.H., Ueland, M. (2023). The use of lipids from textiles as soft-tissue biomarkers of human decomposition. Forensic Science International, 343, 111547. (Chapter 3 and 4).

3. **Collins, S.**, Maestrini, L., Hui, F., Stuart, B.H., Ueland, M. (accepted May 2023). The use of generalized linear mixed models to investigate lipids in textiles as biomarkers of decomposition. iScience. (Chapter 5).

Publications included as an adjunct to this thesis:

1. Stuart, B., Guan, J., **Collins, S**., Thomas, P., & Ueland, M. (2022). A Preliminary study of non-woven fabrics for forensic identification purposes. Australian Journal of Forensic Sciences.

2. Ueland, M., **Collins, S**., Maestrini, L., Forbes, S. L., & Luong, S. (2021). Fresh vs. frozen human decomposition–A preliminary investigation of lipid degradation products as biomarkers of post-mortem interval. Journal of Forensic Chemistry, 24, 100335.

3. **Collins, S**., Stuart, B., & Ueland, M. (2023). Anatomical location dependence of human decomposition products in clothing. Australian Journal of Forensic Sciences, 55, 363-375.

4. **Collins, S**., Stuart, B., & Ueland, M. (2020). Monitoring human decomposition products collected in clothing: an infrared spectroscopy study. Australian Journal of Forensic Sciences, 52(4), 428-438.

Conference Presentations, Invited Talks and Awards Arising from this Thesis

1. **Collins, S.**, Maestrini, L., Ueland, M., Stuart, B.H. (2022). A preliminary investigation to determine the suitability of pigs as human analogues for post-mortem lipid analysis. *EAFS 2022,* Stockholm, Sweden.

2. **Collins, S.** (2021) Lipids in Textiles… A Key to Time Since Death? *Three Minute Thesis,* University of Technology Sydney, Online.
    a. Awardee*: People's Choice Award and Faculty of Science winner.*

3. **Collins, S.** Stuart, B.H., and Ueland, M. (2021) Lipids in Textiles… A Key to Time Since Death? *ANZFSS Research in the Spotlight*, Online.

4. **Collins, S**. Stuart, B.H., and Ueland, M. (2021) The investigation of post-mortem lipid degradation in complex matrices associated with human remains. *Crossing Forensic Borders, Global lecture series, Online.*

5. **Collins, S.** Stuart, B.H., and Ueland, M. (2019) Monitoring Human Decomposition Products Collected in Clothing, *FoSTER,* University of Technology Sydney
    a. Awardee: *Highly Commended Long Talk.*

6. **Collins, S**. Stuart, B.H., and Ueland, M. (2019) Human Decomposition Fluids and Clothing Degradation, *RACI R&D* Topics, Adelaide, South Australia.

Impact of COVID-19 Pandemic on Research

It was the full intention of this thesis to obtain extensive longitudinal samples from several donors, over multiple years. This particular type of longitudinal sampling would have allowed for more concrete conclusions to the proposed aims and objectives of this work. In addition, this longitudinal sampling would have also allowed for the much-needed investigation into the systematic differences that inevitably exists between individuals, and how that impacts on the lipid profiles obtained in the textile samples. However, due to an unfortunate number of uncontrollable circumstances, these intentions were not possible to fulfil.

The work in this thesis commenced on the 23rd August 2019, and during this time, NSW experienced some of the worst bushfires in Australian history, now known as the Black Summer bushfires of 2019-2020. These bushfires directly impacted the ability to gain safe access to the AFTER facility as it was situated in affected areas. Little to no fieldwork was able to be conducted during this time.

In early 2020, COVID-19 directly impacted this work as the university indefinitely suspended the body donation programme. No human donors were received for this project during that time. In June 2021, COVID-19 caused lockdowns to Sydney again. During this time, the FEIT laboratories were completely locked down and no laboratory work could be completed. This lockdown also impacted donor availability again, preventing the ability to collect and analyse samples, causing significant delay.

Table of Contents

List of Tables

List of Figures

Supplementary Information

Chapters 2 – 5 refer to supplementary information related to methods and results. This information is contained within the Appendices or attached files that accompany this thesis.

Ethics

All research conducted within this thesis was approved by the UTS Human Research Ethics Committee (HREC ETH18-2999). Human cadavers were received through the UTS Body Donation Program, with consent provided in accordance with the New South Wales Anatomy Act (1977).

Funding

This research was funded by the Australian Government Research Training Program and UTS.

Thesis Abstract

After death, the human body undergoes a series of biochemical processes as part of decomposition. These processes eventually result in the release of fluids, containing a mixture of water, protein, lipids, carbohydrates and minerals from the tissues into the surrounding environment. Due to their hydrophobicity, lipids are more resistant to harsh environmental conditions than the other constituents of the decomposition fluids. As such, lipids have been a target of archaeological investigations for many years as a means to reconstruct the history of human civilizations across the globe. This has been achieved by analysing the many matrices, clothing in particular, that contain these target lipids and consequently mapping their patterns of degradation. In a forensic context, clothing is commonly recovered at the scene of a crime as physical evidence. Therefore, the application of these archaeological methods could provide an excellent resource for investigators, particularly when faced with complex death investigations, to aid in the reconstruction of events, or most importantly, time since death.

In order to investigate post-mortem lipids in textiles, pig and human remains were clothed and placed on the soil surface at the Australian Facility for Taphonomic Experimental Research (AFTER) and allowed to naturally decompose. Clothing samples were collected in-field and first analysed using attenuated total reflectance Fourier transform infrared (ATR-FTIR) spectroscopy as a preliminary method for the detection of post-mortem lipids. The samples were then extracted and analysed using a method adapted from previous archaeological works using gas chromatography

tandem mass spectrometry (GC-MS/MS) for further elucidation of the lipid profiles collected in the materials.

At the completion of this project, post-mortem lipids proved to be of great use when relating their detection, and monitoring their patterns, in conjunction with the decomposition timeline. In addition, interesting trends relating to interspecies differences between humans and their analogues were revealed. Lipids in textiles therefore, hold great potential in the future of forensic science as an additional means of estimating time since death, providing valuable information that could aid in solving future cases involving human remains.

Chapter 1: Introduction.

Chapter 1: Introduction.

Human remains are often discovered clothed or semi-clothed [1-3], making textile materials a ubiquitous source of physical evidence in forensic cases. Second to residential scenarios, homicide victims are often located in outdoor environments [4], where soft tissue decomposition can be rapid and scavenging activity becomes quite common, providing additional challenges to investigators [5]. In complex death investigations such as this, the analysis of associated evidence becomes critical in providing information concerning the criminal activities in question. Previous research has been focused on how textiles impact the overall decomposition ecology [5-8] and it is understood that the presence of textiles has a significant impact on the rate of decomposition [9]. Recent taphonomic research has also investigated the potential of indirectly monitoring the decomposition timeline through the collection of lipids within textiles associated with remains [10].

The word taphonomy comes from the Greek words *taphos* (grave) and *nomos* (law) and involves the study of an organism from the time of its death, until its discovery [11, 12]. It is a term originally coined by palaeontologist Professor Ivan Antonovich Yefremov who studied the transition of organisms from the biosphere to the lithosphere [11]. During this transition, Yefremov found that organisms often experienced a series of preservation processes, known as fossilisation [11]. Yefremov also recognised that by investigating the features and conditions of the burial environment, he could better understand and predict the post-mortem changes that would occur to an organism [11, 12].

The use of human analogues, such as the domestic pig, in forensic taphonomy has been a commonly accepted and widely practiced method in the past. This is primarily due to the ethical and legal restrictions that exist in most countries which limit the use of human cadavers in taphonomic research studies [13]. However, little research has investigated the efficacy of using pigs as human proxies in taphonomic research. To date, some research has shown differences between humans and domestic pigs in respect to; body composition and gut flora [14], lipid biochemistry [15], visual total body scoring and volatile organic compounds [13].

In 1980, American forensic anthropologist Dr. William Bass, opened the Anthropological Research Facility (ARF) at the University of Tennessee in the United States (US); this facility was the first of its kind and provided the invaluable opportunity to study the decomposition of human cadavers in a controlled environment that was comparable to forensic casework [11]. This influenced the development and establishment of other decomposition facilities across the globe, with seven now located in the US, one in the Netherlands, one in Canada and one in Australia. The Australian Facility for Taphonomic Experimental Research (AFTER) was established in 2016, and is the only facility of its kind in the southern hemisphere. With the development of such facilities and the production of novel research, taphonomy, which was once an archaeologically focused practice, was repurposed with the application to modern forensic casework and so the term forensic taphonomy was developed [11, 12]. Forensic taphonomy focuses on four distinct phases: time of death, death, deposition and recovery [11, 12]. Today, this transdisciplinary field incorporates features of pathology, anthropology, archaeology and palaeontology [11], with the sole purpose to understand the fate of contemporary human remains

[12]. In 2017, Schotsmans et al. [16] proposed that forensic taphonomy encompasses all aspects of peri- and post-mortem assessments; including the stages, recovery and storage of remains.

1.1. Decomposition

Decomposition is the dynamic process whereby a compound is disintegrated into its elementary constituents through physical, chemical, and biological mechanisms [5, 17, 18]. With respect to the decomposition of human remains, it is the process that occurs between heartbeat cessation, up until all soft tissue is resolved, leaving only hard tissues or skeletonised remains [19]. Although there are a series of predictable post-mortem processes that occur, the determination of time since death still presents as a major challenge to law enforcement when faced with decomposing human remains [20]. This is primarily due to the complex idiosyncrasies surrounding each case, and the dynamic relationship that exists between the abiotic and biotic factors involved [21].

In previous years, the post-mortem process has been consolidated to a manner of five predictable stages known as: fresh, bloat, active, advanced and dry remains [22, 23].

1.1.1 Fresh

The first stage of decomposition is known as the fresh stage, and this begins as the heart stops beating, where the remains typically appear as they did in life (Fig. 1.1). This causes an oxygen depletion in the body, consequently leading to an increase of carbon dioxide in the blood [24]. As a result, the blood pH decreases, excess waste products begin to accumulate and aerobic metabolism is inhibited [24].

This initiates the process of autolysis, the enzymatic digestion of cellular membranes, which causes a release of intracellular fluids (lipids, proteins, carbohydrates and

Fig. 1.1 Clothed pig remains in the 'fresh' stage of decomposition

nucleic acids) [18, 19, 25, 26].

During the fresh stage, the remains will also pass through rigor, algor and livor mortis [26, 27]. Rigor mortis may be observed within 2-6 hours post-mortem, whereby the muscles and joints become rigid due to oxygen depletion and a loss of adenosine triphosphate (ATP) [26, 27]. Between 18-20 hours post-mortem, the body will begin to equilibrate with atmospheric temperature, and this is known as algor mortis [26, 27]. In most cases, the blood will also begin to accumulate and settle in the small blood vessels toward the posterior surface of the remains, causing a discoloration of the skin known as livor mortis, or lividity [26, 27]. During the fresh stage, flesh flies (Sacrophagidae) and blow flies (Calliphoridae) are observed; these are known as

early insect colonisers and their egg masses will be located in moist areas of the body [25].

1.1.2. Bloat

The second stage of decomposition is marked by the appearance of abdominal distention, or bloating (Fig. 1.2).

Fig. 1.2 Clothed pig remains in the 'bloat' stage of decomposition

This bloat effect is a direct result of putrefaction, where the accrual of internal gases like hydrogen sulphide and methane produced during autolysis distend the abdomen [19, 25]. When the internal pressure becomes too great, the decomposition fluids and gases will begin to purge from the remains, initiating the onset of the active decay stage [19, 25]. During the bloat stage, carrion beetles such as clown beetles (Histeridae) become more prominent as they feed on the larva of the early insect colonisers as well as the flesh of the decomposing remains [22].

1.1.3. Active

Once the skin has ruptured and the fluids and gases are released into the immediate environment, the remains are in the active decay stage (Fig. 1.3).

Fig. 1.3 Clothed pig remains in the 'active' stage of decomposition

This is typically characterised by the rapid loss of body mass, the appearance of black putrefaction, darkening of the skin and the presence of distinctive decomposition odours due to the volatile organic compounds (VOCs) released [19, 28]. During this stage, insect activity peaks (Calliphoridae, Staphylinidae, Histeridae, Sacrophagidae and Muscidae) and accelerates the degradation of soft tissue, leading to bone exposure [19].

1.1.4. Advanced

The advanced decay stage is primarily marked by the migration of maggots away from the remains where they begin to pupate [25] and there is an increase in

beetle activity [19]. This stage typically occurs weeks, to months, post-mortem and any remaining soft tissue begins to desiccate, leaving predominantly skin, cartilage, hair and bones [19] (Fig. 1.4).

Fig. 1.4 Clothed pig remains in the 'advanced' stage of decomposition

1.1.5. Dry remains

The final stage of decomposition is known as the dry remains stage where any remaining moist, soft tissue becomes mummified and adheres to the bones [26, 28] (Fig. 1.5). Over time, the bones will continue to degrade at a much slower rate, undergoing bleaching and diagenesis in some cases [18]. At the point where > 50% of the bones are exposed, skeletonization is said to have occurred [28].

Fig. 1.5 Clothed pig remains in the 'dry' stage of decomposition

1.2. Covariates impacting decomposition

The overall rate, manner and progression of the decomposition process is highly dependable on a range of extrinsic covariates. Data obtained from both forensic casework and experimental research [16, 29-31] have documented temperature and moisture to be the primary covariates influencing decomposition.

1.2.1. Accumulated-degree-days (ADD)

Work by Megyesi et al. in 2005 [32] demonstrated that 80% of the variation within decomposition can be accounted for by accumulated-degree-days (ADD). ADD are units that represent the accumulation of thermal energy in a chronological combination of time and energy [32]. In this manner, it is said that when equal units of thermal energy (ADD) are applied to remains, a relatively equal amount of decomposition is to be expected [33]. This is because climate effects the time that

will elapse during each stage, and thus determines the overall rate at which remains will decay [16, 29]. Climate can also regulate the microbial environment as it selects for certain decomposer microbes, whilst also eliminating others; this is particularly true when comparing a microbial environment between two contrasting seasons, such as summer and winter [34]. It is also well documented, that warmer climates significantly enhance the biological and chemical taphonomic processes, thus facilitating a much faster rate of decomposition [25, 35]. Warmer climates lead to an increase in entomological activity, which will consequently lead to an escalation in soft tissue consumption [36]. This means that the remains will progress from fresh, to skeletal, at a much more accelerated rate. In contrast, cooler climates evidently slow microbial metabolism, decrease the biological and chemical processes and retard the decomposition process [16]. And under extreme conditions, cooler climates can result in the preservation of the remains [16].

As a result of these variables and the dynamicity of the decomposition process, there is no accurate scoring system that is universally applicable. There are however, a number of teams currently working on developing these systems worldwide. These scoring systems are subjective and it is suspected that a more objective Artificial Intelligence (AI) approach could be a more viable alternative.

1.2.2. Accumulated-relative-humidity (ARH)

Moisture, relative humidity or rainfall, is another important factor to consider when working with remains, as the introduction of water will alter the environment in which the remains are deposited [16]. This excess moisture will percolate into the surrounding soil and can promote waterlogging [35]. In clayey soils, containing a

minimum of 40% clay particles, the diffusion of gasses is restricted, which depletes the soil environment of oxygen and leads to the build-up of moisture [16]. These are optimum conditions for anaerobic microorganisms, which are less effective than aerobes, causing the decomposition process to slow [37]. Under favourable conditions, particularly in these moist environments, triacylglycerols, within adipose tissue, undergo hydrolysis and hydrogenation via intrinsic lipases [15]. During autolysis, elements such as sodium and potassium are released, and these elements may result in the formation of salts by reaction with the cleaved fatty acids [15]. Natural environments often provide other sources of elements that may react with these cleaved fatty acids to form fatty acid salts, for example calcium found in soil [15]. These salts are known to be the primary constituents of adipocere [37]; a grey, wax-like substance, that retards decomposition [18].

In contrast, sandy soils containing a minimum of 85% sand particles, facilitate gas diffusion at a much greater rate and the larger particle size allows moisture to drain away, favouring desiccation [16]. Under these conditions, remains will typically dehydrate; the skin will become dark and leathery, and under stable conditions, the remains can be preserved for years – this is known as mummification [25, 38].

1.3. The great debate: pigs vs humans

Due to legal and ethical restrictions surrounding the use of human cadavers in decomposition research, a majority of taphonomic work in the past has been conducted on domestic pigs (Sus scrofa) as human analogues. The use of pigs as analogues has been widely accepted in forensic science, due to similarities in the skin, digestive, and immunological systems [39-41]. The advantages of using pigs as animal models for human decomposition centre largely around the availability of

subjects, replicability, scalability, and affordability. In addition, when working with animal models, such as pigs, researchers are better able to control systematic nuances in height, age, weight, sex, time of death, cause of death, medical condition etc. to better regulate their experiments. In contrast, when working with human remains, there are limitations with respect to most, if not all, of these aforementioned factors. From a research perspective, conducting taphonomic experimentation on pigs appears to be the most obvious and logical approach. However, the degree of difference, or the standard of error, that exists between species, is yet to be fully understood. And when placed in context of applying animal-obtained data, regarding decomposition, to forensic casework involving human remains, the question is raised as to the accuracy of such application.

The establishment of human taphonomic facilities have provided researchers with the invaluable opportunity to investigate whole human decomposition in a controlled, legal and ethical manner [11]. These facilities allow for the development, optimisation and testing of novel, and existing, techniques for the location, detection, identification and dating of human remains. In addition, these human taphonomic facilities allow for the much-needed comparative studies to evaluate the degree of difference that exists between pigs and humans, in a taphonomic respect.

Recent comparative studies have already investigated the differences between pigs and humans in context of adipose tissues, volatile organic compounds (VOCs) [15], insect succession [13, 42-45], and skeletal muscle tissue [46] to list a few. Each of these unique comparative studies found that the outcome(s) being measured in the investigations were dissimilar between pigs and humans. Thus, providing sound evidence to support the use of human remains in taphonomic

research, as well as highlighting the importance of continuing these comparative studies to deepen our understanding of this degree of difference more accurately between the species.

1.4. Post-mortem lipids

In life, the human body is primarily composed of water, protein, lipids, carbohydrates and minerals which are contained mostly within tissues [47]. However, during the biochemical decomposition processes of autolysis and putrefaction, these molecules, and their resulting by-products, are released from the tissues and into the immediate environment [18]. As a majority of proteins and carbohydrates are hydrophilic molecules [48], they are unfavourable targets when considering naturally occurring covariates such as rainfall. Lipids on the other hand, are mostly hydrophobic molecules [48, 49] and as such, are more resistant to harsh environmental conditions. So much so, that several archaeological studies have successfully extracted lipids from specimens exposed to the environment for hundreds of years [50, 51]. Therefore, the ability to detect and monitor these lipids in textiles, and relate them to the decomposition timeline, holds great potential for use as soft tissue biomarkers of decomposition. These biological lipids are a chemically varied group of compounds [52], and are as functionally diverse as their chemistry. These lipids can be grouped into three major categories: storage lipids, structural lipids and signalling lipids [52]. The most dominant type of lipid present in the body, in life, are triacylglycerols [10, 16] which are primarily storage fats [52]. Triacylglycerols contain a single glycerol

molecule with three fatty acids, joined via ester linkages (Fig. 1.6), and are mostly insoluble in water [10, 16, 52].

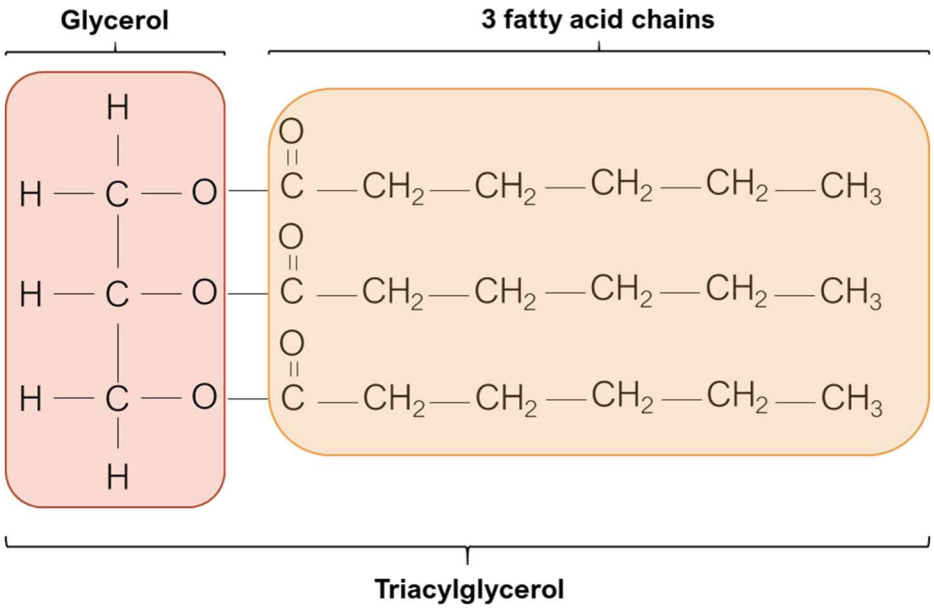

Fig.1. 6 Diagram of triacylglycerol structure with glycerol molecule joined to three fatty acids via ester linkages.

As the body undergoes decomposition, these triacylglycerols undergo hydrolysis, due to enzymatic activity, and produce a mixture of saturated and unsaturated fatty acids [53]. Under aerobic conditions, the oxidation of unsaturated fatty acids can occur due to the activity of microorganisms or oxygen present in the atmosphere. The final products of this aerobic oxidation are aldehydes and ketones. However, under anaerobic conditions the mixture of saturated and unsaturated fatty acids produced during the post-mortem process of hydrolysis, undergo further

hydrolysis and hydrogenation via intrinsic lipases, which result in the transformation of the unsaturated fatty acid double bonds into single bonds (Fig. 1.7.) [10, 15].

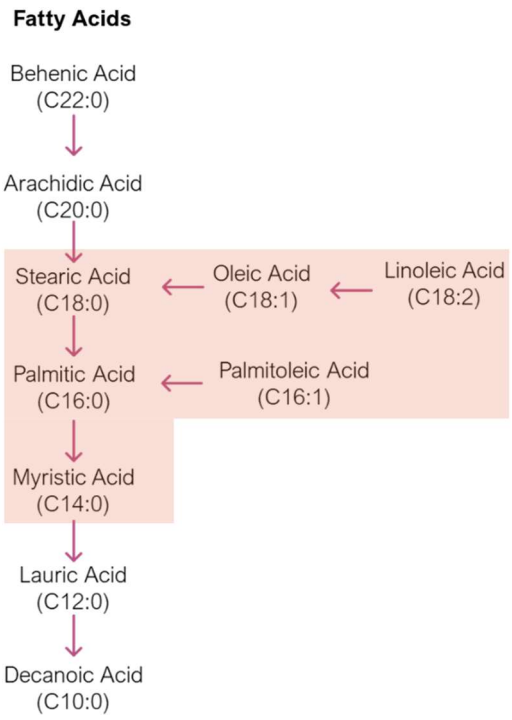

Fig. 1.7 Expected degradation pathway of saturated and unsaturated fatty acids. Fatty acids of particular interest in decomposition are highlighted in orange.

The fatty acids of most importance, according to the available literature are the medium- and long- chained fatty acids: palmitic acid, palmitoleic acid, stearic acid, oleic acid, linoleic acid and myristic acid [49, 54, 55]. However, while these fatty acids have been highlighted in previous research, little work has delved deeper into relating the appearance and subsequent degradation patterns of such lipids, to the

chronology of decomposition. Nor have recent works looked into the contribution of these fatty acids from sources other than decomposition. Because fatty acids are so omnipresent in the environment, it is vital to establish an understanding of the sources of background contamination, to fully comprehend their significance in the decomposition process.

Sterols are another class of lipids which mostly function as structural or signalling lipids however, they differ from most other lipids due to their characteristic tetracyclic ring structure [56] (Fig. 1.8.).

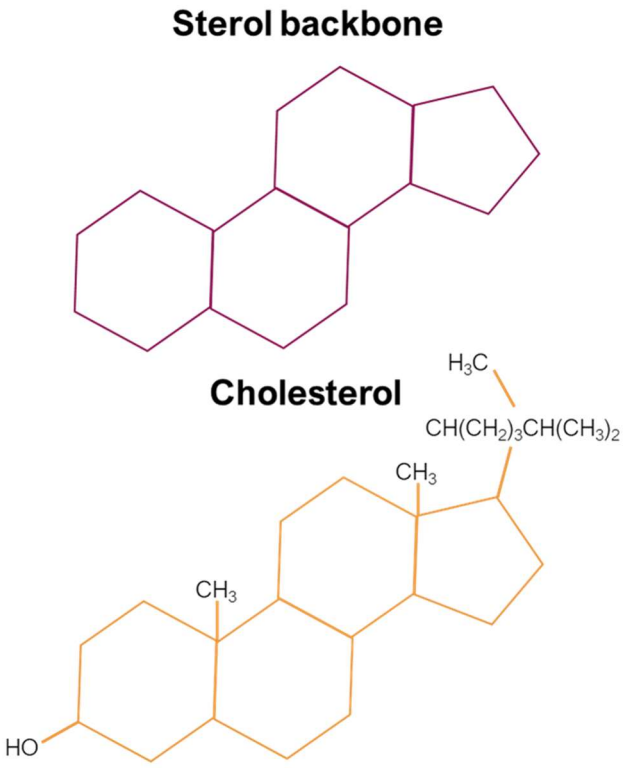

Fig.1.8 Diagram of characteristic sterol tetracyclic backbone and structure of a common sterol: cholesterol.

In comparison to fatty acids, sterols have been somewhat neglected in decomposition studies with respect to their role and importance in understanding the decomposition ecology. Despite this, archaeological investigations have demonstrated how sterols can remain stable in harsh conditions, over extended periods of time [50, 57, 58]. Some recent forensic-focused works, conducted by Luong et al. [51], Ueland et al. [49] and Von der Lühe et al. [56, 59], have shed some light on the role of cholesterol in particular, with respect to decomposition. In life, cholesterol is a ubiquitous tissue sterol in animals, whilst also being detectable in trace levels in some plants [60, 61]. In animals, cholesterol plays an integral part in lipid metabolism as well as being a structural component of plasma membranes [60, 61]. During the processes of decomposition, cholesterol is known to reduce into its stanol derivatives, 5α-cholestanol and coprostanol [62], with 5α-cholestanone being an intermediary of this reduction process [63, 64] (Fig. 1.9). Coprostanol is also a well-known faecal sterol that is produced in the intestines of animals that are warm-blooded, making up approximately 60% of the faecal sterols present in human faeces [63]. The difficulty with targeting sterols in decomposition studies lies in the

background contribution of environmental sterols from plants, animals and fungi [65-67].

A range of different fatty acids and sterols have been targeted in several recent archaeological [57, 58, 68] and forensic [49, 51] investigations for different purposes. Some of the most commonly targeted lipids, based on their potential diagnostic value in context of decomposition [2, 21-23], as well as their ability to capture a more holistic insight into the decomposition ecology are outlined in Table 1.1.

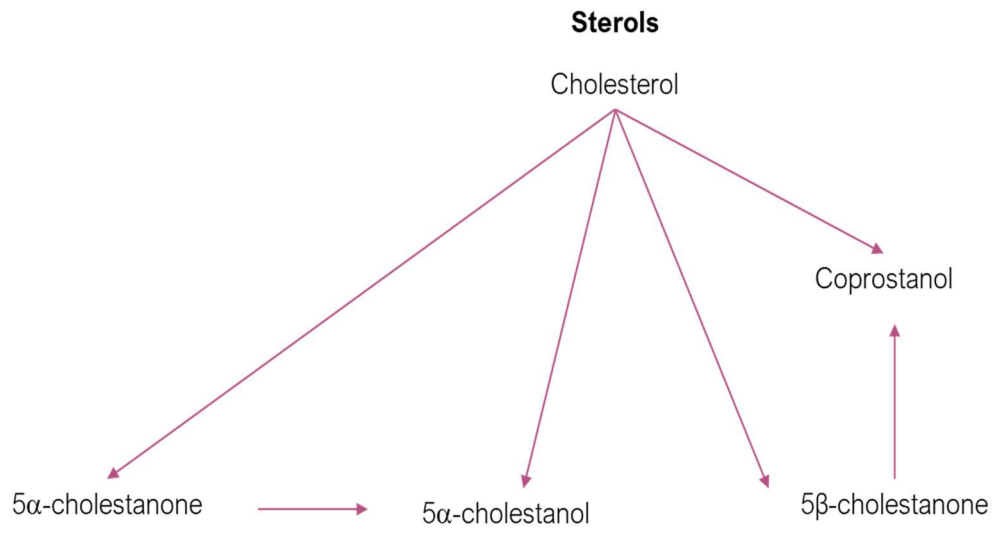

Fig.1.9 Expected degradation pathway of sterols of particular interest in decomposition.

Table 1.1 Commonly targeted lipids for forensic analysis [2, 21-23], organised by category.

Name	***Chemical Formula***
Saturated fatty acids	
Arachidic Acid	C20H40O2
Behenic Acid	C22H44O2
Decanoic Acid	C10H20O2
Deoxycholic Acid	C24H40O4
Heneicosanoic Acid	C21H42O2
Heptadecanoic Acid	C17H34O2
Hexacosanoic Acid	C26H52O2
Lauric Acid	C12H24O2
Myristic Acid	C14H28O2
Palmitic Acid	C16H32O2
Pentadecanoic Acid	C15H30O2
Nonadecanoic Acid	C19H38O2
Tetracosanoic Acid	C24H48O2
Tricosanoic Acid	C23H46O2
Tridecanoic Acid	C13H26O2
Stearic Acid	C18H36O2
Unsaturated fatty acids	
Linoleic Acid	C18H32O2
Lithocholic Acid	C24H40O3
Oleic Acid	C18H34O2
Palmitoleic Acid	C16H30O2
Dicarboxylic acids	
Azelaic Acid	C9H16O4
Sebacic Acid	C10H18O4
Oxysterols	
25-hydroxycholesterol	C27H46O2
Stanols	
5α-cholestanol	C27H48O
Coprostanol	C27H48O
Stanones	
5α-cholestanone	C27H48
Δ^5–sterols	
Cholesterol	C27H46O
Phytosterols	
Ergosterol	C28H44O
Stigmasterol	C29H48O
β-sitosterol	C29H50O

1.5. Post-mortem lipids in textiles as biomarkers of decomposition

The fluids released from a body during decomposition, containing post-mortem lipids, are absorbed and accumulated in associated matrices, such as clothing worn by the individual at death. A report published in 2018 by Balan [69] noted that 97% of homicides resulted in physical evidence, primarily clothing, being collected which makes it a ubiquitous source of evidence at scenes involving the discovery of human remains. A majority of the published literature focuses on textiles from an archaeological perspective [31, 70, 71], on how clothing affects the decomposition process [7, 72-75], or on the interactive relationship between decomposing remains and textiles [5]. Despite often being utilized in criminal cases to aid in the 'how' aspect through forensic textile damage analysis [76], these materials have recently been proven to also be an excellent host for decomposition fluids [10, 53, 77].

Due to the complexity involved with the analysis of decomposition samples alone, the work in this thesis focused on the use of 100% cotton as the textile host to capture the post-mortem lipids. Cotton is a commonly used natural textile that is derived from the seed hair of the many species of the genus Gossypium [78]. These fibers are mostly composed of cellulose and are highly absorbent [31]. As the work in this thesis aimed to develop and test novel analytical methods for the detection of post-mortem lipids in textiles, this material was also considered to be a practical selection to further eliminate variables that could be introduced by fabric dyes or synthetic materials.

1.6. Analytical approach

This research utilised a two-phase approach to investigate whether post-mortem lipids collected in textiles could be associated with the decomposition ecology, and therefore time since death. Phase one involved a non-targeted approach with the use of attenuated total reflectance (ATR) – Fourier transform infrared (FTIR) spectroscopy. This tool served as a presumptive method for the detection and monitoring of post-mortem lipids collected in textiles, alongside the degradation of the textiles themselves. Phase two then utilised a targeted analytical chemical detection to analyse lipids extracted from textiles via gas chromatography (GC) coupled with tandem mass spectrometry (MS/MS).

1.6.1. Phase one: FTIR spectroscopy

FTIR spectroscopy is a technique often utilised in forensic science for the non-destructive characterisation of materials. These materials can vary from the analysis of suspected prohibited drugs, to human hair. Recently, this method has been employed in research for the investigation textile degradation [79-81], as well as the successful detection and monitoring of human decomposition by-products retained in clothing [10, 53].

An ATR accessory is highly advantageous in the application of such work as it is fast and reproducible, whilst also being non-destructive, which allows subsequent analyses of the samples [82, 83]. Additionally, in line with the scope of the current study, this technique allows for the analysis of both the degradation to the clothing materials (cotton), as well as the detection of decomposition by-products (lipids). Table 1.2 outlines the regions of particular interest in this work pertaining to the IR

bands characteristic of the cellulose within the cotton materials, and the post-mortem lipids released during the decomposition process.

Table 1.2 IR band assignments of interest pertaining to the detection and monitoring of post-mortem lipids and cotton cellulose.

IR region ***(cm^{-1})***	***Wavenumber*** ***(cm^{-1})***	***Band Assignment***	***Characterisation***
3000 - 2800	2920	CH_2 asymmetrical stretching	Lipid containing regions
	2850	CH_2 symmetrical stretching	
1800 - 1500	1710, 1720, 1745	C=O stretching	
	1540, 1575	C-O stretching	
1400 - 1200	1430	CH_2 scissoring	Cellulose containing regions
	1335	C-H bending	
	1314	CH_2 rocking	
1200 - 800	1033, 1001, 985	C-O stretching	

In this work, ATR-FTIR spectroscopy was applied as a preliminary method for the detection and monitoring of post-mortem lipids collected in cotton textiles associated with decomposing pig and human remains. The bands of interest outlined in Table 1.2. were focused on in an effort to investigate the simultaneous degradation patterns of these post-mortem lipids, as well as the cotton materials, in conjunction with the decomposition timeline. Specifically, the bands targeted in these regions related to fatty acid salts (1540 cm^{-1} and 1575 cm^{-1}), free fatty acids (1710 cm^{-1}), aldehydes and ketones (1720 cm^{-1}) and triacylglycerols (1745 cm^{-1}) [10, 53]. In

addition, several cellulose containing regions were targeted to simultaneously monitor the degradation of the textile materials during this study. While highly advantageous in most respects, this method does present limitations as it does not allow for more targeted or specific analysis of the lipid profiles that are associated with the decomposition ecology.

1.6.2. Phase two: GC-MS/MS

Gas chromatography – tandem mass spectrometry (GC-MS/MS), is a powerful analytical technique that enables targeted analysis. The use of chromatographic separation coupled with tandem mass spectrometry is a highly advantageous method for the analysis of trace compounds, including lipids, in complex matrices [84]. Gas chromatography (GC) is used as the separation method whereby the volatile liquid or gaseous sample is introduced through a heated injection port and onto the analytical column [85] (Fig. 1.10).

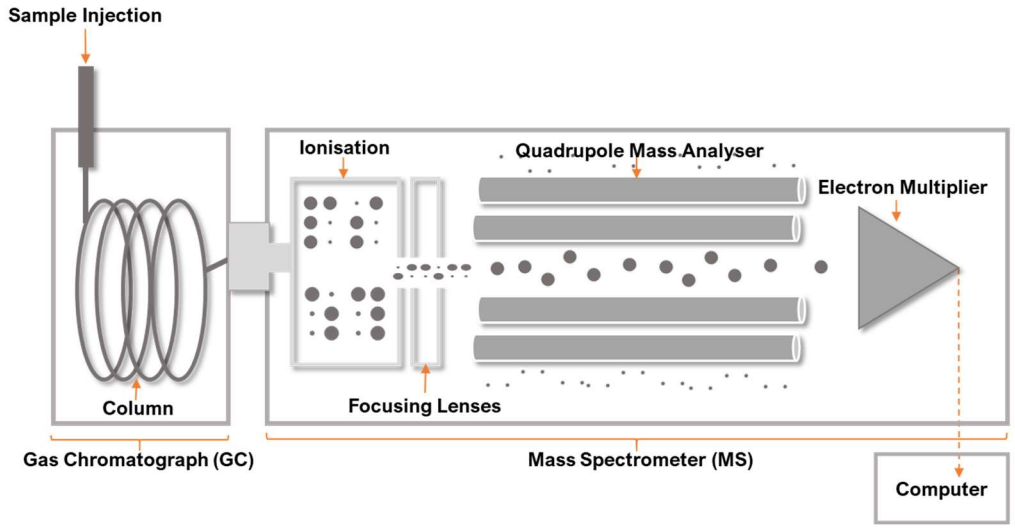

Fig. 1.10 Schematic diagram of gas chromatography quadrupole mass spectrometer (GC-MS/MS).

The sample is then separated in a gaseous state based on its physical and chemical properties and its interaction with the stationary phase of the analytical column [85] (Fig. 1.10). When exiting the analytical column, the compounds enter the tandem mass spectrometer (MS/MS) which is comprised of two scanning mass analysers that are separated by the collision cell (Fig. 1.10). Parent fragments can then be selectively reacted in the collision cell with an inert gas, resulting in further fragmentation to produce daughter ions which are then further resolved in the third quadrupole [86] (Fig. 1.10).

In their native form, lipids are not amenable to detection and analysis via GC-MS/MS due to their low volatility [68]. However, previous lipid work in forensics by Ueland et al. [49] and in archaeology by Luong et al. [68] have demonstrated great success in increasing the volatility of these target lipids via trimethylsilylation derivatisation for analysis using GC-MS/MS. A series of archaeological investigations [87-105] have also successfully demonstrated the use of full scan mode, selected ion monitoring (SIM) mode and multiple reaction monitoring (MRM) mode of GC-MS/MS for the detection and quantification of non-volatile lipids. Additionally, GC-MS/MS has an increased signal to noise ratio, due to reduction of noise from interference ions, lowering the detection limit of the MRM mode relative to SIM [106], proving it to be a superior technique to conventional GC-MS.

1.7. Thesis aims and structure

This thesis documents novel results from the investigation of post-mortem lipids collected in cotton textiles associated with decomposing remains from AFTER. In addition, this work comments on the use of post-mortem lipids as a measurable

outcome to assess the interspecies differences between pigs and humans, as well as its future potential to be developed into an alternative time since death estimator.

In Chapter 2, cotton textile samples associated with decomposing pig and human remains were analysed using ATR-FTIR spectroscopy to measure the relative absorbance of known target lipid regions within the spectra. These lipid regions incorporated fatty acid salts (1540 and 1575 cm^{-1}), free fatty acids (1710 cm^{-1}), aldehydes and ketones (1720 cm^{-1}) and triacylglycerols (1745 cm^{-1}), however did not extend to sterols. The aim of this study was to assess, using semi-parametric regression models in linear mixed model form with Markov chain Monte Carlo (MCMC) sampling, the aforementioned lipid profiles on a time-dependent scale. In addition, this research aimed to provide further insight to the ongoing debate regarding the species comparison between pigs and humans using the lipid profiles obtained.

Despite the major advantages associated with the use of ATR-FTIR spectroscopy in forensic work such as in Chapter 2, this method does not allow for a more specific analysis of the post-mortem lipid profile. Chapter 3 therefore aimed to develop and optimize a novel analytical chemical workflow for the targeted analysis of post-mortem lipids collected in textiles using GC-MS/MS. The specific lipids targeted in this analysis included; arachidic acid, azelaic acid, behenic acid, cholestanol, cholesterol, coprostanol, decanoic acid, deoxycholic acid, ergosterol, heneicosanoic acid, heptadecanoic acid, hexacosanoic acid, lauric acid, linoleic acid, lithocholic acid, myristic acid, nonadecanoic acid, oleic acid, palmitic acid, palmitoleic acid, pentadecanoic acid, sebacic acid, stearic acid, stigmasterol, tetracosanoic acid, tricosanoic acid, tridecanoic acid, 25-hydroxycholesterol, 5α- 5α-cholestanone, and

β-sitosterol. Chapter 3 also aimed to investigate the complex challenges of matrix effects observed in taphonomic samples.

The aim of Chapter 4 was to apply the methods developed in Chapter 3 as a preliminary investigation to examine human decomposition lipid profiles extracted from textiles associated with remains.

While the research in Chapter 4 was fundamental in providing a foundation for future work, the results were mostly descriptive in nature, making it difficult to discern which of the lipids were most appropriate for investigation as soft-tissue biomarkers of decomposition. Therefore, Chapter 5 aimed to thoroughly investigate the impact of ADD, as the unit of measurement for chronological time, on post-mortem lipids in clothing, as the measurable outcome of decomposition, using generalized linear mixed models.

Chapter 5 initially included ARH as a covariate to account for the accumulation of moisture within the taphonomic ecosystem. However, preliminary statistical tests revealed no significant value was attributed by the inclusion of ARH, of which was not already accounted for by the use of ADD. This finding is congruent with recent work by Garrett-Rickman [107] who concluded that ARH accumulates consistently, and that rainfall is unpredictable across all seasons. Therefore, ARH was excluded from further analysis. The data included in this chapter was obtained from both pig and human donors in order to meet sample size requirements for modeling.

1.8. References

[1] R.C. Janaway, Degradation of clothing and other dress materials associated with buried bodies, in: W.D. Haglund, M.H. Sorg (Eds.) Advances in Forensic Taphonomy: Method, theory and archaeological perspectives, CRC Press: Boca Raton, 2002, pp. 379-402.

[2] D.A. Komar, Decay rates in a cold climate region: a review of cases involving advanced decomposition from the Medical Examiner's Office in Edmonton, Alberta, J. Forensic Sci., 43 (1) (1998), 57-61. https://doi.org/ 10.1520/JFS16090J

[3] G.S. Anderson, The use of insects in death investigations: An analysis of cases in British Columbia over a five-year period, J. Can. Soc. Forensic Sci., 28 (4) (1995), 277-292. https://doi.org/10.1080/00085030.1995.10757488

[4] J. Mouzos, Homicidal encounters: A study of homicide in Australia 1989-1999, Canberra: Australian Institute of Criminology, 2000.

[5] M. Ueland, K.D. Nizio, S.L. Forbes, B.H. Stuart, The interactive effect of the degradation of cotton clothing and decomposition fluid production associated with decaying remains, Forensic Sci. Int., 255 (2015) 56-63. https://doi.org/10.1016/j.forsciint.2015.05.029

[6] W.C. Rodriguez, W.M. Bass, Decomposition of buried bodies and methods that may aid in their location, J. Forensic Sci., 30 (3) (1985), 836-852. https://doi.org/ 10.1520/JFS11017J

[7] Mann, R.W., W.M. Bass, and L. Meadows, Time since death and decomposition of the human body: variables and observations in case and experimental field studies, J. Forensic Sci., 35 (1) (1990), 103-11. https://doi.org/ 10.1520/JFS12806J

[8] C.P. Campobasso, G. Di Vella, F. Introna, Factors affecting decomposition and Diptera colonization, Forensic Sci. Int., 120 (1-2) (2001), 18-27. https://doi.org/ 10.1016/s0379-0738(01)00411-x

[9] A. Card, P. Cross, C. Moffatt, T. Simmons, The effect of clothing on the rate of decomposition and Diptera colonization on Sus Scrofa carcasses, J. Forensic Sci., 60 (4) (2015), 979-982. https://doi.org/ 10.1111/1556-4029.12750

[10] S. Collins, B.H. Stuart, M. Ueland, Monitoring human decomposition products collected in clothing: an infrared spectroscopy study, Aust. J. Forensic Sci., 52 (2020) 428-438. https://doi.org/10.1080/00450618.2019.1593504

[11] A.E. Rattenbury, Chapter 2 – Forensic Taphonomy, in: T.K. Ralebitso-Senior (Eds.), Forensic Ecogenomics, Academic Press, 2018, pp. 37-59.

[12] W.D. Haglund, M.H. Sorg, Advances in forensic taphonomy: Method, theory, and archaeological perspectives, Taylor & Francis, 2001.

[13] Z. Knobel, M. Ueland, K.D. Nizio, D. Patel, S.L. Forbes, A comparison of human and pig decomposition rates and odour profiles in an Australian environment, Aust. J. Forensic Sci., 51(2019) 557-572. https://doi.org/10.1080/00450618.2018.1439100

[14] D.L. Cockle, Human decomposition and the factors that affect it: a retrospective study of death scenes in Canada, Doctoral dissertation, Simon Fraser University, Canada, 2013.

[15] S.J. Notter, B.H. Stuart, R. Rowe, N. Langlois, The initial changes of fat deposits during the decomposition of human and pig remains, J. Forensic Sci., 54 (2009) 195-201. https://doi.org/10.1111/j.1556-4029.2008.00911.x

[16] E.M.J. Schotsmans, N. Marquez-Grant, S.L. Forbes, Taphonomy of human remains: forensic analysis of the dead and the depositional environment. John Wiley & Sons, 2017.

[17] M. Ueland, Investigation of the interaction of remains and textiles in soil graves, Doctoral dissertation, University of Technology Sydney, Australia, 2015.

[18] B.H. Stuart, Decomposition chemistry: overview, analysis, and interpretation, in: J.A Siegel, P.J. Saukko, M.M. Houck, (Eds.), Encyclopedia of Forensic Sciences, second ed., Academic Press, 2013, pp. 11–15.

[19] M.A. Iqbal, M. Ueland, S.L. Forbes, Recent advances in the estimation of post-mortem interval in forensic taphonomy, Aust. J. Forensic Sci., 52 (2020) 107-123. https://doi.org/10.1080/00450618.2018.1459840

[20] S.L. Forbes, Time since death: a novel approach to dating skeletal remains, Aust. J. Forensic Sci., 36 (2) (2004), 67-72. https://doi.org/10.1080/00450610409410599

[21] E.R. Hyde, D.P. Haarmann, A.M. Lynne, S.R. Bucheli, J.F. Petrosino, The living dead: bacterial community structure of a cadaver at the onset and end of the bloat stage of decomposition, PLoS ONE 8, (2013). https://doi.org/10.1371/journal.pone.0077733

[22] J.A. Payne, A summer carrion study of the baby pig Sus Scrofa Linnaeus, Ecology. 46 (1965) 592-602. https://doi-org.ezproxy.lib.uts.edu.au/10.2307/1934999

[23] G. Anderson, S. VanLaerhoven, Initial studies on insect succession on carrion in southwestern British Columbia, J. Forensic Sci., 41 (4) (1996) 617-625. https://doi.org/10.1520/JFS13964J

[24] B.G. Ioan, C.N. Manea, B. Hanganu, L. Statescu, L.G. Solovastru, I.S. Manoilescu, The chemistry decomposition in human corpses, Revista De Chimie, 68 (2017) 1352, 1356. https://doi.org/ 10.37358/rc.17.6.5672

[25] D.O. Carter, D. Yellowlees, M. Tibbett, Cadaver decomposition in terrestrial ecosystems. Naturwissenschaften, 94 (1) (2007) 12-24. https://doi.org /10.1007/s00114-006-0159-1

[26] A.A. Vass, S-A. Barshick, G. Sega, J. Carlton, J. Love, J. Synstelien, Decomposition chemistry of human remains: a new methodology for determining the postmortem interval, J. Forensic Sci., 47 (2002) 542-553. https://doi.org/10.1520/JFS15294J

[27] M. Lee Goff, Early post-mortem changes and stages of decomposition in exposed cadavers, Exp. Appl. Acarol., 49 (1-2) (2009) 21-36. https://doi.org/ 10.1007/s10493-009-9284-9

[28] L.M. Swann, S. L. Forbes, S. W. Lewis, Analytical separations of mammalian decomposition products for forensic science: a review, Anal. Chim. Acta., 682 (1-2) (2010) 9-22. https://doi.org/ 10.1016/j.aca.2010.09.052

[29] H. Gill-King, Chemical and ultrastructural aspects of decomposition. in: W.D. Haglund, M. H. Sorg (Eds.) Forensic taphonomy: the postmortem fate of human remains, CRC Press, 1997, pp.93-108.

[30] V. Bugelli, M. Gherardi, M. Focardi, V. Pinchi, S. Vanin, C. P. Campobasso, Decomposition pattern and insect colonization in two cases of suicide by hanging, Forensic Sci. Res., 3 (1) (2018) 94-102. https://doi.org/10.1080/20961790.2017.1418622

[31] R.C. Janaway, Degradation of clothing and other dress materials associated with buried bodies, in: W.D. Haglund, M.H. Sorg (Eds.) Advances in forensic taphonomy: method, theory and archaeological perspectives, CRC Press: Boca Raton, 2002, pp. 379-402.

[32] M.S. Megyesi, S.P. Nawrocki, N.H. Haskell, Using accumulated degree-days to estimate the postmortem interval from decomposed human remains, J. Forensic Sci., 50 (3) (2005) 618-26. https://doi.org/10.1520/jfs2004017

[33] T. Simmons, R. E. Adlam, C. Moffatt, Debugging decomposition data--comparative taphonomic studies and the influence of insects and carcass size on decomposition rate, J. Forensic Sci., 55 (1) (2010) 8-13. https://doi.org/ 10.1111/j.1556-4029.2009.01206.x

[34] D.O. Carter, J.L. Metcalf, A. Bibat, R, Knight, Seasonal variation of postmortem microbial communities, Forensic Sci. Med. Pathol., 11(2) (2015) 202-207. https://doi.org/ 10.1007/s12024-015-9667-7

[35] M. Tibbett, D.O. Carter, Cadaver decomposition and soil: processes, in: D.O. Carter, M. Tibbett, (Eds.) Soil analysis in forensic taphonomy: chemical and biological effects of buried human remains, 2008, CRC Press: pp. 29-52.

[36] S. Blau, D. H. Ubelaker, Handbook of forensic anthropology and archaeology, Walnut Creek: Left Coast Press, 2009.

[37] S.L. Forbes, B.B. Dent, B.H. Stuart, The effect of soil type on adipocere formation, Forensic Sci. Int. 154 (1) (2005) 35-43. https://doi.org/10.1016/j.forsciint.2004.09.108

[38] E.M.J. Schotsmans, W. Van de Voorde, J. De Winne, A.S. Wilson, The impact of shallow burial on differential decomposition to the body: a temperate case study, Forensic Sci. Int., 206 (1-3) (2011) e43-48. https://doi.org/10.1016/j.forsciint.2010.07.036

[39] H.J. Rothkötter, Anatomical particularities of the porcine immune system—A physician's view. Dev. Comp. Immunol., 33 (3) (2009) 267-272. https://doi.org/10.1016/j.dci.2008.06.016

[40] F. Meurens, A. Summerfield, H. Nauwynch, L. Saif, V. Gerdts, The pig: a model for human infectious diseases, Trends Microbiol., 20 (2012) 50-57. https://doi.org/10.1016/j.tim.2011.11.002

[41] K.H. Mair, C. Sedlak, T. Käser, A. Pasternak, B. Levast, W. Gerner, A. Saalmüller, A. Summerfield, V. Gerdts, H.L. Wilson, F. Meurens, The porcine innate immune system: an update, Dev. Comp. Immunol., 45 (2014) 321-343. https://doi.org/10.1016/j.dci.2014.03.022

[42] B.M. Dawson, P.S. Barton, J.F. Wallman, Contrasting insect activity and decomposition of pigs and humans in an Australian environment: A preliminary study. Forensic Sci. Int., 316 (2020) 110515. https://doi.org/10.1016/j.forsciint.2020.110515

[43] Y. Wang, M.Y. Ma, X.Y. Jiang, J.F. Wang, L.L. Li, X.J. Yin, M. Wang, Y. Lai, L.Y. Tao, Insect succession on remains of human and animals in Shenzhen, China, Forensic Sci. Int., 271 (2017) 75-86. https://doi.org/10.1016/j.forsciint.2016.12.032

[44] K. Schoenly, N. Haskell, D. Mills, C. Bieme-Ndi, K. Larsen, Y. Lee, Recreating death's acre in the school yard: using pig carcasses as model corpses, to teach concepts of forensic entomology & ecological succession, Am Biol Teach., 68 (2006) 402-410. https://doi.org/10.2307/4452028

[45] A. Whitaker, Development of blowflies (Diptera: Calliphoridae) on pig and human cadavers: implications for forensic entomology casework, Doctoral dissertation, King's College London (University of London), England 2014.

[46] K.L. Stokes, S.L. Forbes, M. Tibbett, Human versus animal: contrasting decomposition dynamics of mammalian analogues in experimental taphonomy, J. Forensic Sci., 58 (2013) 583-91. https://doi.org/10.1111/1556-4029.12115

[47] R.C. Janaway, S.L. Percival, A.S. Wilson, Decomposition of human remains. Microbiology and aging: clinical manifestations, (2009) 313-334.

[48] G. M. Cooper, R.O. Hausman, A molecular approach. The cell, second ed., Sunderland, MA: Sinauer Associates, 2000.

[49] M. Ueland, S. Collins, L. Maestrini, S.L. Forbes, S. Luong. Fresh vs. frozen human decomposition – A preliminary investigation of lipid degradation products as biomarkers of post-mortem interval, Forensic Chem., 24 (2021) 100335. https://doi.org/10.1016/j.forc.2021.100335

[50] R.P. Evershed, Biomolecular archaeology and lipids. World archaeology, 25 (1) (1993) 74-93. https://doi.org/10.1080/00438243.1993.9980229

[51] S. Luong, S.L. Forbes, J.F. Wallman, R.G. Roberts. Monitoring the extent of vertical and lateral movement of human decomposition products through sediment using cholesterol as a biomarker, Forensic Sci. Int., 285 (2018) 93-104. https://doi.org/10.1016/j.forsciint.2018.01.026

[52] Nelson, D.L. M.M. Cox, Lehninger Principles of Biochemistry: sixth ed., Macmillan Learning, 2008.

[53] S. Collins, B.H. Stuart, M. Ueland. Anatomical location dependence of human decomposition products in clothing, Aust. J. Forensic Sci., 55 (2023) 363-375. https://doi.org/10.1080/00450618.2021.1981443

[54] S.J. Notter, B.H. Stuart, B.B. Dent, J. Keegan, Solid-phase extraction in combination with GC/MS for the quantification of free fatty acids in adipocere, Eur. J. Lipid Sci. Technol., 110 (1) (2008) 73-80. https://doi.org/10.1002/ejlt.200700159

[55] B.B. Dent, S.L. Forbes, B.H. Stuart, Review of human decomposition processes in soil, Environ. Geol., 45 (2004) 576-585. https://doi.org/10.1007/s00254-003-0913-z

[56] B. von der Lühe, L.A. Dawson, R.W. Mayes, S.L. Forbes, S. Fiedler, Investigation of sterols as potential biomarkers for the detection of pig (S. s. domesticus) decomposition fluid in soils, Forensic Sci. Int., 230 (2013) 68-73. https://doi.org/10.1016/j.forsciint.2013.03.030

[57] B. von der Lühe, K. Prost, J.J. Birk, S. Fiedler, Steroids aid in human decomposition fluid identification in soils of temporary mass graves from World War II, J. Archaeol. Sci. Rep., 32 (2020) 102431. https://doi.org/10.1016/j.jasrep.2020.102431

[58] S. Luong, M.W. Tocheri, E. Hayes, T. Sutikna, R. Fullagar, E.W. Saptomo, R.G. Roberts, Combined organic biomarker and use-wear analyses of stone artefacts from Liang Bua, Flores, Indonesia, Sci. Rep., 9 (1) (2019) 1-17. https://doi.org/10.1038/s41598-019-53782-2

[59] B. von der Lühe, J.J. Birk, L. Dawson, R.W. Mayes, S. Fiedler, Steroid fingerprints: Efficient biomarkers of human decomposition fluids in soil, Org. Geochem.,124 (2018) 228-237. https://doi.org/10.1016/j.orggeochem.2018.07.016

[60] W.W. Christie, Lipid analysis, Pergamon press, Oxford, 2003.

[61] W.W. Christie, X.J.S. Han, Lipid analysis: isolation, separation, identification and lipidomic analysis: Fourth Edition, Elsevier Ltd., 2003. https://doi.org/10.1533/9780857097866

[62] R. Leeming, A. Ball, N. Ashbolt, P. Nichols, Using faecal sterols from humans and animals to distinguish faecal pollution in receiving waters, Water research, 30 (1996), 2893-290067.

[63] J.O. Grimalt, P. Fernandez, J.M. Bayona, J. Albaiges, Assessment of faecal sterols and ketones as indicators of urban sewage inputs to coastal waters, Environ. Sci. & Technol., 24 (3) (1990) 357-363. https://doi.org/10.1021/es00073a011

[64] S.J. Gaskell, G. Eglinton, Rapid hydrogenation of sterols in a contemporary lacustrine sediment, Nature, 254 (5497) (1975) 209-211. https://doi.org/10.1038/254209b0

[65] P.G. Hatcher, P.A. McGillivary, Sewage contamination in the New York Bight. Coprostanol as an indicator, Environ. Sci. Technol., 13 (10) (1979) 1225-1229. https://doi.org/10.1021/es60158a015

[66] J.J. Murtaugh, R.L. Bunch, Sterols as a measure of faecal pollution, J. Water Pollut. Control Fed., (1967) 404-409.

[67] M. Noda, M. Tanaka, Y. Seto, T. Aiba, C. Oku, Occurrence of cholesterol as a major sterol component in leaf surface lipids, Lipids 23 (5) (1988) 439-444. https://doi.org/10.1007/BF02535517

[68] S. Luong, E. Hayes, E. Flannery, T. Sutikna, M. Tocheri, E.W. Saptomo, R.G. Jatmiko, R.G. Roberts, Development and application of a comprehensive analytical workflow for the quantification of non-volatile low molecular weight lipids on archaeological stone tools, Anal. Methods, 9 (30) (2017) 4349-4362. https://doi.org/10.1039/C7AY01304C

[69] L. Balan, The importance of clothing examination, Eur. J. Law Publ. Adm., 5 (2) (2018) 137-141. https://doi.org/10.18662/eljpa/49

[70] J. Was-Gubala, R. Salerno-Kochan, The biodegradation of the fabric of soldiers' uniforms. Sci. Justice, 40 (1) (2000)15-20. https://doi.org/ 10.1016/S1355-0306(00)71928-9

[71] J. Wakely, Death, decay and reconstruction — Approaches to archaeology and forensic science. J. Anat., 160 (1988) 233.

[72] S.L. Forbes, B.H. Stuart, B.B. Dent, The effect of the method of burial on adipocere formation. Forensic Sci. Int., 154 (1) (2005) 44-52. https://doi.org/10.1016/j.forsciint.2004.09.109

[73] G. Anderson, Factors that influence insect succession on carrion. In: J.H. Byrd, J.K. Tomberlin (Eds.) Forensic Entomology: The utility of arthropods in legal investigations. second ed., CRC Press, 2010, pp. 103-139.

[74] J.A. Kelly, T.C. van der Linde, G.S. Anderson, The influence of clothing and wrapping on carcass decomposition and arthropod succession during the warmer seasons in central South Africa*. J. Forensic Sci., 54 (5) (2009) 1105-1112. https://doi.org/ 10.1111/j.1556-4029.2009.01113.x

[75] S.C. Voss, D.F. Cook, I.R. Dadour, Decomposition and insect succession of clothed and unclothed carcasses in Western Australia, Forensic Sci. Int., 211 (1-3) (2011) 67-75. https://doi.org/ 10.1016/j.forsciint.2011.04.018

[76] K. Sloan, M. Fergusson, J. Robertson, Australian forensic textile damage examinations – Finding a way forward since PCAST. Sci. Justice, 59 (2) (2019) 145-152. https://doi.org/10.1016/j.scijus.2018.10.004

[77] B.H. Stuart, M. Ueland, Degradation of clothing in depositional environments, in: E.M.J . Schotsmans, N. Márquez-Grant, S.L. Forbes (Eds.) Depositional environments, in taphonomy of human remains: forensic analysis of the dead and the depositional environment, John Wiley & Sons, 2017, pp. 120-133.

[78] S.K. David, M.T. Pailthorpe, Classification of textile fibres: production, structure, and properties, in: J. Robertson, C. Roux, and K.G. Wiggins (Eds.) Forensic examination of fibres, CRC Press, 1999, CRC Press.

[79] K. Kavkler, N. Gunde-Cimerman, P. Zalar, A. Demsar, FTIR spectroscopy of biodegraded historical textiles. Polym. Degrad. Stabil., 96 (2011) 574-580. https://doi.org/10.1016/j.polymdegradstab.2010.12.016

[80] J.S. Church, D.J. Evans, The quantitative analysis of fluorocarbon polymer finishes on wool by FT-IR spectroscopy, J. Appl. Polym. Sci., 57 (13) (1995) 1585-1594. https://doi.org/10.1002/app.1995.070571306

[81] K. Stehfest, M. Boese, G. Kerns, A. Piry, C. Wilhelm, Fourier transform infrared spectroscopy as a new tool to determine rosmarinic acid in situ, J. Plant Physiol., 161 (2) (2004)151-156. https://doi.org/10.1078/0176-1617-01099

[82] M. Ueland, J.M. Howes, S.L. Forbes, B.H. Stuart, Degradation patterns of natural and synthetic textiles on a soil surface during summer and winter seasons studied using ATR-FTIR spectroscopy, Spectrochim. Acta A Mol. Biomol. Spectrosc., 185 (2017) 69-76. https://doi/org/ 10.1016/j.saa.2017.05.044

[83] K.D. Nizio, M. Ueland, B.H. Stuart, S.L. Forbes, The analysis of textiles associated with decomposing remains as a natural training aid for cadaver-detection dogs, Forensic Chem., 5 (2017). https://doi.org/10.1016/j.forc.2017.06.002

[84] P. He, D.S. Aga, Comparison of GC-MS/MS and LC-MS/MS for the analysis of hormones and pesticides in surface waters: advantages and pitfalls, Anal. Methods, 11 (11) (2019) 1436-1448. https://doi.org/10.1039/C8AY02774A

[85] B.H. Stuart, Forensic analytical techniques, John Wiley & Sons, 2012.

[86] A. Varela Coelho, C.D. Matos Ferraz Franco, Tandem mass spectrometry: Molecular characterization, IntechOpen, London. https://doi.org/10.5772/56703

[87] R.P. Evershed, Experimental approaches to the interpretation of absorbed organic residues in archaeological ceramics. World Archaeol., 40 (1) (2008) 26-47. https://doi.org/10.1080/00438240801889373

[88] J.W. Eerkens, GC–MS analysis and fatty acid ratios of archaeological potsherds from the western great basin of North America. Archaeometry, 47 (1) (2005) 83-102. https://doi.org/10.1111/j.1475-4754.2005.00189.x

[89] M.P. Colombini, G. Giachi, F. Modugno, E. Ribechini, Characterisation of organic residues in pottery vessels of the Roman age from Antinoe (Egypt), Microchem. J., 79 (1) (2005) 83-90. https://doi.org/10.1016/j.microc.2004.05.004

[90] J. Baeten, B. Jervis, D. De Vos, M. Waelkens, Molecular evidence for the mixing of Meat, Fish and Vegetables in Anglo-Saxon coarseware from Hamwic, UK. Archaeometry, 55 (6) (2013) 1150-1174. https://doi.org/10.1111/j.1475-4754.2012.00731.x

[91] M. Copley, H.A. Bland, P. Rose, M. Horton, R. Evershed, Gas chromatographic, mass spectrometric and stable carbon isotopic investigations of organic residues of plant oils and animal fats employed as illuminants in archaeological lamps from Egypt, Analyst 130 (6) (2005) 860-871. https://doi.org/10.1039/B500403A

[92] M. Correa-Ascencio, R.P. Evershed, High throughput screening of organic residues in archaeological potsherds using direct acidified methanol extraction, Anal. Methods, 6 (5) (2014) 1330-1340. https://doi.org/10.1039/C3AY41678J

[93] S. E. Fraser, T. Insoll, A. Thompson, B. E. van Dongen, Organic geochemical analysis of archaeological medicine pots from Northern Ghana. The multi-functionality of pottery. J. Archaeol. Sci., 39 (7) (2012) 2506-2514. https://doi.org/10.1016/j.jas.2012.03.015

[94] M. W. Gregg, E. B. Banning, K. Gibbs, G. F. Slater, Subsistence practices and pottery use in Neolithic Jordan: molecular and isotopic evidence, J. Archaeol. Sci., 36 (4) (2009) 937-946. https://doi.org/10.1016/j.jas.2008.09.009

[95] C. Heron, R.P. Evershed, L.J. Goad, Effects of migration of soil lipids on organic residues associated with buried potsherds, J. Archaeol. Sci., 18 (6) (1991) 641-659. https://doi.org/10.1016/0305-4403(91)90027-M

[96] S. Isaksson, F. Hallgren, Lipid residue analyses of Early Neolithic funnel-beaker pottery from Skogsmossen, eastern Central Sweden, and the earliest evidence of dairying in Sweden, J. Archaeol. Sci., 39 (12) (2012) 3600-3609. https://doi.org/10.1016/j.jas.2012.06.018

[97] S. Isaksson, C. Karlsson, T. Eriksson, Ergosterol (5, 7, 22-ergostatrien-3β-ol) as a potential biomarker for alcohol fermentation in lipid residues from prehistoric pottery. J. Archaeol. Sci., 37 (12) (2010) 3263-3268. https://doi.org/10.1016/j.jas.2010.07.027

[98] K. Kimpe, C. Drybooms, E. Schrevens, P.A. Jacobs, R. Degeest, M. Waelkens, Assessing the relationship between form and use of different kinds of pottery from the archaeological site Sagalassos (southwest Turkey) with lipid analysis, J. Archaeol. Sci., 31 (11) (2004) 503-1510. https://doi.org/10.1016/j.jas.2004.03.012

[99] D. Namdar, R.J. Stacey, S.J. Simpson, First results on thermally induced porosity in chlorite cooking vessels from Merv (Turkmenistan) and implications for the formation and preservation of archaeological lipid residues, J. Archaeol. Sci., 36 (11) (2009) 2507-2516. https://doi.org/10.1016/j.jas.2009.07.003

[100] A. Charrié-Duhaut, J. Connan, N. Rouquette, P. Adam, C. Barbotin, M.F. de Rozières, A. Tchapla, P. Albrecht, The canopic jars of Rameses II: real use revealed by molecular study of organic residues, J. Archaeol. Sci., 34 (6) (2007) 957-67. https://doi.org/10.1016/j.jas.2006.09.012

[101] O.E. Craig, G. Taylor, J. Mulville, M.J. Collins, M.P. Pearson, The identification of prehistoric dairying activities in the Western Isles of Scotland: an integrated biomolecular approach, J. Archaeol. Sci., 32 (1) (2005) 91-103. https://doi.org/10.1016/j.jas.2004.06.009

[102] S. N. Dudd, M. Regert, R.P. Evershed, Assessing microbial lipid contributions during laboratory degradations of fats and oils and pure triacylglycerols absorbed in ceramic potsherds, Org. Geochem., 29 (5) (1998) 1345-1354. https://doi.org/10.1016/S0146-6380(98)00093-X

[103] J. Echeverría, M.T. Planella, H.M. Niemeyer, Nicotine in residues of smoking pipes and other artifacts of the smoking complex from an Early Ceramic period archaeological site in central Chile, J. Archaeol. Sci., 44 (2014) 55-60. https://doi.org/10.1016/j.jas.2014.01.016

[104] J. Font, N. Salvado, S. Buti, J. Enrich, Fourier transform infrared spectroscopy as a suitable technique in the study of the materials used in waterproofing of archaeological amphorae, Anal. Chim. Acta, 598 (1) (2007) 119-127. https://doi.org/10.1016/j.aca.2007.07.021

[105] B. Stern, C. Heron, M. Serpico, J. Bourriau, A comparison of methods for establishing fatty acid concentration gradients across potsherds: a case study using late bronze age canaanite amphorae, Archaeometry, 42 (2) (2000) 399-414. https://doi.org/10.1111/j.1475-4754.2000.tb00890.x

[106] N. Homer, S. Kothiya, A. Rutter, B. R. Walker, R. Andrew, Gas chromatography tandem mass spectrometry offers advantages for urinary steroids analysis, Anal. Biochem., 538 (2017) 34-37. https://doi.org/ 10.1016/j.ab.2017.09.002

[107] S. Garrett-Rickman, Assessment of taphonomic effects on biomolecule degradation for the estimation of post-mortem interval of human remains, Doctoral dissertation, University of Technology Sydney, Australia, 2022.

Chapter 2: A preliminary investigation to determine the suitability of pigs as human analogues for post-mortem lipid analysis.

Chapter 2: A preliminary investigation to determine the suitability of pigs as human analogues for post-mortem lipid analysis.

i. Preface

With the exception of minor editorial changes, Chapter 2 reproduces the following research article; **S. Collins,** L. Maestrini, M. Ueland, B.H. Stuart, (2022). A preliminary investigation to determine the suitability of pigs as human analogues for post-mortem lipid analysis. Talanta Open, 5, 100100. https://doi.org/10.1016/j.talo.2022.100100. Permissions for reuse of this article within this dissertation have been obtained.

ii. Statement of Contribution and Declaration

Sharni Collins: conceptualisation; methodology; validation; formal analysis; investigation; writing – original draft; writing - review and editing; Luca Maestrini: methodology; software; formal analysis; writing - review and editing; Maiken Ueland: conceptualisation; methodology; writing - review and editing; supervision; Barbara Stuart: conceptualisation; methodology; writing – review and editing; supervision.

Graduate research student

Production Note:
Signature removed
prior to publication.

Sharni Collins

Principal Supervisor

Production Note:
Signature removed
prior to publication.

Dr. Maiken Ueland

Co-supervisor

Production Note:
Signature removed
prior to publication.

Professor Barbara Stuart

Co-supervisor

Dr. Luca Maestrini

2.1. Introduction

Determination of time since death presents as a major challenge to law enforcement when faced with the discovery of human remains [1]. This is primarily due to complex relationships between biotic and abiotic factors influencing the post-mortem process [2]. Decomposition involves a series of chemical processes that result in the breakdown of soft tissues containing carbohydrates, proteins and lipids [3-6]. This process occurs immediately after death and ultimately results in the disintegration of all soft tissues, leaving dry or skeletal remains [3-6].

For decades, studies investigating post-mortem decomposition and time since death have utilised human analogues, primarily the domestic pig (Sus domesticus) due to ethical and legal restrictions limiting the use of human cadavers in decomposition research [3]. The use of pigs as analogues has been widely accepted in forensic science, due to anatomical similarities in the skin, digestive, and immunological systems [7-9]. As a result, the field of forensic taphonomy has become heavily saturated with information regarding the post-mortem processes gained from pig models.

A review article published in 2020 by Matuszewski et al. [10] detailed selected cadaver studies conducted between 1955 and 2018 related to carrion ecology, forensic entomology and taphonomy. Of the studies listed, more than half were conducted on pigs and less than 10% on humans. However, with the emergence of human taphonomic research facilities, researchers have been able to directly compare the taphonomy of pigs and humans. Recent comparative studies have investigated the differences between pigs and humans with respect to adipose tissues

[11], volatile organic compounds (VOCs) [12], insect succession [13-16], skeletal muscle tissue [17], soil biogeochemistry and microbiology [18] and total body scoring [19, 20]. However, there remains an urgent need to continue these comparative studies in more fields, using different scientific methods in order to adequately assess whether pigs are suitable analogues for human decomposition work. Therefore, the current study aims to investigate the interspecies differences between pigs and humans using post-mortem lipids collected in textiles. Recent forensic studies [21-24] have demonstrated that textiles are a valuable source of physical evidence, particularly as a host for decomposition fluids rich in lipids [21-23].

Lipids contribute to approximately 60-85% of adipose tissues [4], with the predominant type being triacylglycerols [4, 21, 25]. The structure of triacylglycerols is comprised of three fatty acid tails attached via ester linkages to a glycerol molecule [4]. Following death, these lipids undergo hydrolysis due to enzymatic activity, resulting in the release of free fatty acids [4, 21, 22]. Due to their hydrophobic nature, saturated fatty acids are extremely persistent in the environment and are more stable when compared to other soft tissue biomarkers such as proteins, carbohydrates and nucleic acids [26]. Despite the fact that pigs and humans both contain approximately 20% adipose tissue [27], the composition and individual proportions differ greatly between species [11, 28].

For the current study, cotton textile samples were examined using attenuated total reflectance (ATR) - Fourier transform infrared (FTIR) spectroscopy to measure the relative absorbance of target lipid regions. One hundred percent cotton was selected as the baseline for this work due to its known absorptive properties and feasibility for the collection of decomposition products and assessment using FTIR

spectroscopy [21-23]. The ability to identify and monitor trends in the post-mortem lipids collected in textiles over the decomposition timeline and statistically assess these patterns provides a new pathway for the analysis of functional data on a time-dependent scale. This is a useful tool for forensic investigations where time since death is in question.

This preliminary study provides the first assessment of post-mortem lipids collected in textiles to examine interspecies differences between pigs and humans in the southern hemisphere.

2.2. Materials and Methods

2.2.1. Experimental Field Site

This study was conducted at the Australian Facility for Taphonomic Experimental Research (AFTER), an outdoor eucalypt woodland on the Cumberland Plain in Western Sydney, New South Wales, Australia. This field site is privately owned and operated by the University of Technology Sydney (UTS). A description of the facility is documented in Knobel et al. [12]. Weather data were collected using a HOBO® U30 weather station within the AFTER site.

2.2.2. Donor Information

Two human donors and four pig cadavers were placed in a supine position on the soil surface and allowed to decompose naturally. Trial 1 was conducted over the Australian summer – autumn period (commencing January 29, 2021) and included human donor 1 (H1), an 86-year-old male with a height of 174 cm and weight of 63 kg, giving a body mass index (BMI) [29] of 20.8. H1 was directly compared with two

domestic 6-month-old pigs, one female (P1) and one male (P2), both weighing approximately 65 kg. Trial 2 was conducted over the Australian winter – spring period (commencing June 11, 2021) and included human donor 2 (H2), an 84-year-old male with a height of 182 cm and weight of 100 kg, giving a BMI of 30.2. H2 was directly compared with two domestic female 6-month-old pigs (P3 and P4) both weighing approximately 70 kg. All individuals were clothed in a 100% white cotton t-shirt as described in Collins et al. [22].

The human donors (H1 and H2) were received through the University of Technology Sydney (UTS) Body Donation Programme, with consent provided in accordance with the New South Wales Anatomy Act (1977). Ethics approval was provided by the UTS Human Research Ethics Committee (HREC ETH15-0029). The human donors were not treated with any chemicals prior to placement at the facility and were allowed to decompose naturally.

Control sites were created for both trials, containing identically sourced clothing placed on the soil surface at AFTER at a minimum distance of 5 m from the decomposing remains, twice the minimum recommended distance proposed by Luong et al. 2018 [30].

Photographs and visual observations were recorded for human and pigs on each sampling day. Visual decomposition was determined using the five reported stages of decomposition: fresh, bloat, active, advanced, and skeletal [5].

2.2.3. Sample Collection

Textile samples were collected using sterilised scissors from the anterior aspect of the decomposing remains and respective control sites on a series of days

from 0 – 105 days post-placement (Table 2. S1). The scissors were thoroughly washed with acetone between each section. The textile samples were photographed, and any visible changes were documented. Each textile sample was individually packaged and labelled in a paper envelope and stored in a cooler for transportation to the laboratory. The textile samples were dried at ambient temperature to impede bacterial and fungal growth. Adhering soil and hair was also removed. The textile samples were then re-packaged into new, individually labelled envelopes and stored for a maximum of 3 months, at -18°C until further analysis.

Due to a local flooding event, the AFTER facility was closed between 19 March – 4 April 2021, which directly impacted sample collection for Trial 1 between days 42 and 70 post-placement (Table 2. S1).

2.2.4. ATR-FTIR Spectroscopy

ATR-FTIR spectra were obtained using a Nicolet Magna-IR 6700 spectrometer (Thermo Scientific, USA) and an ATR accessory consisting of a diamond crystal with a 45° angle of incidence. Spectra were recorded over a range of 4000 – 400 cm^{-1}, with a spectral resolution of 4 cm^{-1} and averaged over 128 scans. Triplicates were taken for each textile sample and acetone was used to clean the ATR crystal between each sample. OMNIC software (version 8.2, Thermo Scientific, USA) was used to record and baseline-correct the spectra which were then exported as individual comma-separated values (CSV) files. The averaged stacked plots of the IR functions are shown in Figure 2. S1 – 2. S6.

The data was then further processed in accordance with the respective statistical methods (Figure 2. S7).

2.2.5. Data processing and statistical analyses

2.2.5.1. Functional Principal Component Analysis (FPCA)

Principal component analysis (PCA) is a multivariate technique for high-dimensional data which is commonly used as a dimensionality reduction tool for exploratory data analysis and predictive models [31]. The purpose of PCA is often to compress, simplify and extract the most important information present within a dataset [32]. PCA has been applied as an exploration tool for chemometric analysis of IR data [21-23, 33]. However, IR data is functional data due to the dependence of the observations over the wavenumber domain (in this case a scanning range of 4000 – 400 cm^{-1}) [34]. For this reason, the use of an extension of traditional PCA, in the form of functional principal component analysis (FPCA) was selected in the current study to investigate the variation within the full functional dataset more accurately. FPCA replaces vectors with functions, covariance matrices with covariance operators, and scalar products in vector space by scalar products in square-integrable functional space [34 - 37].

For the FPCA, the triplicate absorbance values extracted from the CSV files were averaged to provide a single set of full spectra absorbance values as a representative for each sample collected post-placement. Two datasets were created, one for Trial 1 containing the data for H1, P1 and P2, and one for Trial 2 containing the data for H2, P3 and P4. These datasets were imported directly into the Unscrambler X (version 10.3, CAMO, Norway) statistical software to further process the data prior to (FPCA). The first derivative using the Savitzky-Golay (SG) algorithm with 3 smoothing points and extended multiplicative scattering correction (EMSC) was applied to the datasets. This processing method for ATR-FTIR spectra has

previously been employed as it minimises baseline differences [38-40]. Two FPCAs were produced in R [41] using the package fdapace [42], one for each trial: Trial 1 and Trial 2. The loadings plot for each FPCA were then used to determine the bands of interest (Table 2. S2) for further targeted statistical analysis (2.5.2 and 2.5.3). The residual plots (Figure 2. S8c and 2. S9c) from the projection of the first two FPCs for each trial were used to determine that there are minimal unexplained features of the spectral profiles.

2.2.5.2. Semi-parametric Regression Analysis

In addition to FPCA, the functional data was also analysed using semi-parametric regression models. The baseline corrected triplicate data obtained were used to extract maximum absorbance values within a set boundary for the IR bands of interest (Table 2. S2) revealed from the loadings plots of the FPCAs. Triplicate normalised absorbance ratios were then computed using an adapted method from Ueland et al. 2015 [23]. Each extracted maximum absorbance value was then normalised to the asymmetrical CH2 stretching of the methylene chain ~2920 cm^{-1} present in all spectra as a stable reference point as per Ueland et al. 2015 [23]. This method provided five normalised ratios: ~1540 cm^{-1}/ ~2920cm^{-1}, ~1575 cm-^{1} / ~2920 cm^{-1}, ~1710 cm^{-1} /~2920 cm^{-1}, ~1720 cm^{-1} /~2920 cm^{-1} and ~1745 cm^{-1} / ~2920 cm^{-1}.

Semi-parametric regression models [43] in linear mixed model form were then fitted in R for the normalised ratios on a time dependent scale (days post-placement). The non-parametric components were given by O'Sullivan penalised splines [44]. The number of knots were selected using the simple default indications from Chapter 5 of

Rupert, Wand and Carroll (2003) [45]. Regression lines and 95% confidence bands were obtained for the mean of the underlying process using Markov chain Monte Carlo (MCMC) sampling. The models were validated by checking the assumptions of normality, independence of the residuals and the appropriate convergence of MCMC chains. This analysis allowed a more targeted investigation of the post-mortem lipids on a time-dependent scale.

2.2.5.3. One-way Analysis of Variance

The triplicate normalised ratios computed were averaged to perform one-way analysis of variance (ANOVA) to compare the mean differences between species groups (human v pig) within each trial. As the one-way ANOVA compares the mean differences between groups, the triplicate normalised ratios were averaged to eliminate the influence of intrasample variation on the overall statistical significance. The ratios were log-transformed so that the assumptions of normality and homoscedasticity were not violated. Normality was tested using the Shapiro-Wilk test of the residuals and the hypothesis of equal variances was tested using the Levene test. The resulting p-values were then compared to a reference level of 0.05. Tukey honestly significant different (HSD) post-hoc tests were run to understand the source of the statistically significant differences from the one-way ANOVAs. The ANOVAs, tests for checking assumptions and post-hoc tests were performed using R in-built functions and the package 'car' [44].

2.3. Results and Discussion

2.3.1. Environmental conditions

Mean temperature and total rainfall for the duration of the study is displayed in Fig. 2.1. Two trials were conducted for this study: Trial 1 (January 29, 2021 – May 14, 2021) and Trial 2 (June 11, 2021 – September 24, 2021). H1, P1 and P2 of Trial 1 experienced several rainfall events (Fig. 2.1) and an overall mean temperature of 19.4°C. Trial 2 experienced relatively less rainfall events and a lower overall mean temperature of 14.8°C.

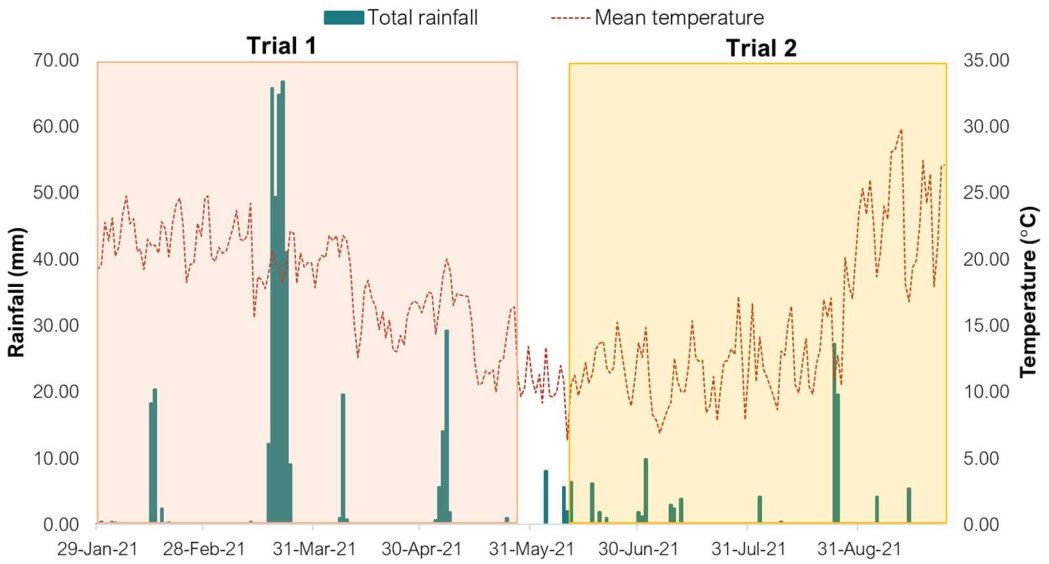

Fig. 2. 1 Total rainfall (mm) and mean temperature (°C) for the duration of Trial 1 and Trial 2. The overall mean temperature for Trial 1 was 19.4°C and Trial 2, 14.8°C.

2.3.2. Visual Decomposition

The visual decomposition of the pigs and humans was considerably different between Trial 1 and Trial 2 (Fig. 2.2). During Trial 1, the pigs and human experienced several periods of heavy rainfall throughout the investigation and an overall mean temperature of 19.4°C (Fig. 2.1). When compared with P1 and P2, there was a

considerable difference in the visual decomposition observed for H1 (Fig. 2.2). H1 progressed from the fresh stage into the bloat stage within the first 10 days post-

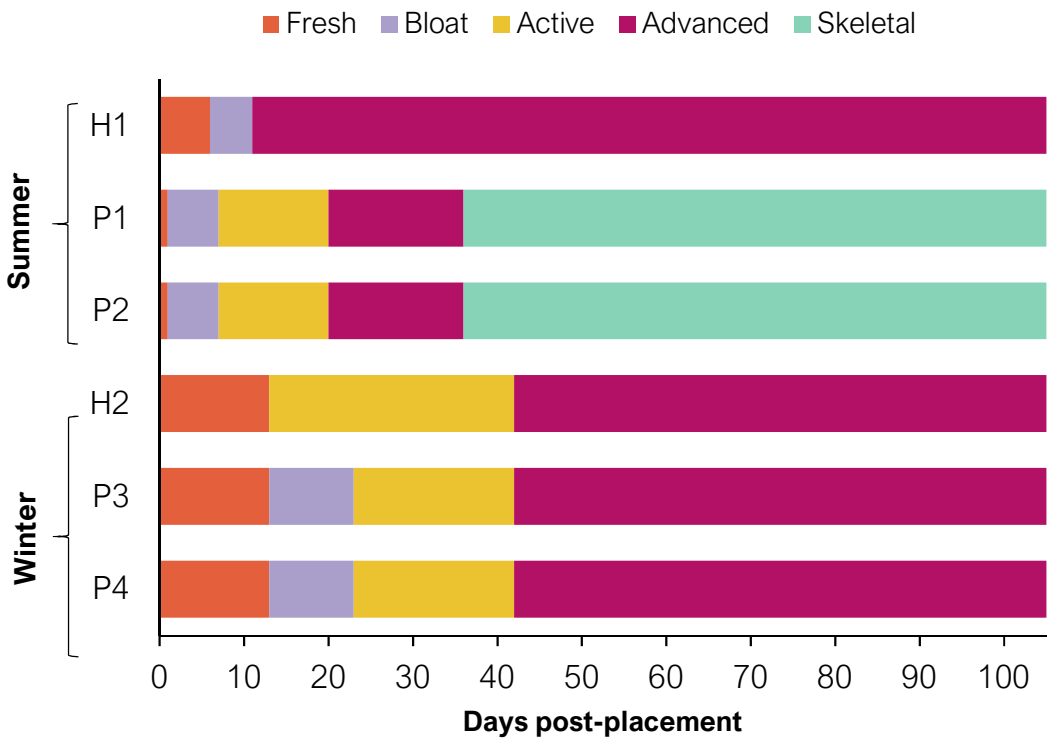

Fig. 2. 2 Occurrence and duration of the stages of decomposition for the summer Trial 1 (H1, P1, P2) and the winter Trial 2 (H2, P3, P4) over the 105-day post-placement period.

placement, however, H1 did not experience a distinct active decay stage. Instead, H1 transitioned from bloat into an advanced decay, relatively stable state of mummification. In contrast, P1 and P2 progressed from fresh, bloat and then active decay within the first 10 days post-placement. During the active period for P1 and P2, there was dense entomological activity which is typically attributed to an abundance of volatile organic compounds (VOCs) being emitted during this stage [45]. Between days 20 and 42 post-placement, P1 and P2 reached an advanced state of decomposition with a significant loss of soft-tissue mass, resulting in skeletonisation. By day 35 post-placement, both pigs were fully skeletonised (Fig. 2.3a and b).

Trial 2 experienced less rainfall than Trial 1 and had a lower overall mean temperature of 14.8°C (Fig. 2.1). In contrast to Trial 1, there were no obvious

Fig. 2. 3 H1 (a) and P1 (b) from Trial 1 on day 35 post-placement. H1 in a stable state of mummification. P1 skeletonized. H2 (c) and P3 (d) from Trial 2 on day 42 post-placement. Both H2 and P3 in an advanced state of decomposition.

differences in the rate and manner of which H2, P3 and P4 progressed through the stages of decomposition (Fig. 2.2), with the exception of H2, which did not exhibit signs of the bloat stage. By day 42 post-placement, H2, P3 and P4 had reached an advanced state of decomposition with a large portion of soft tissue exhibiting signs of mummification (Fig. 2.3c and d). Overall, visual differences between the pigs and humans were evident. This occurred in both seasons, with the human not experiencing bloat in winter. However, the differences were a lot more pronounced in summer.

2.3.3. Textile Analysis

The textile control specimens remained intact until the completion of each trial with moderate discoloration. The IR bands of interest attributed to post-mortem lipids were not visually observed in any of the control specimens throughout the duration of the trials. In contrast, the experimental samples showed considerable visual discoloration as the decomposition fluids were released from decomposing remains and absorbed into the textiles.

2.3.4. Functional Principal Component Analysis (FPCA)

Trial 1

The results from the FPCA for Trial 1 (Fig. 2.4a) were consistent with visual observations in the field for H1, P1 and P2. The fresh sampling days for both species (0, 3 and 7 post-placement) demonstrated a clustering toward the positive portion of functional principal component 1 (FPC-1) and the negative portion of FPC-2 (Fig. 2.4 b). The data for day 10 post-placement from H1 was projected onto the negative portion of FPC-1 and FPC-2, clearly distinguished from P1 and P2 day 10 post-placement which were projected onto the positive portion of FPC-1 and the negative portion of FPC-2. This trend was observed for the remainder of the data for Trial 1, with the data from the human (H1) being distinctly different from the pigs (P1 and P2). This provides preliminary evidence that the data obtained between humans and pigs for Trial 1 are not consistent, indicating interspecies differences.

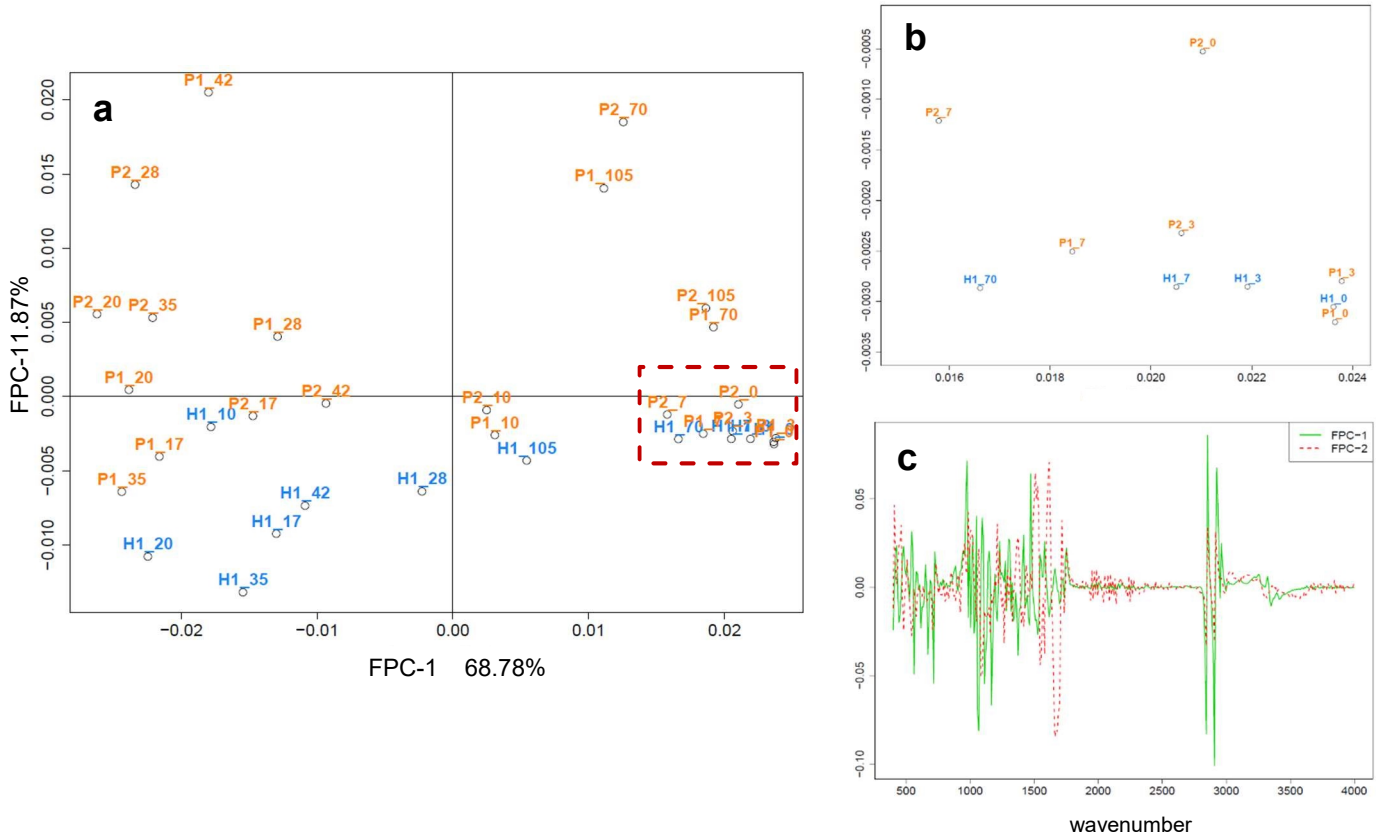

Fig. 2. 4 Functional principal component analysis (FPCA) of the processed correlation matrix for H1, P1 and P2 of Trial 1. Each data point represents the averaged triplicate function for each day post-placement. The red dashed box in a) represents expanded portion displayed in b). Loadings plot of the eigenfunctions c) of the processed correlation matrix for Trial 2 for FPC-1 and FPC-2 that captures 80.65% of the variation. The x-axis represents the wavenumber (cm^{-1}).

The separation and groupings projected in the FPCA (Fig. 2.4a) can be explained by the eigenfunctions in the loadings plot (Fig. 2.4c). It is clear that the carbonyl region pertaining to the 1710 cm^{-1}, 1720 cm^{-1} and 1745 cm^{-1} bands were responsible for the vertical spread of the data along FPC-2 (Fig. 2.4c). In contrast, it appeared that the C-H stretching band 2920 cm^{-1} was responsible for majority of the dispersion in the data along FPC-1 (Fig. 2.4c). During the decomposition process, the post-mortem lipids breakdown from larger triacylglycerols (~1745 cm^{-1}) and release smaller free fatty acids (~1710 cm^{-1}) into the immediate environment, explaining this dispersion. The data shown in Fig. 2.4a between day 10 and 42 post-placement corresponds to this pattern of lipid breakdown and provides evidence that this information is being effectively captured in the associated textile samples collected in-field (Fig. 2.4c).

The data obtained from the final two sampling days (70 and 105 post-placement) from both pig and human were more closely related to the initial cluster (Fig. 2.4b) than the rest of the data. This is likely due to a lower relative amount of post-mortem lipids present in the textile samples collected on those days. The loadings plot (Fig. 2.4c) demonstrated that this trend is due to the data from days 70 and 105 post-placement for H1, P1 and P2 containing lower relative amounts of the ~2920 cm^{-1} band corresponding to CH_2 asymmetrical stretching of the methylene chain, similar to the data obtained from the earlier days (Fig 2.4b). In addition, the loadings plot (Fig. 2.4c) revealed that the data obtained from P1 and P2 for days 70 and 105 post-placement contained higher relative amounts of the ~1540 cm^{-1} and ~1575 cm^{-1} bands corresponding to the C-O stretching from carboxylate bands of fatty acid salts. The ~1710 cm^{-1} band relates to the C=O stretch of free fatty acids and

the lower relative amounts of the ~1745 cm^{-1} band is consistent with the decreased C=O stretch of triacylglycerols.

The data obtained from day 105 post-placement for H1 was grouping with the data obtained from day 10 post-placement from both P1 and P2 in the positive portion of FPC-1 and the negative portion of FPC-2. This correlates to the visual trends observed in-field, as the pigs decomposed at a much more accelerated rate than the human. This grouping provides further preliminary evidence to support the fact that there are considerable interspecies differences, particularly in respect to the decomposition timeline.

Trial 2

The FPCA for Trial 2 (Fig. 2.5a) is also congruent with the visual observations that were made in-field for H2, P3 and P4 with respect to the stages of decomposition. When compared to Trial 1, the data for both human and pigs were more closely related for the early decomposition period (Fig. 2.5b). Due to the lower temperatures observed (compared to Trial 1), there was a delay in the initial onset of visual decomposition from fresh into bloat, or active for both species. This was apparent with the large clustering toward the positive portion of FPC-1 and the negative portion of FPC-2 (Fig. 2.5b) that captured data from day 0 up until approximately day 31 post-placement for both species. This is considerably different to what was seen in Trial 1 (Fig. 2.4b) for H1, P1 and P2, as the early grouping only contained data from days 0 to 3 post-placement. Again, this is likely attributed to the warmer temperatures during the summer Trial 1.

In contrast to Trial 1, the data from the last sampling day (105 post-placement) was clearly distinguishable from the early cluster, with obvious differences in the data obtained from H2 projected in the negative portion of FPC-1 and the positive portion of FPC-2, and P3 projected in the negative portion of both FPC-1 and FPC-2. Overall, the patterns in the FPCAs demonstrate clear interspecies differences, particularly for the data obtained during the later decomposition period.

Several studies have demonstrated the benefit of chemometric analysis via ordinary PCA for IR data [22, 23, 33]. However, as previously mentioned, the application of ordinary PCA for functional data has its limitations [31, 34]. The results of the current study demonstrate the successful application and interpretation of FPCAs for functional IR data. Overall, the loadings plot from the FPCAs of Trial 1 and Trial 2 (Fig. 2.4c and 2.5c) revealed six IR bands of interest for further statistical investigation: ~1540 $cm^{-1,}$ ~1575 cm^{-1}, ~1710 cm^{-1}, ~1720 cm^{-1}, ~1745 cm^{-1} and ~2920 cm^{-1}.

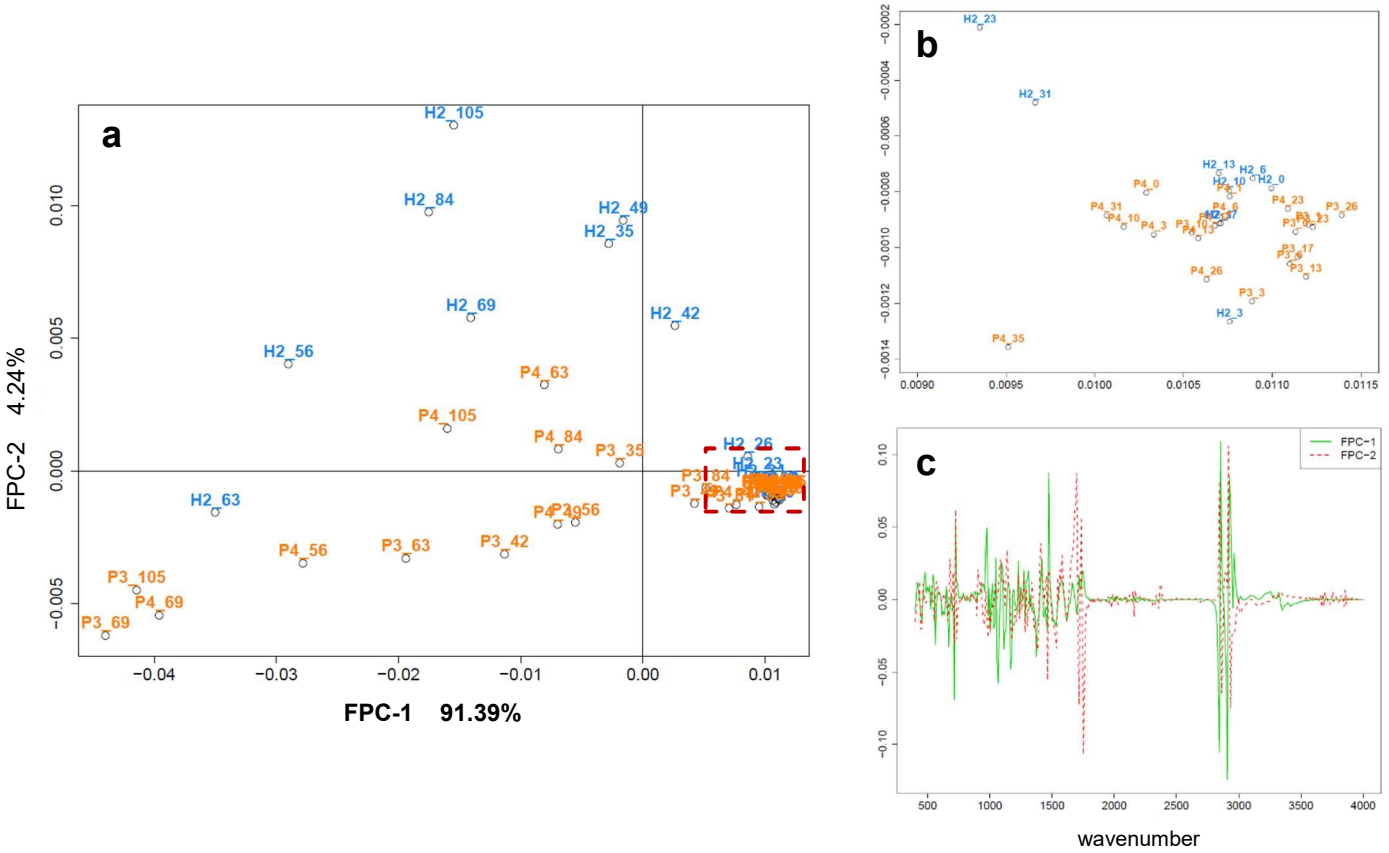

Fig. 2. 5 *Functional principal component analysis (FPCA) of the processed correlation matrix for H2, P3 and P4 of Trial 2. Each data point represents the averaged triplicate function for each day post-placement. The red dashed box in a) represents expanded portion displayed in b). Loadings plot of the eigenfunctions c) of the processed correlation matrix for Trial 1 for FPC-1 and FPC-2 that captures 95.63% of the variation. The x-axis represents the wavenumber (cm^{-1}).*

2.3.5. Semi-parametric regression modelling

In order to further investigate the post-mortem lipid interspecies differences, semi-parametric regression models were fitted. These models were applied to five different band ratios: ~1540 cm^{-1}/ ~2920cm^{-1}, ~1575 cm^{-1} / ~2920 cm^{-1}, ~1710 cm^{-1} /~2920 cm^{-1}, ~1720 cm^{-1} /~2920 cm^{-1} and ~1745 cm^{-1} / ~2920 cm^{-1} on a time-dependent scale (day post-placement). The ~2920 cm^{-1} C-H stretching band was selected as the normalisation factor as per Ueland et al. 2015 [23] and supported by Stuart et al. 2005 [46]. For each ratio and donor or pig, the model parameter estimates were used to produce a continuous ratio mean estimate over time and its 95% confidence bands. The residual scatter plots from the semi-parametric regressions (Figures 2. S10 and 2. S11) show that the residuals are overall randomly distributed, which confirms that the selected model fits the data in most cases. However, in some cases, such as (Figure 2. S10 h), extreme values, as seen on day 35 post-placement for the ratio ~1710/2920 cm^{-1} are not well captured by the models.

Trial 1

The mean daily ratios of the post-mortem lipid bands for H1 (Fig. 2.6a, d, g, j, and m) all exhibited a spike in relative absorbance within the first 20 days post-placement, except for ~1710 cm^{-1}/~2920 cm^{-1}, which peaked at approximately day 40 post-placement. In contrast, the models for P1 (Fig. 2.6b, e, h, k, n) and P2 (Fig. 2.6c, f, i, l, o) did not exhibit this spike during the early period and were generally more stable over the decomposition timeline than H1. This was most pronounced when comparing the free fatty acid ratio ~1710 cm^{-1}/~2920 cm^{-1} between species (Fig. .2.6g – i). The ratios corresponding to the carboxylate bands of the fatty acid salts ~1540 cm^{-1}/~2920 cm^{-1} and ~1575 cm^{-1}/~2920 cm^{-1} demonstrated the most contrasting

results between species. The mean of the underlying process of the relative absorbance for H1 for the carboxylate bands did not exceed 0.6 (Fig. 2.6a and d), whereas the mean of the underlying process of the relative absorbance for P1 (Fig. 2.6b and e) and P2 (Fig. 2.6c and f) far exceeded 0.6 by the final sampling day (105 post-placement). The presence of the ~1540 cm^{-1}/~2920 cm^{-1} and ~1575 cm^{-1}/~2920 cm^{-1} bands are indicative of adipocere formation, which is known to be a late-stage decomposition product [21, 46, 47]. This product is a waxy substance formed by the hydrolysis and hydrogenation of adipose tissues [46, 47]. The results of the semi-parametric regression models provided evidence to support the formation of adipocere during the early stages of decomposition for P1 (Fig. 2.6b and e) and P2 (Fig. 2.6c and f) which continued to increase over the decomposition timeline. In contrast to the semi-parametric regression models for H1 (Fig. 2.6a and d) which provided poor evidence of this same finding.

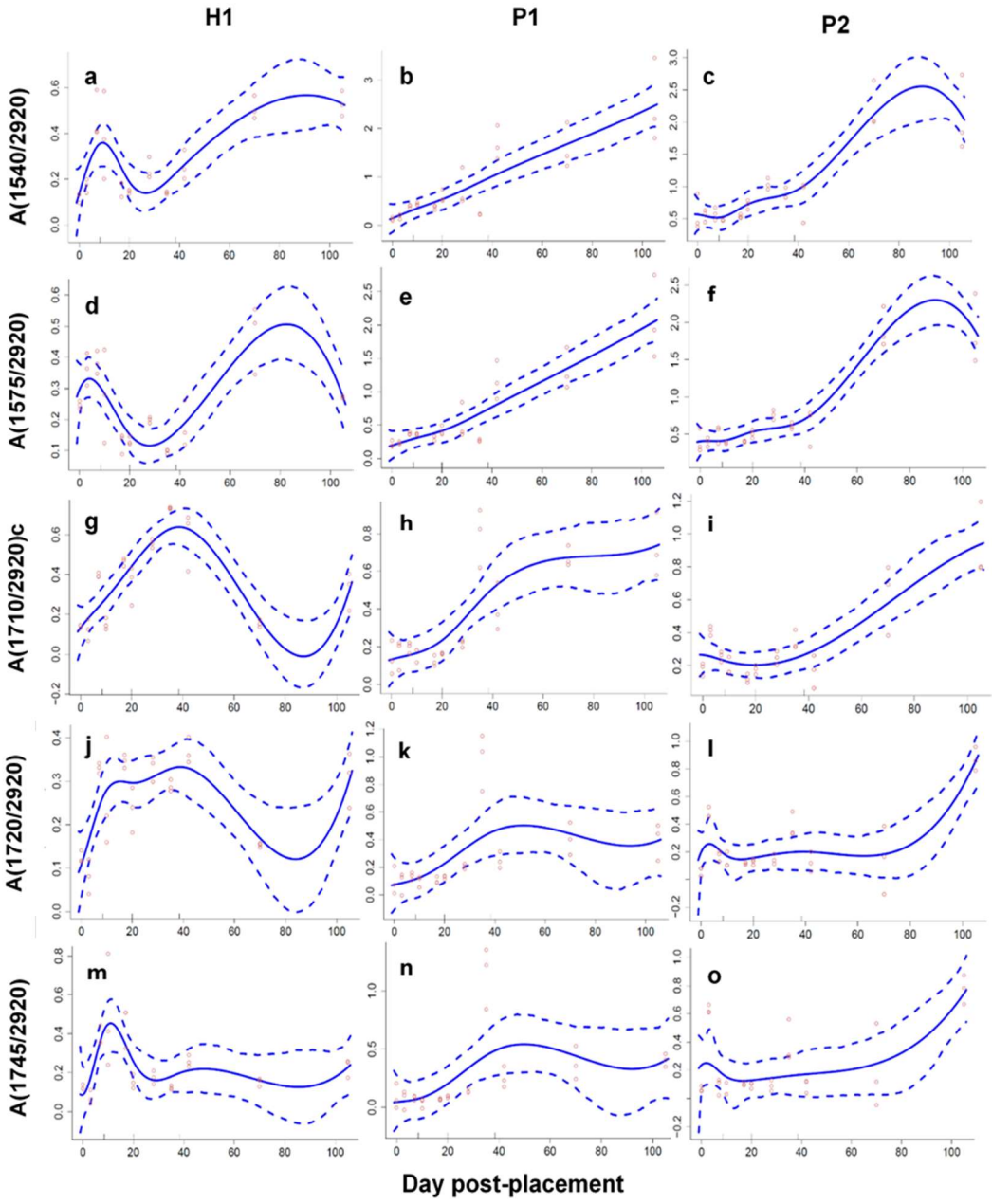

Fig. 2. 6 Semi-parametric regression models for Trial 1 of the five normalised post-mortem lipid ratios: ~1540 cm^{-1}/~2920cm^{-1}, ~1575 cm^{-1}/~2920 cm^{-1}, ~1710 cm^{-1}/~2920 cm^{-1}, ~1720 cm^{-1}/~2920 cm^{-1} and ~1745 cm^{-1}/~2920 cm^{-1}. The y-axis represents the normalised absorbance values, and the x-axis represents the sample period (days post-placement). The red circles represent the normalised absorbance values per sampling day. The solid blue line represents the daily mean of the underlying process, and the dashed blue lines represent the 95% confidence bands.

Trial 2

In contrast to Trial 1, the mean of the underlying process for the carboxylate bands of fatty acid salts ~1540 cm^{-1} /~2920 cm^{-1} and ~1575 cm^{-1} /~2920 cm^{-1} showed a general decreasing trend for Trial 2 (Fig. 2.7a – f), particularly for H2 (Fig. 2.7a and d). The models for the formation of free fatty acids ~1710 cm^{-1} /~2920 cm^{-1} over the decomposition timeline for H2 (Fig. 2.7g) and P4 (Fig. 2.7i) were more similar to each other than P3 (Fig. 2.7h), with a clear increasing trend over the decomposition timeline. The semi-parametric regression model of the free fatty acid band, ~1710 cm^{-1} /~2920 cm^{-1}, for P3 (Fig. 2.7h) spiked within the first few days, providing evidence of post-mortem lipid degradation from triacylglycerols to free fatty acids during the early period. Additionally, there was an increase in the release of triacylglycerols, ~1745 cm^{-1} / ~2920 cm^{-1}, into the textiles for H2 (Fig. 2.7m) around day 40 post-placement which was not observed for P3 or P4. This is likely due to differences in the rate and manner of decomposition between species.

The results of the semi-parametric regression models of the normalised post-mortem lipid bands for Trial 1 and Trial 2 clearly indicate interspecies differences over the decomposition period, particularly for the carboxylate bands of fatty acid salts attributed to the formation of adipocere.

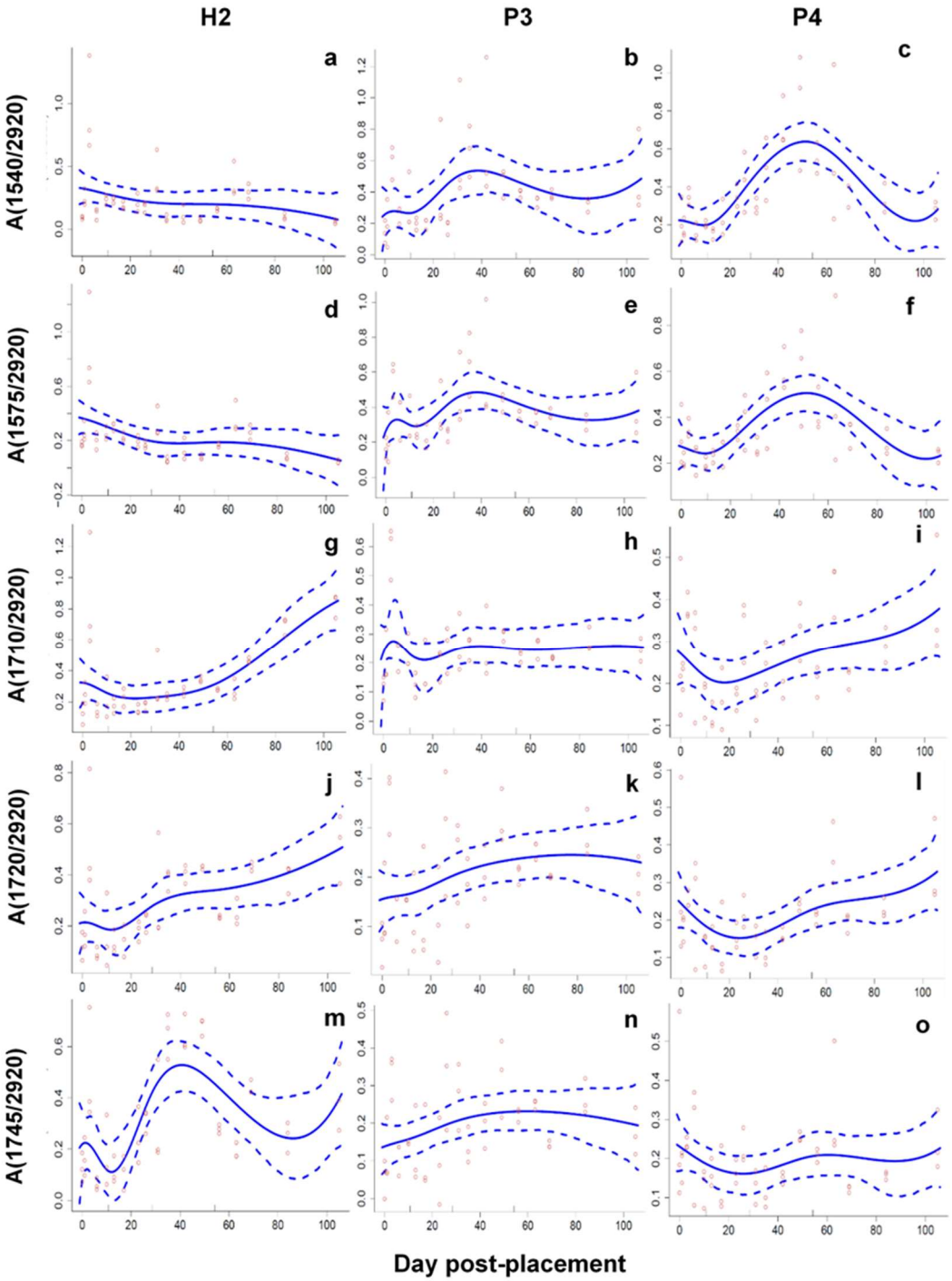

Fig. 2. 7 Semi-parametric regression models for Trial 2 of the five normalised post-mortem lipid ratios: ~1540 cm^{-1}/~2920cm^{-1}, ~1575 cm^{-1}/~2920 cm^{-1}, ~1710 cm^{-1}/~2920 cm^{-1}, ~1720 cm^{-1}/~2920 cm^{-1} and ~1745 cm^{-1}/~2920 cm^{-1}. The y-axis represents the normalised absorbance values, and the x-axis represents the sample period (days post-placement). The red circles represent the normalised absorbance values per sampling day. The solid blue line represents the daily mean of the underlying process, and the dashed blue lines represent the 95% confidence bands.

2.3.6. Analysis of Variance (ANOVA)

One-way ANOVA was performed on the daily averaged normalised ratios (Table 2. S3) used in the semi-parametric regression modelling to statistically assess the mean differences between species groups (human or pig) within each trial. Statistically significant results were obtained between the two species for Trial 1 and Trial 2 for the ratios corresponding to carboxylate bands of the fatty acids ~1540/2920 and ~1575/2920 (Table 2. S3). Post-hoc tests revealed that the statistically significant differences for Trial 1 were between H1 and P1, H1 and P2 and not between P1 and P2 (Table 2. S3). Similarly, the post-hoc tests for Trial 2 showed statistically significant differences between H2 and P3, H2 and P4 and not between P3 and P4. The results of these tests provide strong evidence to support the fact that pigs and humans decompose incongruously as the post-mortem lipids collected in textiles demonstrate clear significant differences.

2.4. Conclusions

The current study has demonstrated the successful application of FPCA to IR data as a dimensionality reduction tool, to reveal underlying patterns in the data collected from cotton textiles associated with decomposing human and pig remains. The FPCA results indicated that post-mortem lipids collected in cotton textiles were the primary influence on the variability within the datasets. In addition, the separation and groupings projected in the FPCAs could be directly correlated to both the visual in-field observations and environmental data recorded.

The application of regression modelling was also explored in this study through the use of semi-parametric regression models of normalised post-mortem lipid bands

to obtain the mean of the underlying process using Markov chain Monte Carlo (MCMC). The results from these models clearly indicate interspecies differences between pigs and humans over the decomposition period, particularly for the carboxylate bands of fatty acid salts attributed to the presence of adipocere. The results from these models also provided sufficient evidence to support the use of normalised lipid ratios to monitor the chemical decomposition on a time-dependent scale. With further studies and an expansion of the current database, these models provide the potential application for casework where unknown textile evidence is yielded. In a forensic context, this could prove to be a useful tool for determining a relative post-mortem interval period, a vital aspect of complex death investigations [1].

Further statistical analysis of the averaged normalised post-mortem lipids bands was conducted via one-way ANOVA. These tests revealed statistically significant interspecies differences for the summer Trial 1 and the winter Trial 2 for the normalised ratios corresponding to the C-O stretch of the carboxylate bands of fatty acid salts at ~1540 cm^{-1}/~2920 cm^{-1} and ~1575 cm^{-1}/~2920 cm^{-1}. No other normalised ratios for Trial 1 or Trial 2 revealed statistically significant results. These findings provide strong evidence to question the suitability of pigs as human analogues for taphonomic investigation as the lipid contents of the adipose tissues are not consistent between species over the decomposition period.

Overall, the results of this study provide preliminary evidence that pigs are not statistically interchangeable analogues for human decomposition with respect to post-mortem lipids collected in textiles in an Australian summer or winter season. It is important to recognise that there were several uncontrollable and systematic

differences between the pigs and humans used in each trial including age, sex, cause of death and mass which could have influenced the findings. Such factors are difficult to control when conducting decomposition studies including human donors. Recommendations for future investigations include further comparative studies to adequately assess the influence of these systematic differences with an increased sample size. In addition, it is advised that future work incorporate a direct comparison between classical PCA and FPCA to provide an insight to the benefits of using FPCA over the classical approach.

The assessment of different textile types to determine the universality of this method is also suggested. In particular, synthetic varieties such as polyester, which contains a sharp ester band in the carbonyl region of the infrared spectrum, would likely impact the investigation of the free fatty acids and triacylglycerols at ~1710 and ~1745 cm^{-1} [22, 33].

2.5. References

[1] S.L. Forbes, Time since death: a novel approach to dating skeletal remains, Aust. J. Forensic Sci., 36 (2004) 67-72. https://doi.org/10.1080/00450610409410599.

[2] E.R. Hyde, D.P. Haarmann, A.M. Lynne, S.R. Bucheli, J.F. Petrosino, The living dead: bacterial community structure of a cadaver at the onset and end of the bloat stage of decomposition, PLoS ONE 8, (2013). https://doi.org/10.1371/journal.pone.0077733

[3] M.A. Iqbal, M. Ueland, S.L. Forbes, Recent advances in the estimation of post-mortem interval in forensic taphonomy, Aust. J. Forensic Sci., 52 (2020) 107-123. https://doi.org/10.1080/00450618.2018.1459840

[4] B.H. Stuart, Decomposition chemistry: overview, analysis, and interpretation, in: J.A Siegel, P.J. Saukko, M.M. Houck, (Eds.), Encyclopedia of Forensic Sciences, second ed., Academic Press, 2013, pp. 11–15.

[5] J.A. Payne, A summer carrion study of the baby pig Sus Scrofa Linnaeus, Ecology. 46 (1965) 592-602. https://doi-org.ezproxy.lib.uts.edu.au/10.2307/1934999

[6] A.A. Vass, S-A. Barshick, G. Sega, J. Carlton, J. Love, J. Synstelien, Decomposition chemistry of human remains: a new methodology for determining the postmortem interval, J. Forensic Sci., 47 (2002) 542-553. https://doi.org/10.1520/JFS15294J

[7] H.J. Rothkotter, Anatomical particularities of the porcine immune system--a physician's view, Dev. Comp. Immunol., 33 (2009) 267-272. https://doi.org/10.1016/j.dci.2008.06.016

[8] F. Meurens, A. Summerfield, H. Nauwynch, L. Saif, V. Gerdts, The pig: a model for human infectious diseases, Trends Microbiol., 20 (2012) 50-57. https://doi.org/10.1016/j.tim.2011.11.002

[9] K.H. Mair, C. Sedlak, T. Käser, A. Pasternak, B. Levast, W. Gerner, A. Saalmüller, A. Summerfield, V. Gerdts, H.L. Wilson, F. Meurens, The porcine innate immune system: an update, Dev. Comp. Immunol., 45 (2014) 321-343. https://doi.org/10.1016/j.dci.2014.03.022

[10] S. Matuszewski, M.J.R. Hall, G. Moreau, K.G. Schoenly, A.M. Tarone, M.H. Villet, Pigs vs people: the use of pigs as analogues for humans in forensic entomology and taphonomy research, Int. J. Legal Med., 134 (2020) 793-810. https://doi.org/10.1007/s00414-019-02074-5

[11] S.J. Notter, B.H. Stuart, R. Rowe, N. Langlois, The initial changes of fat deposits during the decomposition of human and pig remains, J. Forensic Sci., 54 (2009) 195-201. https://doi.org/10.1111/j.1556-4029.2008.00911.x

[12] Z. Knobel, M. Ueland, K.D. Nizio, D. Patel, S.L. Forbes, A comparison of human and pig decomposition rates and odour profiles in an Australian environment, Aust. J. Forensic Sci., 51(2019) 557-572. https://doi.org/10.1080/00450618.2018.1439100

[13] B.M. Dawson, P.S. Barton, J.F. Wallman, Contrasting insect activity and decomposition of pigs and humans in an Australian environment: A preliminary study, Forensic Sci. Int., 316 (2020) 110515. https://doi.org/10.1016/j.forsciint.2020.110515

[14] Y. Wang, M.Y. Ma, X.Y. Jiang, J.F. Wang, L.L. Li, X.J. Yin, M. Wang, Y. Lai, L.Y. Tao, Insect succession on remains of human and animals in Shenzhen, China, Forensic Sci. Int., 271 (2017) 75-86. https://doi.org/10.1016/j.forsciint.2016.12.032

[15] K. Schoenly, N. Haskell, D. Mills, C. Bieme-Ndi, K. Larsen, Y. Lee, Recreating death's acre in the school yard: using pig carcasses as model corpses, to teach concepts of forensic entomology & ecological succession, Am Biol Teach., 68 (2006) 402-410. https://doi.org/10.2307/4452028

[16] A. Whitaker, Development of blowflies (Diptera: Calliphoridae) on pig and human cadavers: implications for forensic entomology casework, Doctoral dissertation, King's College London (University of London), 2014.

[17] K.L. Stokes, S.L. Forbes, M. Tibbett, Human versus animal: contrasting decomposition dynamics of mammalian analogues in experimental taphonomy, J. Forensic Sci., 58 (2013) 583-91. https://doi.org/10.1111/1556-4029.12115

[18] J.M. DeBruyn, K.M. Hoeland, L.S. Taylor, J.D. Stevens, M.A. Moats, S. Bandopadhyay, S.P. Dearth, H.F. Castro, K.K. Hewitt, S.R. Campagna, A.M. Dautartas, G.M. Vidoli, A.Z.

Mundorff, D.W. Steadman, Comparative decomposition of humans and pigs: soil biogeochemistry, microbial activity and metabolomic profiles, Front. Microbiol., 11 (2021) 608856. https://doi.org/10.3389/fmicb.2020.608856

[19] M. Connor, C. Baigent, E.S. Hansen, Testing the use of pigs as human proxies in decomposition studies, J. Forensic Sci., 63 (2018) 1350-1355. https://doi.org/10.1111/1556-4029.13727

[20] A. Dautartas, M.W. Kenyhercz, G.M. Vidoli, L. Meadows Jantz, A. Mundorff, D.W. Steadman, Differential decomposition among pig, rabbit, and human remains, J. Forensic Sci., 63 (2018) 1673-1683. https://doi.org/10.1111/1556-4029.13784

[21] S. Collins, B.H. Stuart, M. Ueland, Monitoring human decomposition products collected in clothing: an infrared spectroscopy study, Aust. J. Forensic Sci., 52 (2020) 428-438. https://doi.org/10.1080/00450618.2019.1593504

[22] S. Collins, B.H. Stuart, M. Ueland. Anatomical location dependence of human decomposition products in clothing, Aust. J. Forensic Sci., 55 (2023) 363-375. https://doi.org/10.1080/00450618.2021.1981443

[23] M. Ueland, K.D. Nizio, S.L. Forbes, B.H. Stuart, The interactive effect of the degradation of cotton clothing and decomposition fluid production associated with decaying remains, Forensic Sci. Int., 255 (2015) 56-63. https://doi.org/10.1016/j.forsciint.2015.05.029

[24] F. Zapata, M.Á.F. de la Ossa, C. García-Ruiz, Differentiation of body fluid stains on fabrics using external reflection Fourier transform infrared spectroscopy (FT-IR) and chemometrics, Appl. Spectrosc., 70 (2016) 654-665. https://doi.org/10.1177/0003702816631303

[25] M. Ueland, S. Collins, L. Maestrini, S.L. Forbes, S. Luong, Fresh vs. frozen human decomposition – A preliminary investigation of lipid degradation products as biomarkers of post-mortem interval, Forensic Chem., 24 (2021) 100335. https://doi.org/10.1016/j.forc.2021.100335

[26] G. Eglington, G.A. Logan, R. P. Ambler, J.J Boon, W. R. K. Perizonius, Molecular preservation [and discussion], Philos. Trans. R. Soc. Lond., B, Biol. Sci., 333 (1991), 315-328. https://www.jstor.org/stable/55419

[27] S. Meeuwsen, G.W. Horgan, M. Elia, The relationship between BMI and percent body fat, measured by bioelectrical impedance, in a large adult sample is curvilinear and influenced by age and sex, Clin. Nutr., 29 (2010) 560-566. https://doi.org/10.1016/j.clnu.2009.12.011

[28] K.L. Miles, D.A. Finaughty, V.E. Gibbon, A review of experimental design in forensic taphonomy: moving towards forensic realism, Forensic Sci. Res., 5 (2020) 249-259. https://doi.org/10.1080/20961790.2020.1792631

[29] A. Misra, N.V. Dhurandhar, Current formula for calculating body mass index is applicable to Asian populations, Nutr. Diabetes., 9 (2019) 3. https://doi.org/10.1038/s41387-018-0070-9

[30] S. Luong, S.L. Forbes, J.F. Wallman, R.G. Roberts, Monitoring the extent of vertical and lateral movement of human decomposition products through sediment using cholesterol as a

biomarker, Forensic Sci. Int., 285 (2018) 93-104. https://doi.org/10.1016/j.forsciint.2018.01.026

[31] R. Viviani, G. Grön, M. Spitzer, Functional principal component analysis of fMRI data: Functional PCA of fMRI Data, Hum. Brain Mapp., 24 (2005) 109-129. https://doi.org/10.1002/hbm.20074

[32] H. Abdi, L.J. Williams, Principal component analysis, Wiley Interdiscip. Rev. Comput. Stat. 2 (2010) 433-459. https://doi.org/10.1002/wics.101

[33] M. Ueland, J.M. Howes, S.L. Forbes, B.H. Stuart, Degradation patterns of natural and synthetic textiles on a soil surface during summer and winter seasons studied using ATR-FTIR spectroscopy, Spectrochim. Acta A Mol. Biomol., 185 (2017) 69-76. https://doi.org/10.1016/j.saa.2017.05.044

[34] C. Hernández-Murillo, S. García, P. Fernández, Matthieu Ménager, M.L. Montero, Integrated mineralogical and typological study of Axe-God pendants from the Jade and pre-Columbian Culture Museum in Costa Rica. Cuadernos de Antropología,31 (2021) 1-17. 10.15517/cat.v31i1.47146

[35] H.L. Shang, A survey of functional principal component analysis. AStA Adv Stat Anal., 98 (2014) 121-142. https://doi-org.ezproxy.lib.uts.edu.au/10.1007/s10182-013-0213-1

[36] R. Burfield, C. Neumann, C.P. Saunders, Review and application of functional data analysis to chemical data—The example of the comparison, classification, and database search of forensic ink chromatograms, Chemom. Intell. Lab. Syst., 149 (2015) 91-106. https://doi.org/10.1016/j.chemolab.2015.07.006

[37] M. Febrero-Bande, M.O. de la Fuente, Statistical computing in functional data analysis: the R package fda.usc., J. Stat. Softw., 51 (2012) 1-28. https://doi.org/10.18637/jss.v051.i04

[38] M.S. Fahelelbom Khairi, A. Saleh, R. Mansour, S. Sadik, First derivative ATR-FTIR spectroscopic method as a green tool for the quantitative determination of diclofenac sodium tablets, F1000Research, 9 (2020). https://doi.org/10.12688/f1000research.22274.2

[39] B. Zimmermann, A. Kohler, Optimizing Savitzky-Golay parameters for improving spectral resolution and quantification in infrared spectroscopy, Appl. Spectrosc., 67 (2013) 892-902. https://doi.org/10.1366/12-06723

[40] O.E. Adedipe, T.A. Jacot, A.R. Thurman, G.F. Doncel, M.R. Clark, Rapid measures of user's adherence to vaginal drug products using attenuated total reflectance Fourier transform infrared spectroscopy (ATR-FTIR) and multivariate discriminant techniques, PLoS ONE 1, (2018) e0197906. https://doi.org/10.1371/journal.pone.0197906

[41] Rstudio Team, R: A language and environment for statistical computing, R Core Team, R Foundation for Statistical Computing, Vienna, Austria, 2021.

[42] A. Gajardo, C. Carroll, Y. Chen, X. Dai, J. Fan, P. Z. Hadjipantelis, K. Han, H. Ji, H. Mueller, J. Wang, fdapace: Functional Data Analysis and Empirical Dynamics, (R package version 0.5.7), 2021.

[43] D. Ruppert, M.P. Wand, R.J. Carroll, Semiparametric Regression, Cambridge University Press, Cambridge, 2003.

[44] J. Fox, S. Weisberg, An R Companion to Applied Regression, Third edition, Sage, Thousand Oaks, 2019.

[45] C. von Hoermann, J. Ruther, S. Reibe, B. Madea, M. Ayasse, The importance of carcass volatiles as attractants for the hide beetle Dermestes maculatus (De Geer), Forensic Sci. Int., 212 (2011) 173-179. https://doi.org/10.1016/j.forsciint.2011.06.009

[46] B.H. Stuart, S. Forbes, B.B. Dent, G. Hodgson, Studies of adipocere using diffuse reflectance infrared spectroscopy, Vib. Spectrosc., 24 (2000) 233-242. https://doi.org/10.1016/S0924-2031(00)00097-7

[47] B.H. Stuart, L. Craft, S.L. Forbes, B.B. Dent, Studies of adipocere using attenuated total reflectance infrared spectroscopy, Forensic Sci. Med. Pathol., 1(3) (2005) 197-201. https://doi.org/10.1385/FSMP:1:3:197

Chapter 3: The development and adaptation of an analytical chemical method for the extraction and detection of post-mortem lipids collected in textiles associated with decomposing human remains using GC-MS/MS.

Chapter 3: The development and adaptation of an analytical chemical method for the extraction and detection of post-mortem lipids collected in textiles associated with decomposing human remains using GC-MS/MS.

i. Preface

With the exception of minor editorial changes and the addition of extraction efficiency results, Chapter 3 reproduces part of the following research article; **S. Collins,** B.H. Stuart, M Ueland, (2023). The use of lipids from textiles as soft-tissue biomarkers of human decomposition. Forensic Science International, 111547. https://doi.org/10.1016/j.forsciint.2022. Permissions for reuse of this article within this dissertation have been obtained.

ii. Statement of Contribution and Declaration

Sharni Collins: conceptulisation; methodology; formal analysis; investigation; writing – original draft; writing - review and editing; Barbara Stuart: conceptulisation; methodology; writing – review and editing; supervision; Maiken Ueland: conceptulisation; methodology; writing – review and editing; supervision.

Graduate research student

Production Note:
Signature removed
prior to publication.

Sharni Collins

Principal Supervisor

Production Note:
Signature removed
prior to publication.

Dr. Maiken Ueland

Co-supervisor

Production Note:
Signature removed
prior to publication.

Professor Barbara Stuart

3.1. Introduction

Lipid analysis is an emerging area of research in forensic taphonomy [1-6] and it is used to better understand the complex processes involved in human decomposition chemistry. By pursuing soft-tissue biomarkers, such as lipids, researchers are able to monitor the microstructural changes that occur during the disintegration of human remains [5-7]. This allows for the identification of patterns that are related to the decomposition processes. The documentation and analysis of such patterns furthers the impact of taphonomic research by allowing longitudinal information to be recorded. This longitudinal information can provide the opportunity to make measurable predictions which could then be applied in real forensic casework involving human remains. This could aid in the vital determination of time since death, which still presents as a major challenge to law enforcement [8].

A recent study by Ueland et al. in 2021 [5] demonstrated the successful adaptation of an analytical chemical method for the analysis of lipids in decomposing human tissue samples. This study was the first of its kind that utilised a targeted gas chromatography (GC) coupled with tandem mass spectrometry (MS/MS) method originally developed for the analysis of archaeological samples [9], for the analysis of post-mortem lipids in decomposition samples. Other work by Ueland et al. [4] has revealed the ability to indirectly monitor decomposition through the extraction and detection of post-mortem lipids collected in textiles, using a non-targeted gas chromatography – mass spectrometry (GC-MS) method.

In the previous chapter, post-mortem lipids collected in textiles were analysed using attenuated total reflectance (ATR) – Fourier transform infrared (FTIR)

spectroscopy to assess interspecies differences between pigs and humans [10]. The results of this study provided further evidence to support the use of post-mortem lipids collected in textiles for investigating the complex processes of decomposition. The patterns that emerged in the degradation of the post-mortem lipids in that study could be related not only to species, but also to the decomposition timeline [10]. Despite the major advantages that accompany the use of a non-destructive ATR-FTIR technique in a forensic context, the method used in the previous chapter did not allow for a more specific analysis of the lipid profiles that are associated with species or the decomposition timeline.

Therefore, the aim of this chapter was to develop and optimise a novel analytical chemical workflow for the targeted analysis of post-mortem lipids in textiles using GC-MS/MS. Using methods adapted from Ueland et al. [5] and Luong et al. [9], this chapter details the processes of extraction, separation, detection and analysis of post-mortem lipids in textiles. In addition, this chapter also reports and discusses novel information regarding the complex challenges of matrix effects observed with decomposition samples.

3.2. Materials and methods

3.2.1. Field Site

The study was conducted at the Australian Facility for Taphonomic Experimental Research (AFTER), an open eucalypt woodland on the Cumberland Plain in Western Sydney, privately owned by the University of Technology, Sydney (UTS). Soils at the site are classified broadly as sandy clay loam or gravelly clay, with a pH range from 5.5 – 6.5 [11].

3.2.2. Experimental Design

Human cadavers were received through the UTS Body Donation Program, with consent provided by each donor in accordance with the NSW Anatomy Act (1977). Ethics approval was provided by the UTS Human Research Ethics Committee (HREC ETH18-2999). None of the human donors involved in these taphonomic experiments were treated with any chemicals prior to placement at the facility and were allowed to decompose naturally.

For the purpose of method development and optimisation in the current study, textile samples were obtained on day 0 and day 84 post-placement from an 86-year-old male (H2) with a height of 174 cm and weight of 63 kg, giving a body mass index (BMI) [12] of 20.8. Prior to placement, the donor was clothed in a 100% white cotton t-shirt and placed in the centre of a 5 m x 5 m plot, directly on the soil surface in a supine position. A wire mesh cage was placed over the donor to ensure prevention of vertebrate scavenging whilst not impeding entomological succession. An environmental control site was also created at the same time point with identically sourced clothing. Each control site is erected in a clean zone of the facility to ensure that no decomposition fluids contaminated the sample.

3.2.3. Textile Matrix

The textile matrix used in this study consisted of a plain white cotton t-shirt (Anko, Kmart, Australia) composed of 100% viscose and cotton. The textiles were not washed or cleaned prior to placement or analysis so as to acquire a baseline lipid profile of the store-bought textiles.

3.2.4. Sample Collection

Textile samples were collected using sterilised scissors. Each textile sample was photographed in-situ prior to collection and individually packaged in paper envelopes and stored in a cooler box for transportation to the laboratory, where the samples were kept at -18 °C when not in use. Each sample was dried in a fume cupboard at ambient temperature to inhibit bacterial and fungal growth, with adhering soil, hair and tissue removed. Samples selected for this study represent the fresh stage of decomposition (day 0 post-placement) (Fig. 3.1a) and the advanced stage of decomposition (day 84 post-placement) (Fig. 3.1b). The day 0 post-placement sample was relatively clean while the day 84 post-placement sample was heavily saturated in decomposition matter. These timepoints were selected to provide representative data from contrasting decomposition samples to allow a more efficient assessment of the analytical methods across the decomposition timeline.

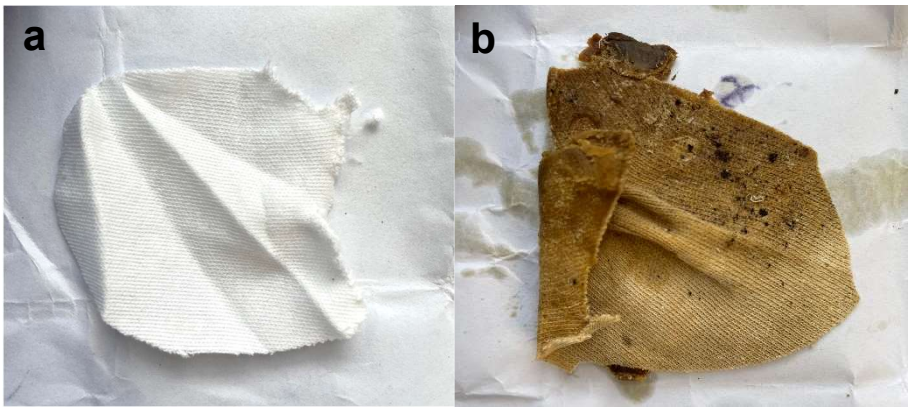

Fig. 3. 1 Visual comparison of the day 0 (a) and day 84 (b) post-placement samples.

3.2.5. GC-MS/MS instrument parameters

The instrument method and GC-MS/MS parameters were adapted from Luong et al. [9] and Ueland et al. [5]. This served as a baseline for the separation and detection of non-volatile lipid analytes. The current investigation utilised a GCMS-TQ8030 Triple Quadrupole Gas Chromatograph fitted with an AOC-20i auto injector (Shimadzu, Kyoto, Japan). Samples were injected in split mode at a temperature of 270 °C onto an Agilent HP-5MS (30 m x 0.250 mm) column with a film thickness of 0.25 µm. The initial column temperature was 80 °C and was held for 3 min before being increased at a rate of 20 °C per min, until the temperature reached 315°C. This temperature was held for 4 min. Sample flow through the column was at a rate of 1.40 mL/min. The total run time of 18.75 min was selected to enable efficient separation and detection of lighter analytes (fatty acids) and heavier analytes (sterols). After initial testing, a 6-min solvent delay was used to safeguard that majority of the solvent had passed through the system before the filament was powered on [13]. This prolonged the life of the electron multiplier and filament by preventing large amounts of solvent ions to bombard the system with each injection. Samples were analysed using GCMS RealTime Analysis (LabSolutions, Shimadzu Corporation) and data was processed using GCMS Postrun Analysis (LabSolutions, Shimadzu Corporation). Full scan mode was used to identify and obtain the chromatogram of each reference standard for optimisation purposes.

3.2.6. Selection of lipids

A suite of lipids were selected for targeted analysis in this study that included: Δ^5-sterols (cholesterol), oxysterols (25-hydroxycholesterol), stanols (coprostanol, 5α-

cholestanol), stanones (5α-cholestanone), phytosterols (stigmasterol, ergosterol, β-sitosterol), bile acids (deoxycholic acid, lithocholic acid), saturated fatty acids (arachidic acid, azelaic acid, behenic acid, decanoic acid, heneicosanoic acid, heptadecanoic acid, hexacosanoic acid, lauric acid, myristic acid, nonadecanoic acid, palmitic acid, pentadecanoic acid, sebacic acid, stearic acid, tetracosanoic acid, tricosanoic acid, tridecanoic acid), and unsaturated fatty acids (linoleic acid, oleic acid, palmitoleic acid). These lipids were selected based on their diagnostic value in context of human decomposition [2, 14-16], as well as their ability to capture a more holistic insight to the decomposition ecology. The 30 targeted lipids, along with their chemical formulae, and additional comments, are detailed in Table 3.1.

Surrogates were utilised for the purposes of method development in this chapter in the form of two deuterated standards, stearic acid-d3 for the fatty acids and cholesterol-d7 for the sterols. For all subsequent chapters, these deuterated standards were subsequently treated as internal standards and used to monitor instrument variability in addition to normalise against as quantitation was not the outcome.

Table 3. 1 Suite of 30 lipids targeted for analysis, along with their chemical formula, additional comments and references.

Name	***Chemical Formula***	***Additional Comments***
25-hydroxycholesterol	C27H46O2	Oxygenated sterol derivative of cholesterol [17]. High degradation propensity; usually found in arid environments [18, 19]. Targeted mostly in archaeological investigations.
5α-cholestanol	C27H48O	Stanol; usually produced by microbial degradation processes from sterol precursors such as β-sitosterol and cholesterol [20-22]. Used as a faecal biomarker of omnivores [23].
5α-cholestanone	C27H48	Intermediate steroidal ketone of intestinal and environmental reduction of cholesterol to produce 5α-cholestanol and coprostanol [24-26].
Arachidic Acid	C20H40O2	Major component of mammalian cell membranes [27]. Incorporated into human tissues from dietary sources [28-31]. Degradation product of behenic acid.
Azelaic Acid	C9H16O4	Dicarboxylic acid found in grains such as wheat and barley [32]. Strong antibacterial properties [33]. High amounts of this diacid are used in archaeological studies to indicate that unsaturated fatty acids have undergone oxidation [34]. Not very stable in environmental conditions due to increased solubility in water [35].
Behenic Acid	C22H44O2	Carboxylic acid, not very common in nature, mainly found in plant waxes [34].
Cholesterol	C27H46O	Common Δ^5-sterol of higher animals, found in trace amounts in eukaryotes and fungi; widespread in soils [36-38]. In soils, reduction of cholesterol leads to the production of 5α-cholestanol [21]
Coprostanol	C27H48O	Produced in the gut of higher animals due to the microbial degradation of cholesterol [21]. Used in environmental and agricultural research as a faecal biomarker [39-41]. Coprostanol is the primary 5β-stanol found in human faeces [21].
Decanoic Acid	C10H20O2	Degradation product of lauric acid.
Deoxycholic Acid	C24H40O4	Secondary bile acid formed in the intestines due to microbial action [42, 43]. Deoxycholic acid and lithocholic acid are the main bile acids found in human faeces [39].
Ergosterol	C28H44O	The main endogenous sterol found in fungi and some microalgae [44]. Can be used in soil as an indicator of living fungal biomass [45].

Heneicosanoic Acid	C21H42O2	Found in trace amounts in ruminant milk [46]. Not usually found in biological systems.
Heptadecanoic Acid	C17H34O2	Incorporated into human tissues in trace amounts from dietary intake [47]. Found particularly in ruminant fat and milk [48].
Hexacosanoic Acid	C26H52O2	In living human tissues, high amounts of hexacosanoic acid are linked to coronary artery disease [49]. Major structural component of myelin sphingolipids in eukaryotic cell membranes [50].
Lauric Acid	C12H24O2	Known component of human sweat [51, 52]. Degradation product of myristic acid.
Linoleic Acid	C18H32O2	An essential fatty acid for animals; plants can synthesise linoleic acid from oleic acid; abundant in nuts, seeds and vegetable oils [31]; a dietary fatty acid in humans. Known component of adipocere [53, 54]; it is hydrogenated to cis-12-octadecanoic (positional isomer of oleic acid) acid during the process of adipocere formation [55]. Most abundance polyunsaturated fatty acid in human diets [56].
Lithocholic Acid	C24H40O3	Secondary bile acid formed in the intestines due to microbial action [48-50]. Lithocholic acid and deoxycholic acid are the main bile acids found in human faeces [39].
Myristic Acid	C14H28O2	Component of adipocere [53, 54]. Found in small quantities in living animal and human tissues [57, 58], degradation product of palmitic acid. Component of human sweat [59].
Nonadecanoic Acid	C19H38O2	Secreted by termites [60]; a fungal metabolite [61]; a bacterial metabolite [62]
Oleic Acid	C18H34O2	Component of adipocere [53, 54] and human sweat [59]. Found in various animal and vegetable sources [63, 64]. Degradation product of linoleic acid.
Palmitic Acid	C16H32O2	Component of adipocere [53, 54] and human sweat [59]. Most common saturated fatty acid in living human tissue (20-30% of total human fatty acid content) [65]. Degradation product of palmitoleic acid.
Palmitoleic Acid	C16H30O2	One of the most abundant fatty acids in human serum and tissues [66]; component of adipocere [53, 54].
Pentadecanoic Acid	C15H30O2	Product of ruminant microbial fermentation [48]. Incorporated into human tissues in trace amounts from dietary intake [47].
Sebacic Acid	C10H18O4	Often used as a monomer for nylon, plasticisers, lubricants, cosmetics, and candles [67].
Stearic Acid	C18H36O2	Component of adipocere [53, 54] and human sweat [59]. Abundant in animal fat (up to 30%) [68]. Known background contaminant in analytical systems due to plastic labware sources [69]; textile industries react stearic acid with cellulose fibres to produce hydrophobic cotton materials [70, 71].

Stigmasterol	C29H48O	Most abundant phytosterol, plays a role in plant physiology and cell membranes [72].
Tetracosanoic Acid	C24H48O2	Major structural component of myelin sphingolipids in eukaryotic cell membranes [50]. Other sources include leaf waxes [73]
Tricosanoic Acid	C23H46O2	Found in ruminant milk and is incorporated into human tissues in trace amounts from dietary intake [74].
Tridecanoic Acid	C13H26O2	Found in ruminant milk [75]; likely incorporated into human tissues from dietary intake like pentadecanoic and heptadecanoic acids.
β-sitosterol	C29H50O	Faecal biomarker of herbivores [23].

3.2.7. Reference standards

High-performance liquid chromatography (HPLC) grade reference standards were sourced from a multitude of manufacturers and ranged in purity from ≥ 85% to ≥ 99.5%. Saturated fatty acids including: arachidic acid, behenic acid, decanoic acid, heptadecanoic acid, hexacosanoic acid, myristic acid, palmitic acid, pentadecanoic acid, stearic acid-d3, tricosanoic acid, tridecanoic acid, tetracosanoic acid and (≥ 95 - ≥ 99%) were sourced from Sigma-Aldrich (St. Louis, United States). Nonadecanoic acid and stearic acid (≥ 99.5%) were obtained from Honeywell (Sydney, Australia) while lauric acid (≥ 98%) was sourced from European Pharmacopeia (Strasbourg, France). All unsaturated fatty acids including linoleic acid, oleic acid, palmitoleic acid (≥ 98.5 - ≥ 99%) were sourced from Sigma-Aldrich (St. Louis, Missouri, United States). Dicarboxylic acids including: azelaic acid (≥ 98.5%) and sebacic acid (99%) were sourced from Fluka Analytical (Gillman, Australia) and Sigma-Aldrich (St. Louis, United States), respectively. Bile acids, deoxycholic acid (≥ 95%) and lithocholic acid (≥ 95%), were sourced from Sigma-Aldrich (St. Louis, United States). Sterols including: 25-hydroxycholesterol, 5α-cholestanone, cholesterol, ergosterol, stigmasterol, β-sitosterol and coprostanol (≥ 85 - ≥ 99%), were sourced from Sigma-Aldrich (St. Louis, United States), while cholesterol-d7 (≥ 99%), was sourced form Avanti Polar Lipids, Inc. (Alabaster, United States).

3.2.8. Chemical reagents

Acetonitrile (ACN) was obtained from RCI Labscan Ltd. (Gillman, Australia). N, O-bis (trimethylsilyl) trifluoroacetamide with 1% trimethyl-chlorosilane (TMCS) silylation reagent was purchased from United Chemical Reagents (Bristol, United

States). HPLC grade acetone (≥ 99.8%) and chloroform (≥ 99.9%) were obtained from Sigma-Aldrich (St. Louis, United States).

3.2.9. MRM optimisation

The initial method development and optimisation was carried out using standards. Reference standards were prepared at 10 ppm for identification by GC-MS/MS in full scan mode and multiple reaction monitoring (MRM) mode. Hexane was used as the solvent to prepare the liquid standards. Once prepared at 10 ppm, compounds were then analysed as outlined in the derivatisation procedure described in Section 3.2.10. Optimisation of the MS parameters were adapted from Luong et al. [9] and involved the selection of the neat lipid standards. This required careful consideration of both the specificity and abundance of the ions. The highest abundance m/z ions were generally selected as most characteristic and were then used as the precursor ions for collision induced dissociation (CID). This was conducted using the Smart MRM Optimisation Tool operating environment in LabSolutions (Shimadzu, Japan). All duplicate samples were injected in triplicates, with a single injection using full scan mode for quality control purposes and duplicate injections in MRM mode for analysis.

3.2.10. Preparation of standards for identification

Standards were prepared at 10 ppm and derivatised for identification by GC-MS/MS in full scan mode and MRM mode as described in the previous section, and retention times were recorded. The derivatisation procedure involved drying down under a gentle stream of nitrogen at 40 °C, followed by reconstitution using 40 µL

BSTFA + 1% TMCS and 10 µL acetonitrile. These were then heated at 70 °C for 30 minutes and transferring into 250 µL polymer inserts (Agilent Technologies, Australia).

3.2.11. Preparation of standards for calibration

After identification, all standards, except for stearic acid, were serially diluted from 0.5 to 8 ppm to produce a five-point calibration curve. Due to the lower detection limit of stearic acid, this analyte was prepared in concentrations ranging from 0.001 to 10 ppm. These standards were then derivatised as outlined in 3.2.10. All standards were created in duplicate, and injected on the GC-MS/MS in duplicate, with a single injection using full scan mode, giving a total of four replicate data points per concentration.

3.2.12. Investigation of lipid extraction efficiency from textiles

Textile samples associated with decomposing human remains were collected in field from the same donor (H2) on day 0 and day 84 post-placement. These samples were used to test the efficiency of extracting post-mortem lipids in textiles at contrasting decomposition time points. Duplicate textile samples were prepared using a method adapted from Ueland et al. [4], with 35 mg of textile weighed per sample. Measuring the sample by weight allowed for a more controlled, repeatable process and accounted for the increasing cumulative weight of the samples as the textiles became more saturated in decomposition fluids over time. All textile samples were spiked directly, pre-extraction, with 10 ppm of deuterated analytes, 20 uL of stearic acid-d3 and 50 uL of cholesterol-d7. Four simple monophasic extraction solvents were tested (Table 3.2) at a total extraction volume of 4 mL. In addition, four blanks were created containing a mixture of 10 ppm of stearic acid-d3 and cholesterol-d7

(with no textile matrix) using the four different solvent compositions. These blanks were used to compare the results of the experimental textile samples to calculate the extraction efficiency.

Table 3. 2 Solvent methods tested for the extraction of lipids from textiles.

Method	***Solvent (s)***	***Volume (mL)***
1 [76, 77]	Acetone	4
2 [1]	Hexane	4
3 [3, 4, 9]	Chloroform	4
4 [78, 79]	Acetone—chloroform	2:2

All samples were sonicated for 20 min without heat and refrigerated for 16 h at 4 °C. 1 mL of the sample was subsequently extracted and filtered through a 0.2 µm hydrophobic PTFE syringe filter (MicroAnalytix, NSW, Australia). 25 µL of the filtered aliquots were then derivatised as outlined in 3.2.10. All samples were extracted and injected in duplicate with the addition of a full scan injection, giving four replicate data points per sample.

3.2.13. Investigation of matrix effects

Matrix effects occur when undesired, co-eluting components alter the ionisation efficiency of a system, impacting the ionisation of the target analyte as well as the instrument response to the target analyte [80, 81]. These matrix effects often lead to significantly suppressed or enhanced sensitivity, altering the experimental results [80, 81]. The matrix effects in a system can be measured by comparing the response of an analyte in a standard solution to the response of the same analyte in

matrix. In the current study, the sample matrix was highly complex, containing a mixture of the host (textile), the target (lipids) bound in decomposition fluids and other unwanted environmental debris such as soil, leaf litter, hair, tissue or insects. As such, the target compounds (lipids) were endogenous to the matrix. In order to adequately assess the effects of the matrix on the analysis, deuterated lipid analytes (stearic acid-d3 and cholesterol-d7) were used.

Textile samples associated with decomposing human remains collected in field from the same donor H2 on day 0 and day 84 post-placement, were used for the assessment of matrix effects. 25 µL of the filtered aliquots were then spiked with either a low (1 ppm) or high (10 ppm) concentration of deuterated acid and sterol standards, stearic acid-d3 and cholesterol-d7. These were then dried down, reconstituted, and transferred to polymer inserts as outlined in the derivatisation procedure described in Section 3.2.10. All samples were extracted in duplicate, and injected in triplicate, with the use of a full scan injection for quality control purposes and four MRM data points.

3.2.14. Investigation of background lipid contamination

Since lipids are ubiquitous in nature and are found at detectable limits in most plant and animal fats, it was essential for this study to explore possible sources of lipid contamination that could impact the experimental results. As this research is novel, it was imperative to document all possible aspects of lipid contamination. Three control sets were created. A laboratory control containing no matrix (textile), an environmental control containing matrix (textile) exposed to the field environment for 84 days post-placement, and a textile control containing store-bought matrix (textile).

All of these controls were spiked post-extraction with of 20 uL of 10 ppm stearic acid-d3 and 50 µL of10 ppm cholesterol-d7.

3.3. Results and Discussion

3.3.1. MRM optimisation

A total of 30 lipids, and two internal standards, were successfully identified and optimised for GC-MS/MS analysis. In all cases, one quantifying transition and two qualifying transitions were selected for each lipid. The five-point calibration curves, respective R^2 values and linear equations are displayed in Figure 3.S1A – 3.S1F. Linearity ranges below 0.99 were accepted in this work as the aims and objectives of this work was to conduct normalisation instead of quantitation. In future, to reach the threshold for validation, and thus quantitation, R^2 values $\geq$ 0.99 should be considered. The retention times, MRM transitions, collision energies and limit of detection (LOD) for the fatty acids are detailed in Table 3.3 and the sterols in Table 3.4. LOD was calculated using the standard procedure of 3.3*σ /S, where σ was the standard deviation of the response and S was the slope of the calibration curve.

*Table 3. 3 Retention time (RT), MRM ion transitions, optimized collision energies and LOD for the targeted fatty acids. *internal standard used for the acid analytes.*

Analyte	***RT***	***Transition 1***	***CE***	***Transition 2***	***CE***	***Transition 3***	***CE***	***R^2***	***LOD***
Decanoic Acid	8.031	229>75	15	229>131	10	229>81	10	0.94	0.04
Lauric Acid	9.280	257>75	15	257>131	10	257>95	10	0.96	0.01
Tridecanoic Acid	9.900	271>75	15	271>131	10	271>95	10	0.96	0.04
Azelaic Acid	10.170	201>83	5	317>149	10	317>123	10	0.99	0.02
Myristic Acid	10.391	285>75	20	285>131	10	285>95	10	0.93	0.05
Sebacic Acid	10.630	331>149	10	215>55	10	331>95	10	0.87	0.07
Pentadecanoic Acid	10.900	299>75	15	299>131	10	299>95	15	0.93	0.05
Palmitoleic Acid	11.282	311>75	25	236>67	25	311>131	10	0.98	0.03
Palmitic Acid	11.470	313>141	25	313>113	10	313>75	10	0.93	0.05
Heptadecanoic Acid	11.860	327>75	15	327>131	10	327>95	10	0.99	0.01
Linoleic Acid	12.150	337>75	25	220>79	10	337>93	25	0.99	0.04
Stearic Acid-d3*	12.268	344>75	30	375>213	15	344>95	15	0.89	0.07
Oleic Acid	12.270	339>75	25	339>131	10	222>67	25	0.95	0.05
Stearic Acid	12.278	341>75	15	341>131	10	341>95	10	0.93	0.05
Nonadecanoic Acid	12.710	355>75	25	355>131	10	355>95	15	0.96	0.04
Arachidic Acid	13.270	369>75	20	369>131	15	369>95	10	0.93	0.05
Heneicosanoic Acid	13.529	383>75	25	383>131	15	383>95	10	0.78	0.23
Behenic Acid	13.945	397>75	25	397>131	15	397>95	20	0.99	0.02
Tricosanoic Acid	14.345	411>75	25	411>131	20	411>81	20	0.97	0.04
Tetracosanoic Acid	14.670	425>75	25	425>131	15	425>95	15	0.92	0.05
Hexacosanoic Acid	15.610	453>75	25	453>131	15	453>95	15	0.93	0.05

*Table 3. 4 Retention time (RT), MRM ion transitions, optimized collision energies and LOD for the targeted sterol analytes. **internal standard used for sterol analytes.*

Analyte	***RT***	***Transition 1***	***CE***	***Transition 2***	***CE***	***Transition 3***	***CE***	***R^2***	***LOD***
Coprostanol	15.980	403>73	45	370>215	15	370>355	15	0.94	0.05
Cholesterol	16.150	329>95	25	368>353	15	368>339	15	0.99	0.01
5α-cholestanol	16.224	403>73	45	460>215	15	355>91	45	0.99	0.02
Cholesterol-d7**	16.235	336>95	20	375>213	15	375>255	15	0.93	0.05
5a-cholestanone	16.308	429>167	20	458>429	20	401>195	20	0.98	0.03
Lithocholic Acid	16.705	257>161	15	215>105	10	430>325	15	0.98	0.02
Stigmasterol	16.904	255>105	25	394>83	15	394>211	15	0.99	0.02
Ergosterol	16.945	379>69	30	379>255	30	379>83	30	0.94	0.05
Deoxycholic Acid	16.985	255>159	15	266>119	25	428>255	10	0.99	0.02
β-sitosterol	17.270	129>73	20	357>95	20	396>145	25	0.99	0.02
25-hydroxycholesterol	17.870	255>145	10	255>159	10	255>147	10	0.94	0.05

3.3.2. Investigation of extraction efficiency

While it is recognised that the traditional Folch method (2:1 chloroform/methanol) [82] remains the benchmark for most lipid extraction techniques, recent studies [1, 3, 4, 9, 76, 77] have demonstrated great success with other, more simpler extraction methods. Four methods were tested (Table 3.2) for the purpose of post-mortem lipid extraction from textiles at using a total extraction volume of 4 mL in this study. A novel extraction method was also included in these tests, which combined two common lipid extraction solvents (acetone and chloroform) in a simple 1:1 ratio. This method was adapted from Leikola et al. 1965 [78] and Koeppen et al. 1979 [79] who both looked at the extraction of lipids from post-mortem tissues using an acetone—chloroform mixture.

The extraction efficiency percentage was calculated by dividing the mean area of the deuterated analytes yielded in the experimental samples (Table 3. S1 and 3.S2) by the mean area of the neat deuterated analytes in the blanks (Table 3.S3), multiplied by 100 (Table 3.5 and 3.6) [13, 83]. Overall, the results indicated that there was sample loss in the percentage yield of the deuterated sterol analyte (cholesterol-d7) in both the day 0 and day 84 post-placement samples, across all four extraction methods tested. A loss in percentage yield is to be expected when testing extraction efficiency, as there are various manual steps in the extraction procedure where sample loss can occur, such as syringe filtration. However, it is possible that these results could also be indicative of ion suppression due to matrix effects [13, 84]. This is explored in the next section 3.3.3.

Table 3. 5 Extraction efficiency percentage (%) calculated for the four extraction methods on the day 0 and day 84 post-placement experimental samples ± relative standard deviation (%RSD)

	Stearic acid-d3		***Cholesterol-d7***	
Method	***Day 0***	***Day 84***	***Day 0***	***Day 84***
1	154.0% ± 141.0%	1905.0% ± 42.5%	39.0% ± 17.3%	49.0% ± 36.5%
2	1800.0% ± 139.9%	2150.0% ± 28.8%	45.0% ± 11.4%	67.0% ±6.5%
3	31.0% ± 149.8%	2249.0% ± 57.7%	78.0% ± 13.7%	66.0% ± 58.7%
4	53.0% ± 168.4%	2554.0% ± 2.3%	92.0% ± 14.4%	72.0% ± 38.2%

Overall, the novel method four, acetone—chloroform, performed best for the deuterated sterol analyte (cholesterol-d7), with the highest percentage yield for both the day 0 and day 84 post-placement samples with 92.0% ± 14.4% (Table 3.5) and 72.0% ± 38.2% (Table 3.5) recovery yield, respectively

In contrast, the results for the deuterated acid analyte (stearic acid-d3) indicated a general trend of ion enhancement in both the day 0 and day 84 post-placement samples using method one and method two. Dissimilarly, methods three and four resulted in samples loss or ion suppression for the deuterated acid analyte for the day 0 post-placement sample, whereas the results of the day 84 post-placement samples demonstrated ion enhancement (Table 3.5). Results of 2249.0%± 57.7% and 2554.0%± 2.3% recovery yield for the deuterated acid analyte (stearic acid-d3) in methods three and four, were respectively calculated.

These findings clearly demonstrate that the representative textile sample containing a greater saturation of decomposition fluid (day 84 post-placement) significantly impacted the efficiency of all extraction methods tested for the deuterated acid analyte. In contrast, the deuterated sterol analyte demonstrated to be more stable when exposed to the day 84 post-placement sample. The false ion

enhancement of the deuterated acid analyte is likely due to matrix effects of the complex decomposition samples [84].

Overall, method four, acetone—chloroform in a 1:1 ratio, performed soundly when compared to the other three methods, for both the acid and sterol deuterated analyte, across both representative decomposition stages. In general, biphasic extractions work by creating two distinct solvent layers – one with the desired analytes and the other with the undesired components. This is advantageous in some applications [85, 86]. However, when working with analytes of differing properties and polarity, biphasic extraction systems can result in favouring one specific sub-group of the desired analytes, subsequently introducing an unwanted target bias [85, 86]. Because of this, monophasic extraction methods are superior to biphasic extraction methods at recovering a broader range of lipid classes, including the more polar lipids that may not be favoured in biphasic systems [85, 86]. When combining polar acetone and non-polar chloroform in a 1:1 ratio, the two solvents are miscible and do not separate into two distinct extraction layers. This results in a monophasic extraction system with dual-polarity. Based on the biochemical profile of the human body, it can be expected that the post-mortem lipid profile obtained from textiles associated with decomposing human remains will contain both hydrophobic and hydrophilic targets [4, 76, 77, 81]. Thus, supporting the selection of method four, an extraction technique that combines both polar and non-polar solvents.

3.3.3. Investigation of matrix effects

In order to accurately assess matrix effects, the response of the deuterated standards in a standard solution was compared to the response of the same

deuterated standards spiked onto the textile matrix post-extraction [13, 83]. The post-extraction spike eliminates the effects of the extraction procedure that may impact the results, however, does not eliminate effects introduced from the derivatisation and reconstitution process. The effects of the decomposition matrix were tested on both the day 0 and day 84 post-placement decomposition samples from H2, at a low concentration spike (1 ppm of stearic acid-d3 and cholesterol-d7) and a high concentration spike (10 ppm of stearic acid-d3 and cholesterol-d7).

The results of the matrix effects tests (Table 3.6) demonstrated minimal matrix effects when exposed to the day 0 post-placement sample for both the acid and sterol deuterated standards. However, at a low concentration spike (1 ppm), both stearic acid-d3 and cholesterol-d7 exhibited ion suppression with 45.9 ± 8.0% and 70.5 ± 4.4%, respective recovery. At a high concentration spike (10 ppm) stearic acid-d3 and cholesterol-d7 yielded a 67.0 ± 2.0% and 74.8 ± 1.7% respective recovery. This indicates that it is possible that sample loss is occurring from incomplete silylation during the derivatisation and reconstitution process [87]. Alternatively, this could be the result of matrix-induced diminishment, a phenomenon first described by Hajslova et al. in 2007 [88].

Table 3. 6 Matrix effects results in percentage (%) for extraction method four tested on the day 0 and day 84 post-placement samples at a low (1 ppm) and high (10 ppm) spike ± standard error.

	1 ppm		***10 ppm***	
	Day 0	***Day 84***	***Day 0***	***Day 84***
Stearic acid -d3	45.9% ± 8.0%	205.0% ± 78.1%	67% ± 2.8%	150.5% ± 6.3%
Cholesterol-d7	70.5% ± 3.8%	3.2% ± 1.5%	74.8% ± 2.6%	0.7% ± 0.08%

In contrast, ion enhancement was detected for the acid standard (stearic acid-d3) when exposed to the day 84 post-placement sample (Table 3.6). At a low

concentration spike (1 ppm) stearic acid-d3 yielded 205.0 ± 8.0%, while at a high concentration spike (10 ppm) the results were 150.5 ± 6.3%. At a lower concentration spike (1 ppm) the standard error was greater, 78.1%, than at a higher concentration spike (10 ppm), 6.3%. These results demonstrate that the deuterated acid standard (stearic acid-d3) is more stable and reproducible in highly saturated decomposition matrix, when spiked at a higher concentration. These results show a clear ion enhancement effect that is introduced with the complex decomposition matrix. This phenomenon was first described in 1993 by Erney et al. [89] who noted that neat standards could be thermally degraded and adsorbed onto the active sites of the GC column, blocking the active sites when real sample extracts are injected into the system. This results in false signal enhancement of the target analyte, and thus ion enhancement effect is observed [89].

The deuterated sterol standard (cholesterol-d7) showed to be influenced by the advanced decomposition matrix (day 84 post-placement) at both low (1 ppm) and high (10 ppm) concentrations, with 3.21 ± 1.5% and 0.71 ± 0.08%, respectively. Despite low recovery yield percentages, the calculated standard errors remain low, signifying that the sample means are closely distributed around the population mean, therefore the results of the matrix effects are true and reliable. Overall, the results of these matrix effects tests present considerable issues with conducting accurate and repeatable quantitative analysis of post-mortem lipids collected in textiles associated with decomposing human remains. However, as all calculated standard errors were below 8.0%, except for 1 ppm of stearic acid-d3 exposed to the day 84 post-placement sample, it is possible to overcome some of these issues of quantitation. This can be achieved by utilising a post-extraction spike of known amounts of

deuterated acid and sterol standards (as internal standards) and hence normalising the data to these internal standard(s). This was included in the experimental analysis process whereby 4 ppm of stearic acid-d3 and 10 ppm of cholesterol-d7 were used, and the subsequent analyte responses were normalised to their respective (acid or sterol) internal standard response. This method of normalisation has been successfully used in previous work by Ueland et al. [5] for the analysis of decomposition samples.

3.3.4. Investigation of background lipid contamination

Three types of controls were used in this study to examine potential sources of background lipid contamination: laboratory, environmental and textile. A laboratory control was used to assess contamination levels of lipids contributed from potential leachates of plastic labware consumables, apparatuses, and solvents [53, 69, 90]. Environmental controls were established for all experimental works in this study and consisted of identically sourced textiles placed on the soil surface of the experimental field-site, at the same time point as each cadaver. These environmental controls capture information about the natural deterioration of the textile over time [91], as well as providing an opportunity to establish the contribution of environmental lipids to the textiles. Textile controls were also used to investigate the presence of lipids on the store-bought textiles.

The results showed a considerably high normalised abundance of stearic acid in all three control types (Fig. 3.1). For the textile controls, stearic acid was found to be present at a normalised abundance of 11.5 ppm (Fig. 3.1). Cotton is a natural material composed of cellulose fibres which are naturally hydrophilic [92]. As such,

most industrial processes in the creation of cotton materials have adopted the application of chemical treatments to meet the demands of consumers [93]. Stearic acid treatment is a common form of chemical treatment to increase fibre hydrophobicity and involves the reaction of the stearic acid group with the hydroxyl group of the cotton fibres [94]. Thus, the stearic acid at such high normalised concentrations, particularly in the textile controls, can be explained by the manufacturing process of the cotton materials. In addition, stearic acid is one of the most abundant fatty acids in biological fluids, such as human sweat [51, 59, 95-98]. And so, it is also highly likely that additional stearic acid contributions were made to the textile controls from the manual handling of the material during the production and sale processes. While stearic acid was also present in the other two controls, the environmental and labware, the normalised abundances were ≤ 1 ppm. The presence of stearic acid in the labware controls, containing no textiles, is likely due to the single-use plastic labware implements used during the extraction procedure, such as syringes and syringe filters [69]. A high normalised abundance of stearic acid has also been reported in Ueland et al. in 2021 [5] and Luong et al. 2017 [9], from which the current method has been adapted. This provides further evidence to support the fact that stearic acid is a contaminant in this system and was thus removed from all subsequent analyses.

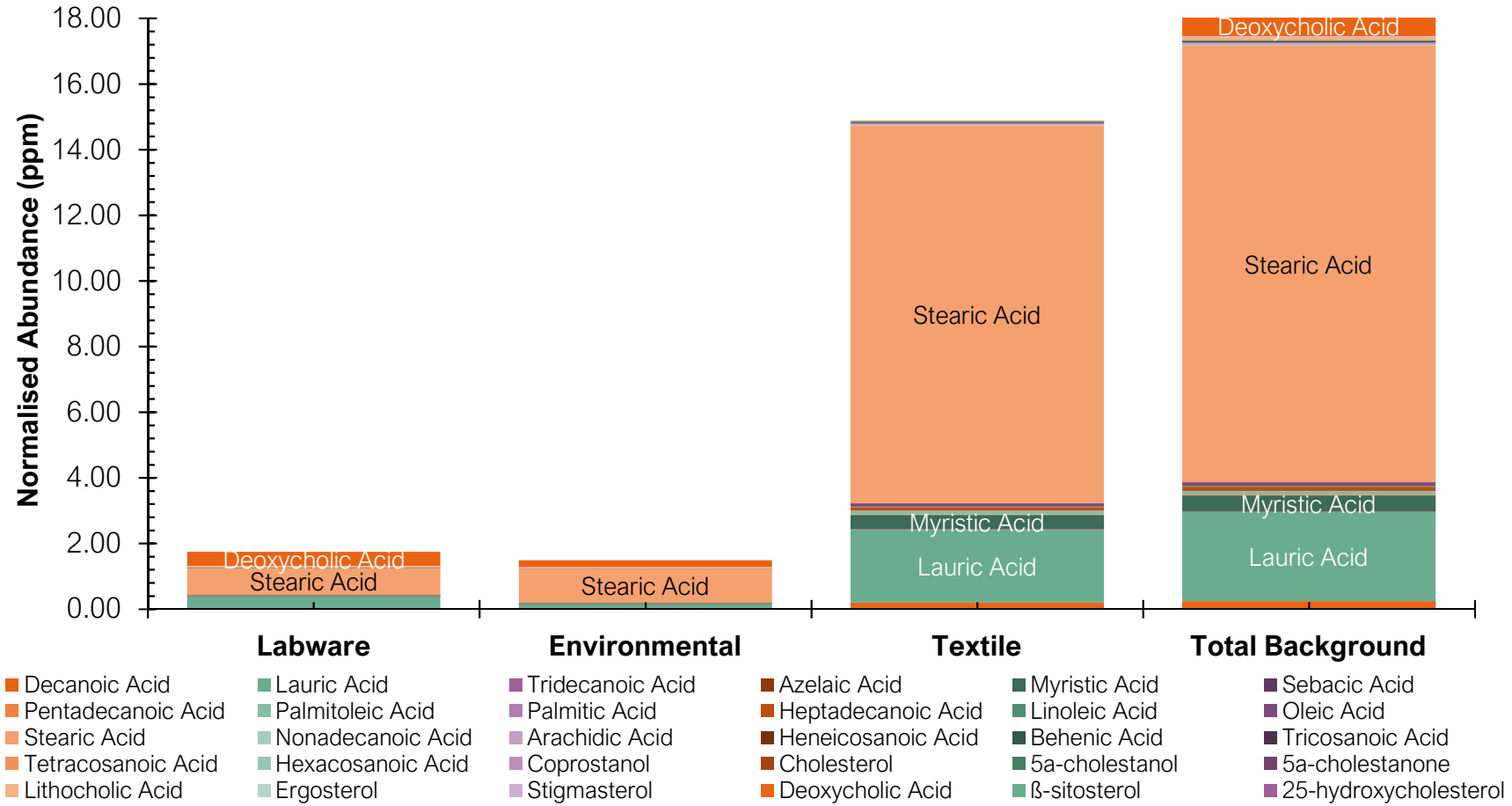

Fig. 3. 2 Normalised abundance (ppm) of the 30 target lipids from the three contamination tests: textile, environmental, labware and the calculated total background. Acid analytes were normalised to the deuterated acid internal standard (stearic acid-d3) and sterol analytes were normalised to the deuterated sterol internal standard (cholesterol-d7)

Lauric acid, myristic acid and deoxycholic acid were also detected in the contamination tests. Lauric acid was found in all three control sets at a low normalised abundance that did not exceed 0.5 ppm, except for the textile controls (2.2 ppm, Fig. 3.1). Myristic acid was only detected in the textile controls, at 0.43 ppm. Lauric acid and myristic acid are also known components of human sweat [51, 59] and it is likely that these analytes, detected at such low levels, have been introduced into the controls from manual handling and contamination of gloves. Deoxycholic acid was also detected in two out of the three sets tested, however, this lipid was present in both the labware and environmental controls at less than 0.5 ppm in each case.

Overall, the investigation of background lipid contamination through the use of these three controls was extremely useful for establishing an understanding of baseline lipid levels. These results demonstrated the importance of having controls in experiments investigating lipids and has led to the development of an exclusion criteria to establish a threshold for experimental analysis, adapted from Forbes et al. 2016 [99] and Ueland et al. 2021 [100]. In summary, the original lipid response was retained for analysis if it was exclusive to the experimental samples. Or if the experimental response was ≥ 50% when divided by the sum of the experimental response and the control response, multiplied by 100. This threshold therefore accounts for extracting useful information regarding lipids, from any potential background lipid contamination. In addition, this threshold also accounts for lipids that are exclusive only to the experimental samples. If this threshold was not met, the lipid response was discarded for future analysis.

3.4. Conclusions

Overall, a novel analytical workflow for the extraction, separation and detection of 30 post-mortem lipids collected in textiles associated with human remains was successfully developed. In addition, the results of the extraction efficiency and matrix effects tests revealed significant challenges associated with working with decomposition samples. Specifically, the impact of the complex decomposition matrix to quantitative work. Despite the use of a targeted method in the form of MRM, chromatographic baselines often differ between injections and batches due to thermal degradation or vaporisation of the stationary phase in the chromatographic column [101, 102]. In addition, other undesirable variations such as detector non-linearity [103], ionisation suppression or enhancement [104] and most predominantly in the case of this investigation, matrix effects [101]. If not corrected, these variations can have a significant impact on downstream data analyses, particularly when developing multivariate models.

Sources of lipid contamination were also explored in this investigation and it was reported that stearic acid, lauric acid, myristic acid and deoxycholic acid were found at detectable limits in most controls. Stearic acid, lauric acid and myristic are likely contaminants from human sweat and manual handling in the manufacturing and selling processes, while deoxycholic acid was likely an instrument contaminant. This study highlights the importance of controls in such experimental work and led to the application of a simple classification system to establish a threshold for further experimental analysis.

In context of these findings, recommendations have been developed and applied for future data analysis. For improved accuracy and the ability to perform

quantitative analysis, the method requires validation. However, it is recommended to perform data normalisation by internal standards that are representative of the target lipid classes, in this case stearic acid-d3 for the acid analytes and cholesterol-d7 for the sterol analytes. This normalisation process reduces the variation from the sample handling process (as presented in the extraction efficiency tests), data-acquisition (as indicated by thermal degradation or vaporisation of the stationary phase) and matrix effects [105]. This data normalisation technique provides useful information about the relative abundance of the target lipids in each sample on a time dependent scale and can therefore provide insight to the degradation patterns of the lipids collected in the textiles over time.

3.5. References

[1] S. Luong, S.L. Forbes, J.F. Wallman, R.G. Roberts. Monitoring the extent of vertical and lateral movement of human decomposition products through sediment using cholesterol as a biomarker, Forensic Sci. Int., 285 (2018) 93-104. https://doi.org/10.1016/j.forsciint.2018.01.026

[2] P.S. Barton, A. Reboldi, B.M. Dawson, M. Ueland, C. Strong, J.F. Wallman. Soil chemical markers distinguishing human and pig decomposition islands: a preliminary study. Forensic Sci. Med. Pathol.,16 (2020) 605-12. https://doi.org/10.1007/s12024-020-00297-2

[3] M. Ueland, S.L. Forbes, B.H. Stuart. Seasonal variation of fatty acid profiles from textiles associated with decomposing pig remains in a temperate Australian environment. Forensic Chem., 11 (2018) 120-127. https://doi.org/10.1016/j.forc.2018.10.008

[4] M. Ueland, K.D. Nizio, S.L. Forbes, B.H. Stuart. The interactive effect of the degradation of cotton clothing and decomposition fluid production associated with decaying remains, Forensic Sci. Int., 255 (2015) 56-63. https://doi.org/10.1016/j.forsciint.2015.05.029

[5] M. Ueland, S. Collins, L. Maestrini, S.L. Forbes, S. Luong. Fresh vs. frozen human decomposition – A preliminary investigation of lipid degradation products as biomarkers of post-mortem interval, Forensic Chem., 24 (2021) 100335. https://doi.org/10.1016/j.forc.2021.100335

[6] S. Collins, B.H. Stuart, M. Ueland. Anatomical location dependence of human decomposition products in clothing, Aust. J. Forensic Sci., 55 (2023) 363-375. https://doi.org/10.1080/00450618.2021.1981443

[7] S. Collins, B.H. Stuart, M. Ueland. Monitoring human decomposition products collected in clothing: an infrared spectroscopy study, Aust. J. Forensic Sci., 52 (2020) 428-438. https://doi.org/10.1080/00450618.2019.1593504

[8] S.L. Forbes. Time since death: a novel approach to dating skeletal remains, Aust. J. Forensic Sci., 36 (2004) 67-72. https://doi.org/10.1080/00450610409410599.

[9] S. Luong, E. Hayes, E. Flannery, T. Sutikna, M. Tocheri, E.W. Saptomo, R.G. Jatmiko, R.G. Roberts, Development and application of a comprehensive analytical workflow for the quantification of non-volatile low molecular weight lipids on archaeological stone tools, Anal. Methods, 9 (30) (2017) 4349-4362. https://doi.org/10.1039/C7AY01304C

[10] S. Collins, L. Maestrini, M. Ueland, B.H. Stuart. A preliminary investigation to determine the suitability of pigs as human analogues for post-mortem lipid analysis. Talanta Open. (2022) 100100. https://doi.org/10.1016/j.talo.2022.100100

[11] Z. Knobel, M. Ueland, K.D. Nizio, D. Patel, S.L. Forbes, A comparison of human and pig decomposition rates and odour profiles in an Australian environment, Aust. J. Forensic Sci., 51 (5) (2019) 557-572. https://doi.org/10.1080/00450618.2018.1439100

[12] A. Misra, N.V. Dhurandhar, Current formula for calculating body mass index is applicable to Asian populations, Nutr. & Diabetes., 9 (1) (2019) 3. https://doi.org/10.1038/s41387-018-0070-9

[13] S. Bidny, K. Gago, P. Chung, D. Albertyn, D. Pasin, Simultaneous screening and quantification of basic, neutral and acidic drugs in blood using UPLC-QTOF-MS, J. Anal. Toxicol.,41 (3) (2016) 181-195. https://doi.org/10.1093/jat/bkw118

[14] B. von der Lühe, L.A. Dawson, R.W. Mayes, S.L. Forbes, S. Fiedler, Investigation of sterols as potential biomarkers for the detection of pig (S. s. domesticus) decomposition fluid in soils, Forensic Sci. Int., 230 (2013) 68-73. https://doi.org/10.1016/j.forsciint.2013.03.030

[15] C.-W. Lin, P.-H. Wang, W. Ismail, Y.-W. Tsai, A. El Nayal, C.-Y. Yang, F.-C. Yang, C.-H. Wang, Y.-R. Chiang, Substrate uptake and subcellular compartmentation of anoxic cholesterol catabolism in Sterolibacterium denitrificans, J. Biol. Chem., 290 (2) (2015) 1155. https://doi.org/10.1074/jbc.M114.603779

[16] S.S. Pfeiffer, S. Milne, R.M. Stevenson, The natural decomposition of adipocere. J. Forensic Sci., 43 (1998) 368-370. https://doi.org/10.1520/JFS16147J

[17] W. Luu, L.J. Sharpe, I. Capell-Hattam, I.C. Gelissen, A.J. Brown, Oxysterols: old tale, new twists, Annu. Rev. Pharmacol. Toxicol., 56 (1) (2016) 447-467. https://doi.org/10.1146/annurev-pharmtox-010715-103233

[18] S. Luong, M.W. Tocheri, E. Hayes, T. Sutikna, R. Fullagar, E.W. Saptomo, R.G. Roberts, Combined organic biomarker and use-wear analyses of stone artefacts from Liang Bua, Flores, Indonesia, Sci. Rep., 9 (1) (2019) 1-17. https://doi.org/10.1038/s41598-019-53782-2

[19] M. Copley, H.A. Bland, P. Rose, M. Horton, R. Evershed, Gas chromatographic, mass spectrometric and stable carbon isotopic investigations of organic residues of plant oils and

animal fats employed as illuminants in archaeological lamps from Egypt, Analyst 130 (6) (2005) 860-871. https://doi.org/10.1039/B500403A

[20] K. Schubert, G. Kaufmann, Bildung von Sterinestern in der Bakterienzelle, Biochim. Biophys. Acta. Mol. Cell Biol. Lipids,106 (3) (1965) 592-597.

[21] I.D. Bull, M.J. Lockheart, M.M. Elhmmali, D.J. Roberts, R.P. Evershed, The origin of faeces by means of biomarker detection, Environ. Int., 27 (8) (2002) 647-654. https://doi.org/10.1016/S0160-4120(01)00124-6

[22] D. Nash, R. Leeming, L. Clemow, M. Hannah, D. Halliwell, D. Allen, Quantitative determination of sterols and other alcohols in overland flow from grazing land and possible source materials, Water Res., 39 (13) (2005) 2964-2978. https://doi.org/10.1016/j.watres.2005.04.063

[23] L. Harrault, K. Milek, E. Jardé, L. Jeanneau, M. Derrien, D.G. Anderson, Faecal biomarkers can distinguish specific mammalian species in modern and past environments, PLoS One 14 (2) (2019) e0211119. https://doi.org/10.1371/journal.pone.0211119

[24] J.O. Grimalt, P. Fernandez, J.M. Bayona, J. Albaiges, Assessment of faecal sterols and ketones as indicators of urban sewage inputs to coastal waters, Environ. Sci. & Technol., 24 (3) (1990) 357-363. https://doi.org/10.1021/es00073a011

[25] S.J. Gaskell, G. Eglinton, Rapid hydrogenation of sterols in a contemporary lacustrine sediment, Nature, 254 (5497) (1975) 209-211. https://doi.org/10.1038/254209b0

[26] I. Björkhem, J.Å. Gustafsson, Mechanism of microbial transformation of cholesterol into coprostanol, Eur. J. Biochem., 21 (3) (1971) 428-432. https://doi.org/10.1111/j.1432-1033.1971.tb01488.x

[27] L. Zhou, Å. Nilsson, Sources of eicosanoid precursor fatty acid pools in tissues, J. Lipid Res., 42 (10) (2001) 1521-1542. https://doi.org/10.1016/S0022-2275(20)32206-9

[28] D. Li, A. Ng, N.J. Mann, A.J. Sinclair, Contribution of meat fat to dietary arachidonic acid, Lipids, 33 (4) (1998) 437-440. https://doi.org/10.1007/s11745-998-0225-7

[29] L. Taber, C.H. Chiu, J. Whelan, Assessment of the arachidonic acid content in foods commonly consumed in the American diet, Lipids 33 (12) (1998) 1151-1157. https://doi.org/10.1007/s11745-998-0317-4

[30] T. Komprda, J. Zelenka, E. Fajmonova, M. Fialova, D. Kladroba, Arachidonic acid and long-chain n− 3 polyunsaturated fatty acid contents in meat of selected poultry and fish species in relation to dietary fat sources, J. Agric. Food & Chem., 53 (17) (2005) 6804-6812. https://doi.org/10.1021/jf0504162

[31] E. Abedi, M.A. Sahari, Long-chain polyunsaturated fatty acid sources and evaluation of their nutritional and functional properties, Food Sci. & Nutr., 2 (5) (2014) 443-463. https://doi.org/10.1002/fsn3.121

[32] J. Genebriera, M. Davis, Chapter 70 - Acne, in: S.A. Waldman, A. Terzic, L.J. Egan, J.-L. Elghozi, A. Jahangir, G.C. Kane, W.K. Kraft, L.D. Lewis, J.D. Morrow, L.V. Zingman, D.R.

Abernethy, A.J. Atkinson, N.L. Benowitz, D.C. Brater, J. Gray, P.K. Honig, G.L. Kearns, B.A. Levey, S.P. Spielberg, R. Weinshilboum, R.L. Woosley (Eds.), Pharmacology and Therapeutics, W.B. Saunders, Philadelphia, 2009, pp. 973-981.

[33] K. Holland, R. Bojar, Antimicrobial effects of azelaic acid, J. Dermatolog. Treat., 4 (sup1) (1993) S8-S11. https://doi.org/10.3109/09546

[34] M.P. Colombini, G. Giachi, F. Modugno, E. Ribechini, Characterisation of organic residues in pottery vessels of the Roman age from Antinoe (Egypt), Microchem. J., 79 (1) (2005) 83-90. https://doi.org/10.1016/j.microc.2004.05.004

[35] M. Regert, H.A. Bland, S.N. Dudd, P.v. Bergen, R.P. Evershed, Free and bound fatty acid oxidation products in archaeological ceramic vessels, Proc. Royal Soc. B., 265 (1409) (1998) 2027-2032. https://doi.org/10.1098/rspb.1998.0536

[36] W.W. Christie, X.J.S. Han, Lipid analysis: isolation, separation, identification and lipidomic analysis: Fourth Edition, Elsevier Ltd., 2003. https://doi.org/10.1533/9780857097866

[37] J.D. Weete, M. Abril, M. Blackwell, Phylogenetic distribution of fungal sterols, PloS One 5 (5) (2010) e10899. https://doi.org/10.1371/journal.pone.0010899

[38] O.G. Mouritsen, M.J. Zuckermann, What's so special about cholesterol?, Lipids 39 (11) (2004) 1101-1113. https://doi.org/10.1007/s11745-004-1336-x

[39] K. Prost, J.J. Birk, E. Lehndorff, R. Gerlach, W. Amelung, Steroid biomarkers revisited - improved source identification of faecal remains in archaeological soil material, PLoS One 12 (1) (2017) e0164882. https://doi.org/10.1371/journal.pone.0164882

[40] V. Campos, R. Fracácio, L.F. Fraceto, A.H. Rosa, Faecal sterols in estuarine sediments as markers of sewage contamination in the Cubatão area, São Paulo, Brazil, Aquat. Geochem., 18 (5) (2012) 433-443. https://doi.org/10.1007/s10498-012-9167-2

[41] P.G. Hatcher, P.A. McGillivary, Sewage contamination in the New York Bight. Coprostanol as an indicator, Environ. Sci. Technol., 13 (10) (1979) 1225-1229. https://doi.org/10.1021/es60158a015

[42] P. Gérard, Metabolism of cholesterol and bile acids by the gut microbiota, Pathogens 3 (1) (2013) 14-24. https://doi.org/10.3390/pathogens3010014

[43] E. Stellwag, P. Hylemon, 7alpha-Dehydroxylation of cholic acid and chenodeoxycholic acid by Clostridium leptum, J. Lipid Res., 20 (3) (1979) 325-333. https://doi.org/10.1016/S0022-2275(20)40615-7

[44] P. Battilani, G. Chiusa, C. Cervi, M. Trevisan, C. Ghebbioni, Fungal growth and ergosterol content in tomato fruits infected by fungi, Ital. J. Food Sci., (1996) 283-289.

[45] A. West, W. Grant, G. Sparling, Use of ergosterol, diaminopimelic acid and glucosamine contents of soils to monitor changes in microbial populations, Soil Biology and Biochemistry 19 (5) (1987) 607-612. https://doi.org/10.1016/0038-0717(87)90106-4

[46] R. Oliveira, M. Faria, R. Silva, L. Bezerra, G. Carvalho, A. Pinheiro, J. Simionato, A. Leão, Fatty acid profile of milk and cheese from dairy cows supplemented a diet with palm kernel cake, Molecules, 20 (8) (2015) 15434-48. https://doi.org/10.3390/molecules200815434

[47] L. Hodson, H.C. Eyles, K.J. McLachlan, M.L. Bell, T.J. Green, C.M. Skeaff, Plasma and erythrocyte fatty acids reflect intakes of saturated and n–6 PUFA within a similar time frame, Nutr. J., 144 (1) (2014) 33-41. https://doi.org/10.3945/jn.113.183749

[48] W.N. Ratnayake, Concerns about the use of 15: 0, 17: 0, and trans-16: 1n–7 as biomarkers of dairy fat intake in recent observational studies that suggest beneficial effects of dairy food on incidence of diabetes and stroke, Am. J. Clin. Nutr., 101 (5) (2015) 1102-1103. https://doi.org/10.3945/ajcn.114.105379

[49] T. Miyazaki, K. Shimada, M. Hiki, A. Kume, Y. Kitamura, K. Oshida, N. Yanagisawa, T. Kiyanagi, R. Matsumori, H.J.A. Daida, High hexacosanoic acid levels are associated with coronary artery disease, Atherosclerosis, 233 (2) (2014) 429-433. https://doi.org/10.1016/j.atherosclerosis.2014.01.031

[50] H. Singh, N. Derwas, A. Poulos, β-oxidation of very-long-chain fatty acids and their coenzyme A derivatives by human skin fibroblasts, Arch. Biochem. Biophys., 254 (2) (1987) 526-533. https://doi.org/10.1016/0003-9861(87)90133-0

[51] T. Takemura, P.W. Wertz, K. Sato, Free fatty acids and sterols in human eccrine sweat, Br. J. Dermatol., 120 (1) (1989) 43-7. https://doi.org/10.1111/j.1365-2133.1989.tb07764.x

[52] M. Harker, H. Coulson, I. Fairweather, D. Taylor, C.A. Daykin, Study of metabolite composition of eccrine sweat from healthy male and female human subjects by 1 H NMR spectroscopy, Metabolomics, 2 (3) (2006) 105-112. https://doi.org/10.1007/s11306-006-0024-4

[53] S.J. Notter, B.H. Stuart, B.B. Dent, J. Keegan, Solid-phase extraction in combination with GC/MS for the quantification of free fatty acids in adipocere, Eur. J. Lipid Sci. Technol., 110 (1) (2008) 73-80. https://doi.org/10.1002/ejlt.200700159

[54] S.J. Notter, B.H. Stuart, R. Rowe, N. Langlois, The initial changes of fat deposits during the decomposition of human and pig remains, J. Forensic Sci., 54 (1) (2009) 195-201. https://doi.org/10.1111/j.1556-4029.2008.00911.x

[55] H. Nushida, J. Adachi, A. Takeuchi, M. Asano, Y. Ueno, Adipocere formation via hydrogenation of linoleic acid in a victim kept under dry concealment, Forensic Sci. Int., 175 (2) (2008) 160-165. https://doi.org/10.1016/j.forsciint.2007.06.008

[56] T.A.B. Sanders, 37 - Polyunsaturated fatty acid status in vegetarians, in: F. Mariotti (Ed.), Vegetarian and Plant-Based Diets in Health and Disease Prevention, Academic Press, 2017, pp. 667-681.

[57] V. Rioux, F. Pédrono, P. Legrand, Regulation of mammalian desaturases by myristic acid: N-terminal myristoylation and other modulations, Biochim. Biophys. Acta 1811 (1) (2011) 1-8. https://doi.org/10.1016/j.bbalip.2010.09.005

[58] V. Saraswathi, N. Kumar, W. Ai, T. Gopal, S. Bhatt, E.N. Harris, G.A. Talmon, C.V. Desouza, Myristic acid supplementation aggravates high fat diet-induced adipose inflammation and systemic insulin resistance in mice, Biomolecules 12 (6) (2022) 739. https://doi.org/10.3390/biom12060739

[59] Y. Nunome, T. Tsuda, K. Kitagawa, Determination of fatty acids in human sweat during fasting using GC/MS, Anal. Sci., 26 (8) (2010) 917-9.

[60] M.S. Blum, T.H. Jones, D.F. Howard, W.L. Overal, Biochemistry of termite defenses: Coptotermes, rhinotermes and Cornitermes species, Comp. Biochem. Physiol. B, Biochem., 71 (4) (1982) 731-733. https://doi.org/10.1016/0305-0491(82)90489-8

[61] J.K.R.P. Felisbino, B.S. Vieira, A. de Oliveira, N.A. da Silva, C.H.G. Martins, M.B. Santiago, R.A.A. Munoz, L.C.S. Cunha, R.M.F. Sousa, Identification of substances produced by cercospora brachiata in absence of light and evaluation of antibacterial activity, J. Fungus, 7 (9) (2021) 680. https://doi.org/10.3390/jof7090680

[62] Z.A. Ktsoyan, N.V. Beloborodova, A.M. Sedrakyan, G.A. Osipov, Z.A. Khachatryan, D. Kelly, G.P. Manukyan, K.A. Arakelova, A.I. Hovhannisyan, A.Y. Olenin, A.A. Arakelyan, K.A. Ghazaryan, R.I. Aminov, Profiles of microbial fatty acids in the human metabolome are disease-specific, Front. Cell. Infect. Microbiol., (2010) 148-148. https://doi.org/10.3389/fmicb.2010.00148

[63] G.R. List, Chapter 6 - Minor high-oleic oils, in: F.J. Flider (Ed.), High Oleic Oils, AOCS Press, 2022, pp. 125-142.

[64] N.H. Choulis, Chapter 49 - Miscellaneous drugs, materials, medical devices, and techniques, in: J.K. Aronson (Ed.), Side Effects of Drugs Annual, Elsevier, 2011, pp. 1009-1029.

[65] G. Carta, E. Murru, S. Banni, C. Manca, Palmitic acid: physiological role, metabolism and nutritional implications, Front. physiol., 8 (2017). https://doi.org/10.3389/fphys.2017.00902

[66] M.E. Frigolet, R. Gutiérrez-Aguilar, The role of the novel lipokine palmitoleic acid in health and disease, Adv Nutr., 8 (1) (2017) 173s-181s. https://doi.org/10.3945/an.115.011130

[67] M. Siotto, M. Tosin, F. Degli Innocenti, V.J.W. Mezzanotte, Air, S. Pollution, Mineralization of monomeric components of biodegradable plastics in preconditioned and enriched sandy loam soil under laboratory conditions, Water Air Soil Pollut., 221 (1) (2011) 245-254. https://doi.org/10.1007/s11270-011-0787-8

[68] Z. Zhen, T.F. Xi, Y.F. Zheng, 11 - Surface modification by natural biopolymer coatings on magnesium alloys for biomedical applications, in: T.S.N.S. Narayanan, I.-S. Park, M.-H. Lee (Eds.), Surface Modification of Magnesium and its Alloys for Biomedical Applications, Woodhead Publishing, 2015, pp. 301-333.

[69] Y.Y. Cheng, J.Z. Yu, Minimizing contamination from plastic labware in the quantification of c16 and c18 fatty acids in filter samples of atmospheric particulate matter and their utility in apportioning cooking source contribution to urban PM2.5, Atmosphere, 11 (10) (2020) 1120. https://doi.org/10.3390/atmos11101120

[70] A.M. Varghese, V. Mittal, 5 - Surface modification of natural fibers, in: N.G. Shimpi (Ed.), Biodegradable and Biocompatible Polymer Composites, Woodhead Publishing, 2018, pp. 115-155.

[71] 1 - Natural fibers and their composites, in: N. Chand, M. Fahim (Eds.), Tribology of Natural Fiber Polymer Composites, Woodhead Publishing, 2008, pp. 1-58.

[72] A. Ferrer, T. Altabella, M. Arró, A. Boronat, Emerging roles for conjugated sterols in plants, Prog. Lipid Res., 67 (2017) 27-37. https://doi.org/10.1016/j.plipres.2017.06.002

[73] M.M.J.P. Bender, Variations in the 13C/12C ratios of plants in relation to the pathway of photosynthetic carbon dioxide fixation, Phytochemistry, 10 (6) (1971) 1239-1244. https://doi.org/10.1016/S0031-9422(00)84324-1

[74] G. Stanaitytė, J. Damašius, D. Čižeikienė, R. Kazernavičiūtė, Ž. Druktenytė, Comparative analysis of biologically active compounds from cow colostrum and milk fats, animals, (2017) 37. https://doi.org/10.3390/ani9121070

[75] V. Fievez, E. Colman, J.M. Castro-Montoya, I. Stefanov, B. Vlaeminck, Milk odd- and branched-chain fatty acids as biomarkers of rumen function—An update, Anim. Feed Sci. Technol., 172 (1) (2012) 51-65. https://doi.org/10.1016/j.anifeedsci.2011.12.008

[76] Drochioiu, G. Turbidometric lipid assay in seed flours, J. Food Lipids., 12 (1) (2005) 12-22. https://doi.org/10.1111/j.1745-4522.2005.00002.x

[77] Ren, X., Wei, C., Yan, Q., Shan, X., Wu, M., Zhao, X., Song, Y. Optimization of a novel lipid extraction process from microalgae. Sci. Rep., 11(1) (2021) 1-10. https://doi.org/10.1038/s41598-021-99356-z

[78] Leikola, E., Nieminen, E., Salomaa, E. Occurrence of methyl esters in the pancreas, J. Lipid Res., 6(4) (1965) 490-493. https://doi.org/10.1016/S0022-2275(20)39611-5

[79] Koeppen, A.H., Mitzen, E.J., Papandrea, J.D. Lipid labelling after intracerebral injection of radioactive malonic acid, J. Neurochem., 34 (2) (1980) 261-268. https://doi.org/10.1111/j.1471-4159.1980.tb06591.x

[80] P. Panuwet, R.E. Hunter, Jr., P.E. D'Souza, X. Chen, S.A. Radford, J.R. Cohen, M.E. Marder, K. Kartavenka, P.B. Ryan, D.B. Barr, Biological matrix effects in quantitative tandem mass spectrometry-based analytical methods: advancing biomonitoring, Crit. Rev. Anal. Chem., 46 (2) (2016) 93-105. https://doi.org/10.1080/10408347.2014.980775

[81] P.J. Taylor, Matrix effects: the Achilles heel of quantitative high-performance liquid chromatography–electrospray–tandem mass spectrometry, Clin. Biochem., 38 (4) (2005) 328-334. https://doi.org/10.1016/j.clinbiochem.2004.11.007

[82] J. Folch, M. Lees, G.H. Sloane Stanley. A simple method for the isolation and purification of total lipides from animal tissues. J. Biol. Chem., 226 (1957) 497-509.

[83] B.K. Matuszewski, M. Constanzer, C. Chavez-Eng. Strategies for the assessment of matrix effect in quantitative bioanalytical methods based on HPLC− MS/MS. Anal. Chem., 73 (2003) 3019-3030. https://doi.org/10.1021/ac020361s

[84] W.S. Zhou, S. Yang, P.G. Wang. Matrix effects and application of matrix effect factor, Bioanalysis, 23 (2017) 1839-1844. https://doi.org/10.4155/bio-2017-0214

[85] M.W.K. Wong, N. Braidy, R. Pickford, P.S. Sachdev, A. Poljak. Comparison of Single Phase and Biphasic Extraction Protocols for Lipidomic Studies Using Human Plasma. Front. Neurol., 10 (2019) 879. https://doi.org/10.3389/fneur.2019.00879

[86] C.W.M. Adams, O.B. Bayliss. Histochemistry of Myelin Vi. Solvent Action of Acetone on Brain and Other Lipid-Rich Tissues, J. Histochem. Cytochem., 16 (1968) 115-118. https://doi.org/10.1177/16.2.115

[87] S.C. Moldoveanu, V. David. Derivatization Methods in GC and GC/MS. in Gas Chromatography - Derivatization, Sample Preparation, Application. in: P. Kusch, (Eds.), Intechopen, 2018.

[88] J. Hajslová, T. Cajka. Chapter 12-Gas chromatography-mass spectrometry (GC-MS), in: Y. Pico, (Eds.), Food Toxicants Analysis, Elsevier, 2007 pp. 419-473.

[89] D. R. Erney, A.M. Gillespie, D.M. Gilvydis, C.F. Poole. Explanation of the matrix-induced chromatographic response enhancement of organophosphorus pesticides during open tubular column gas chromatography with splitless or hot on-column injection and flame photometric detection, J. Chromatogr. A, 638 (1993) 57-63. https://doi.org/10.1016/0021-9673(93)85007-T

[90] M.R. Prasad, R.M, Jones, H.S. Young, L.B. Kaplinsky, D.K. Das. Analysis of tissue free fatty acids isolated by aminopropyl bonded-phase columns, J. Chromatogr., 428 (1988) 221-228. https://doi.org/10.1016/S0378-4347(00)83912-2

[91] M. Ueland, J.M. Howes, S.L. Forbes, B.H. Stuart. Degradation patterns of natural and synthetic textiles on a soil surface during summer and winter seasons studied using ATR-FTIR spectroscopy, Spectrochim. Acta A Mol. Biomol., 185 (2017) 69-76. https://doi.org/10.1016/j.saa.2017.05.044

[92] A.M. Varghese, V. Mittal, 5 - Surface modification of natural fibers, in: N.G. Shimpi (Ed.), Biodegradable and Biocompatible Polymer Composites, Woodhead Publishing, 2018, pp. 115-155.

[93] S. Rabia, M. Muhammad, R. Naveed, A.S. Waqas, H.G.J.I.T. Qutab, Development of free fluorine and formaldehyde oil and water-repellent finishes for cotton fabrics through polymerization of bio-based stearic acid with carboxylic acids, Industria Textila, 71 (2) (2020) 145-155. https://doi.org/10.35530/IT.071.02.1731

[94] N. Chand, M. Fahim, Natural fibers and their composites, in: N. Chand, M. Fahim (Eds.), Tribology of Natural Fiber Polymer Composites, Woodhead Publishing, 2008, pp. 1-58.

[95] V.P. Kutyshenko, M. Molchanov, P. Beskaravayny, V.N. Uversky, M.A. Timchenko, Analyzing and mapping sweat metabolomics by high-resolution NMR spectroscopy, PLOS one, 6 (12) (2011) e28824. https://doi.org/10.1371/journal.pone.0028824

[96] M. Calderón-Santiago, F. Priego-Capote, B. Jurado-Gámez, M.L. de Castro, Optimization study for metabolomics analysis of human sweat by liquid chromatography–tandem mass

spectrometry in high resolution mode, J. Chromatogr. A, 1333 (2014) 70-78. https://doi.org/10.1016/j.chroma.2014.01.071

[97] M. Calderón-Santiago, F. Priego-Capote, N. Turck, X. Robin, B. Jurado-Gámez, J.C. Sanchez, M.D.L. De Castro, Human sweat metabolomics for lung cancer screening, Anal. Bioanal. Chem., 407 (18) (2015) 5381-5392. https://doi.org/10.1007/s00216-015-8700-8

[98] M.M. Delgado-Povedano, M. Calderón-Santiago, F. Priego-Capote, M.L. de Castro, Development of a method for enhancing metabolomics coverage of human sweat by gas chromatography–mass spectrometry in high resolution mode, Anal. Chim. Acta., 905 (2016) 115-125. https://doi.org/10.1016/j.aca.2015.11.048

[99] S.L. Forbes, A.N. Troobnikoff, M. Ueland, K.D. Nizio, K.A. Perrault, Profiling the decomposition odour at the grave surface before and after probing, Forensic Sci. Int., 259 (2016) 193-199. https://doi.org/10.1016/j.forsciint.2015.12.038

[100] M. Ueland, S. Harris, S.L. Forbes, Detecting volatile organic compounds to locate human remains in a simulated collapsed building, Forensic Sci. Int., 323 (2021) 110781. https://doi.org/10.1016/j.forsciint.2021.110781

[101] Z. Wang, P. Chen, L. Yu, P.D. Harrington. Authentication of organically and conventionally grown basils by gas chromatography/mass spectrometry chemical profiles, Anal. Chem., 85 (2013) 2945-2953. https://doi.org/10.1021/ac303445v

[102] Z. Xu, X. Sun, P.D.B. Harrington. Baseline correction method using an orthogonal basis for gas chromatography/mass spectrometry data. Anal. Chem., 83 (2011) 7464-7471. https://doi.org/10.1021/ac2016745

[103] X. Wang, P.D.B. Harrington. Differentiating Rice Varieties by Inductively Coupled Plasma Mass Spectrometry Chemical Profiling with Singular Value Decomposition Background Correction. J. Anal. Test., 2 (2018) 138-148. https://doi.org/10.1007/s41664-018-0055-7

[104] X. Wang, P.D. B. Harrington, S.F. Baugh. Effect of preprocessing high-resolution mass spectra on the pattern recognition of Cannabis, hemp, and liquor. Talanta, 180 (2018) 229-238. https://doi.org/10.1016/j.talanta.2017.12.032

[105] J.P. Koelmel, J.A. Cochran, C.Z. Ulmer, A. J. Levy, R.E. Patterson, B. C. Olsen, R. A. Yost, J.A Bowden, T.J. Garrett. Software tool for internal standard based normalization of lipids, and effect of data-processing strategies on resulting values, BMC Bioinformatics, 20 (2019) 217. https://doi.org/10.1186/s12859-019-2803-8

Chapter 4:
The investigation of lipids from textiles as soft-tissue biomarkers of human decomposition.

Chapter 4: The investigation of lipids from textiles as soft-tissue biomarkers of human decomposition.

i. Preface

With the exception of minor editorial changes, Chapter 4 reproduces the remainder of the following research article; **S. Collins,** B.H. Stuart, M Ueland, (2023). The use of lipids from textiles as soft-tissue biomarkers of human decomposition. Forensic Science International, 111547. https://doi.org/10.1016/j.forsciint.2022.111547. Permissions for reuse of this article within this dissertation have been obtained.

ii. Statement of Contribution and Declaration

Sharni Collins: conceptulisation; methodology; formal analysis; investigation; writing – original draft; writing - review and editing; Barbara Stuart: conceptulisation; methodology; writing – review and editing; supervision; Maiken Ueland: conceptulisation; methodology; writing – review and editing; supervision.

Graduate research student

Production Note:
Signature removed
prior to publication.

Sharni Collins

Principal Supervisor

Production Note:
Signature removed
prior to publication.

Dr. Maiken Ueland

Co-supervisor

Production Note:
Signature removed
prior to publication.

Professor Barbara Stuart

4.1 Introduction

Chapter 3 demonstrated the successful adaptation and optimisation of a targeted GC-MS/MS workflow for the analysis of lipids in textiles associated with human remains. In addition, novel information regarding the complex challenges of matrix effects were presented and consequently, a data processing classification system was also developed to streamline analysis. The aim of the current chapter was to apply the methods presented in Chapter 3, as a preliminary investigation to identify if lipids in textiles could be utilised as biomarkers of decomposition. This study reports the lipid profiles obtained from textiles associated with two human donors, in contrasting seasons in an Australian environment. The use of accumulated degree days (ADD), developed by Megyesi et al. in 2005 [1], allows this comparison across seasons as ADD units represent the accumulation of thermal energy in a chronological combination of time and energy [1].

4.2 Materials and methods

4.2.1 Field Site

The study was conducted at the Australian Facility for Taphonomic Experimental Research (AFTER), an open eucalypt woodland on the Cumberland Plain in Western Sydney, privately owned by the University of Technology, Sydney (UTS). Soils at the site are classified broadly as sandy clay loam or gravelly clay, with a pH range from 5.5 – 6.5 [2].

4.2.2 Donors

Two human donors were received through the University of Technology Sydney (UTS) Body Donation Programme, with consent provided in accordance with the New South Wales Anatomy Act (1977). Ethics approval was provided by the UTS Human Research Ethics Committee (HREC ETH18-2999). Human donor 1 (H1), was an 86-year-old male with a height of 174 cm and weight of 63 kg, giving a body mass index (BMI) [3] of 20.8. And human donor 2 (H2), was an 84-year-old male with a height of 182 cm and weight of 100 kg, giving a BMI of 30.2. H1 was placed on January 29, 2021, and H2 on June 11, 2021, corresponding to Australian summer and winter seasons, respectively. Both donors were clothed in a 100% white cotton t-shirt as described in Collins et al. [4], laid in a supine position on the soil surface at AFTER, and allowed to decompose naturally. Control sites were created for both donors, containing identically sourced clothing placed on the soil surface at AFTER at a minimum distance of 5 m from the decomposing remains, twice the minimum recommended distance proposed by Luong et al. 2018 [5]. Textile samples were collected from H1 and H2 on a series of days between day 0 and day 105 post-placement, these are explicitly outlined in Appendix 3, Table 4. S.1. Photographs and visual observations were recorded for both donors on each sampling day. Visual decomposition was determined using the five reported stages of decomposition: fresh, bloat, active, advanced, and skeletal [6].

4.2.3 Sample collection

Textile samples were collected in duplicates, at different time points during decomposition using sterilised scissors. Each textile sample was photographed in-situ

prior to collection and individually packaged in paper envelopes and stored in a cooler box for transportation to the laboratory, where the samples were kept at -18 °C when not in use. Each sample was dried in a fume cupboard at ambient temperature to inhibit bacterial and fungal growth, with adhering soil, hair and tissue removed.

4.2.4 GC-MS/MS sample preparation

Samples were prepared according to [7]. In brief, 35 mg of textile matrix was weighed per sample. 2 mL of HPLC-grade acetone (Sigma Aldrich, Sydney, Australia) and 2 mL of HPLC-grade chloroform (ChemSupply, Port Adelaide, Australia) were added to each vial and sonicated, without heat, for 20 min. The samples were then left at 4 °C for 16 hours to extract. 1 mL of the resulting extract was filtered through a 0.2 µm hydrophobic PTFE syringe filter (MicroAnalytix, Taren Point, Australia). 25 µL of the filtered aliquots were then spiked with 20 µL 10 ppm stearic acid-d3 (Merck, Macquarie Park, Australia) and 50 µL of 10 ppm cholesterol-d7 were then added as internal standards to. These were then dried down under a gentle stream of nitrogen at 40 °C. Samples were then reconstituted in 40 µL of N,O-bis(trimethylsilyl)trifluoroacetamide (BSTFA) with trimethylchlorosilane (TMCS) (PM Separations, Capalaba, Australia) and 10 µL of HPLC acetonitrile (Labscan Ltd., Gillman, Australia) and heated for 30 min at 70°C prior to being transferred into 250 µL polymer inserts (Agilent Technologies, Mulgrave, Australia). All samples were extracted and aliquoted in duplicates and injected onto the GC-MS/MS, where duplicate runs were conducted, giving a total of four data points per sample with the addition of a full scan injection for quality control purposes.

4.3 Results and discussion

4.3.1 Visual decomposition

The visual stages of decomposition for the summer donor H1, and the winter donor H2, were considerably different and are described in detail in Collins et al. 2022 [8]. Despite these differences, the decomposition period could be differentiated into three distinct groups: 'early', 'middle' and 'late' for each donor (Fig. 4.1). During summer, H1 experienced periods of heavy rainfall and a mean temperature of 19.4°C. H1 progressed from the fresh stage of decomposition, day 0 (ADD 0), to bloat, by sampling day 10 (ADD 222). This was classified as the 'early' period for H1 as it was also the first point that decomposition fluids were noticeably absorbed by the textiles. By day 17 (ADD 371), H1 had reached a relatively stable state of mummification. However, between days 17 (ADD 371) and 42 (ADD 907), decomposition fluids were still being released from the remains and absorbed by the textiles. This was classified as the 'middle' period for H1. Beyond, but not inclusive of day 42 (ADD 907), minimal changes were observed for the remains and the textiles of H1. This was thus classified as the 'late' stage for H1. In contrast, during winter, H2 was exposed to less rainfall and a lower mean temperature of 14.8°C. The 'early' stage for H2 was characterised by samples collected between day 0 (ADD 0) and day 17 (ADD 196). The 'middle' stage was documented between sampling days 23 (ADD 263) and 35 (ADD 385). And the 'late' stage included samples collected beyond day 42 (ADD 457), where the soft tissue had mostly mummified, like H1.

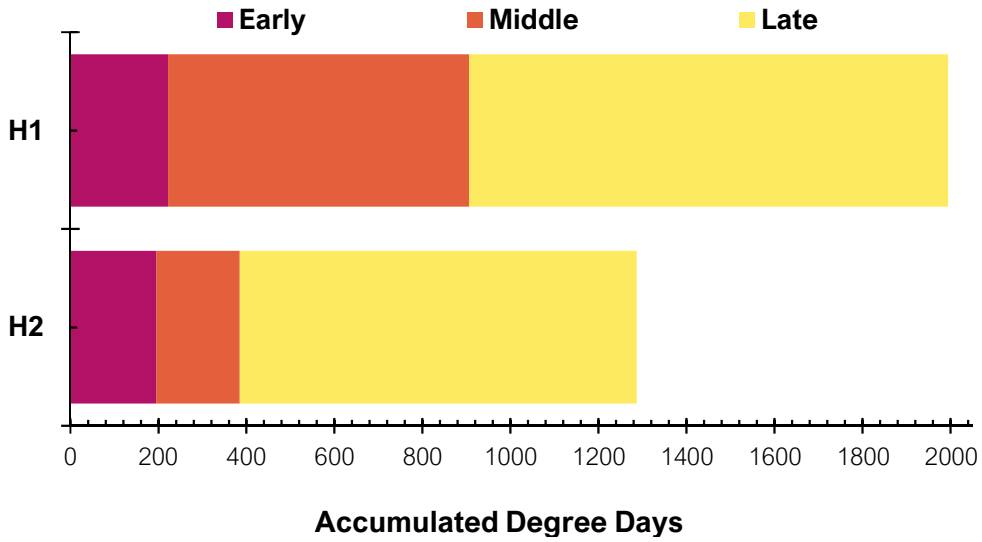

Fig. 4. 1 Occurrence and duration of the three decomposition classifications for each donor over the 105-day sampling periods represented by ADD (x-axis) for comparison. H1 refers to the summer donor and H2 the winter donor.

4.3.2 Human lipid profiles

When analysing the relative abundances of the 30 lipids as a function of ADD, patterns related to the decomposition stages, and seasons, were noted, Appendix 3, Figure 4. S1 – 4. S30. For both the summer donor, H1, and the winter donor, H2, the lipid profiles could be correlated with the three distinct visual decomposition stages established prior; 'early', 'middle' and 'late'. The cumulative relative abundance of each stage, for each donor (Fig. 4.2 and Fig. 4.3) was therefore calculated, using a method adapted from Perrault et al. 2015 [9].

4.3.2.1 H1 (summer)

Overall, the trends observed in the lipid profiles for H1 (Fig. 4.2) were typical of what was expected to occur during the decomposition process. The unsaturated fatty acids demonstrated hydrogenation, which lead to a subsequent increase in the saturated fatty acids over time [10-12]. This was evident when comparing the results of the cumulative relative abundances of the 'early' stage to the 'late' stage for H1

(Fig. 4.2). The degradation of unsaturated fatty acids palmitoleic acid and linoleic acid, are expected to yield palmitic acid and oleic acid, respectively [13, 14], reflected in the results of the current study (Fig. 4.2). The cumulative relative abundance of palmitoleic acid was reduced from 35% during the 'early' stage, to 17% in the 'late' stage. This was also coupled with an increase in the cumulative relative abundance of its degradation product, palmitic acid, from 0% to 12%. Additionally, the cumulative relative abundance of linoleic acid was reduced from 10% to 1% between the 'early' and 'late' stages, while its degradation product, oleic acid, increased from 1% to 4% (Fig. 4.2). Interestingly, myristic acid demonstrated a high cumulative relative abundance during the 'early' and 'middle' stages for H1, with 37% and 49% respectively. However, this was then reduced to 1% during the 'late' stage (Fig. 4.2). Typically, it would be expected that the cumulative relative abundance of the shorter chain fatty acids, such as decanoic acid (C10:0) and azelaic acid (C9:0), would increase as a result of the decrease in myristic acid (C14:0), however this was not documented in the current results. Several explanations could account for this, ranging from inter-sample variability, to superposed concentrations of other more abundant lipids, resulting in overshadowing the abundance of these shorter chain fatty acids. Another interesting result was the increase in the cumulative relative abundance of arachidic acid from 0% in the 'early' stage, to 8% in the 'late' stage (Fig. 4.2). This provides some evidence to suggest the degradation of large chain fatty acids, such as behenic acid (C22:0).

Bile acids, deoxycholic and lithocholic acid, were also evident in the lipid profiles obtained from H1 (Fig. 4.2). Deoxycholic acid increased from a cumulative relative abundance of 6% in the 'early' stage, to 36% in the 'late' stage, while

lithocholic increased only from 1% to 4%, respectively (Fig. 4.2). Deoxycholic acid and lithocholic acid are secondary bile acids produced in the intestines as a result of microbial activity [15] and are the major bile constituents found in human faeces [15, 16]. The increase in the cumulative relative abundances of these secondary bile acids from the 'early' to the 'late' stages, suggests that the epithelial tissues of the gastro-intestinal tract had disintegrated, and released faecal matter as part of the decomposition fluids absorbed into the textiles [17].

Sterols did not demonstrate to be a significant factor in the lipid profiles obtained for H1 (Fig. 4.2), with the exception of stigmasterol which increased in its cumulative relative abundance from the 'early' stage of 1%, to the 'late' stage of 8%. Stigmasterol is a phytosterol [18] and so these results provide some evidence to suggest the growth of fungi or mould on the textiles.

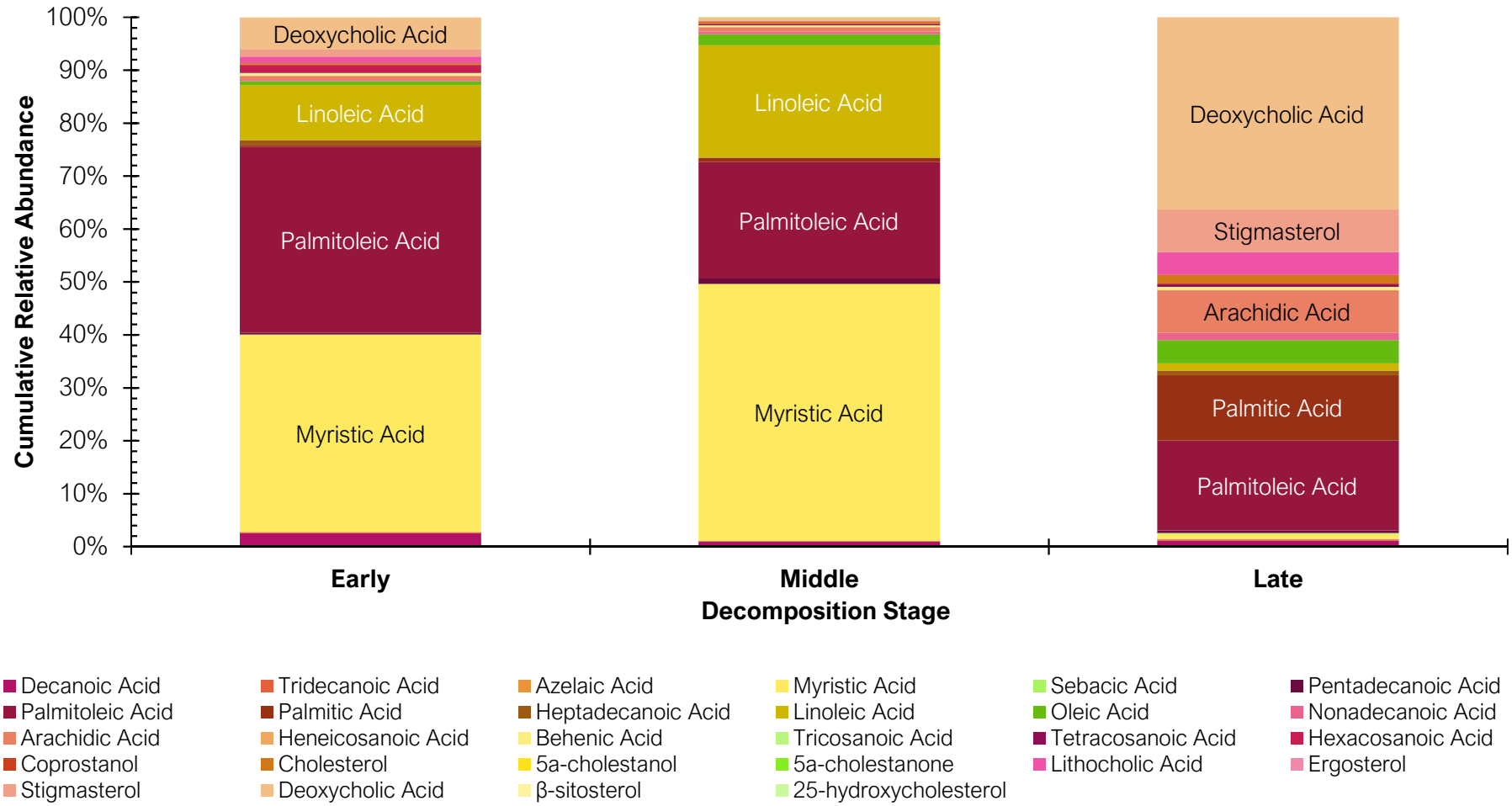

Fig. 4. 2 The cumulative relative abundances (%) of the lipid profiles obtained from textiles collected from H1, grouped by 'early', 'middle' and 'late' stages of decomposition.

4.3.2.2 H2 (winter)

In comparison, the lipid profiles obtained from H2 (Fig. 4.3) were less typical, and this is likely attributed to the contrasting seasons in which the donors were placed. This is typical of what is documented in cooler climates, particularly in Australia [8, 13], where decomposition is often delayed as the conditions are not conducive to soft-tissue degradation. Thus, explaining the poor degradation of lipids in this case. The cumulative relative abundance of the 'early' lipid profile for H2 (Fig. 4.3) was much less dominated by saturated and unsaturated fatty acids, than H1 (Fig. 4.2), with the exceptions of myristic acid (17%) and decanoic acid (12%). In addition, the 'early' lipid profile for H2 contained both bile acids, deoxycholic acid and lithocholic acid at respective cumulative relative abundances of 19% and 6% (Fig. 4.3).

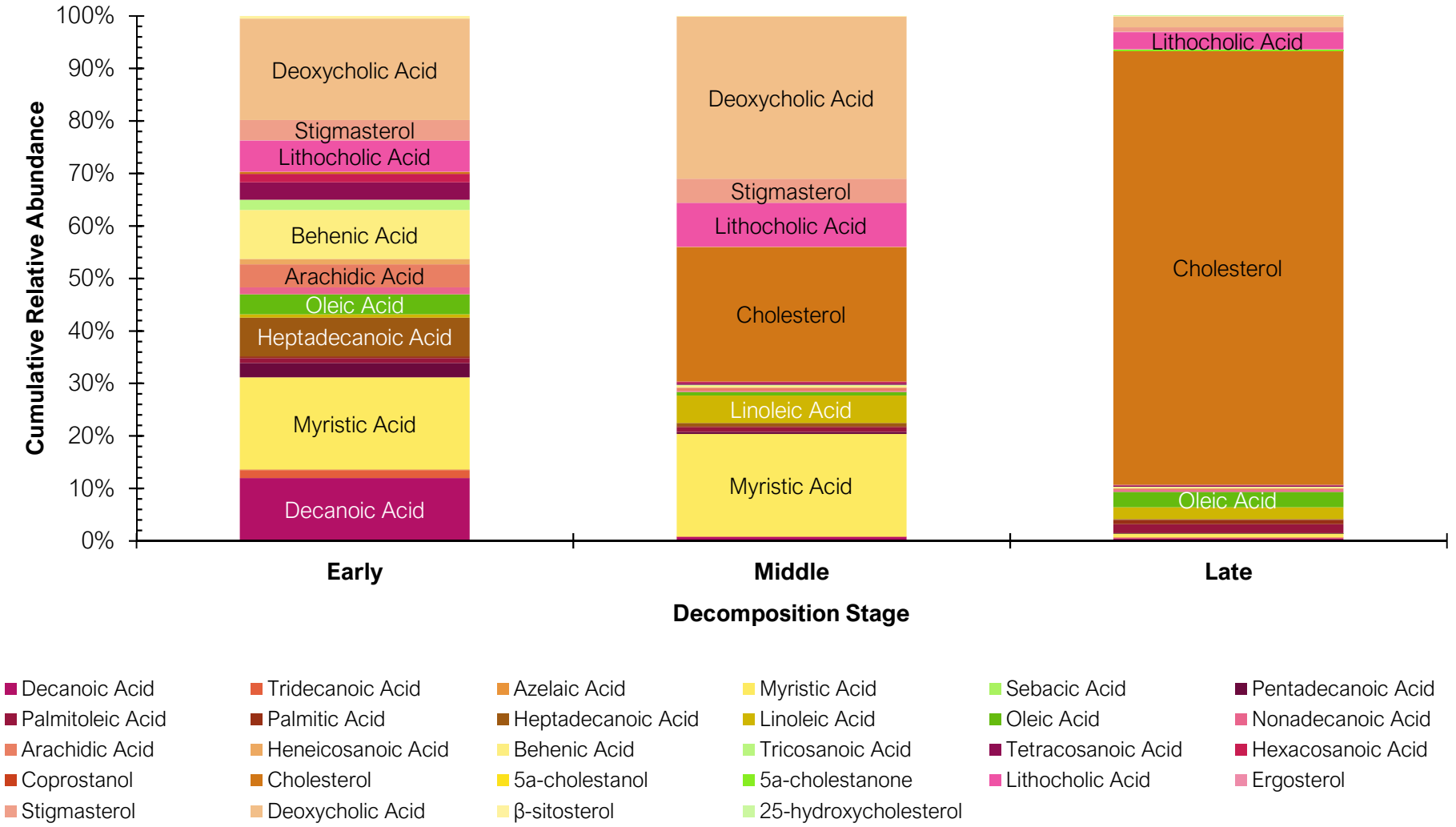

Fig. 4. 3 The cumulative relative abundances (%) of the lipid profiles obtained from textiles collected from H2, grouped by 'early', 'middle' and 'late' stages of decomposition.

During the 'middle' stage of decomposition for H2, the lipid profiles showed a greater relative cumulative abundance of myristic acid, 20%, deoxycholic acid, 31%, and cholesterol, 26% (Fig. 4.3). Interestingly, the lipid profile of the 'late' stage for H2 was heavily concentrated in cholesterol, with a cumulative relative abundance of 87%. This is in complete contrast to the summer donor H1, where little to no sterols were detected across any of the stages (Fig. 4.2). This is likely attributed to the seasonal differences mentioned previously, whereby the sub-optimal soft-tissue degradation conditions experienced in winter result in poor lipid degradation. In addition, the cumulative relative abundances represent 100% of all analytes, i.e., the overall lipid profile, and not the exact amount of each analyte. Therefore, when fewer lipids were present, this can overinflate the cumulative relative abundance of the analytes that were detected. Although cholesterol is a tissue-derived sterol in higher animals [19, 20], it is also ubiquitously found in soils as a result of plant and fungal contributions [21, 22]. In soil environments, the reduction pathway of cholesterol typically yields 5α-cholestanol, however this product can also be detected at trace concentrations in plants, faeces, and animal tissues [23, 24, 25]. An archaeological study by von der Lühe [26] investigated the use of sterols as biomarkers of human decomposition fluids in soil graves from World War II. In that study, the authors found high concentrations of the Δ^5-sterols, cholesterol, β-sitosterol and stigmasterol, which were consequently considered as the natural 'sterol background' in those soils [26]. In addition, these Δ^5-sterols were found to be ubiquitous across both test and reference samples, making it difficult to discern input source from human, plants, fungi or other eukaryotes [22, 26-28]. In contrast, a forensic decomposition study conducted by Luong et al. [5] successfully utilised cholesterol as a biomarker to track the lateral and vertical

migration of human decomposition fluids in a soil environment. The conflicting results obtained by von der Lühe [26] and Luong et al. [5] are likely attributed to the age of the samples, the former being of more archaeological origin and the latter, of forensic. In addition, the lipid profiles obtained from the present investigation support the conclusions of Luong et al [5], particularly when directly comparing the cumulative abundances of the samples obtained from H2, to the environmental control samples (Fig. 4.4). Here, the results clearly indicate, particularly during the 'middle' and 'late' stages, that the source of cholesterol is directly attributed to the decomposition ecology, and not just the environment (Fig. 4.4). Thus, further emphasising the importance of including the appropriate controls in such research and the use of a threshold. Particularly where the targets, in this case lipids, are ubiquitous in nature, and not exclusive to the test samples.

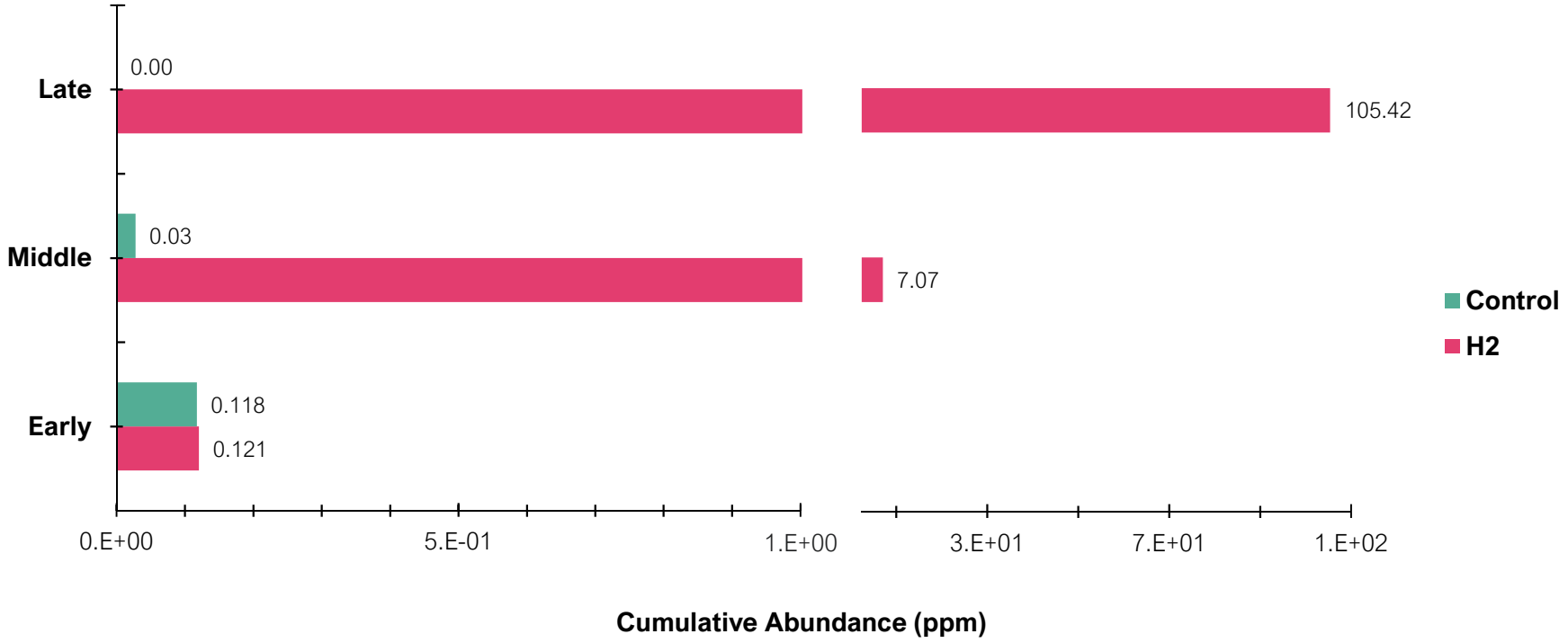

Fig. 4. 4 Comparison of the cumulative abundance (ppm) of cholesterol for H2 and respective controls across each decomposition stage.

4.4 Conclusions

When comparing the results of the post-mortem human lipid profiles obtained in the present study, to recent taphonomic work involving lipids obtained from decomposing human tissues [10] and sediments exposed to decomposition fluids [5], the trends are promising. Textiles have thus proven to be an excellent host for the collection and detection of decomposition lipids over time. In addition, due to the ubiquity of lipids in nature, the results of this study further highlight the importance of including controls, and reference samples, in such research in order to logically deduce conclusions regarding the decomposition ecology. These results also emphasise the urgency for future work to continue in this area in order expand the current dataset so that systematic differences between donors, and environmental variables, can be properly considered. With these considerations explored, lipids in textiles are a promising biomarker for human decomposition, with the potential to aid in future operational environments involving human remains. Particularly, in complex investigations where other target matrices, such as tissue or soil, are unavailable for analysis.

4.5 References

[1] M.S. Megyesi, S.P. Nawrocki, N.H. Haskell, Using accumulated degree-days to estimate the postmortem interval from decomposed human remains, J. Forensic Sci., 50 (3) (2005) 618-26. https://doi.org/10.1520/jfs2004017

[2] Z. Knobel, M. Ueland, K.D. Nizio, D. Patel, S.L. Forbes, A comparison of human and pig decomposition rates and odour profiles in an Australian environment, Aust. J. Forensic Sci., 51 (5) (2019) 557-572. https://doi.org/10.1080/00450618.2018.1439100

[3] A. Misra, N.V. Dhurandhar, Current formula for calculating body mass index is applicable to Asian populations, Nutr. & Diabetes, 9 (1) (2019) 3. https://doi.org/10.1038/s41387-018-0070-9

[4] S. Collins, B.H. Stuart, M. Ueland. Anatomical location dependence of human decomposition products in clothing, Aust. J. Forensic Sci., 55 (2023) 363-375. https://doi.org/10.1080/00450618.2021.1981443

[5] S. Luong, S.L. Forbes, J.F. Wallman, R.G. Roberts. Monitoring the extent of vertical and lateral movement of human decomposition products through sediment using cholesterol as a biomarker, Forensic Sci. Int., 285 (2018) 93-104. https://doi.org/10.1016/j.forsciint.2018.01.026

[6] J.A. Payne, A summer carrion study of the baby pig Sus Scrofa Linnaeus, Ecology, 46 (1965) 592-602. https://doi-org.ezproxy.lib.uts.edu.au/10.2307/1934999

[7] S. Collins, B.H. Stuart, M. Ueland. The use of lipids from textiles as soft-tissue biomarkers of human decomposition. Forensic Sci. Int., (2023) 111547. https://doi.org/10.1016/j.forsciint.2022.111547

[8] S. Collins, L. Maestrini, M. Ueland, B. Stuart, A preliminary investigation to determine the suitability of pigs as human analogues for post-mortem lipid analysis, Talanta Open, 5 (2022) 100100. https://doi.org/10.1016/j.talo.2022.100100

[9] K.A. Perrault, T. Rai, B.H. Stuart, S.L. Forbes, Seasonal comparison of carrion volatiles in decomposition soil using comprehensive two-dimensional gas chromatography–time of flight mass spectrometry, Anal. Methods, 7 (2) (2015) 690-698. https://doi.org/10.1039/C4AY02321H

[10] M. Ueland, S. Collins, L. Maestrini, S.L. Forbes, S. Luong. Fresh vs. frozen human decomposition – A preliminary investigation of lipid degradation products as biomarkers of post-mortem interval, Forensic Chem., 24 (2021) 100335. https://doi.org/10.1016/j.forc.2021.100335

[11] S.J. Notter, B.H. Stuart, R. Rowe, N. Langlois, The initial changes of fat deposits during the decomposition of human and pig remains, J. Forensic Sci., 54 (1) (2009) 195-201. https://doi.org/10.1111/j.1556-4029.2008.00911.x

[12] S.L. Forbes, B.B. Dent, B.H. Stuart, The effect of soil type on adipocere formation, Forensic Sci. Int. 154 (1) (2005) 35-43. https://doi.org/10.1016/j.forsciint.2004.09.108

[13] M. Ueland, S.L. Forbes, B.H. Stuart, Seasonal variation of fatty acid profiles from textiles associated with decomposing pig remains in a temperate Australian environment, Forensic Chem., 11 (2018) 120-127. https://doi.org/10.1016/j.forc.2018.10.008

[14] S.J. Notter, B.H. Stuart, B.B. Dent, J. Keegan, Solid-phase extraction in combination with GC/MS for the quantification of free fatty acids in adipocere, Eur. J. Lipid Sci. Technol., 110 (1) (2008) 73-80. https://doi.org/10.1002/ejlt.200700159

[15] P.G. Hatcher, P.A. McGillivary, Sewage contamination in the New York Bight. Coprostanol as an indicator, Environ. Sci. Technol., 13 (10) (1979) 1225-1229. https://doi.org/10.1021/es60158a015

[16] P. Gérard, Metabolism of cholesterol and bile acids by the gut microbiota, Pathogens, 3 (1) (2013) 14-24. https://doi.org/10.3390/pathogens3010014

[17] B.G. Ioan, C.N. Manea, B. Hanganu, L. Statescu, L.G. Solovastru, I.S. Manoilescu, The chemistry decomposition in human corpses, Revista De Chimie, 68 (2017) 1352, 1356. https://doi.org/ 10.37358/rc.17.6.5672

[18] D. Erney, A. Gillespie, D. Gilvydis, C. Poole, Explanation of the matrix-induced chromatographic response enhancement of organophosphorus pesticides during open tubular column gas chromatography with splitless or hot on-column injection and flame photometric detection, J. Chromatogr. A, 638 (1) (1993) 57-63. https://doi.org/10.1016/0021-9673(93)85007-T

[19] B. von der Lühe, J.J. Birk, L. Dawson, R.W. Mayes, S. Fiedler, Steroid fingerprints: Efficient biomarkers of human decomposition fluids in soil, Org. Geochem.,124 (2018) 228-237. https://doi.org/10.1016/j.orggeochem.2018.07.016

[20] M.D. Pickering, S. Ghislandi, M.R. Usai, C. Wilson, P. Connelly, D.R. Brothwell, B.J. Keely, Signatures of degraded body tissues and environmental conditions in grave soils from a Roman and an Anglo-Scandinavian age burial from Hungate, York, J. Archaeol. Sci., 99 (2018) 87-98. https://doi.org/10.1016/j.jas.2018.08.007

[21] J.D. Weete, M. Abril, M. Blackwell, Phylogenetic distribution of fungal sterols, PLoS One, 5 (5) (2010) e10899. https://doi.org/10.1371/journal.pone.0010899

[22] O.G. Mouritsen, M.J. Zuckermann, What's so special about cholesterol?, Lipids 39 (11) (2004) 1101-1113. https://doi.org/10.1007/s11745-004-1336-x

[23] E. Stellwag, P. Hylemon, 7alpha-Dehydroxylation of cholic acid and chenodeoxycholic acid by Clostridium leptum, J. Lipid Res., 20 (3) (1979) 325-333. https://doi.org/10.1016/S0022-2275(20)40615-7

[24] J.J. Murtaugh, R.L. Bunch, Sterols as a measure of fecal pollution, J. Water Pollut. Control Fed., 39 (1967) 404-409.

[25] M. Noda, M. Tanaka, Y. Seto, T. Aiba, C. Oku, Occurrence of cholesterol as a major sterol component in leaf surface lipids, Lipids, 23 (5) (1988) 439-444. https://doi.org/10.1007/BF02535517

[26] B. von der Lühe, K. Prost, J.J. Birk, S. Fiedler, Steroids aid in human decomposition fluid identification in soils of temporary mass graves from World War II, J. Archaeol. Sci. Rep., 32 (2020) 102431. https://doi.org/10.1016/j.jasrep.2020.102431

[27] W.W. Christie, X.J.S. Han, Lipid analysis: isolation, separation, identification and lipidomic analysis: Fourth Edition, Elsevier Ltd., 2003. https://doi.org/10.1533/9780857097866

[28] J.D. Weete, M. Abril, M. Blackwell, Phylogenetic distribution of fungal sterols, PLoS One, 5 (5) (2010) e10899. https://doi.org/10.1371/journal.pone.0010899

Chapter 5: The use of generalized linear mixed models to investigate lipids in textiles as biomarkers of decomposition.

Chapter 5: The use of generalized linear mixed models to investigate lipids in textiles as biomarkers of decomposition.

i. Preface

With the exception of minor editorial changes, Chapter 5 reproduces the following research manuscript; **S. Collins**, L. Maestrini, F.K.C. Hui, B.H. Stuart, M Ueland, (accepted May 2023). The use of generalized linear mixed models to investigate lipids in textiles as biomarkers of decomposition, iScience. Permissions for reuse of this article within this dissertation have been obtained.

ii. Statement of Contribution and Declaration

Sharni Collins: conceptualisation; methodology; validation; formal analysis; investigation; writing – original draft; writing - review and editing; Luca Maestrini: methodology; software; formal analysis; writing - review and editing; Francis K.C. Hui: methodology; software; formal analysis; writing - review and editing; Barbara Stuart: conceptualisation; methodology; writing – review and editing; supervision; Maiken Ueland: conceptualisation; methodology; writing - review and editing; supervision.

Graduate research student

Sharni Collins

Principal Supervisor

Production Note:
Signature removed
prior to publication.

Dr. Maiken Ueland

Co-supervisor

Production Note:
Signature removed
prior to publication.

Professor Barbara Stuart

Co-supervisor

Production Note:
Signature removed
prior to publication.

Dr. Luca Maestrini

Additional author

Production Note:
Signature removed
prior to publication.

Dr. Francis. K. Hui

5.1 Introduction

The overall rate, manner and progression of human decomposition is highly complex and dependent on a range of intrinsic and extrinsic variables. Because of this, time since death estimation continues to be a major challenge for forensic investigators when faced with the discovery of human remains. After death, the body undergoes a series of semi-predictable stages: fresh, bloat, active, advanced and skeletal [1]. However, the time that elapses between these stages can be unpredictable and often non-linear [2], making it very difficult to estimate the time since death.

Data obtained from both forensic casework and experimental research [3-6] have documented temperature to be one of the main extrinsic covariates influencing the rate and manner of decomposition. Work by Megyesi et al. in 2005 [7] demonstrated that 80% of the variation within decomposition can be accounted for by accumulated-degree-days (ADD). ADD are units that represent the accumulation of thermal energy in a chronological combination of time and energy [7]. In this manner, it is said that when equal units of thermal energy (ADD) are applied to remains, a relatively equal amount of decomposition is to be expected [8]. This is because climate affects the time expected to elapse during each decomposition stage, and thus determines the overall rate at which the remains will decay [3, 5]. Therefore, the ability to assess the impact of ADD on measurable outcomes of decomposition holds great potential for elucidating clarity regarding the problem of determining time since death.

Post-mortem lipid analysis is a promising new area of research in forensic taphonomy, with several recent works [9-12] demonstrating great success with the use of clothing as a host to capture these decomposition lipids. As the human body contains approximately 15% of adipose tissues [13], during the decomposition process, the lipids contained within these tissues are released into the immediate environment. Hence, by analysing the patterns in these post-mortem lipids, in conjunction with ADD, it is possible to use lipids as soft-tissue biomarkers of decomposition.

This idea was recently put forward in Chapters 3 and 4 where a method was successfully developed for the extraction and targeted analysis of post-mortem lipids in textiles using gas chromatography (GC) coupled with tandem mass spectrometry (MS/MS). That work provided novel results which related the cumulative relative abundance of 30 lipids, to three broad decomposition categories: 'early', 'middle' and 'late'. While the research in those chapters was fundamental in providing a foundation for future work, the results were mostly descriptive in nature, making it difficult to discern which of the lipids were most appropriate for investigation as soft-tissue biomarkers of decomposition.

The current chapter investigates the impact of ADD, as the unit of measurement for chronological time, on post-mortem lipids in clothing, as the measurable outcome of decomposition, using GC-MS/MS. Furthermore, this work uses generalized linear mixed models (GLMMs), containing both fixed and random effects where the latter is used to account for heterogeneity between individuals, to perform rigorous statistical analyses on the 30 lipid outcomes in combination with ADD. For the purpose of sample size requirements, the current study supplemented four pig cadavers, in

addition to two human donors. Pigs have often been utilised and widely accepted in taphonomic research due to anecdotal similarities to humans with respect to skin, digestive, and immunological systems [14-16], in addition to the natural limitations that come with working with human remains. As such, this study also provides a unique research opportunity to further investigate the interspecies differences between pigs and humans previously addressed in Chapter 2. The overall aim of the current chapter is to assess which of the 30 lipids were suitable for use as soft-tissue biomarkers of human decomposition.

5.2. Materials and methods

5.2.1. Field site

This study was conducted at the Australian Facility for Taphonomic Experimental Research (AFTER), an open eucalypt woodland on the Cumberland Plain in Western Sydney, privately owned by the University of Technology, Sydney (UTS). Weather conditions at the field site were monitored using a HOBO Weather Station with a HOBO® U30 No Remote Communication (NRC) data logger (OneTemp, Marleston).

5.2.2. Donors

A total of two human and four pig cadavers were utilised in this study. The human donors were received through the UTS Body Donation Program, with consent provided in accordance with the New South Wales Anatomy Act (1977). Ethics approval was provided by the UTS Human Research Ethics Committee (HREC ETH18-2999). The study consisted of two trials: Trial 1 commenced during the

Australian summer on January 29, 2021 and included one human donor (H1) and two pigs (P1 and P2). Trial 2 began in the Australian winter on June 11, 2021, and also included one human donor (H2) and two pigs (P3 and P4). All individuals were clothed in a white 100% cotton t-shirt, as described in [10], laid in a supine position on the soil surface at AFTER, and were allowed to decompose naturally. Anti-scavenging cages were used to allow natural entomological activity to progress, while preventing scavenging from local fauna. Donor information for all six individuals is summarised in Table 5. S1.

5.2.3. Sample collection

Textile samples were collected as outlined in [11]. In summary, textile samples were acquired in duplicates, at different time points, between day 0 and day 105 post-placement (Table 5. S1) from the anterior surface of the remains, using sterilised scissors. Each textile sample was photographed in-situ prior to collection and individually packaged in paper envelopes and stored in a cooler box for transportation to the laboratory, where the samples were kept at -18 °C when not in use. Each sample was dried in a fume cupboard at ambient temperature to inhibit bacterial and fungal growth, with adhering soil, hair and tissue removed.

5.2.4. GC-MS/MS sample preparation

Samples were prepared according to [12]. Specifically, 35 mg of textile matrix was weighed per sample. Afterward, 2 mL of HPLC-grade acetone (Sigma Aldrich, Sydney, Australia) and 2 mL of HPLC-grade chloroform (ChemSupply, Port Adelaide, Australia) were added to each vial and sonicated, without heat, for 20 minutes. The samples were then left at 4°C for 16 hours for extraction. Afterward, 1 mL of the

resulting extract was filtered through a 0.2 µm hydrophobic PTFE syringe filter (MicroAnalytix, Taren Point, Australia). Then, 25 µL of the filtered aliquots were spiked with 20 µL 10 ppm stearic acid-d3 (Merck, Macquarie Park, Australia) and 50 µL of 10 ppm cholesterol-d7 were added as internal standards. These were dried down under a gentle stream of nitrogen at 40°C. Samples were then reconstituted in 40 µL of N,O-bis(trimethylsilyl)trifluoroacetamide (BSTFA) with trimethylchlorosilane (TMCS) (PM Separations, Capalaba, Australia) and 10 µL of HPLC acetonitrile (Labscan Ltd., Gillman, Australia), and heated for 30 minutes at 70°C prior to being transferred into 250 µL polymer inserts (Agilent Technologies, Mulgrave, Australia). All samples were extracted and aliquoted in duplicates and injected onto the GC-MS/MS, where duplicate runs were conducted, giving a total of four data points per sample with the addition of a full scan injection for quality control purposes.

5.2.5. GC-MS/MS analysis

Analysis was performed using the method developed by [12] using a GCMS-TQ8030 Triple Quadrupole Gas Chromatograph fitted with an AOC-20i auto injector (Shimadzu, Kyoto, Japan). In detail, samples were injected in split mode at a temperature of 270 °C onto an Agilent HP-5MS (30 m x 0.250 mm) column with a film thickness of 0.25 µm. The system was run in multiple reaction monitoring (MRM) mode as outlined in [12], with a total run time of 18.75 minutes. A total of 30 lipids, containing a mixture of fatty acids and sterols, were selected for targeted analysis: arachidic acid, azelaic acid, behenic acid, cholesterol, coprostanol, decanoic acid, deoxycholic acid, ergosterol, heneicosanoic acid, heptadecanoic acid, hexacosanoic acid, lauric acid, linoleic acid, lithocholic acid, myristic acid, nonadecanoic acid, oleic

acid, palmitic acid, palmitoleic acid, pentadecanoic acid, sebacic acid, stearic acid, stigmasterol, tetracosanoic acid, tricosanoic acid, tridecanoic acid, β-sitosterol, 5α-cholestanol, 5α-cholestanone and 25-hydroxycholesterol.

5.2.6. Data processing and statistical analysis

The mean area results obtained from the GC-MS/MS MRMs were processed in accordance with [12]. In summary, the lipids were normalised to their respective internal standards; fatty acids to stearic acid-d3 and the sterols to cholesterol-d7. The normalised abundances were then subject to the exclusion criteria proposed in [12]; the original lipid response was retained for analysis if it was exclusive to the experimental samples. Or if the experimental response was ≥ 50% when divided by the sum of the experimental response and the control response, multiplied by 100. After the criteria was applied as in [12]; the analytes were further standardised by dividing the grand population standard deviation, per lipid (i.e. individuals aggregated). ADD was calculated as outlined in [7], and further standardised. As a covariate, ADD was also standardised by dividing by the cluster-specific standard deviation (i.e. by individual). These standardisation procedures are commonly used to stabilise mixed-effects model fitting, and do not have any statistical influence on the final model conclusions [17]. The standardised outcomes and ADD values were plotted using `R` [18] via the package `ggplot2` [19] (Figure 5. S1).

Generalized linear mixed models (GLMMs, [20-22]) were used as the principal method of statistical analysis in the study. GLMMs offer the capacity to handle non-continuous and non-normally distributed responses, where the fixed effects are shared among all the individuals (thus representing population-level effects) while the

random effects account for potential sources of heterogeneity across the six individuals (pigs and humans, thus representing individual-level effects). Put another way, the random effects are specific to a single individual, and are included to allow for the fact that analyte readings within an individual are likely to be more similar compared to readings between individuals i.e., the analyte readings within an individual are correlated over time.

In this study, a Tweedie distribution was used to model the response (analyte) in the GLMM, as this is well suited to data which are heavy-tailed and includes an excess of zero values [23], as is the case with many analytes used in the analysis (see Figure 5. S2 – S7). GLMMs with Tweedie responses were fitted for each outcome in `R` [18] using the `glmmTMB` package [24]. In more detail, let y_{ijk} denote the reading of the kth analyte ($k = 1,..., 30$) for the ith individual ($i = 1, \ldots, 6$) at the jth time point ($j = 1, \ldots, n$). Then the Tweedie-response GLMM is specified as follows:

$$[y_{ijk} \mid u_{ik}] \sim \text{Tweedie}\,(y_{ijk} | u_{ik}, \mu_{ijk}, p_k, \phi_k),$$

$$\log(\mu_{ijk}) = \beta_{0k} + \text{ADD}_i\beta_{1k} + \text{ADD}_i^2\beta_{2k} + \text{Human}_i\beta_{3k} + u_{ik}, \qquad u_{ik} \sim \mathit{Normal}\,(0, \sigma^2_k),$$

where, conditionally on the random effect u_i, the analytes y_{ijk} are independent observations from a Tweedie distribution with mean $\mu_{ijk} = E[y_{ijk}|u_{ik}]$, power parameter $1 < p_k < 2$ and dispersion parameter $\phi_k > 0$. Here, the fixed effects included in the GLMM are the intercept term, the standardised ADD value, its squared term (ADD^2), and the binary indicator of whether the ith individual was a human carcass or not (1=human; 0=pig). The squared effect of ADD, given by the inclusion of ADD2, was incorporated into the GLMMs as exploratory analysis suggested there was evidence for a quadratic relationship with ADD for several of the analytes. The random intercept ui was the only

random effect included in the model. Residual analysis (Table 5. S. 3) was performed using the `DHARMa` package [25], which in tandem with exploratory data analysis was used to both check model assumptions and decide on the final form of the fixed and random effects structure to include. After fitting GLMMs separately to each analyte, the point estimates of the fixed effects from each model were used to construct a matrix plot in `R` [18] to visualise the results.

5.3. Results and discussion

5.3.1. Visual decomposition

The visual stages of decomposition for all six individuals are described in detail in [12]. To summarise, the visual decomposition observed for the pigs and humans was considerably different between the summer and winter trials. During summer, H1, P1 and P2 were exposed to periods of heavy rainfall, with an overall mean temperature of 19.4°C. H1 underwent changes from the fresh stage to the bloat stage within the first ten days post-placement, and entered into an advanced state of mummification without a distinctive active stage. In contrast, P1 and P2 progressed from fresh to bloat and then into active decay within the first ten days post-placement, while later reaching full skeletonisation by day 35 post-placement.

The winter donors H2, P3 and P4 experienced less rainfall and a lower overall mean temperature of 14.8°C. As a result, all three individuals of the winter trial desiccated by day 42 post-placement, with less distinctive differences in the visual stages of decomposition between species compared to the summer trial.

5.3.2. GLMMs

Model selection was performed manually and began with running the full model proposed in Section 5.2.6. Backward selection was then performed by removing non-significant fixed effects (using a nominal significance level of 5%) and checking the residuals. Also, in some cases analysis of variance (ANOVA) was used to determine whether it was beneficial to switch to a purely fixed effect only model or not i.e., removing the random effect from the model. The point estimates and corresponding 95% confidence intervals of the fixed effects for all selected GLMMs are reported in Table 5. S2. For the analytes where a mixed effect model was used, point estimates and confidence intervals for the random intercept variance parameter, σ^2_k, are also displayed in Table 5. S2. The point estimates of fixed effects for the selected models are presented in the matrix plot (Fig. 5.1).

Of the 30 lipids analysed, the binary indicator for human was not statistically significant for 10 lipids, namely cholesterol, coprostanol, deoxycholic acid, 5α-cholestanone, hexacosanoic acid, lithocholic acid, palmitoleic acid, stigmasterol, β-sitosterol and 25-hydroxycholesterol (Table 5. S2). That is, for these 10 lipids, there was no statistically clear difference between pigs or humans in terms of the (log mean) lipid readings.

Of the above 10 lipids, the models for cholesterol, 5α-cholestanone and palmitoleic acid were of most interest, particularly when considering a forensic research perspective where lipid analysis (irrespective of species) is the goal. These three analytes were all found to exhibit a quadratic relationship with the covariate (ADD) (Fig. 5.1). Specifically, as ADD increased over time the lipid value also increased before the rate of increase slowed and eventually the analyte values

plateaued by the end of the study. This finding was consistent with the fact that, during the earlier stages of decomposition prior to the release of fluids into the environment, many zero readings are recorded for the lipids during this period (Figure 5. S2 – S7). Afterwards, once the fluids are released from the body, there is a sudden influx recorded for the outcomes. This influx then plateaus, reaching a point of saturation despite the continuum of ADD.

As discussed in the previous chapter, cholesterol is a tissue-derived sterol in higher animals [26, 27], however it is also ubiquitously found in soil environments due to plant and fungal contributions [28, 29]. In animals, cholesterol plays an integral part in lipid metabolism as well as being a structural component of plasma membranes [30, 31]. During the processes of decomposition, cholesterol is known to reduce into its stanol derivatives, 5α-cholestanol and coprostanol [32], with 5α-cholestanone being an intermediary of this reduction process [33, 34]. The difficulty with targeting sterols in decomposition studies lies in the background contribution of environmental sterols from plants, animals and fungi [35-37]. Thus, some caution should be employed when examining cholesterol in isolation for certain studies; instead, researchers should also consider targeting its degradation stanone intermediary, 5α-cholestanone.

On the other hand, palmitoleic acid is one of the most abundant unsaturated fatty acids in human serum and tissues [38] and has also been well documented to be a component in the decomposition by-product, adipocere [39, 40]. Adipocere is a grey, wax-like substance that is formed by the anaerobic bacterial hydrolysis of lipids [41, 42]. Thus, in context of the results from the model, it appears that palmitoleic acid can be used to track the formation of adipocere during decomposition. In

addition, due to the quadratic relationship exhibited between ADD and ADD^2 for the model of palmitoleic acid, it is clear that adipocere formation follows the aforementioned trend whereby this product is formed, it accumulates and then eventually dissipates to some degree over time. Thus, providing further insight to the decomposition timeline by the appearance and timing of these decomposition by-products.

The model for cholesterol included fixed effects only (Table 5. S2), suggesting that the (baseline) readings for this analyte were relatively similar across the individuals, while the models for palmitoleic acid and 5α-cholestanone included both fixed and random effects, suggesting more evidence of heterogeneity across the individuals (Table 5. S2). Considering this, cholesterol, 5α-cholestanone and palmitoleic acid provide great potential for future use as soft-tissue biomarkers of decomposition with studies that involve both pigs and humans.

The binary indicator for human showed a statistically significant and positive effect for the remaining 20 lipids (Fig. 5.1), meaning that there was evidence to suggest that all 20 of these lipids could potentially be used to differentiate between pigs and humans. However, the particular models for each analyte must be further considered in context of the available decomposition literature in order to extract any meaningful conclusions. Several of these 20 lipids can be traced to sources other than soft-tissue decomposition e.g., dietary (i.e. heptadecanoic acid [43]) or environmental (i.e. ergosterol [44]) factors. Although some of these lipids may provide some useful insight to the decomposition ecology as a whole, the aim of the current study was to identify lipids that could be suitable as soft-tissue biomarkers of decomposition.

With this in mind, the models for unsaturated oleic acid and saturated palmitic acid were the most interesting (Fig. 5.1). Both of these lipids, which are known decomposition by-products [39, 40], ended up requiring the full GLMM outlined in Section 5.2.6 (Table 5. S2). Like cholesterol, 5α-cholestanol and palmitoleic acid, the models for oleic acid and palmitic acid also established a clear quadratic relationship between the log mean of the outcome and the covariate. This trend directly reflects the dynamicity of the decomposition process itself, whereby lipids are released from the body and absorbed by the textiles as a result of active decay, and slowly reduce over time as the remains enter into the advanced and skeletal stages of decomposition. This again offers evidence that these particular lipids could be suitable for further investigation as soft-tissue biomarkers of human decomposition.

It is important to recognise that some of the heterogeneity observed for several of the analytes, namely myristic acid, oleic acid, palmitic acid and palmitoleic acid were influenced by some extreme observations for H1, as shown in the scatter plots (Figure 5. S1) and random effects plots (Figure 5. S8). While it is conceivable that the placement season [3-6], being summer for H1 and winter for H2, could have impacted on these results, it is just as likely that systematic differences could have driven this. As such, it must be acknowledged that H1 may be responsible for driving the strong positive effect for the binary indicator of human group for some of these analytes. In order to draw meaningful conclusions as to which lipids are best suitable as human-specific biomarkers of decomposition, further investigation is required.

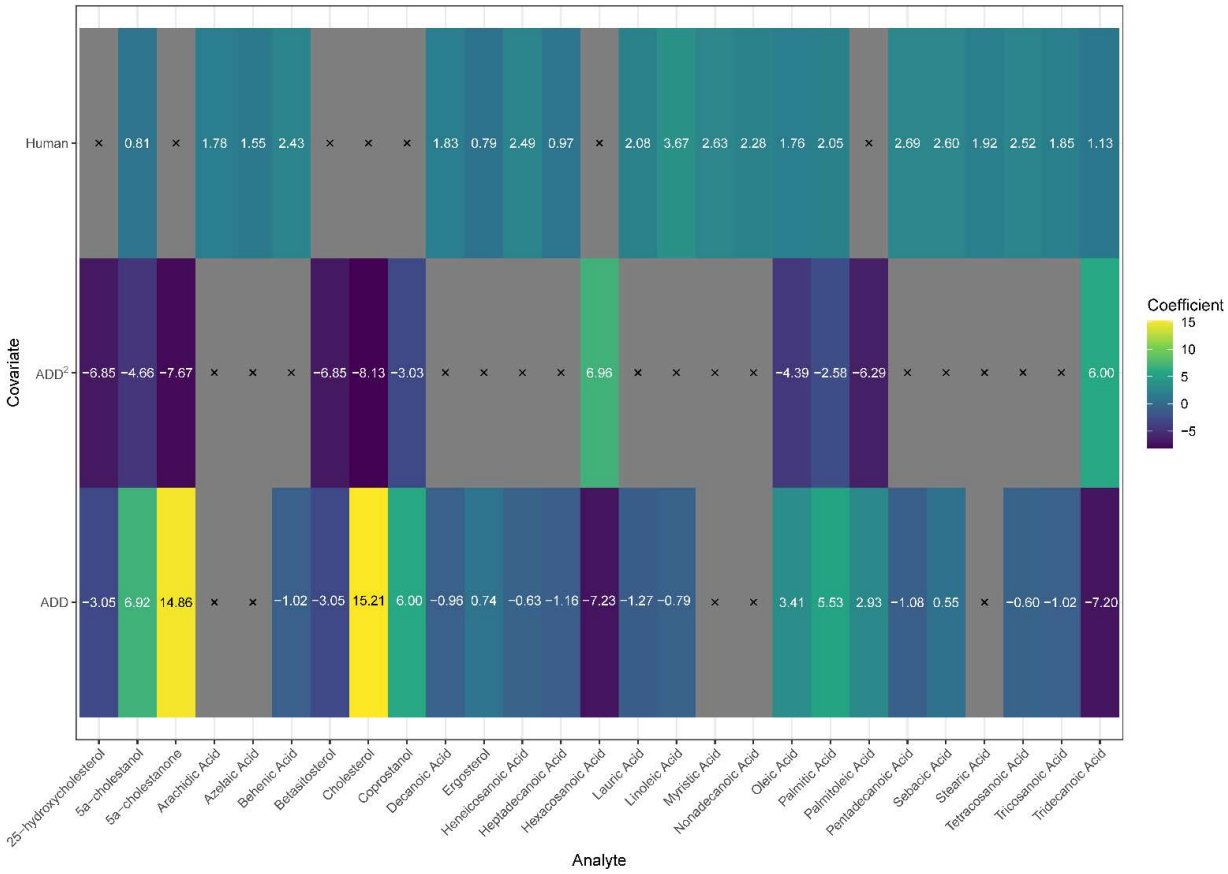

Fig. 5. 1 Matrix plot displaying the estimated fixed effects for the models fitted to the analytes. x indicates the corresponding covariate was not included in the selected model. Yellow indicates the covariate had a high positive effect on the analyte in question while dark blue indicates the covariate had a high negative impact.

5.4. Conclusions

Overall, the results of this study serve as a cornerstone for the future of decomposition lipid analysis. Success was achieved in this work, which could relate ADD, as the chronological measurement of time, to lipids in textiles, as the measurable outcomes of decomposition. In addition, the results provided further insight to the interspecies differences addressed in [11] and Chapter 2, with particular mention to the lipids related to the formation of adipocere. Although the study presented results obtained from lipids in textiles, it is possible that the approach could be applied to other matrices that host decomposition lipids, such as tissue or soil.

Based on preliminary findings, these results indicate that oleic acid and palmitic acid would be the most suitable lipids for future use as soft-tissue biomarkers of human decomposition. However, in order to fully reach meaningful conclusions, the authors recommend future work to include several more donors, with samples obtained over many years. This type of longitudinal analysis would allow for the detection of changes in the lipid characteristics at both the group and individual level, which would provide understanding about the efficacy and stability of these lipids as potential biomarkers. With a larger dataset, it could be possible to make predictions of ADD, given the measurable lipid outcomes.

5.5. References

[1] J.A. Payne, A summer carrion study of the baby pig Sus Scrofa Linnaeus, Ecology. 46 (1965) 592-602. https://doi-org.ezproxy.lib.uts.edu.au/10.2307/1934999

[2] Z. Knobel, M. Ueland, K.D. Nizio, D. Patel, S.L. Forbes, A comparison of human and pig decomposition rates and odour profiles in an Australian environment, Aust. J. Forensic Sci., 51(2019) 557-572. https://doi.org/10.1080/00450618.2018.1439100

[3] H. Gill-King, Chemical and ultrastructural aspects of decomposition. in: W.D. Haglund, M. H. Sorg (Eds.) Forensic taphonomy: the postmortem fate of human remains, CRC Press, 1997, pp.93-108.

[4] V. Bugelli, M. Gherardi, M. Focardi, V. Pinchi, S. Vanin, C. P. Campobasso, Decomposition pattern and insect colonization in two cases of suicide by hanging, Forensic Sci. Res., 3 (1) (2018) 94-102. https://doi.org/10.1080/20961790.2017.1418622

[5] E.M.J. Schotsmans, N. Marquez-Grant, S.L. Forbes, Taphonomy of human remains: forensic analysis of the dead and the depositional environment. John Wiley & Sons, 2017.

[6] R.C. Janaway, Degradation of clothing and other dress materials associated with buried bodies, in: W.D. Haglund, M.H. Sorg (Eds.) Advances in Forensic Taphonomy: Method, theory and archaeological perspectives, CRC Press: Boca Raton, 2002, pp. 379-402.

[7] M.S. Megyesi, S.P. Nawrocki, N.H. Haskell, Using accumulated degree-days to estimate the postmortem interval from decomposed human remains, J. Forensic Sci 50 (3) (2005) 618-26. https://doi.org/10.1520/jfs2004017

[8] T. Simmons, R. E. Adlam, C. Moffatt, Debugging decomposition data--comparative taphonomic studies and the influence of insects and carcass size on decomposition rate, J. Forensic Sci., 55 (1) (2010) 8-13. https://doi.org/ 10.1111/j.1556-4029.2009.01206.x

[9] S. Collins, B.H. Stuart, M. Ueland, Monitoring human decomposition products collected in clothing: an infrared spectroscopy study, Aust. J. Forensic Sci., 52 (2020) 428-438. https://doi.org/10.1080/00450618.2019.1593504

[10] S. Collins, B.H. Stuart, M. Ueland. Anatomical location dependence of human decomposition products in clothing, Aust. J. Forensic Sci., 55 (2023) 363-375. https://doi.org/10.1080/00450618.2021.1981443

[11] S. Collins, L. Maestrini, M. Ueland, B.H. Stuart. A preliminary investigation to determine the suitability of pigs as human analogues for post-mortem lipid analysis. Talanta Open. (2022) 100100. https://doi.org/10.1016/j.talo.2022.100100

[12] S. Collins, B.H. Stuart, M. Ueland. The use of lipids from textiles as soft-tissue biomarkers of human decomposition. Forensic Sci. Int., (2023) 111547. https://doi.org/10.1016/j.forsciint.2022.111547

[13] D.L. Nelson, M.M. Cox, Lehninger Principles of Biochemistry: sixth ed., Macmillan Learning, 2008.

[14] H.J. Rothkotter, Anatomical particularities of the porcine immune system--a physician's view, Dev. Comp. Immunol., 33 (2009) 267-272. https://doi.org/10.1016/j.dci.2008.06.016

[15] F. Meurens, A. Summerfield, H. Nauwynch, L. Saif, V. Gerdts, The pig: a model for human infectious diseases, Trends Microbiol., 20 (2012) 50-57. https://doi.org/10.1016/j.tim.2011.11.002

[16] K.H. Mair, C. Sedlak, T. Käser, A. Pasternak, B. Levast, W. Gerner, A. Saalmüller, A. Summerfield, V. Gerdts, H.L. Wilson, F. Meurens, The porcine innate immune system: an update, Dev. Comp. Immunol., 45 (2014) 321-343. https://doi.org/10.1016/j.dci.2014.03.022

[17] G.W. Milligan, M.C. Cooper, A study of standardization of variables in cluster analysis, J. Classif., 5 (1988) 181-204.

[18] Rstudio Team, R: A language and environment for statistical computing, R Core Team, R Foundation for Statistical Computing, Vienna, Austria, 2021.

[19] H. Wickham, W. Chang, M.H. Wickham, Package 'ggplot2', Create elegant data visualisations using the grammar of graphics. Version 2.1 (2016) 1-189.

[20] W.W. Stroup, Generalized linear mixed models: modern concepts, methods and applications, CRC press, 2012.

[21] S.R. Searle, C.E. McCulloch, J.M. Neuhaus, Generalized, linear, and mixed models, John Wiley & Sons, 2011.

[22] J.J. Faraway, Extending the linear model with R: generalized linear, mixed effects and nonparametric regression models, Chapman and Hall/CRC, 2016.

[23] M.C. Tweedie, An index which distinguishes between some important exponential families, In: Statistics: Applications and new directions: Proc. Indian statistical institute golden Jubilee International conference, 1984.

[24] A. Magnusson, H. Skaug, A, Nielsen, C. Berg, K. Kristensen, M. Maechler, K. van Bentham, B. Bolker, M. Brooks, M.M. Brooks, Package 'glmmtmb', R Package Version 0.2.0 (2017).

[25] F. Hartig, M.F. Hartig, Package 'DHARMa', *Vienna, Austria: R Development Core Team* (2017).

[26] B. von der Lühe, J.J. Birk, L. Dawson, R.W. Mayes, S. Fiedler, Steroid fingerprints: Efficient biomarkers of human decomposition fluids in soil, Org. Geochem.,124 (2018) 228-237. https://doi.org/10.1016/j.orggeochem.2018.07.016

[27] M.D. Pickering, S. Ghislandi, M.R. Usai, C. Wilson, P. Connelly, D.R. Brothwell, B.J. Keely, Signatures of degraded body tissues and environmental conditions in grave soils from a Roman and an Anglo-Scandinavian age burial from Hungate, York, J. Archaeol. Sci., 99 (2018) 87-98. https://doi.org/10.1016/j.jas.2018.08.007

[28] J.D. Weete, M. Abril, M. Blackwell, Phylogenetic distribution of fungal sterols, PloS one 5 (5) (2010) e10899. https://doi.org/10.1371/journal.pone.0010899

[29] O.G. Mouritsen, M.J. Zuckermann, What's so special about cholesterol?, Lipids 39 (11) (2004) 1101-1113. https://doi.org/10.1007/s11745-004-1336-x

[30] W.W. Christie, Lipid analysis, Pergamon press, Oxford, 2003.

[31] W.W. Christie, X.J.S. Han, Lipid analysis: isolation, separation, identification and lipidomic analysis: Fourth Edition, Elsevier Ltd., 2003. https://doi.org/10.1533/9780857097866

[32] R. Leeming, A. Ball, N. Ashbolt, P. Nichols, Using faecal sterols from humans and animals to distinguish faecal pollution in receiving waters, Water research, 30 (1996), 2893-2900

[33] J.O. Grimalt, P. Fernandez, J.M. Bayona, J. Albaiges, Assessment of faecal sterols and ketones as indicators of urban sewage inputs to coastal waters, Environ. Sci. & Technol., 24 (3) (1990) 357-363. https://doi.org/10.1021/es00073a011

[34] S.J. Gaskell, G. Eglinton, Rapid hydrogenation of sterols in a contemporary lacustrine sediment, Nature, 254 (5497) (1975) 209-211. https://doi.org/10.1038/254209b0

[35] P.G. Hatcher, P.A. McGillivary, Sewage contamination in the New York Bight. Coprostanol as an indicator, Environ. Sci. Technol., 13 (10) (1979) 1225-1229. https://doi.org/10.1021/es60158a015

[36] J.J. Murtaugh, R.L. Bunch, Sterols as a measure of fecal pollution, J. Water Pollut. Control Fed., (1967) 404-409.

[37] M. Noda, M. Tanaka, Y. Seto, T. Aiba, C. Oku, Occurrence of cholesterol as a major sterol component in leaf surface lipids, Lipids, 23 (5) (1988) 439-444. https://doi.org/10.1007/BF02535517

[38] M.E. Frigolet, R. Gutiérrez-Aguilar, The role of the novel lipokine palmitoleic acid in health and disease, Adv Nutr., 8 (1) (2017) 173s-181s. https://doi.org/10.3945/an.115.011130

[39] S.J. Notter, B.H. Stuart, R. Rowe, N. Langlois, The initial changes of fat deposits during the decomposition of human and pig remains, J. Forensic Sci., 54 (2009) 195-201. https://doi.org/10.1111/j.1556-4029.2008.00911.x

[40] S.J. Notter, B.H. Stuart, B.B. Dent, J. Keegan, Solid-phase extraction in combination with GC/MS for the quantification of free fatty acids in adipocere, Eur. J. Lipid Sci. Technol., 110 (1) (2008) 73-80. https://doi.org/10.1002/ejlt.200700159

[41] B.H. Stuart, L. Craft, S.L. Forbes, B.B. Dent, Studies of adipocere using attenuated total reflectance infrared spectroscopy, Forensic Sci. Med. Pathol., 1(3) (2005) 197-201. https://doi.org/10.1385/FSMP:1:3:197

[42] B.H. Stuart, Decomposition chemistry: overview, analysis, and interpretation, in: J.A Siegel, P.J. Saukko, M.M. Houck, (Eds.), Encyclopedia of Forensic Sciences, second ed., Academic Press, 2013, pp. 11–15.

[43] L. Hodson, H.C. Eyles, K.J. McLachlan, M.L. Bell, T.J. Green, C.M. Skeaff, Plasma and erythrocyte fatty acids reflect intakes of saturated and n–6 PUFA within a similar time frame, Nutr. J., 144 (1) (2014) 33-41. https://doi.org/10.3945/jn.113.183749

[44] P. Battilani, G. Chiusa, C. Cervi, M. Trevisan, C. Ghebbioni, Fungal growth and ergosterol content in tomato fruits infected by fungi, Ital. J. Food Sci., (1996) 283-289.

Chapter 6: Conclusions and recommendations for future work.

Chapter 6: Conclusions and recommendations for future work

6.1. Overview

Clothing materials are a ubiquitous source of physical evidence in forensic cases, particularly when involving human remains. Despite often being used in criminal cases to aid in the determination of the nature of the death or the identification of the victim, these materials have also proven to be an excellent host for decomposition fluids. Therefore, the ability to assess the patterns in the decomposition fluids captured in textiles, in conjunction with the decomposition timeline, holds great potential for elucidating clarity regarding the enigma that is time since death. Henceforth also increasing the evidentiary value of clothing evidence found at crime scenes.

In Chapter 2, a comparative study was undertaken on decomposing pigs and humans from AFTER, using cotton materials as the host for decomposition lipids. ATR-FTIR spectroscopy was used to target known lipid regions and semi-parametric regression models in linear mixed model form with Markov chain Monte Carlo (MCMC) sampling was employed to statistically investigate the lipids on a time-dependent scale. Overall, the results of this study provided preliminary evidence that pigs and humans are not statistically interchangeable with respect to their post-mortem lipids, in an Australian winter or summer season. The research in this chapter also provided the first comparative study of its kind to utilise post-mortem lipids as a measurable outcome to assess the degree of difference between these species in the southern hemisphere. Despite the major advantages that come with using attenuated total reflectance – Fourier transform infrared (ATR-FTIR) spectroscopy, particularly in

a forensic context, the completion of this work highlighted the need for a more specific and targeted method to analyse lipids in textiles.

Chapter 3 therefore documented the development and optimisation of a novel targeted analytical workflow for the analysis of post-mortem lipids in textiles using gas chromatography (GC) tandem mass spectrometry (MS-MS). This work led to the development of a novel analytical workflow for the extraction, separation and detection of 30 post-mortem lipids collected in textiles. The work in this chapter also revealed significant challenges associated with working with decomposition samples in relation to extraction efficiencies and matrix effects that could have a significant impact on work that aimed to be more quantitative. As lipids are ubiquitous in nature, sources of lipid contamination were also explored in this chapter. It was reported that stearic acid, lauric acid, myristic acid and deoxycholic acid were found at detectable limits in most controls and were likely contaminants from human sweat and manual handling in the manufacturing and selling processes of the materials. The results in this study highlighted the importance of controls in such experimental work and led to the application of a simple classification system to establish a threshold for further experimental analysis. This data normalisation technique provided useful information about the relative abundance of the target lipids in each sample on a time dependent scale which was able to provide insight to the degradation patterns of the lipids collected in the textiles over time.

In Chapter 4, the methods developed in Chapter 3 were applied as a preliminary investigation to examine human decomposition lipid profiles extracted from textiles associated with remains. The results of that chapter provided novel results which could relate the cumulative relative abundance of 30 lipids, to three

broad decomposition categories: ‘early’, ‘middle’ and ‘late’. While this research was fundamental in providing a proof-of-concept and a foundation for future work, the results were mostly descriptive in nature.

Therefore, the final chapter of this thesis, Chapter 5, set out to thoroughly investigate the impact of Accumulated Degree Days (ADD), as the unit of measurement for chronological time, on post-mortem lipids in clothing, as the measurable outcome of decomposition, using generalized linear mixed models. The data included in this chapter was obtained from both pig and human remains in order to meet sample size requirements for modelling. The results of this indicated that oleic acid and palmitic acid would be the most suitable lipids to target in future as soft-tissue biomarkers of human decomposition. In addition, this work also highlighted that cholesterol, 5α-cholestanone and palmitoleic acid would be great potential targets for use as soft-tissue biomarkers of decomposition with studies that involved both pigs and humans.

6.2. Future recommendations and concluding remarks

The work in this thesis highlights the great potential that lipids in textiles hold for the future of decomposition research. Through the application of both ATR-FTIR spectroscopy and GC-MS/MS, it was possible to detect, monitor and relate lipids captured in textiles to the decomposition timeline. However, given the natural limitations that are involved when working with human remains, further work is needed.

While the methods employed in this work, particularly relating to the GC-MS/MS component, were found to be successful in the extraction and detection of

post-mortem lipids in textiles for the purposes of this thesis, they remain strictly experimental. In order to reach a point where the methods within this thesis could be employed operationally in a forensic context, significant work is needed to validate such methods. It is expected that such work could also expand beyond textiles, incorporating several other decomposition matrices that serve as a host for lipids, such as soil or even tissue. Therefore, providing a variety of target matrices for forensic investigators to target if faced with an assortment of scenarios relating to complex death investigations.

With respect to the methods, the exploration and testing of other chromatographic columns that are lipid-specific to increase limit of detection and reduce noise, in addition to alternative derivatization protocols is recommended. These changes hold great potential for enhancing the quality and repeatability of the work.

It is recommended that comparative studies, involving both human and pig donors, be repeated, over different seasons, and extending over multiple years. This repetition and longitudinal type of sampling will only improve the current understanding and provide a clear insight regarding the intra- and inter-donor variability that inevitably exists due to systematic differences. The use of both human and pig donors also provides the opportunity to simultaneously continue the assessment of species differences, a comparison that is of major interest in the field of forensic taphonomy. In addition, by repeating these studies and consequently expanding the database, the results from future statistical modelling are likely to reach more concrete conclusions, particularly with respect to determining biomarkers of decomposition. The success founded by the use of generalised linear mixed models

(GLMMs) for the GC-MS/MS data in Chapter 5 serves as a cornerstone for the future of forensic taphonomy. With the aforementioned recommendations, GLMMs hold the potential to work retrogressively, given the value of a lipid outcome, to predict ADD. A capability that could greatly impact on the world of operational forensic science. Furthermore, exploring the full metabolomic pathways could provide further insight to whether certain lipids are converted or released over the decomposition timeline.

With respect to the textiles themselves, it is recommended that various different textile types be investigated for their suitability as hosts for post-mortem lipids. It is expected that textiles of differing materials, dyes and compositions will have some impact on the overall chemistry, and so it would be of great benefit to explore a variety of materials encountered in casework such as nylon, polyester and elastane.

Overall, this work demonstrated that cotton textiles serve as an excellent medium for post-mortem lipids released from decomposing remains. Furthermore, these lipids proved to be of substantial use when relating their detection and monitoring their patterns, in conjunction with the decomposition timeline. Lipids in textiles therefore, hold considerable potential in the future of forensic science as an additional means of estimating time since death, providing valuable information that could aid in solving future cases involving human remains.

Appendices

Appendix 1: Supplementary information associated with Chapter 2

i. https://doi.org/10.1016/j.talo.2022.100100

Table of Contents

Appendix 1: Supplementary information associated with Chapter 2

Table 2.S. 1 Samples collected for Trial 1 and Trial 2

Trial	*Day (post-placement)*	*Start and End Dates*
1	0, 3, 7, 10, 17, 20, 28, 35, 42, facility closed due to local floods, 70, 105	29/01/21 – 14/05/21
2	0, 1, 3, 6, 10, 13, 17, 23, 26, 31, 35, 42, 49, 56, 63, 69, 84, 105	11/06/21 – 24/09/21

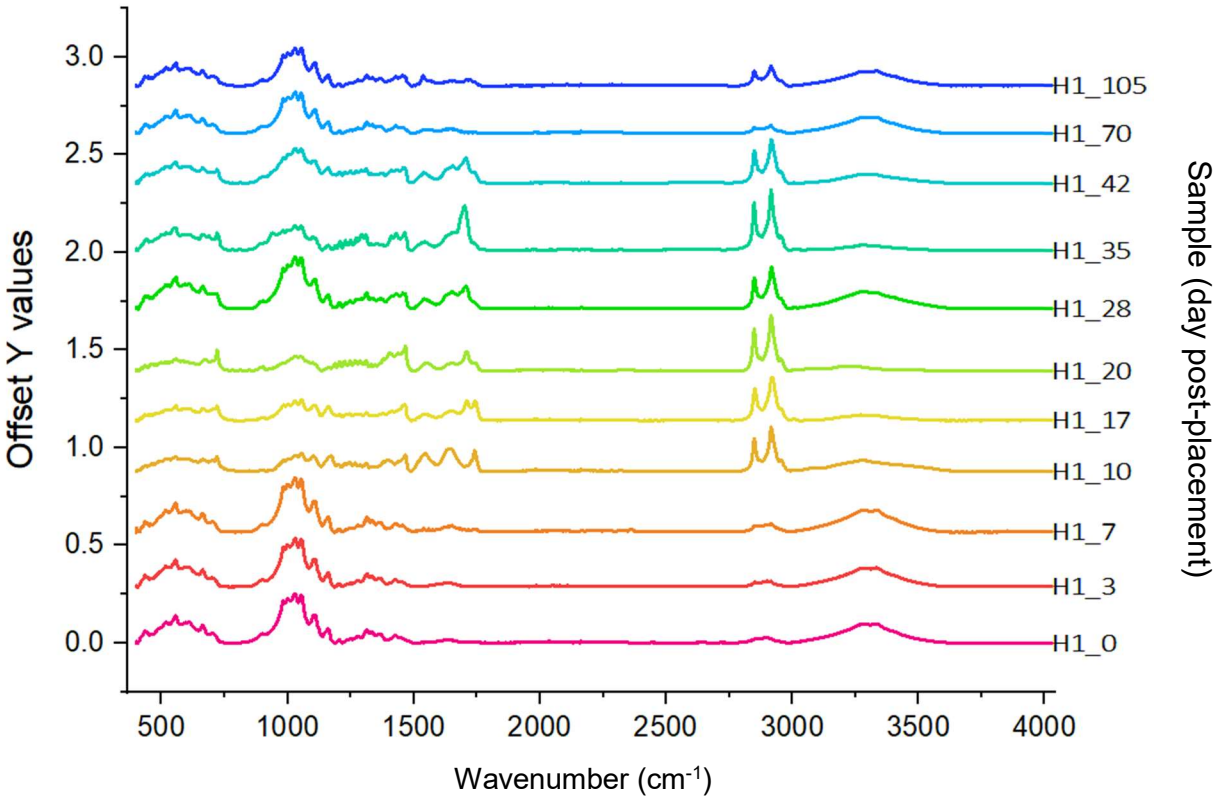

Figure 2.S. 2 Averaged stacked IR spectra for H1 of Trial 1. The x-axis represents the wavenumber (cm-1) and the y-axis represents the offset Y (absorbance values).

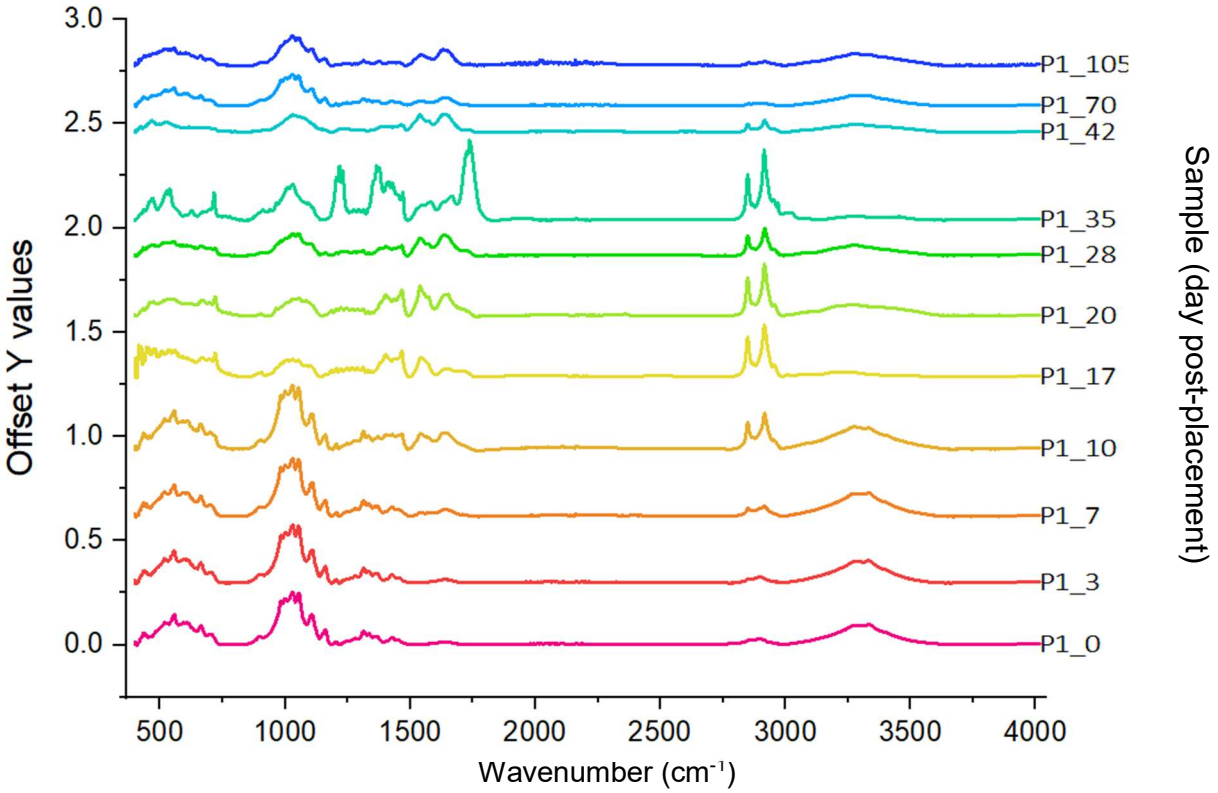

Figure 2.S. 1 Averaged stacked IR spectra for P1 of Trial 1. The x-axis represents the wavenumber (cm-1) and the y-axis represents the offset Y (absorbance values).

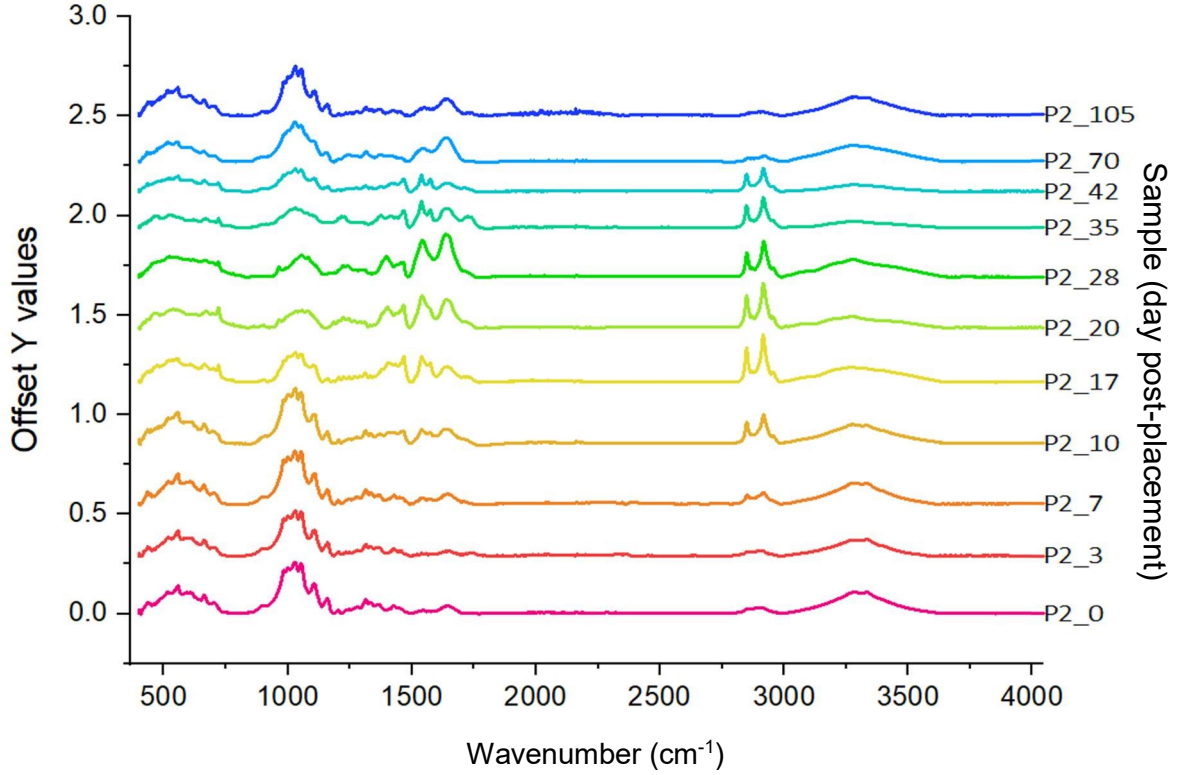

Figure 2.S. 3 Averaged stacked IR spectra for P2 of Trial 1. The x-axis represents the wavenumber (cm-1) and the y-axis represents the offset Y (absorbance values).

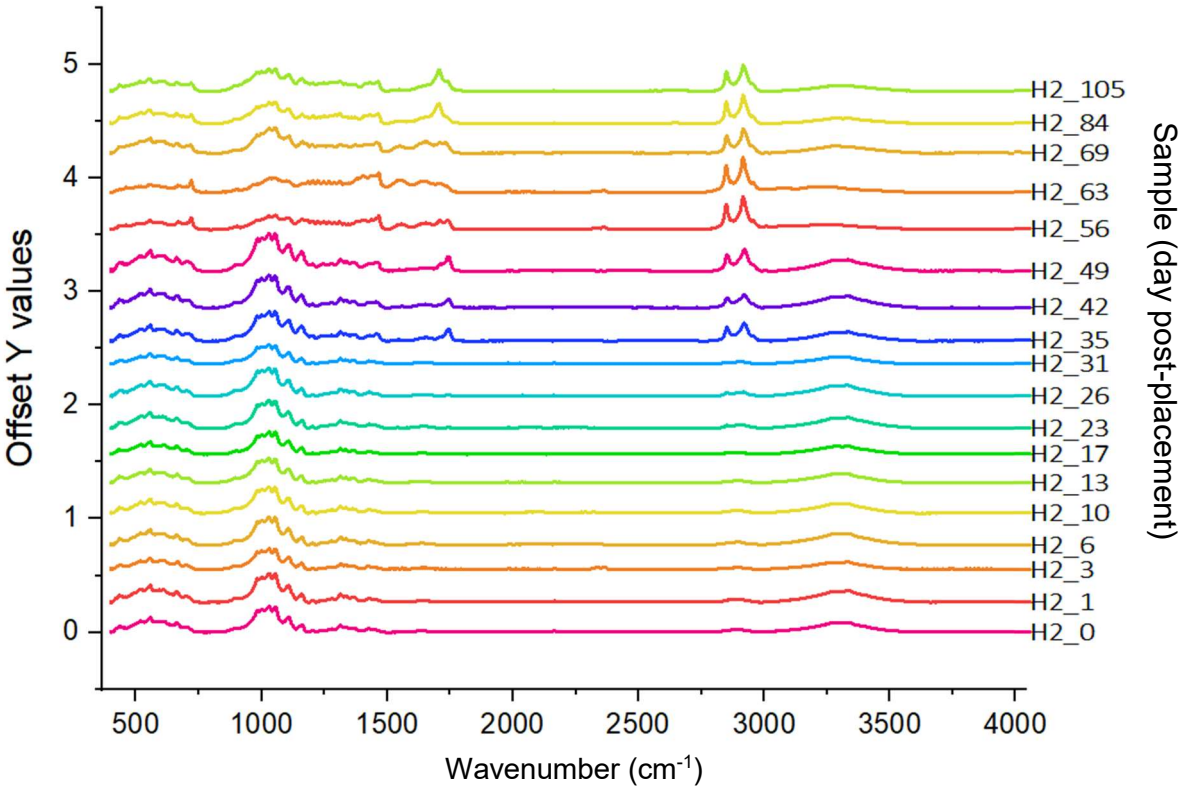

Figure 2.S. 4 Averaged stacked IR spectra for H2 of Trial 2. The x-axis represents the wavenumber (cm-1) and the y-axis represents the offset Y (absorbance values).

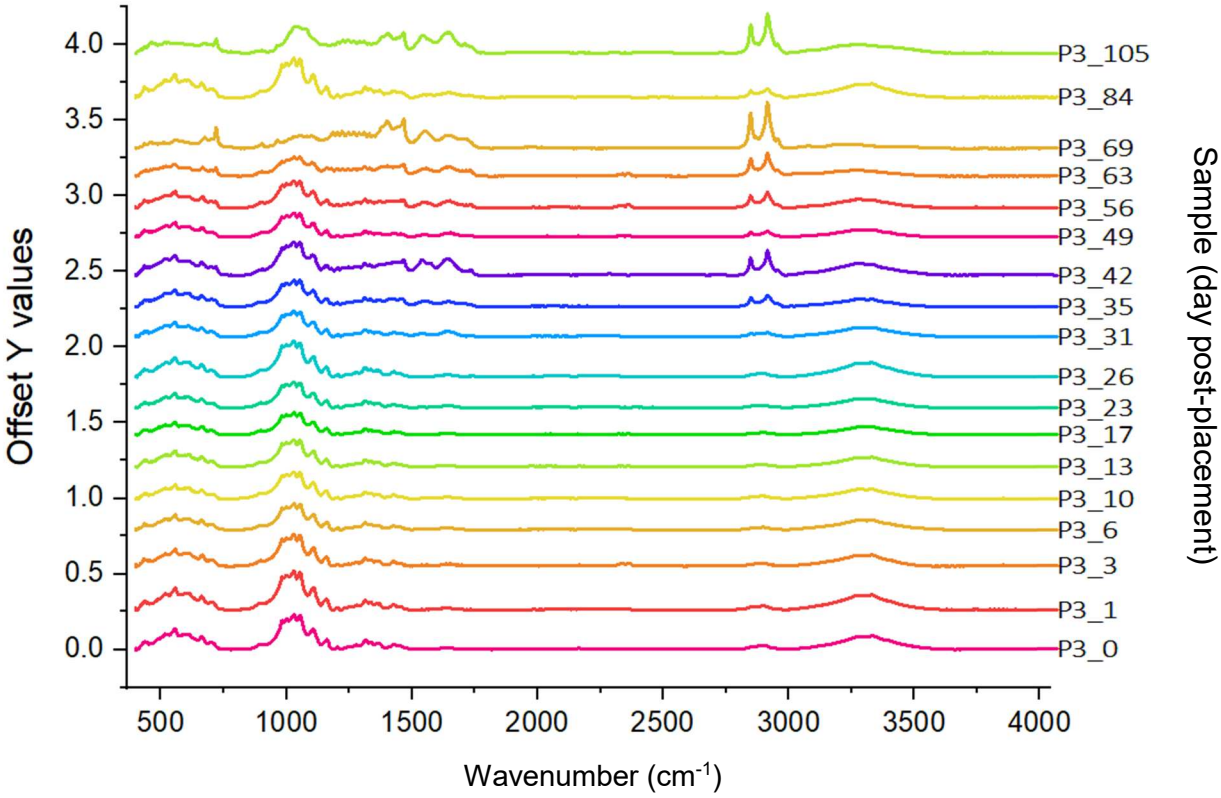

Figure 2.S. 5 Averaged stacked IR spectra for P3 of Trial 2. The x-axis represents the wavenumber (cm-1) and the y-axis represents the offset Y (absorbance values).

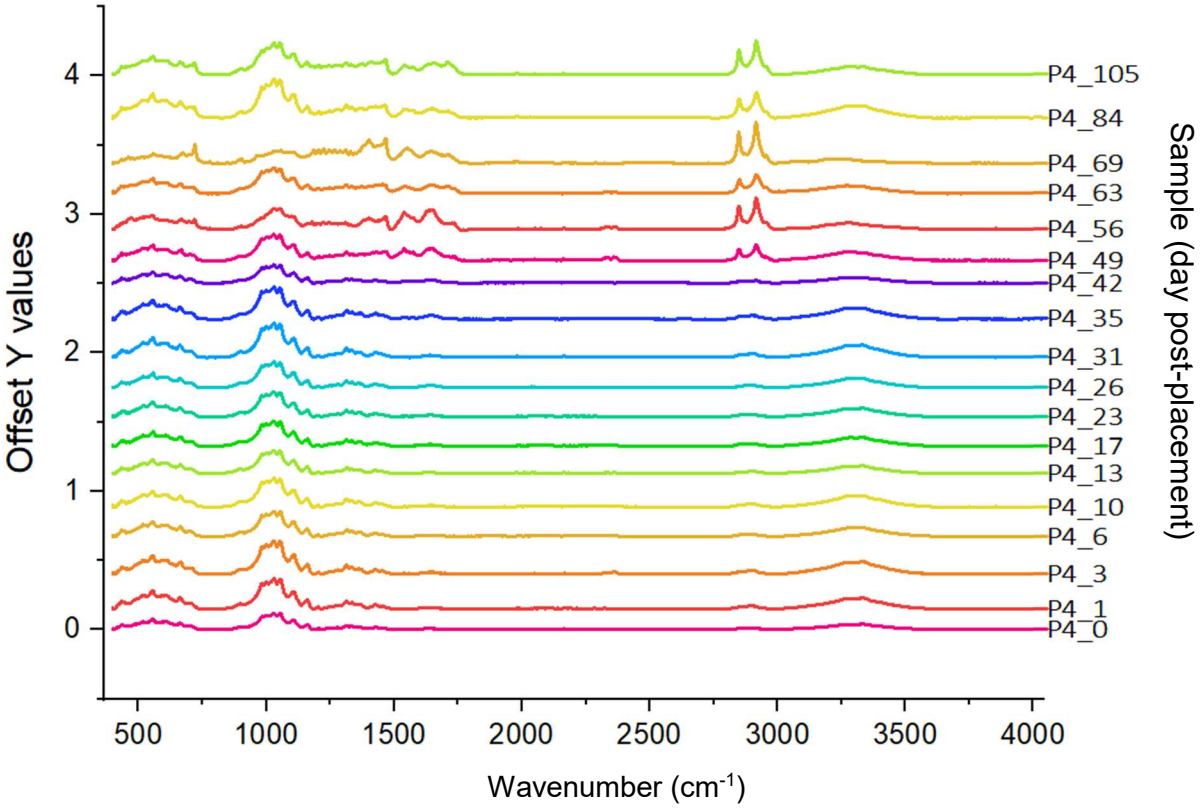

Figure 2.S. 6 Averaged stacked IR spectra for P4 of Trial 2. The x-axis represents the wavenumber (cm-1) and the y-axis represents the offset Y (absorbance values).

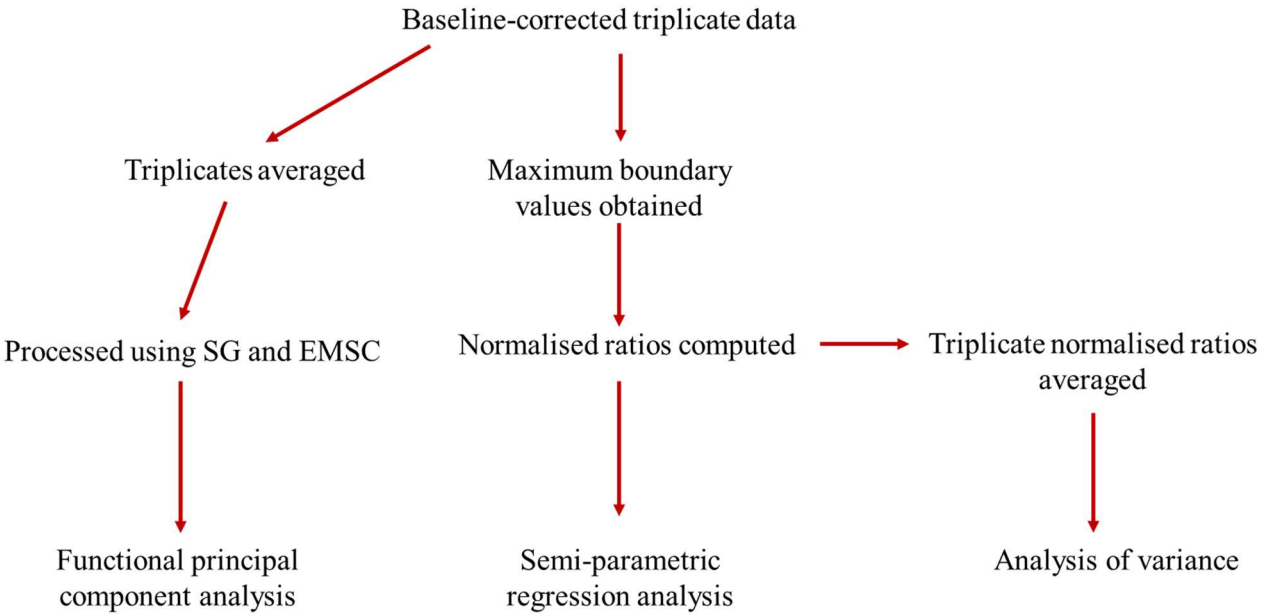

Figure 2.S. 7 Statistical workflow of data processing methods. SG: Savitzky-Golay; EMSC: extended multiplicative scattering correction.

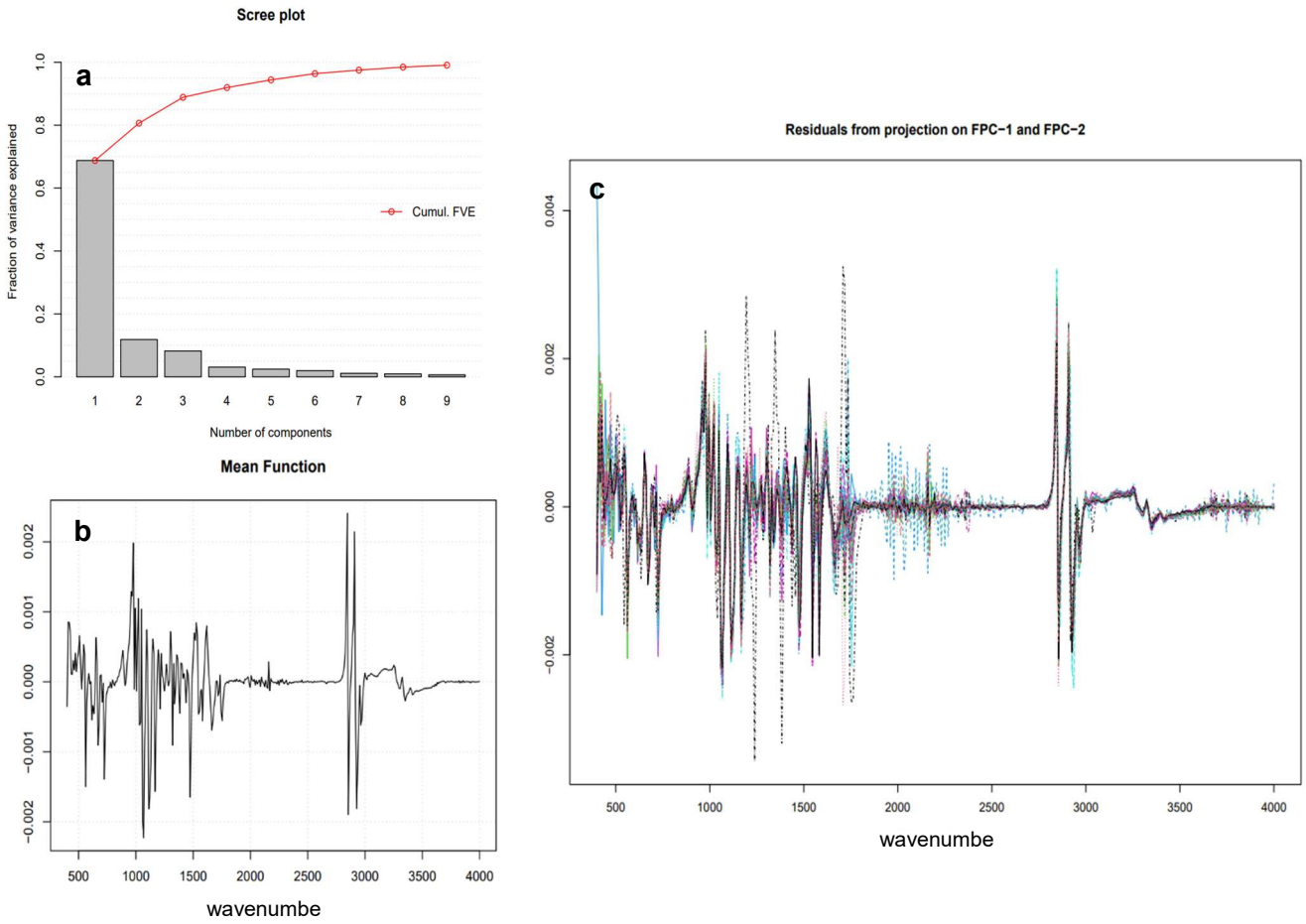

Figure 2.S. 8 Scree plot a), mean function b) and residuals c) of the processed correlation matrix for Trial 1. FPC-1 an FPC-2 captures 80.65% of the variation.

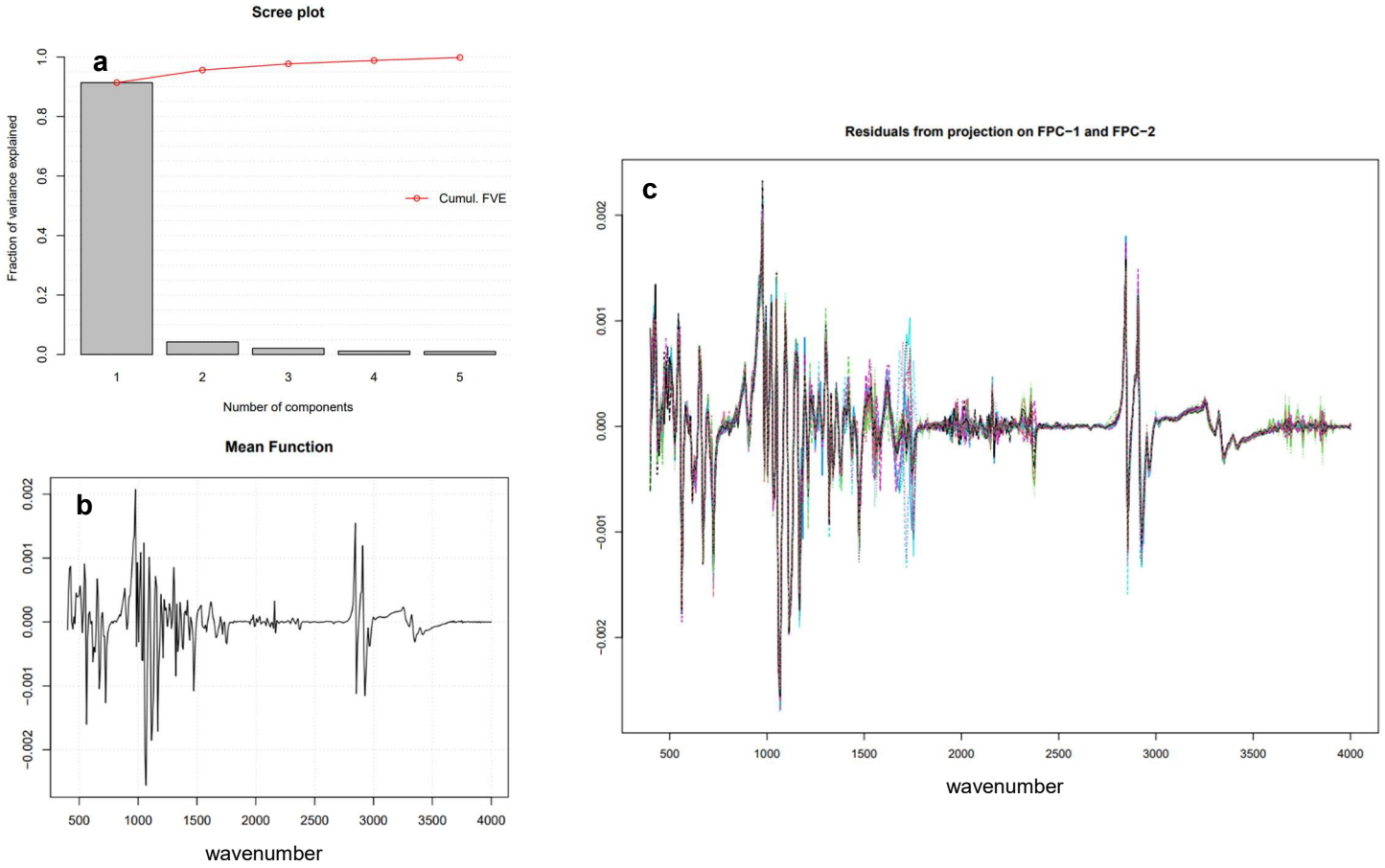

Figure 2.S. 9 Scree plot (a), mean function (b) and residuals c) of the processed correlation matrix for Trial 2. FPC-1 an FPC-2 captures 95.63% of the variation.

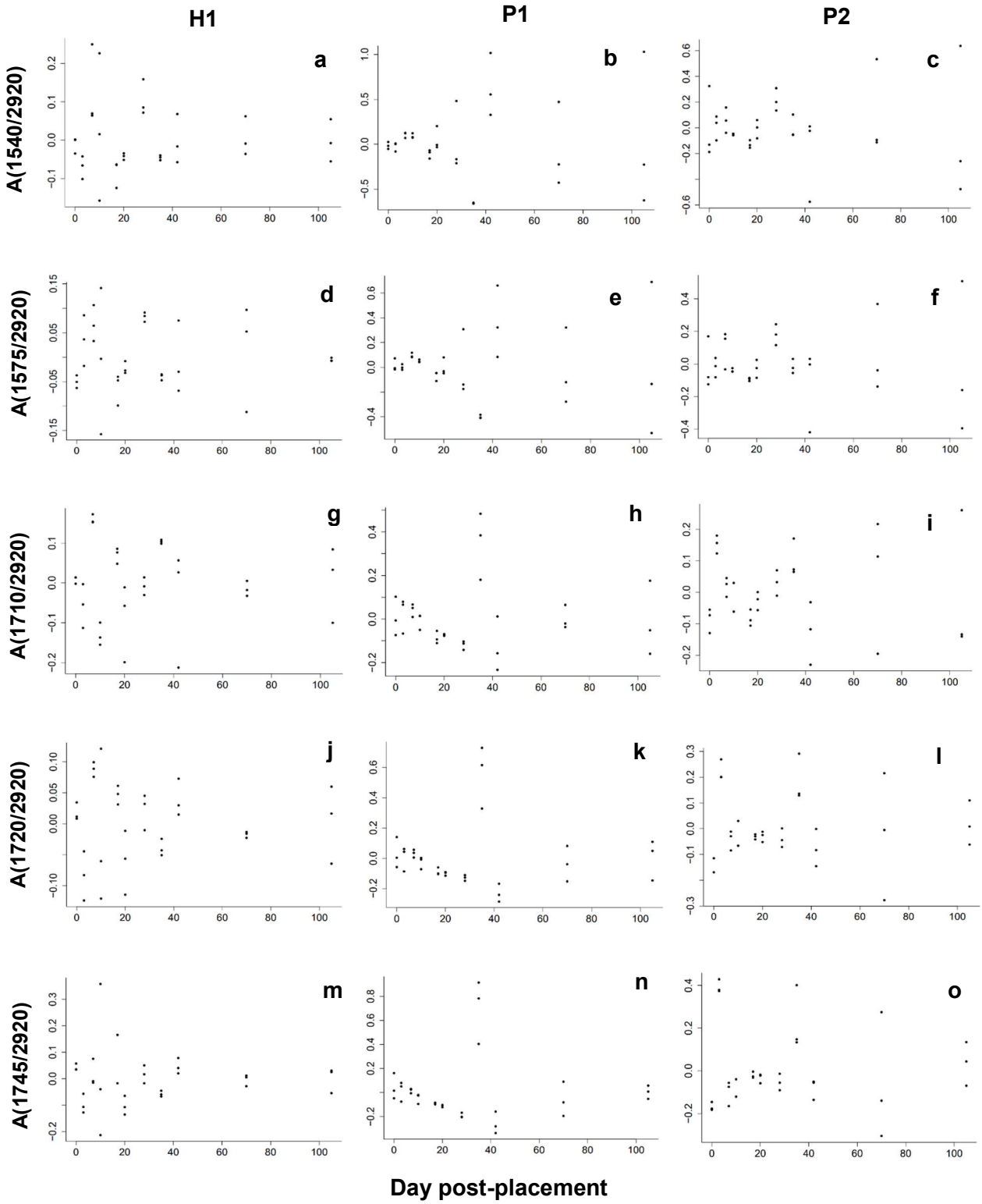

Figure 2.S. 10 Residual scatter plots from the semi-parametric regression models for Trial 1.

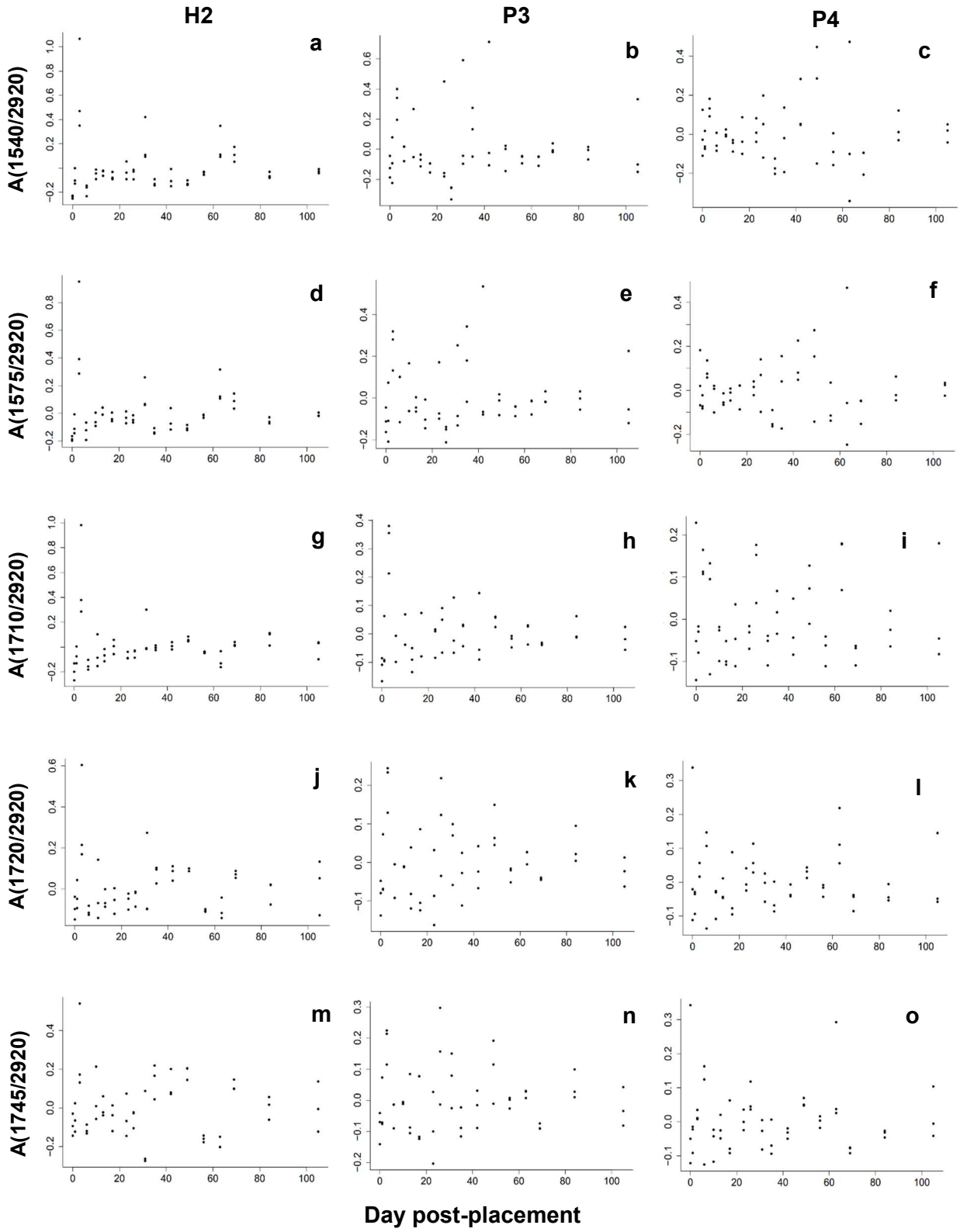

Figure 2.S. 11 Residual scatter plots from the semi-parametric regression models for Trial 2.

Table 2.S. 2 IR bands of interest revealed from loadings plots of FPCAs and the boundaries used to extract the maximum value of desired bands for semi-parametric regression analysi

Band no.	*Desired band (cm^{-1})*	*Boundary (cm^{-1})*	*Assignment*	*References*
1	~1540	1530.26 - 1550.99	C-O stretch: carboxylate bands of fatty acid salts	[11, 21-23, 47]
2	~1575	1560.15 - 1580.89		
3	~1710	1695.15 - 1715.88	C=O stretch: free fatty acids	
4	~1720	1718.29 - 1730.83	C=O stretch: aldehydes and ketones	
5	~1745	1735.17 -1750.59	C=O stretch: triacylglycerols	
6	~2920	2910.10 - 2925.53	Asymmetrical CH_2 stretching of the methylene chain	

Table 2.S. 3 Results from one-way ANOVA test and post-hoc tests using the Tukey honestly

Trial 1

		1540/2920	*1575/2920*	*1710/2920*	*1720/2920*	*1745/2920*
One-way ANOVA	*H1 – P1 – P2*	0.0015	0.0014	0.8940	0.7070	0.6570
Post-hoc tests	*H1 - P1*	0.0405	0.1652	0.8930	0.7752	0.6881
	H1 - P2	0.0011	0.0014	0.9353	0.7296	0.7274
	P1 - P2	0.3417	0.6105	0.9939	0.9967	0.9977

Trial 2

		1540/2920	*1575/2920*	*1710/2920*	*1720/2920*	*1745/2920*
One-way ANOVA	*H2 – P3 – P4*	0.0019	0.0009	0.6220	0.2490	0.1870
Post-hoc tests	*H2 - P3*	0.0029	0.0014	0.6369	0.2324	0.1772
	H2 - P4	0.0110	0.0062	0.7238	0.5058	0.4068
	P3 - P4	0.8872	0.8732	0.9891	0.8549	0.8633

Appendix 2: Supplementary information associated with Chapter 3

Table of Contents

Appendix 2: Supplementary information associated with Chapter 3

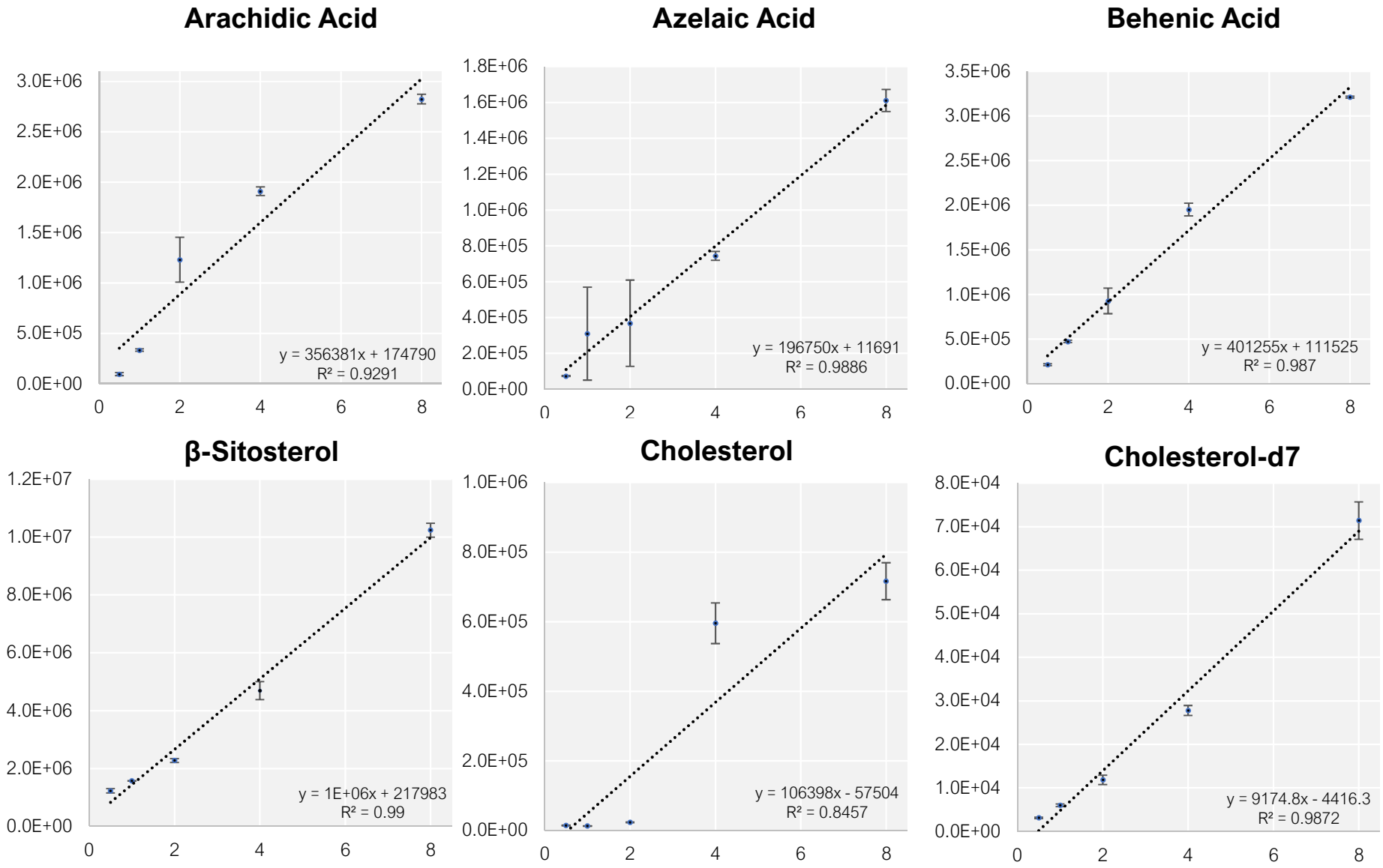

Figure 3.S.1. a Five-point calibration curves displaying the equation of the line, R2 values and error bars calculated by the standard deviation of individual data points (n=3).

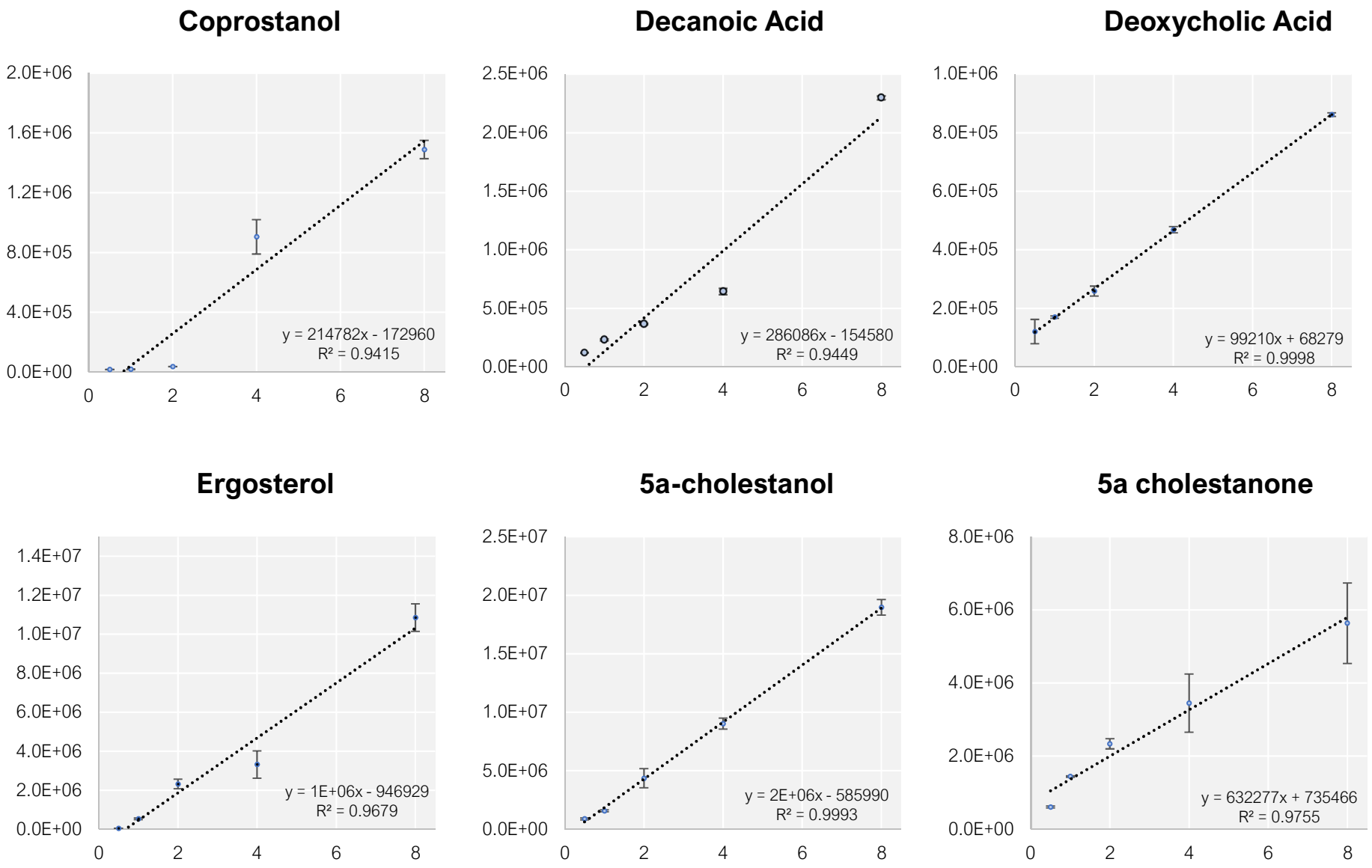

Figure 3.S.1. b Five-point calibration curves displaying the equation of the line, R2 values and error bars calculated by the standard deviation of individual data points (n=3).

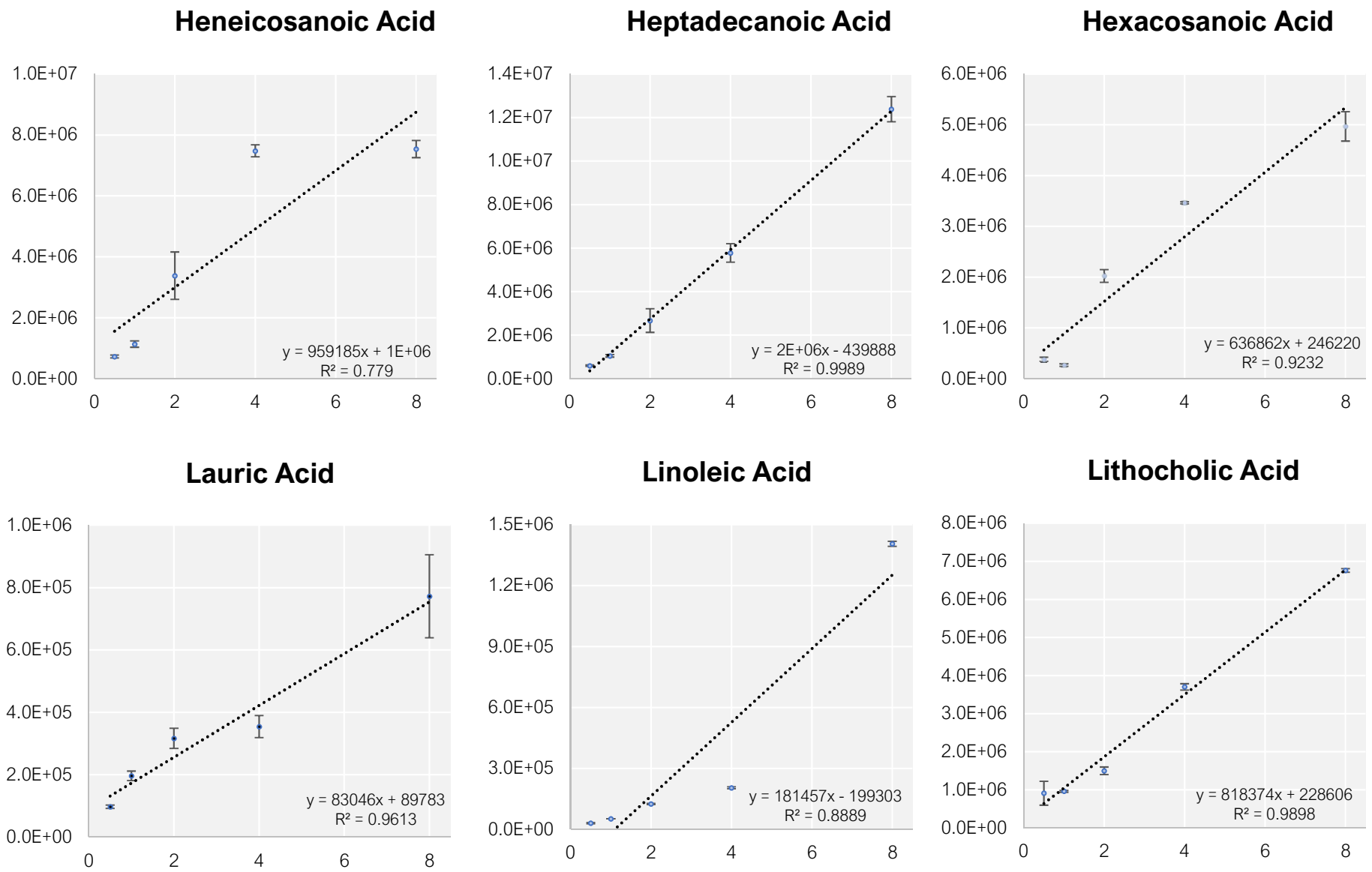

Figure 3.S.1. c Five-point calibration curves displaying the equation of the line, R2 values and error bars calculated by the standard deviation of individual data points (n=3).

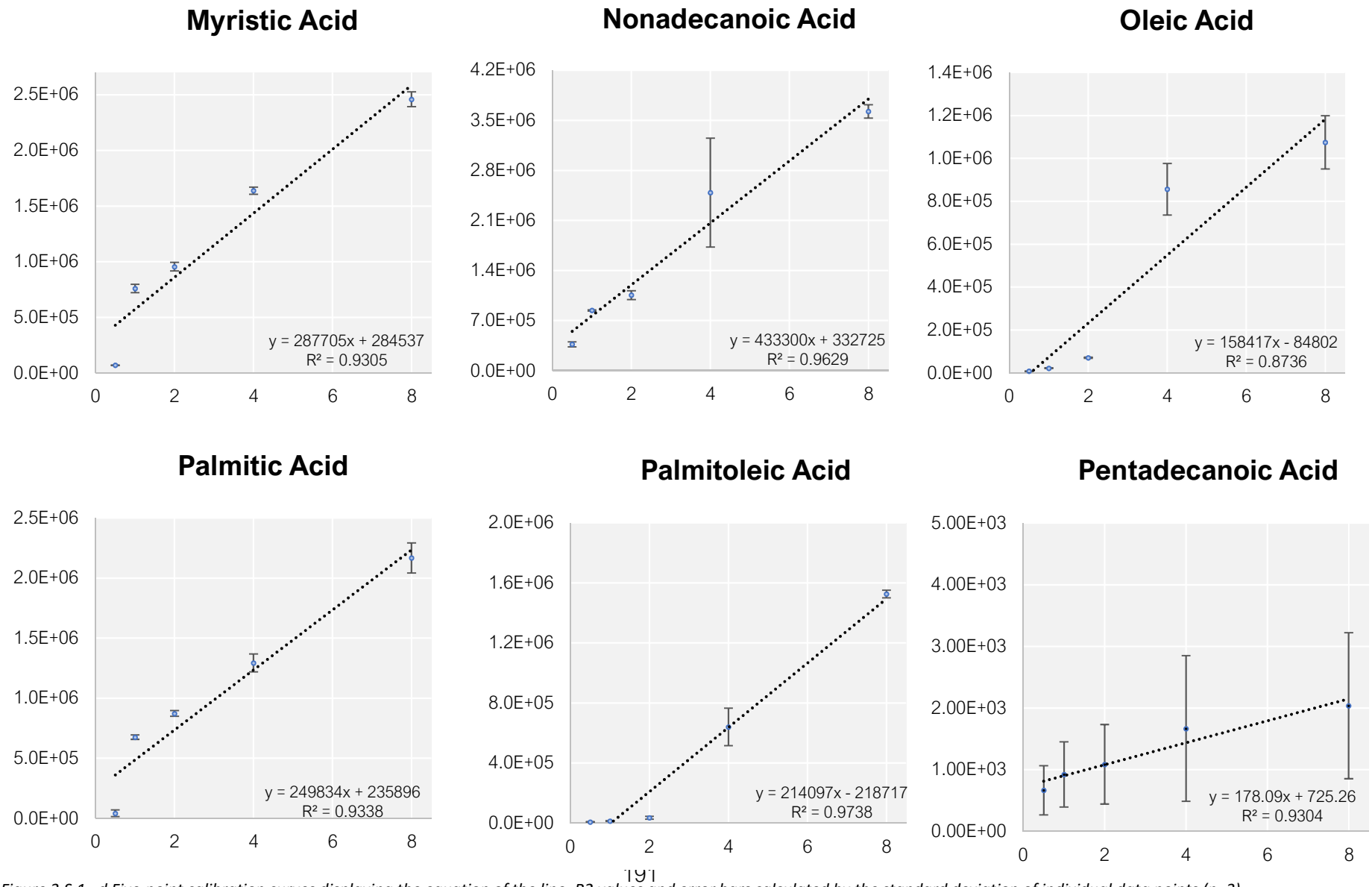

Figure 3.S.1. d Five-point calibration curves displaying the equation of the line, R2 values and error bars calculated by the standard deviation of individual data points (n=3).

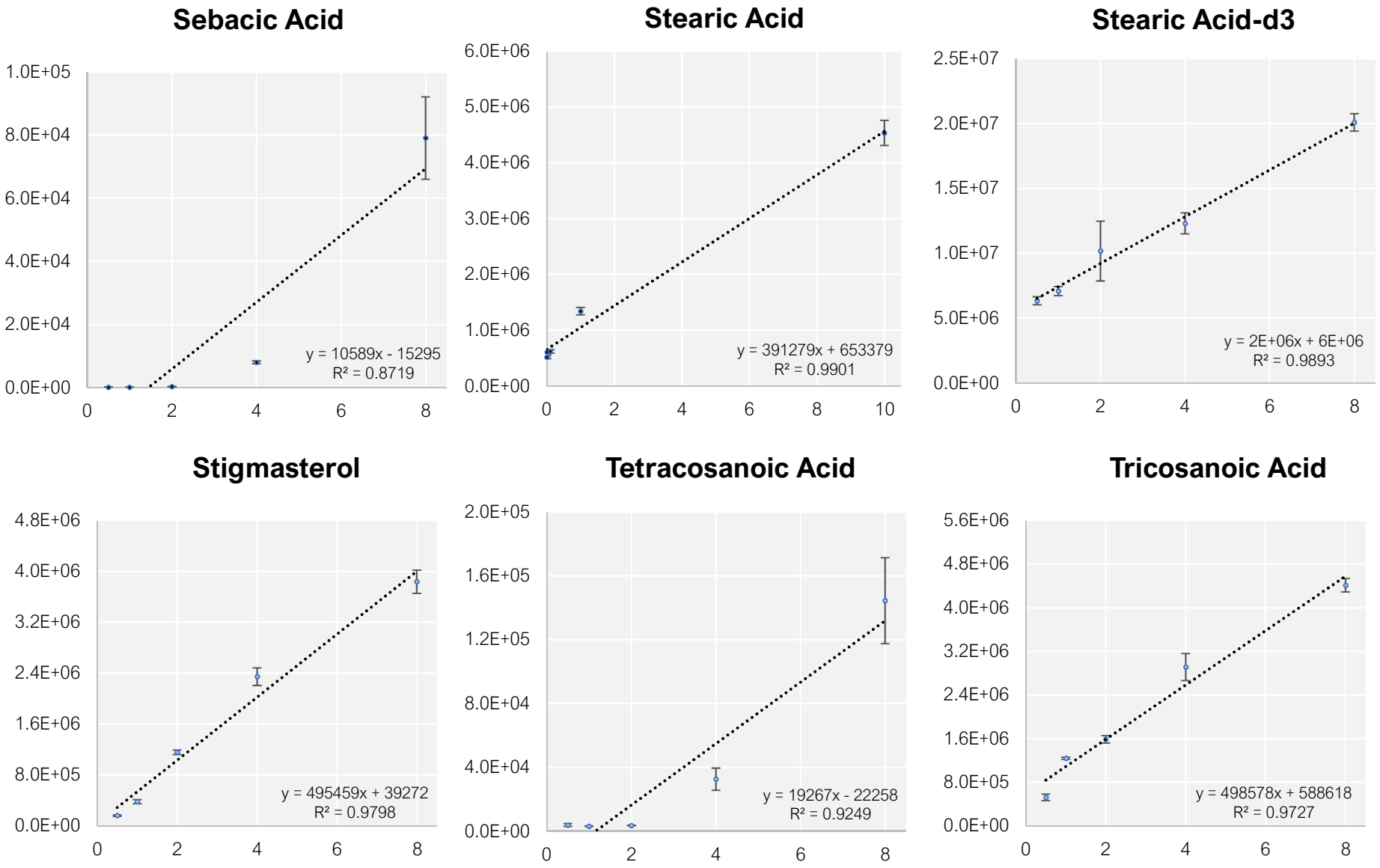

Figure 3.S.1. e Five-point calibration curves displaying the equation of the line, R2 values and error bars calculated by the standard deviation of individual data points (n=3).

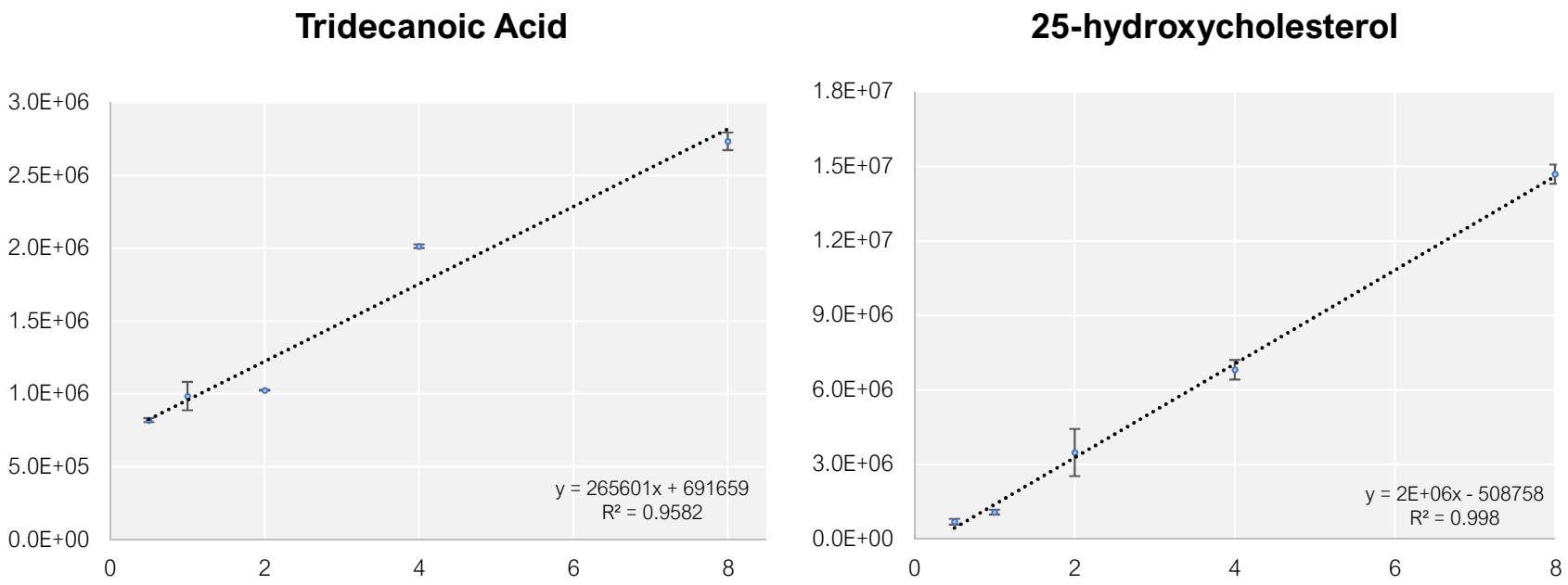

Figure 3.S.1. ƒ Five-point calibration curves displaying the equation of the line, R2 values and error bars calculated by the standard deviation of individual data points (n=3).

Table 3.S. 1 Mean area ($\bar{x}$ A) and relative standard deviation (%RSD) of the deuterated standards yielded for each extraction method in the day 0 post-placement samples.

	1		2		3		4	
	$\bar{x}$ A	%RSD	$\bar{x}$ A	%RSD	$\bar{x}$ A	%RSD	$\bar{x}$ A	%RSD
Stearic acid -d3	1252	141.00	1206	139.92	2445	149.81	2162	168.41
Cholesterol-d7	132	17.28	136	11.43	223	13.69	223	14.41

Table 3.S. 2 Mean area ($\bar{x}$ A) and relative standard deviation (%RSD) of deuterated standards yielded for each extraction method in the day 84 post-placement samples.

	1		2		3		4	
	$\bar{x}$ A	%RSD	$\bar{x}$ A	%RSD	$\bar{x}$ A	%RSD	$\bar{x}$ A	%RSD
Stearic acid -d3	15509	42.46	1441	28.82	177812	57.75	205546	2.28
Cholesterol-d7	163	36.51	201	6.53	190	58.66	176	38.16

Table 3.S. 3 Mean area ($\bar{x}$ A) and relative standard deviation (%RSD) of the deuterated standards yielded for each extraction method in the standard blanks.

	1		2		2		4	
	$\bar{x}$ A	%RSD	$\bar{x}$ A	%RSD	$\bar{x}$ A	%RSD	$\bar{x}$ A	%RSD
Stearic acid -d3	814	32.64	67	61.25	7906	57.79	8045	1.24
Cholesterol-d7	334	17.22	299	8.10	286	10.90	243	14.76

Appendix 3: Supplementary information associated with Chapter 4

Table of contents

Appendix 3: Supplementary information associated with Chapter 4

Appendix 3: Supplementary information associated with Chapter 4

Table 4. S. 1 Summary of human donor information. DPP: days post-placement. ADD: accumulated degree days.

Donor	Date of placement	Sex	Age (years)	Body mass (kg)	Placement season	Cause of death	Samples collected (DPP)	Samples collected (ADD)
H1	29/01/2021	M	86	63	Summer	Alzheimer's disease	0, 3, 7, 10, 17, 20, 28, 35, 42, facility closed due to floods, 70, 105	0, 64, 222, 371, 431, 604, 757, 907, 1437, 1995
H2	11/06/2021	M	84	94	Winter	Metastatic bladder cancer, prostate cancer, peripheral vascular disease, atrial fibrillation	0, 1, 3, 6, 10, 13, 17, 23, 26, 31, 35, 42, 49, 56, 63, 69, 84, 105	0, 9, 28, 59, 110, 146, 196, 263, 297, 337, 385, 457, 541, 620, 704, 776, 967, 1287

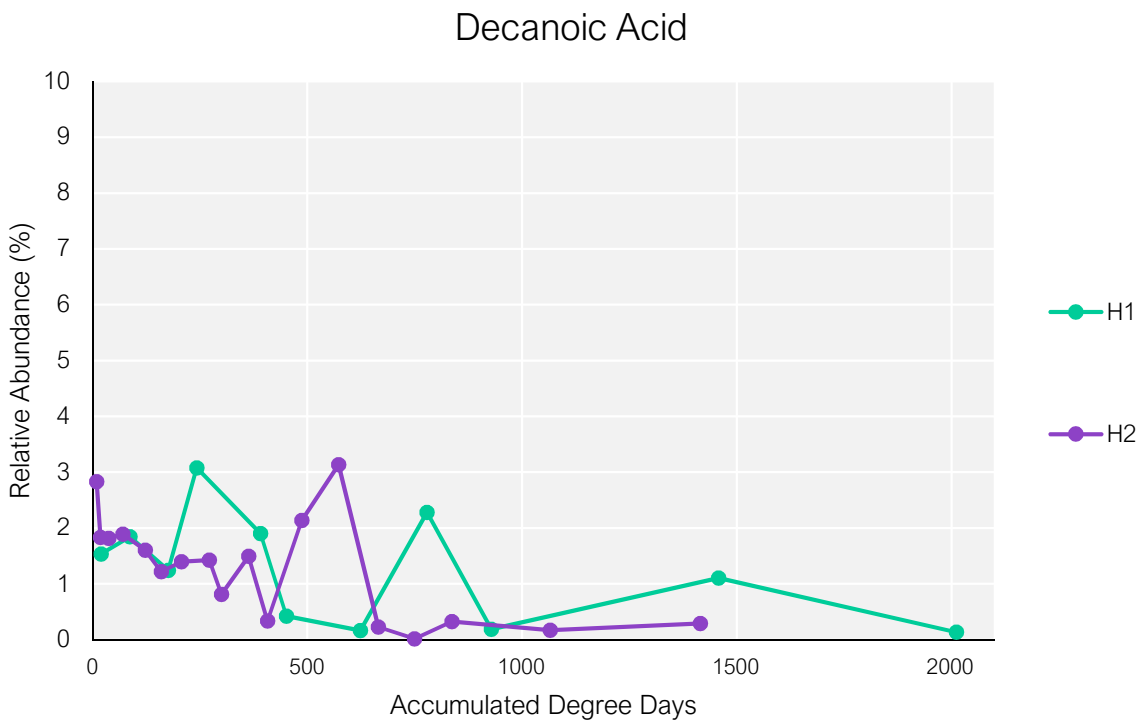

Figure 4.S. 1 Relative abundance (%) of decanoic acid plotted against accumulated degree days for H1 and H2.

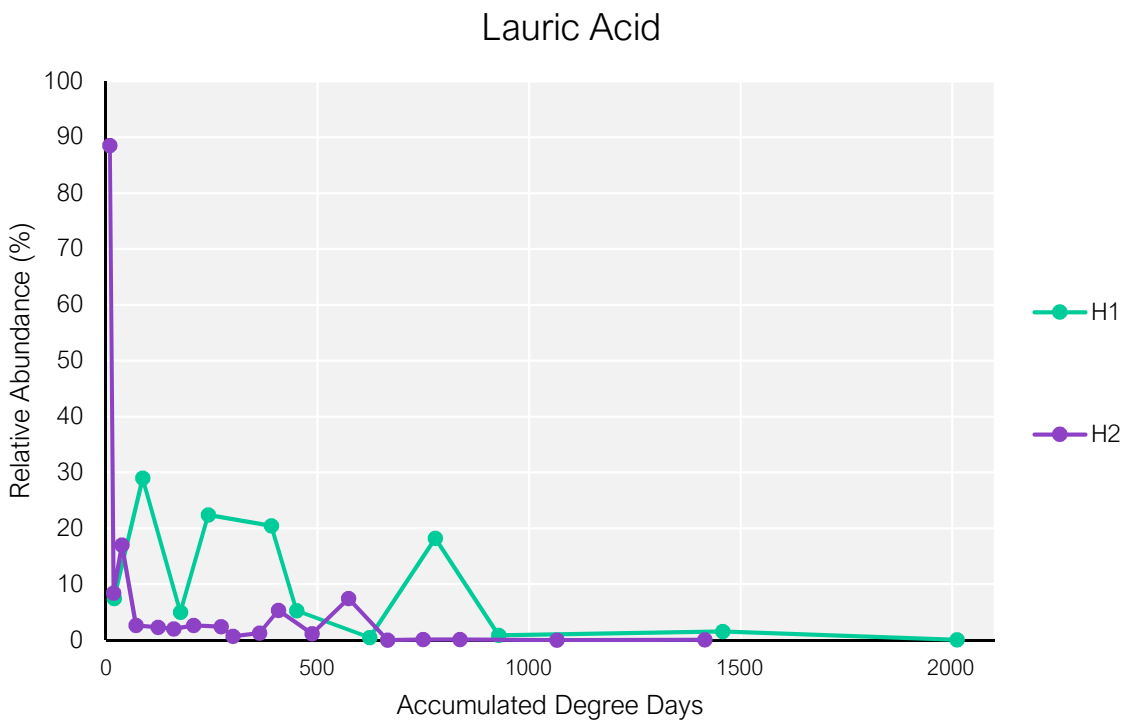

Figure 4.S. 2 Relative abundance (%) of lauric acid plotted against accumulated degree days for H1 and H2.

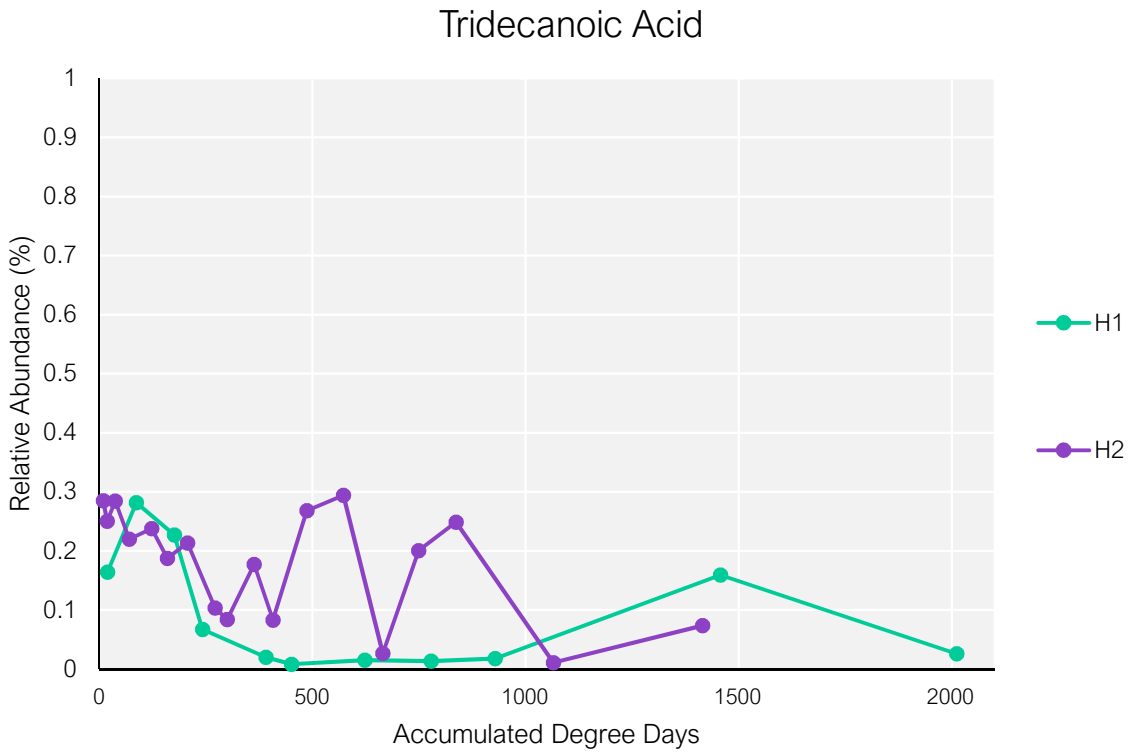

Figure 4.S. 3 Relative abundance (%) of tridecanoic acid plotted against accumulated degree days for H1 and H2.

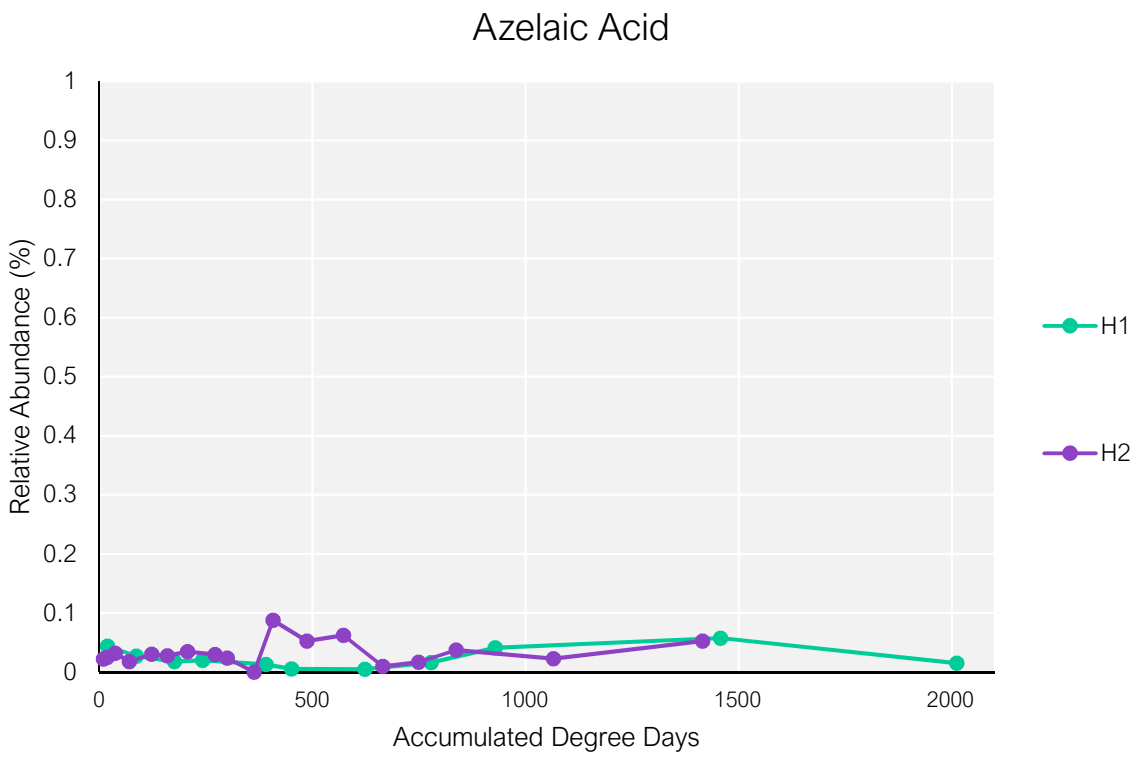

Figure 4.S. 4 Relative abundance (%) of azelaic acid plotted against accumulated degree days for H1 and H2.

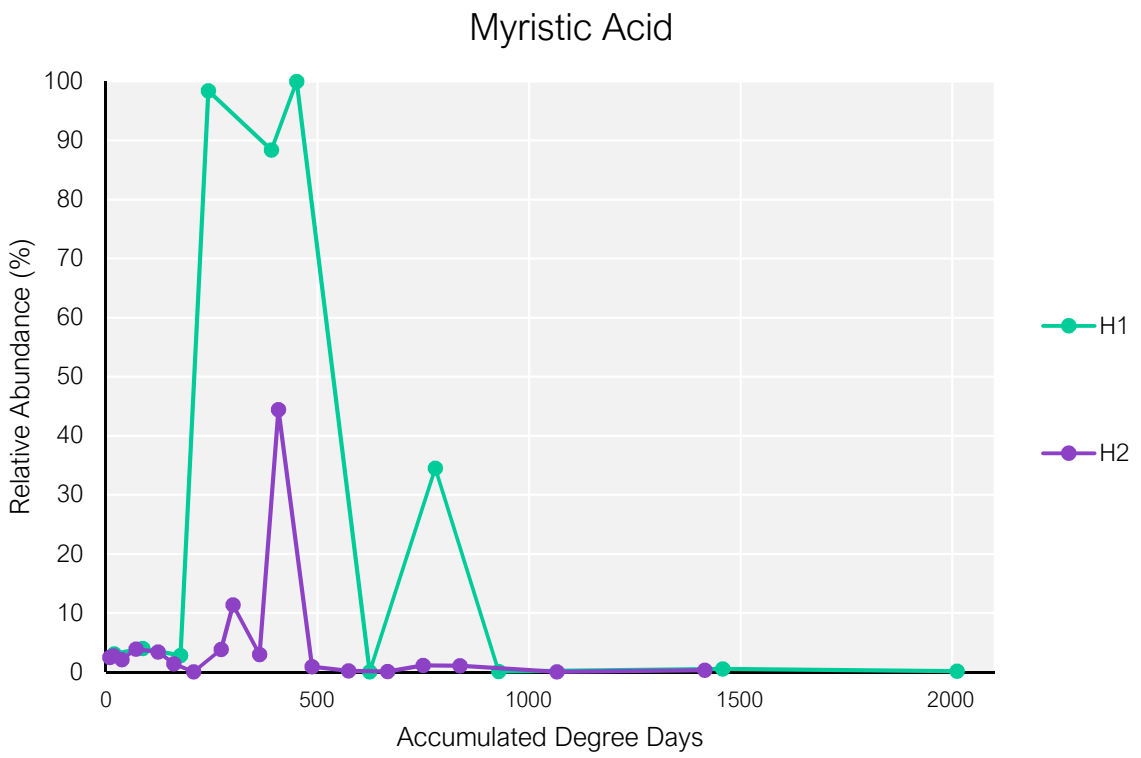

Figure 4.S. 5Relative abundance (%) of myristic acid plotted against accumulated degree days for H1 and H2.

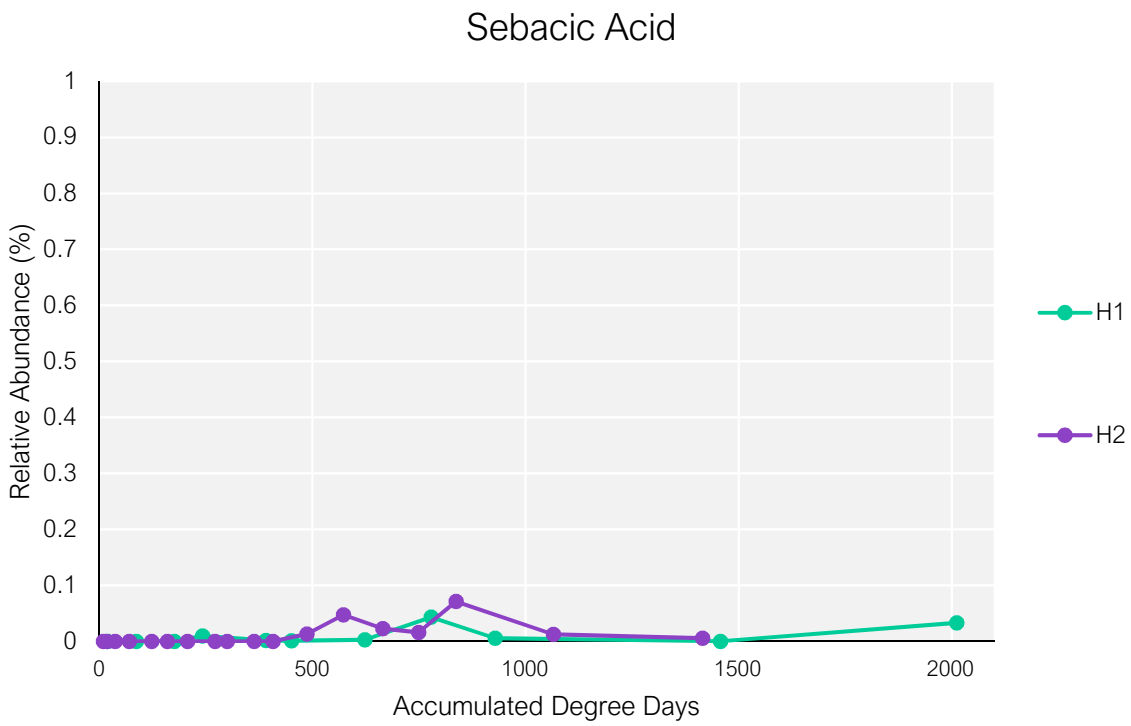

Figure 4.S. 6 Relative abundance (%) of sebacic acid plotted against accumulated degree days for H1 and H2.

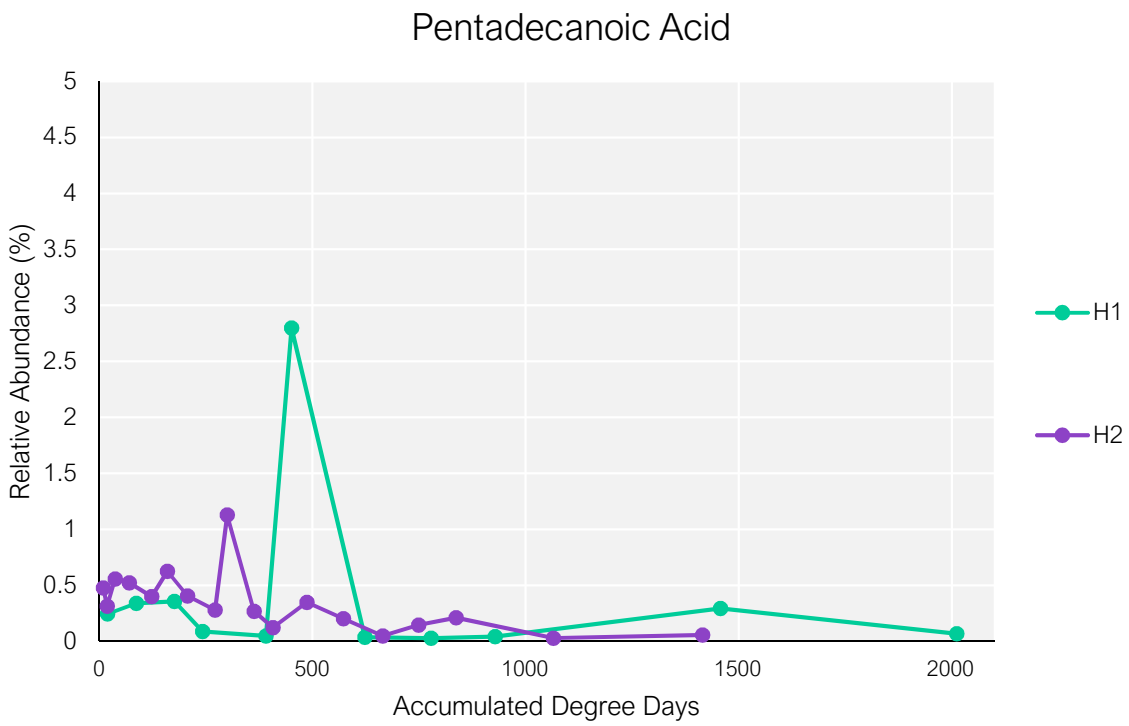

Figure 4.S. 7 Relative abundance (%) of pentadecanoic acid plotted against accumulated degree days for H1 and H2.

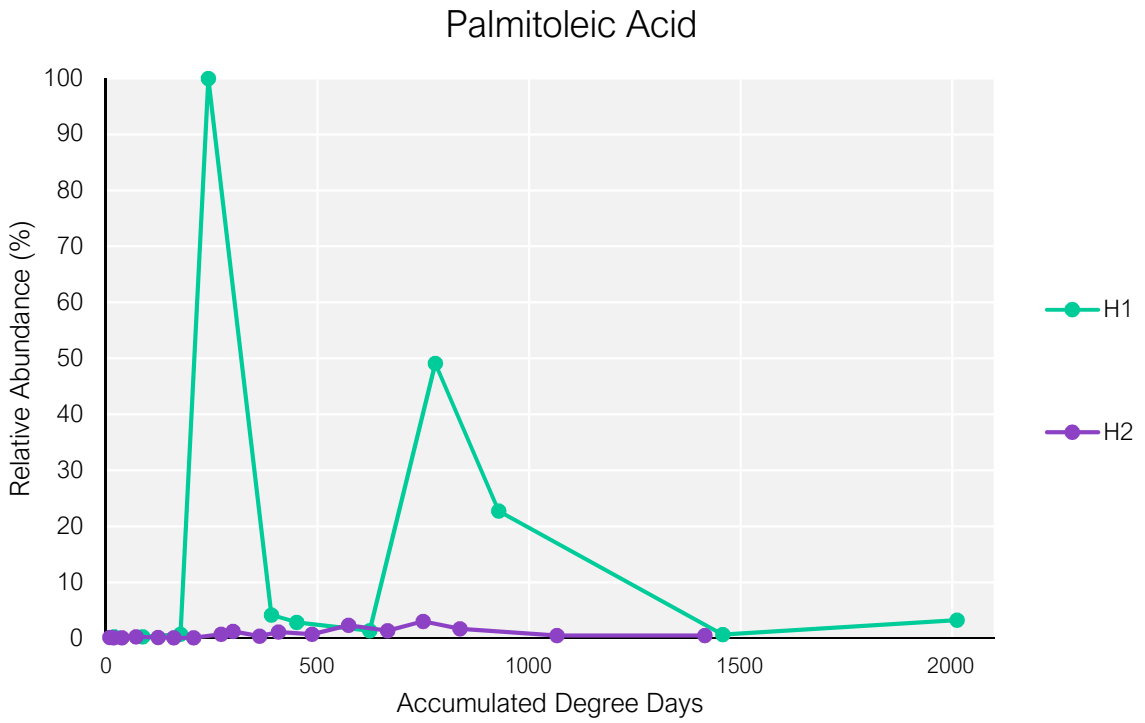

Figure 4.S. 8 Relative abundance (%) of palmitoleic acid plotted against accumulated degree days for H1 and H2.

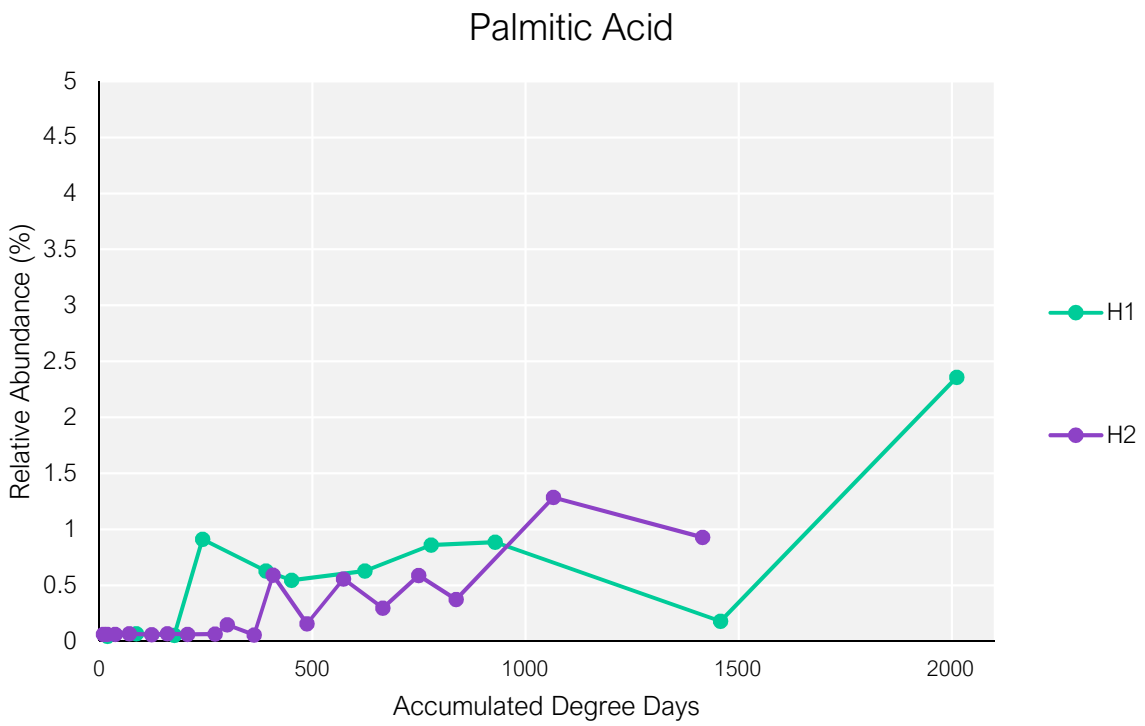

Figure 4.S. 9 Relative abundance (%) of palmitic acid plotted against accumulated degree days for H1 and H2.

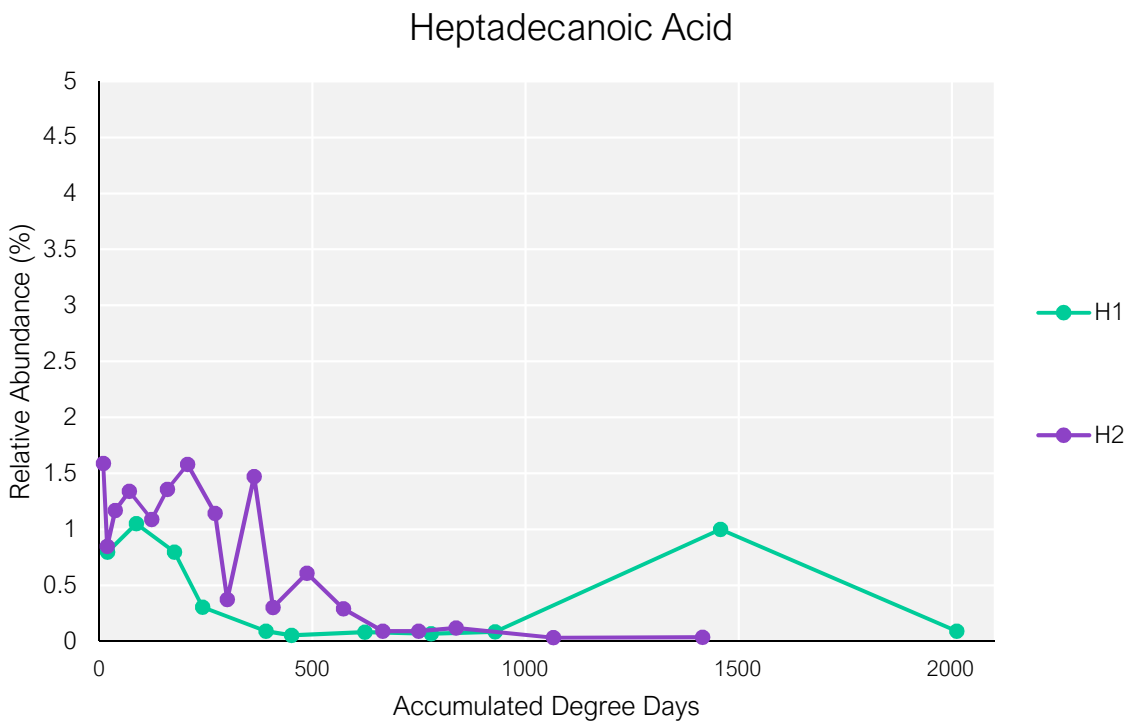

Figure 4.S. 10 Relative abundance (%) of heptadecanoic acid plotted against accumulated degree days for H1 and H2.

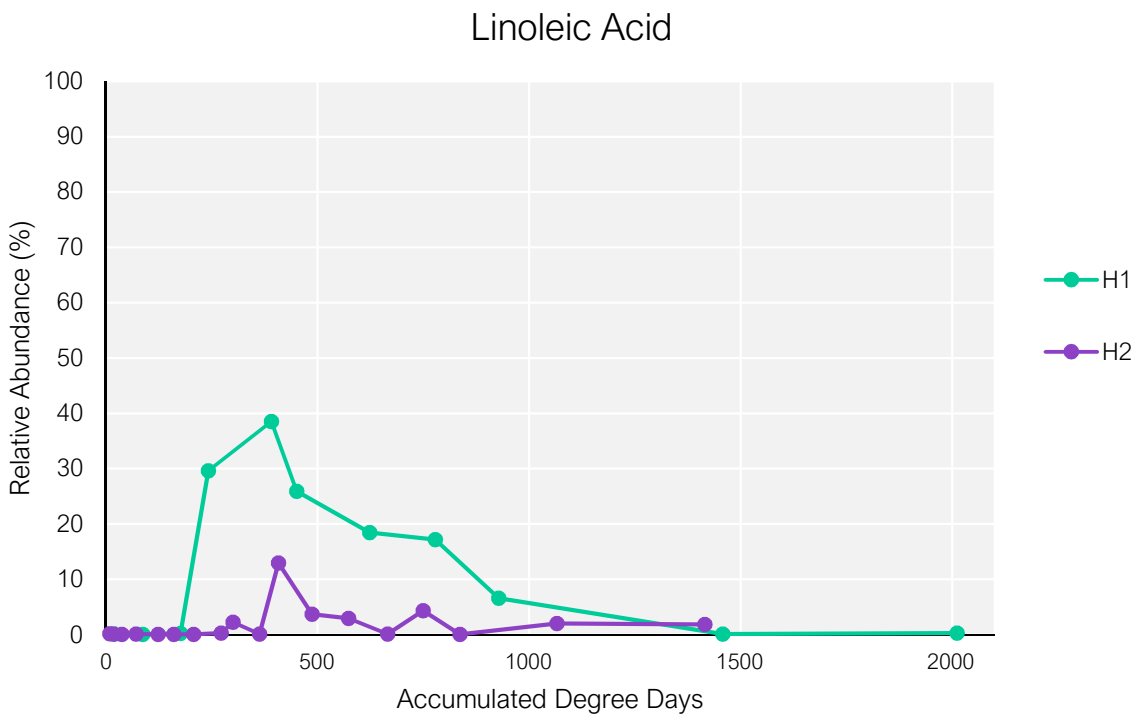

Figure 4.S. 11 Relative abundance (%) of linoleic acid plotted against accumulated degree days for H1 and H2.

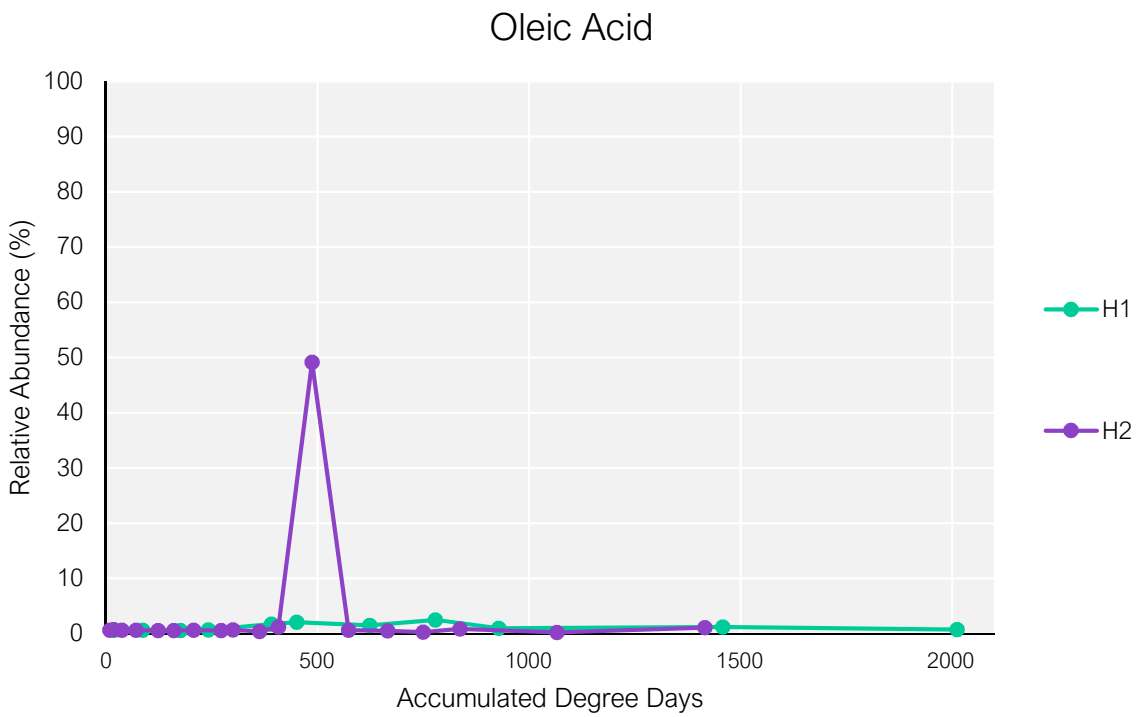

Figure 4.S. 12 Relative abundance (%) of oleic acid plotted against accumulated degree days for H1 and H2.

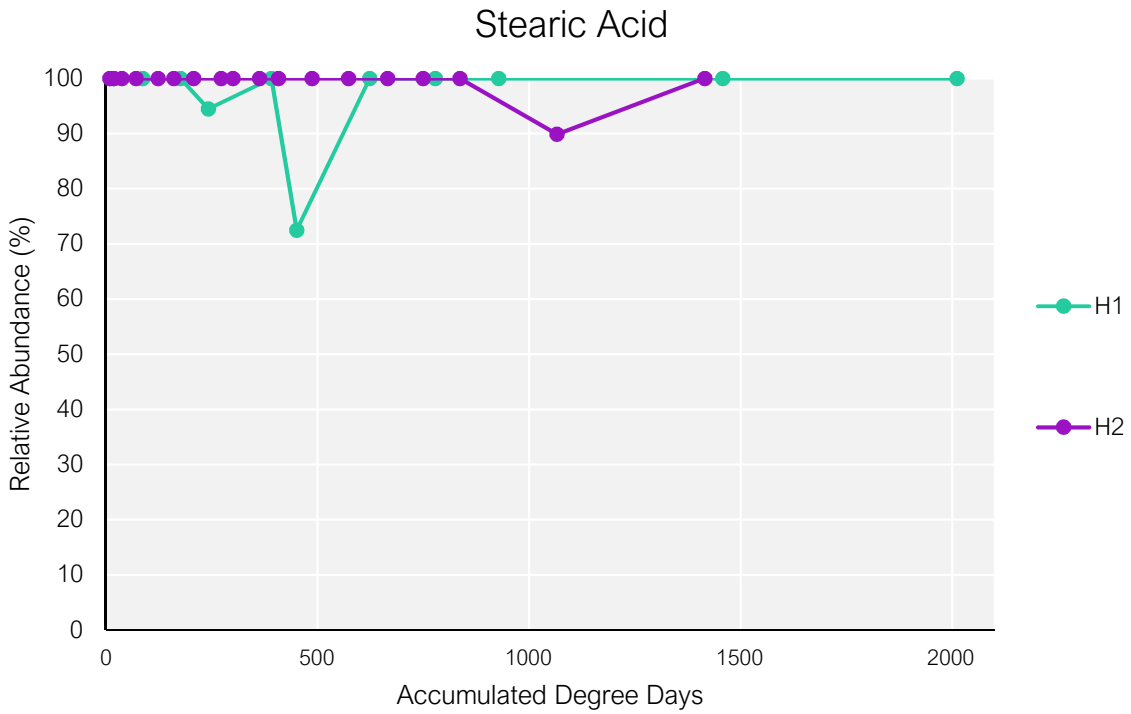

Figure 4.S. 13 Relative abundance (%) of stearic acid plotted against accumulated degree days for H1 and H2.

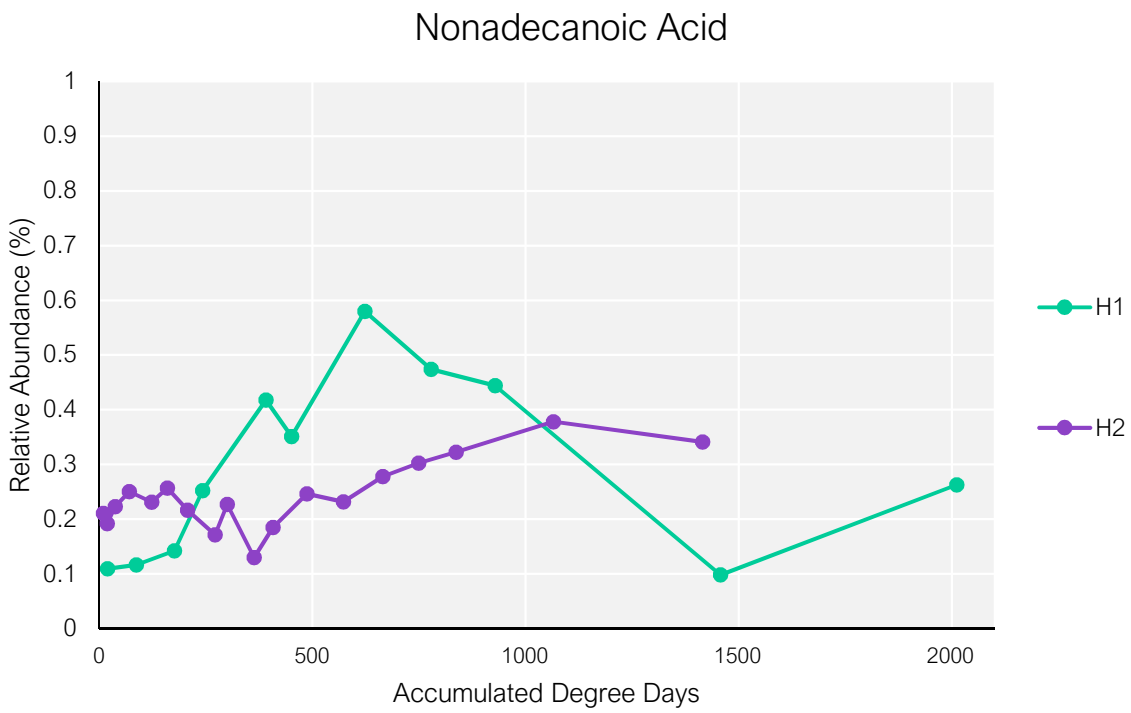

Figure 4.S. 14 Relative abundance (%) of nonadecanoic acid plotted against accumulated degree days for H1 and H2.

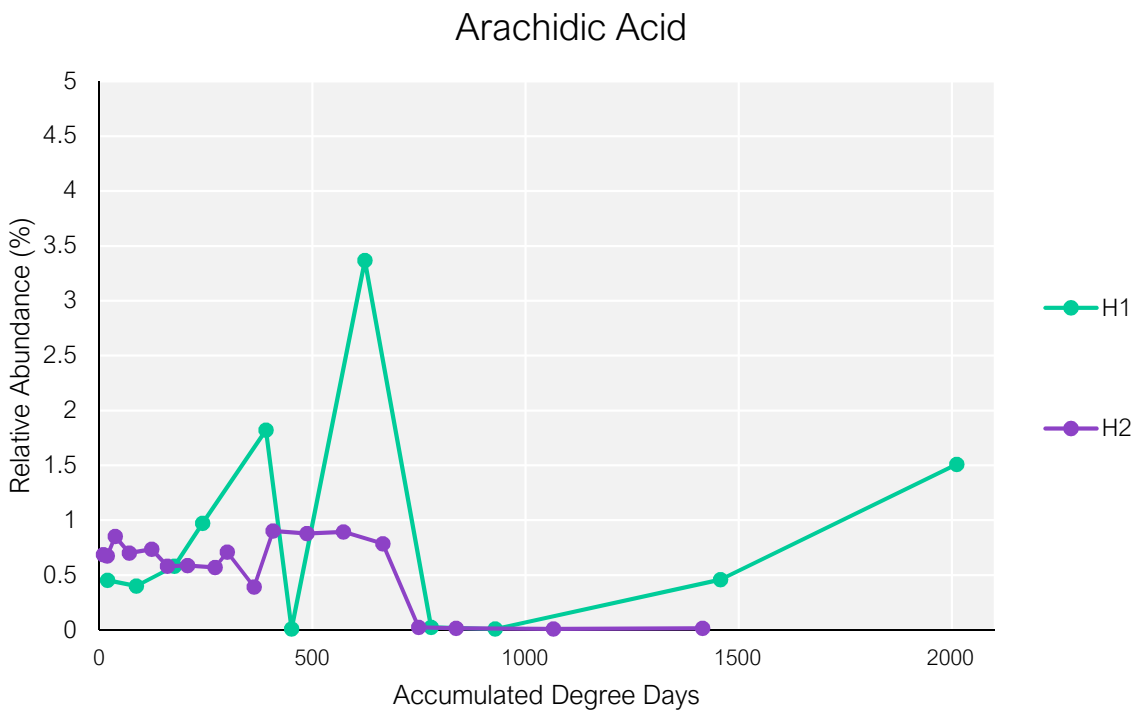

Figure 4.S. 15 . Relative abundance (%) of arachidic acid plotted against accumulated degree days for H1 and H2.

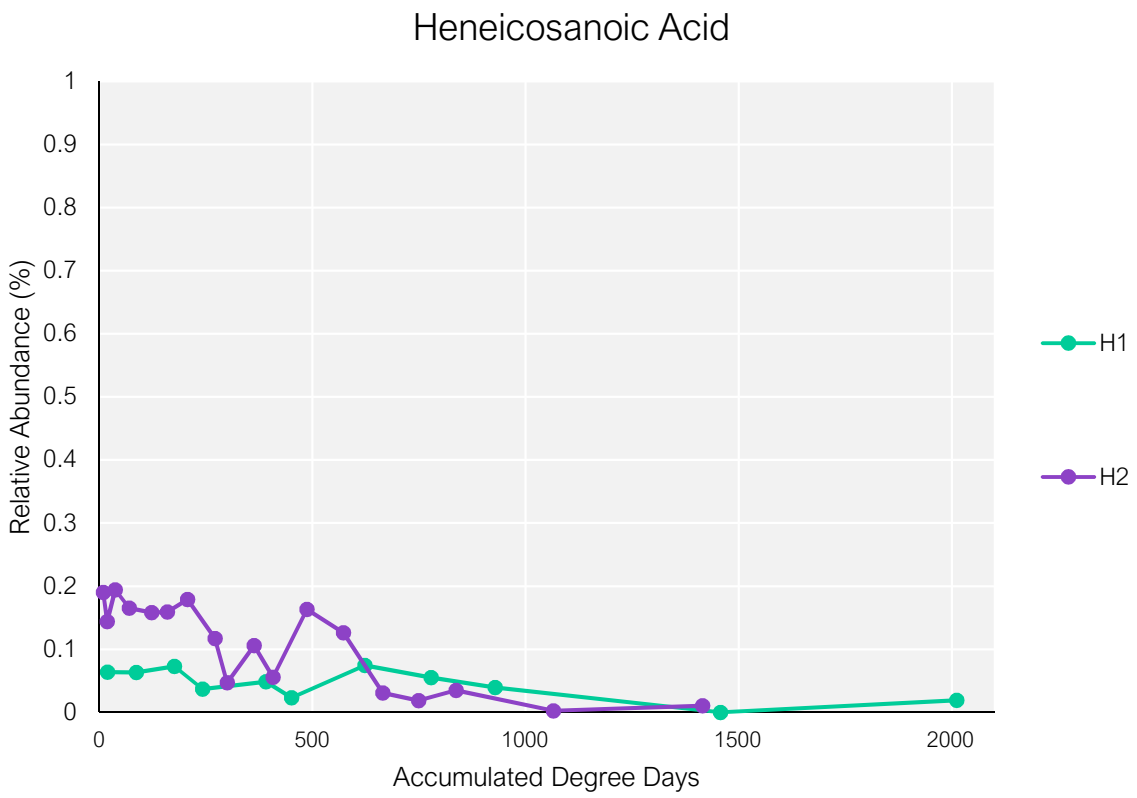

Figure 4.S. 16 Relative abundance (%) of heneicosanoic acid plotted against accumulated degree days for H1 and H2.

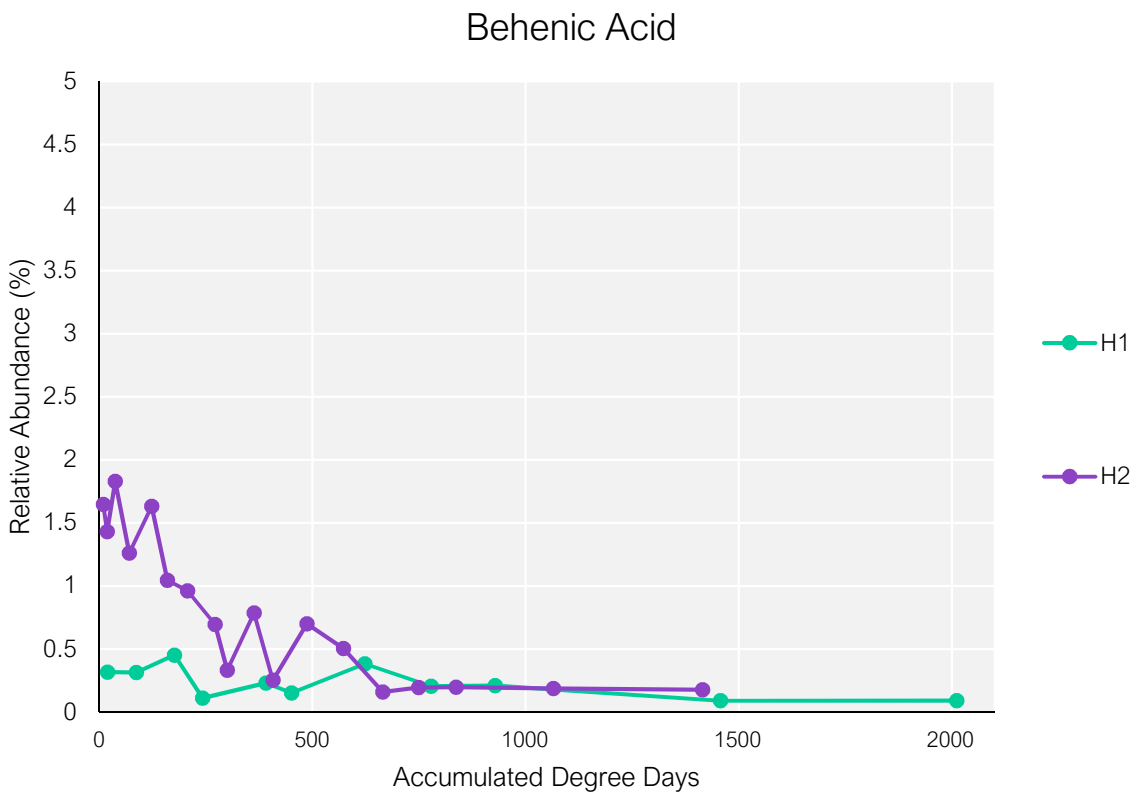

Figure 4.S. 17 Relative abundance (%) of behenic acid plotted against accumulated degree days for H1 and H2.

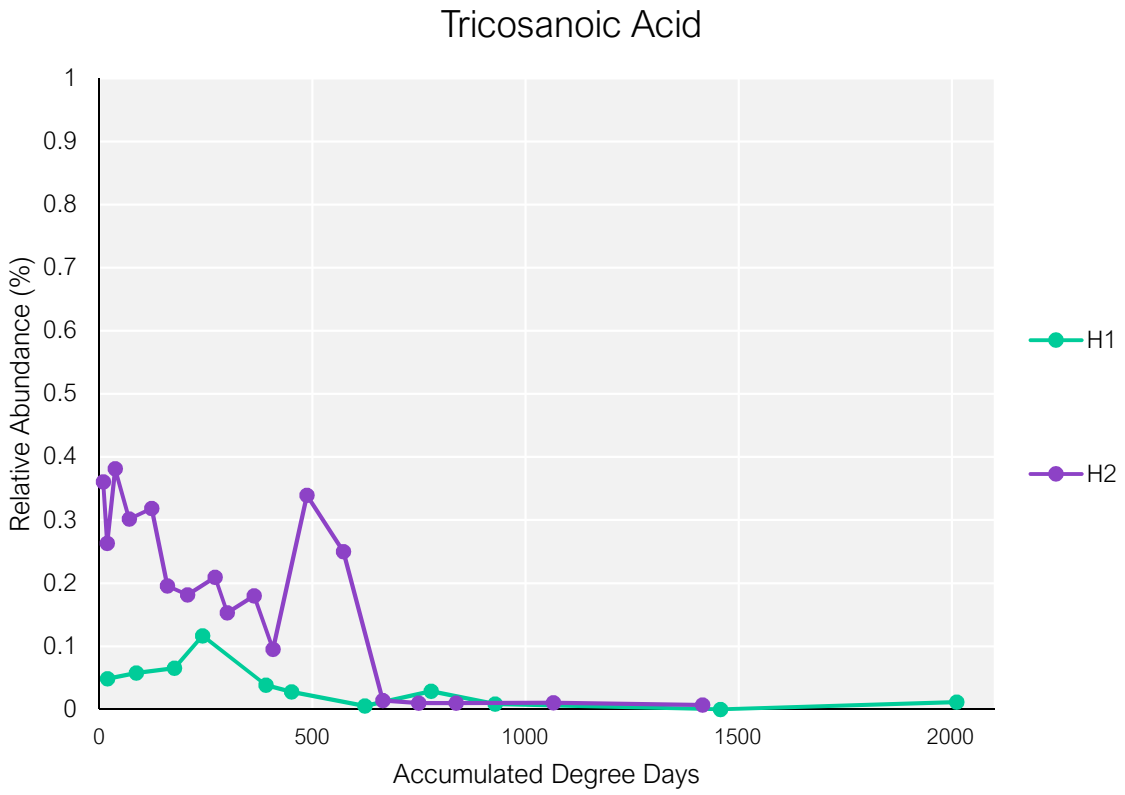

Figure 4.S. 18 Relative abundance (%) of tricosanoic acid plotted against accumulated degree days for H1 and H2.

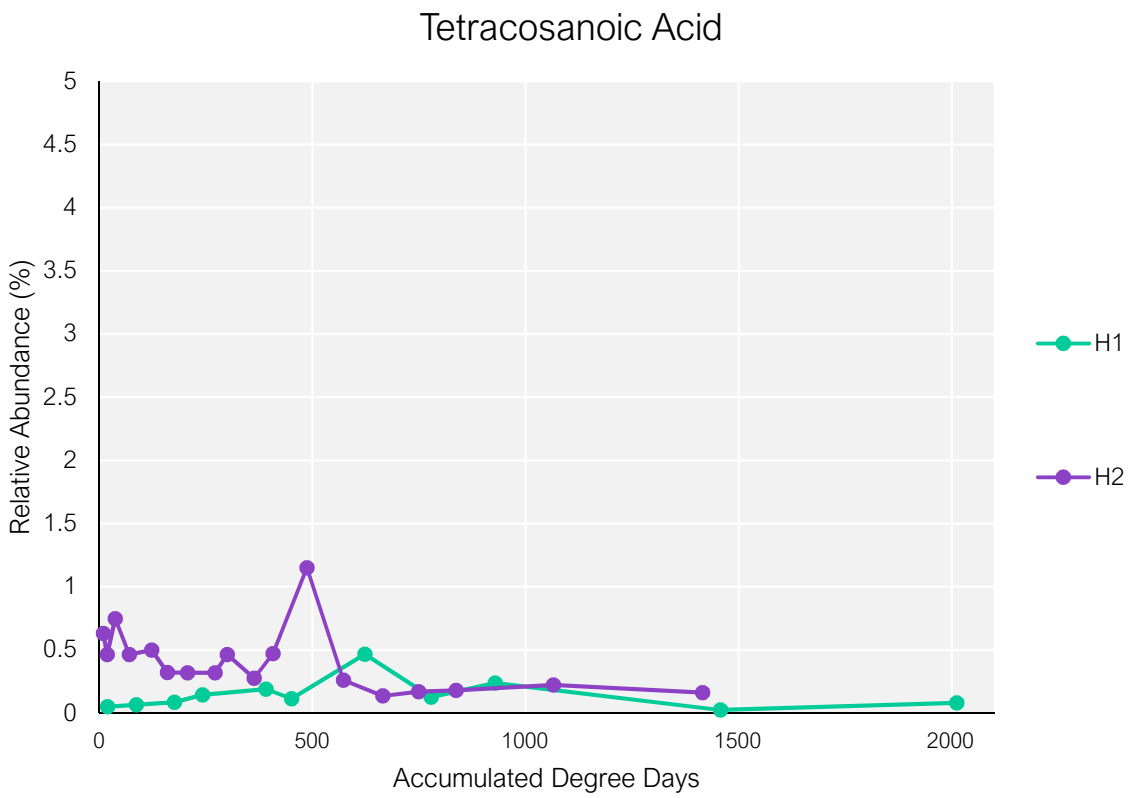

Figure 4.S. 19 Relative abundance (%) of tetracosanoic acid plotted against accumulated degree days for H1 and H2.

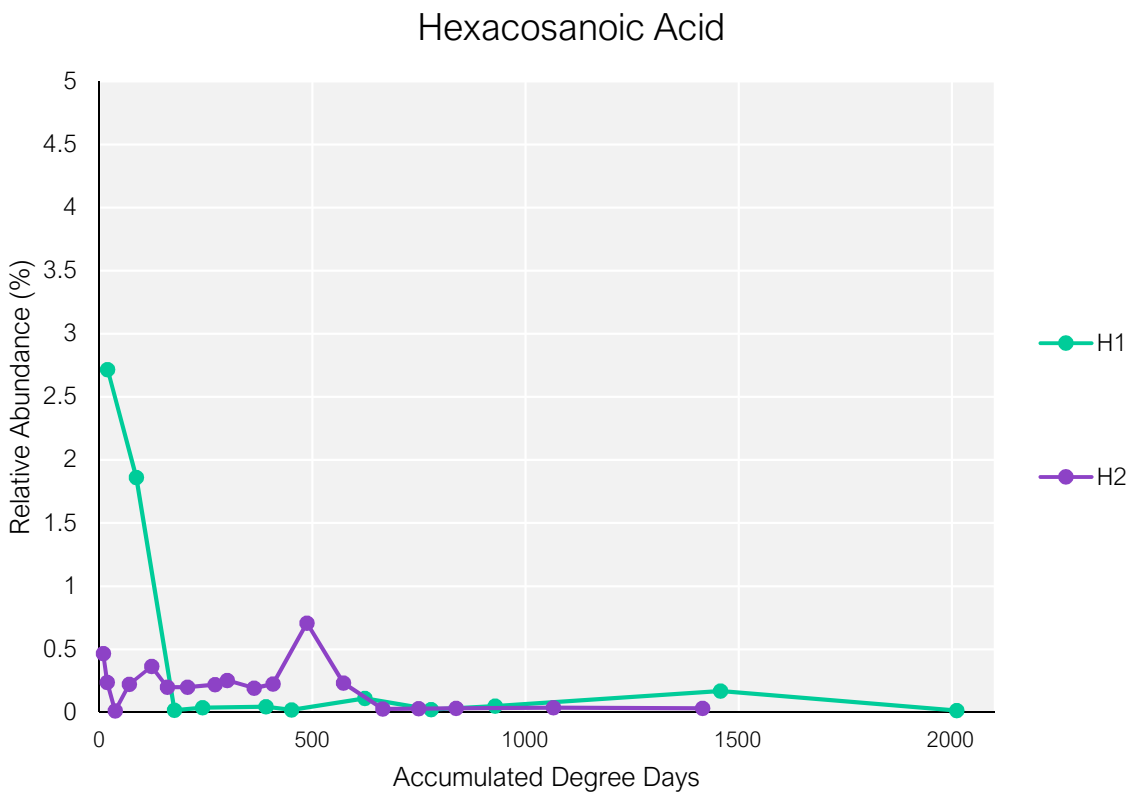

Figure 4.S. 20 Relative abundance (%) of hexacosanoic acid plotted against accumulated degree days for H1 and H2.

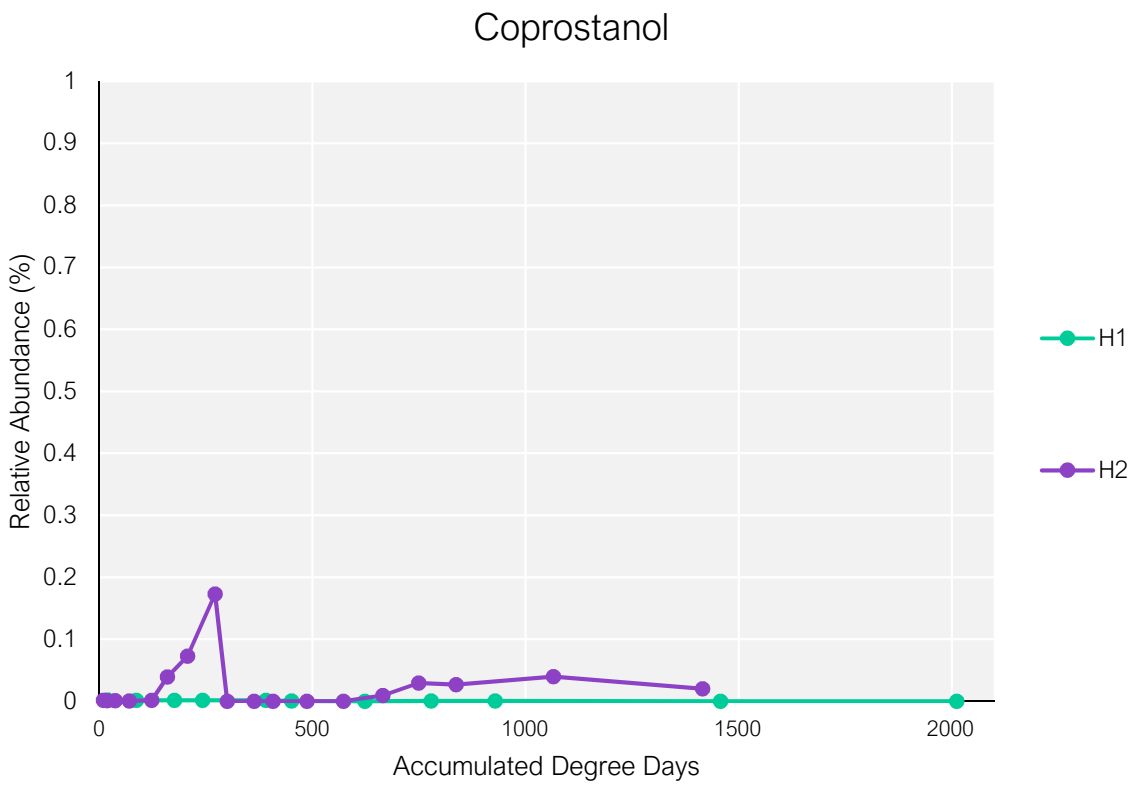

Figure 4.S. 21 Relative abundance (%) of coprostanol plotted against accumulated degree days for H1 and H2.

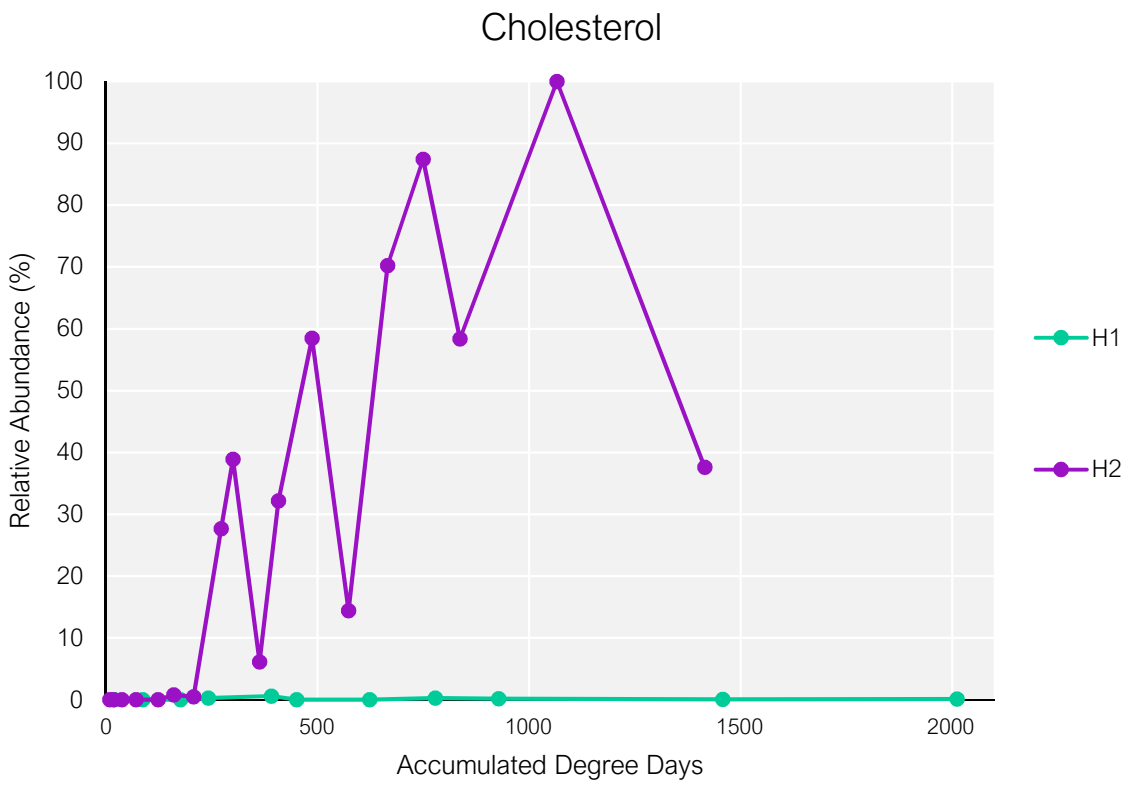

Figure 4.S. 22 Relative abundance (%) of cholesterol plotted against accumulated degree days for H1 and H2.

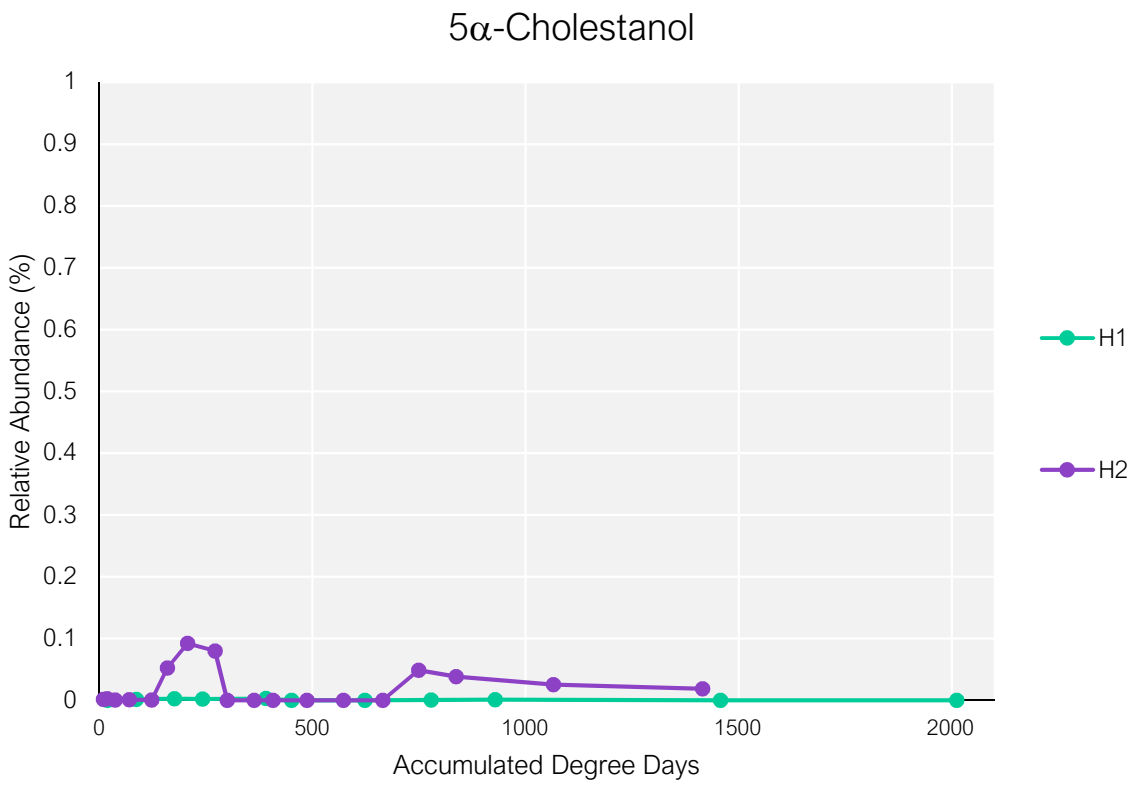

Figure 4.S. 23 Relative abundance (%) of 5α-cholestanol plotted against accumulated degree days for H1 and H2.

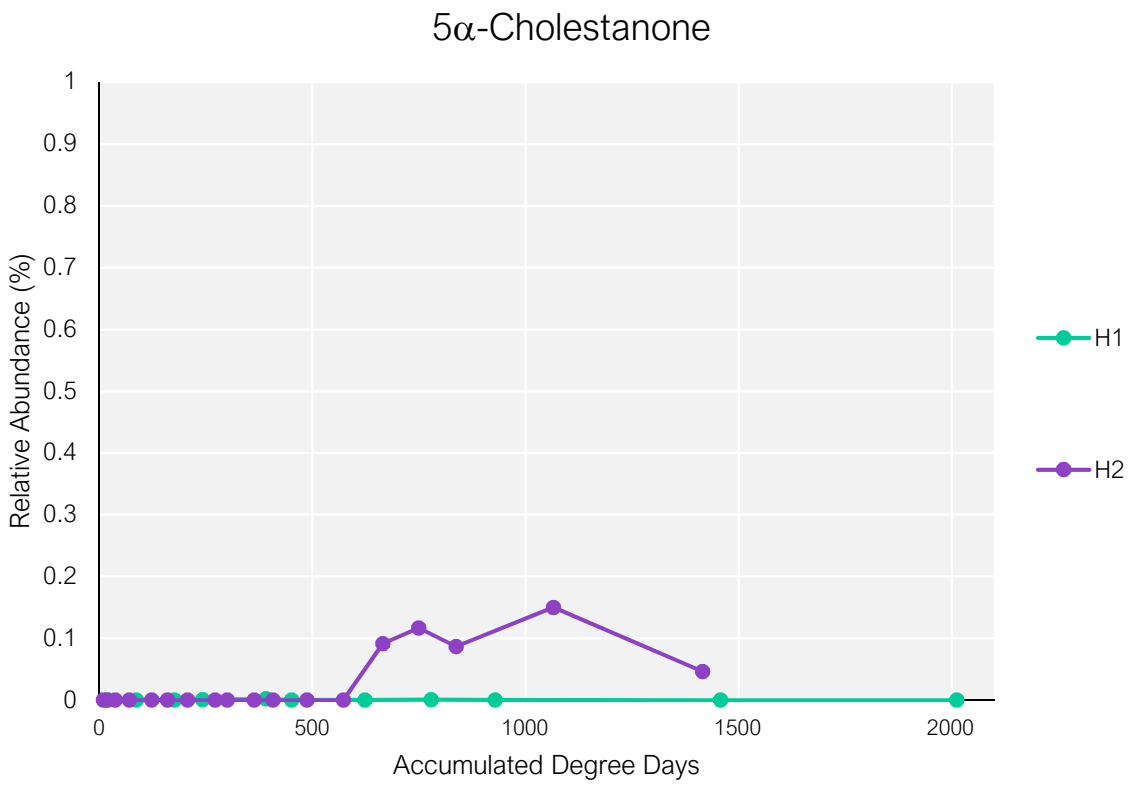

Figure 4.S. 24 Relative abundance (%) of 5α--cholestanone plotted against accumulated degree days for H1 and H2.

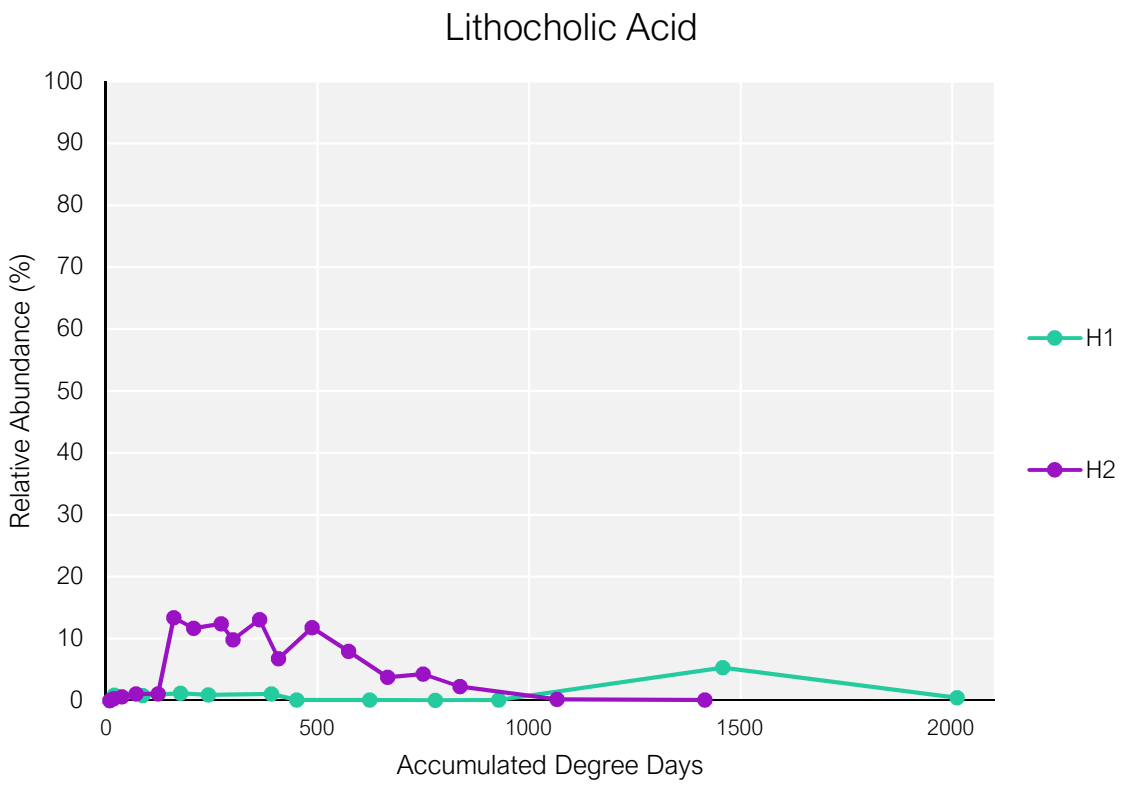

Figure 4.S. 25 Relative abundance (%) of lithocholic acid plotted against accumulated degree days for H1 and H2.

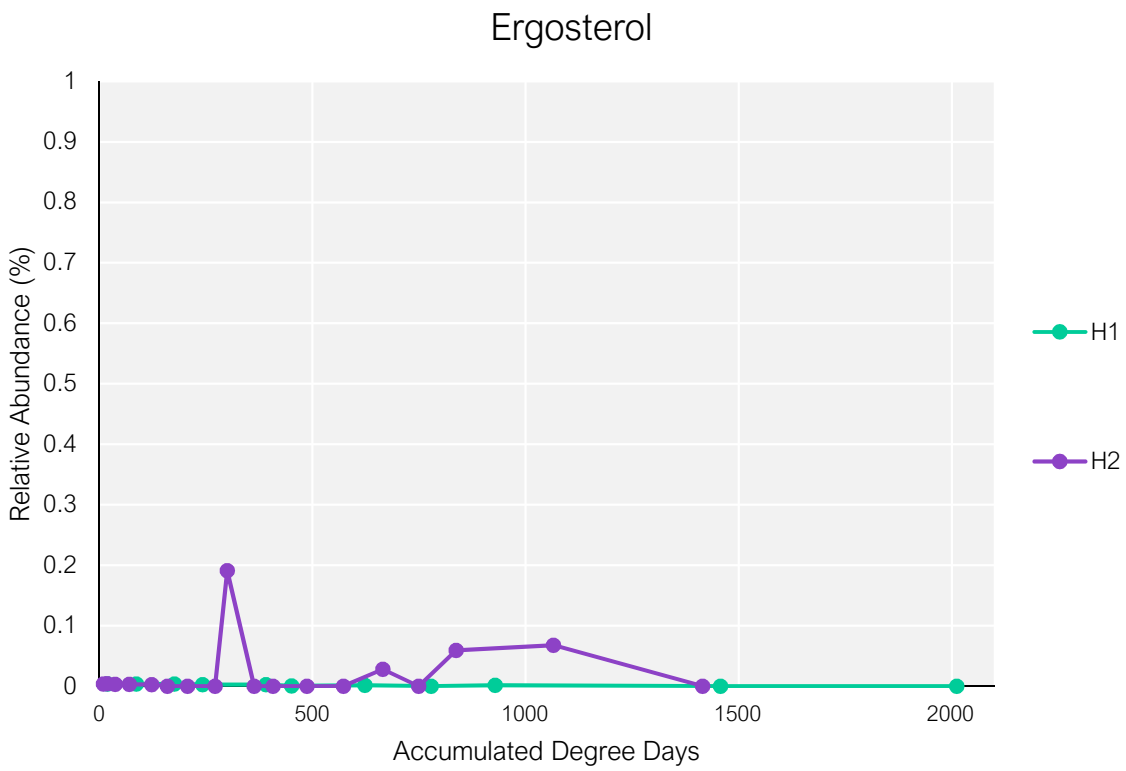

Figure 4.S. 26 Relative abundance (%) of ergosterol plotted against accumulated degree days for H1 and H2.

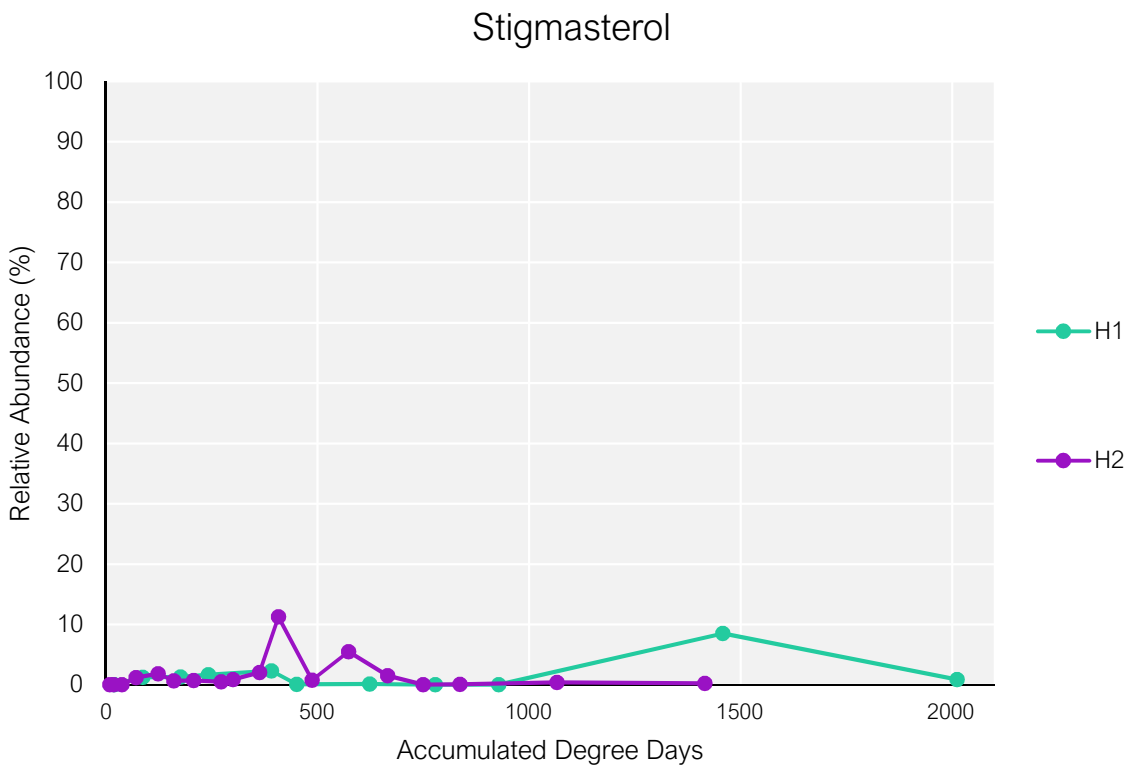

Figure 4.S. 27 Relative abundance (%) of stigmasterol plotted against accumulated degree days for H1 and H2.

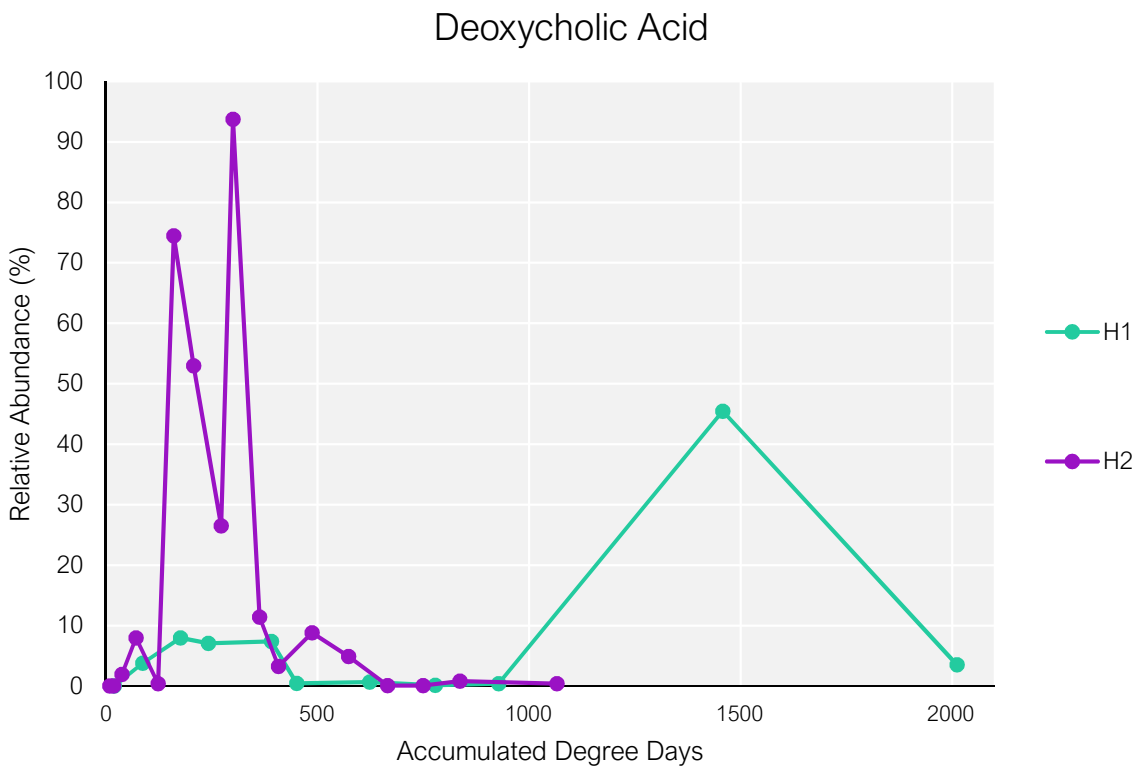

Figure 4.S. 28 Relative abundance (%) of deoxycholic acid plotted against accumulated degree days for H1 and H2.

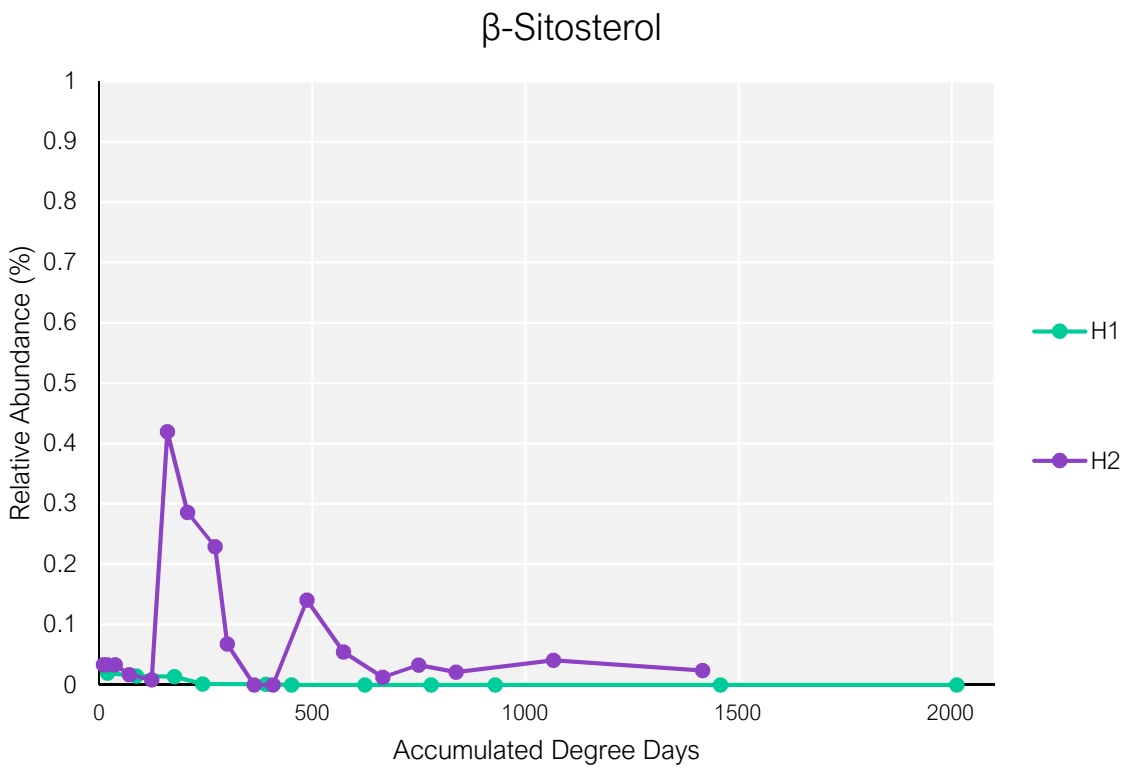

Figure 4.S. 29 Relative abundance (%) of β-sitosterol acid plotted against accumulated degree days for H1 and H2.

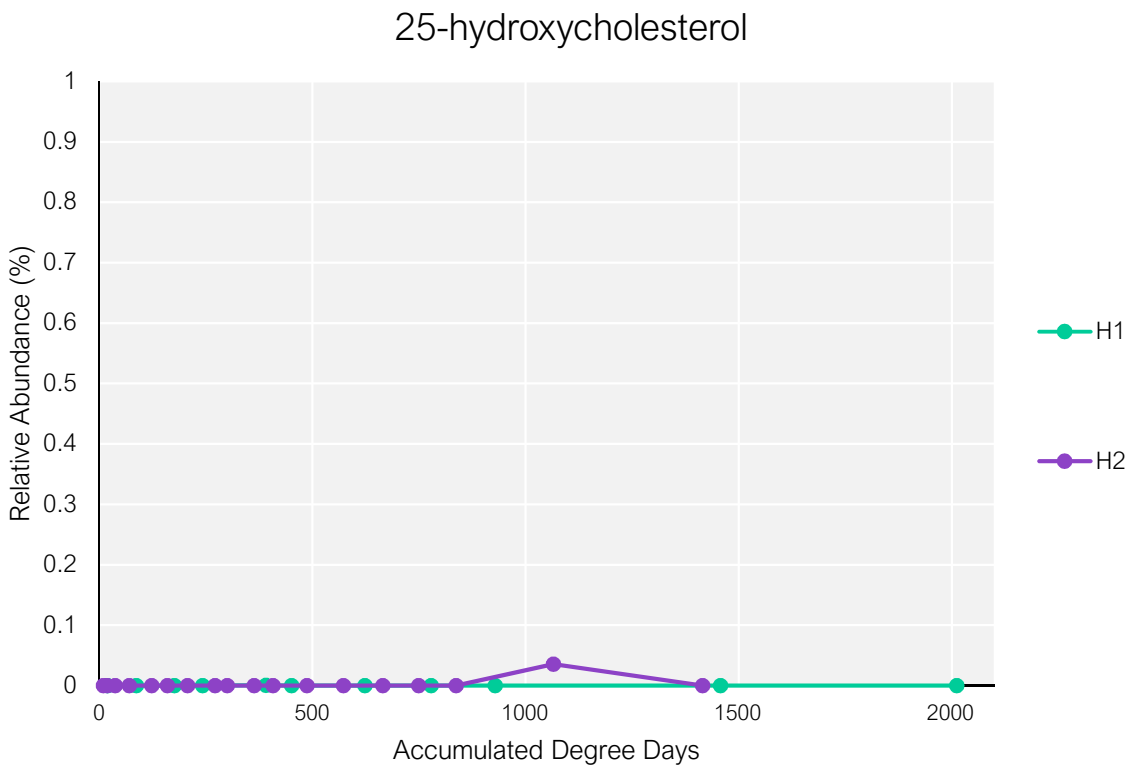

Figure 4.S. 30 Relative abundance (%) of 25-hydroxycholesterol plotted against accumulated degree days for H1 and H2.

Appendix 4: Supplementary information associated with Chapter 5

Table of contents

Table 5. S. 1 Summary of donor information, samples collected in days post-placement (DPP) and accumulated degree days (ADD)

	Donor	Body mass (kg)	Age (years)	Sex	Trial commencement	Placement Season	Samples collected (DPP)	Samples collected (ADD)
Trial 1	H1	63	86	M	29/01/21	Summer	0, 3, 7, 10, 17, 20, 28, 35, 42, facility closed due to floods, 70, 105	0, 64, 151, 222, 371, 431, 604, 757, 907, 1437, 1995
	P1	65	0.5	M				
	P2	65	0.5	F				
Trial 2	H2	100	84	M	11/06/21	Winter	0, 1, 3, 6, 10, 17, 23, 26, 31, 35, 42, 49, 56, 63, 69, 84, 105	0, 9, 28, 59, 110, 146, 263, 297, 337, 620, 704, 967, 1287
	P3	70	0.5	F				
	P4	70	0.5	F				

Figure 5. S 1 Scatter plot of the standardised lipid outcomes (y-axis) plotted over the standardised ADD (x-axis).

Figure 5. S. 2 Histograms of the standardised outcomes (y-axis) over the standardised ADD (xaxis),

Figure 5. S. 3 Histograms of the standardised outcomes (y-axis) over the standardised ADD

Figure 5. S. 4 Histograms of the standardised outcomes (y-axis) over the standardised ADD

Figure 5. S. 5 Histograms of the standardised outcomes (y-axis) over the standardised ADD

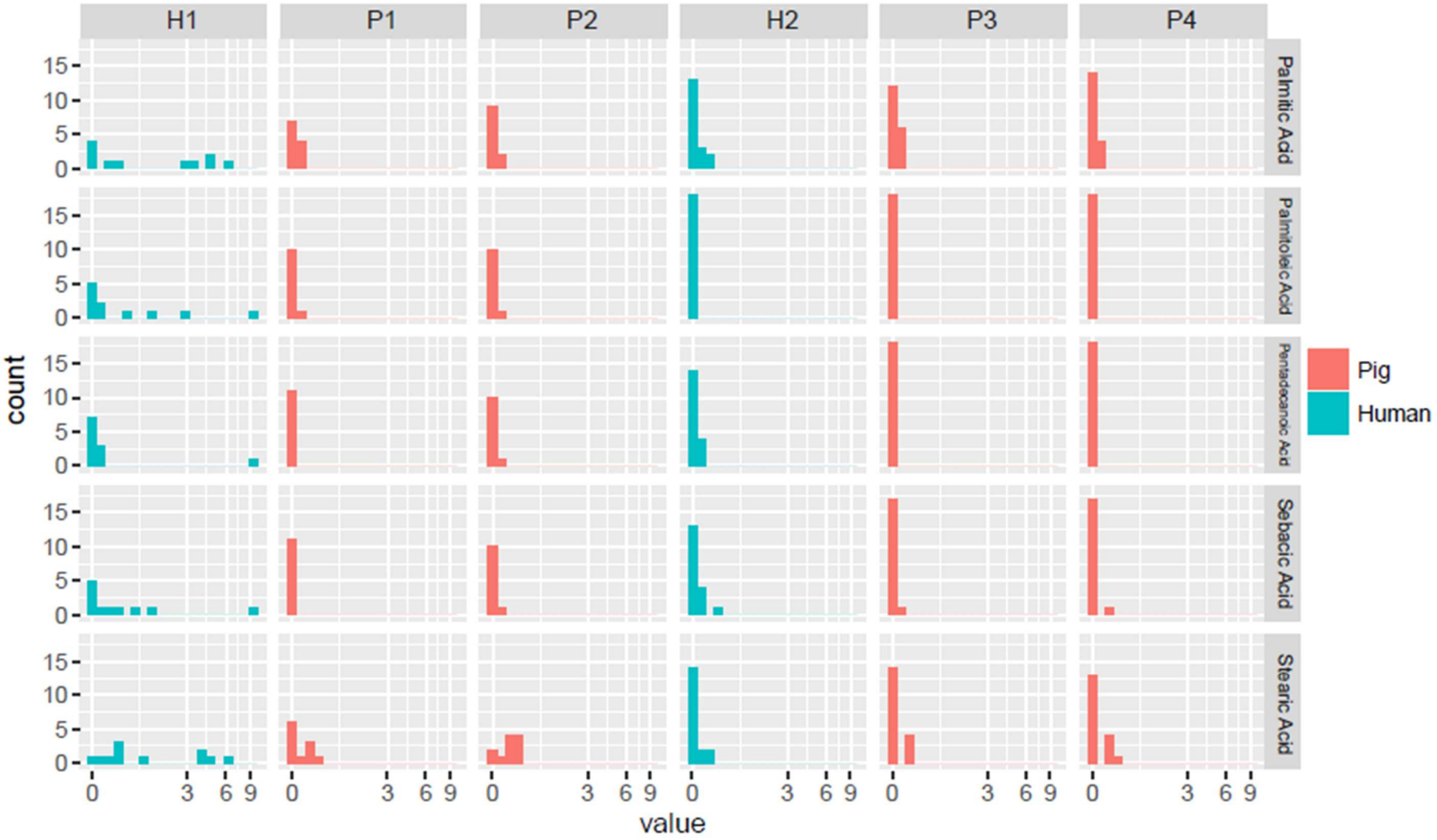

Figure 5. S. 6 Histograms of the standardised outcomes (y-axis) over the standardised ADD

Figure 5. S. 7 Histograms of the standardised outcomes (y-axis) over the standardised ADD

Table 5. S. 2 Summary of coefficient estimates of the GLMMs for the 30 lipid outcomes and their 95% confidence intervals

	Intercept	*ADD*	*ADD²*	*Human*	σ^2
Arachidic Acid	- 2.63 (3.21, - 2.06)	-	-	1.78 (0.95, 2.61)	-
Azelaic Acid	- 2.25 (- 3.14, - 1.37)	-	-	1.55 (0.11, 2.99)	0.66 (0.27,1.59)
Behenic Acid	- 1.56 (- 2.51, - 0.61)	- 1.02 (- 1.47, - 0.57)	-	2.43 (1.00, .86)	0.69 (0.26, 0.86)
β-sitosterol	- 0.89 (- 1.64, - 0.15)	- 3.05 (- 7.31,1.20)	- 6.85 (- 11.07, - 2.63)	-	0.76 (0.35,1.66)
Cholesterol	- 1.68 (- 1.98, - 1.40)	15.21 (12.65, 17.78)	- 8.13 (- 10.40, - 5.90)	-	-
Coprostanol	- 0.85 (- 1.31, - 0.38)	6.00 (3.07, 8.94)	- 3.03 (0.04, 2.05)	-	0.30 (0.04, 2.05)
Decanoic Acid	- 1.84 (- 2.91, - 0.78)	-0.96 (-1.52, -0.39)	-	1.83 (0.19, 3.47)	0.80 (0.36, 1.77)
Deoxycholic Acid	- 0.39 (- 0.83, 0.05)	-	-	-	-
Ergosterol	- 2.26 (- 2.94, - 1.57)	0.74 (0.45, 1.02)	-	0.79 (0.09, 1.48)	-
5α-cholestanol	- 1.44 (- 1.95, - 0.93)	6.92 (3.46, 10.39)	- 4.66 (- 7.84, -1.47)	0.81(0.10, 1.51)	-
5α-cholestanone	- 1.87 (- 2.47, - 1.27)	14.86 (10.78, 18.95)	- 7.67 (- 10.80, - 4.54)	-	0.33 (0.06, 1.83)
Heneicosanoic Acid	- 2.22 (-3.43, - 1.01)	- 0.63 (- 1.28, 0.02)	-	2.49 (0.94, 4.05)	0.63 (0.18, 2.12)
Heptadecanoic Acid	- 0.18 (-0.75, 0.39)	-1.16 (- 1.65, - 0.67)	-	0.97 (0.22, 1.72)	-
Hexacosanoic Acid	- 6.48 (-12.55, - 0.41)	- 7.23 (- 12.88, - 1.58)	6.96 (1.54, 12.38)	-	5.12 (1.71, 15.35)
Lauric Acid	-1.78 (-3.02, - 0.54)	-1.27 (- 2.04, - 0.50)	-	2.08 (0.31, 3.85)	0.73 (0.24, 2.22)
Linoleic Acid	- 3.35 (- 4.17, - 2.52)	- 0.79 (- 1.32, - 0.25)	-	3.67 (2.71, 4.63)	-
Lithocholic Acid	0.18 (- 0.08, 0.43)	-	-	-	-
Myristic Acid	- 4.94 (- 6.72, - 3.17)	-	-	2.63 (-0.37, 5.63)	1.63 (0.85, 3.13)
Nonadecanoic Acid	- 3.26 (- 4.48, - 2.04)	-	-	2.28 (0.25, 4.31)	1.11 (0.57, 2.12)
Oleic Acid	- 2.94 (- 3.98, - 1.89)	3.41 (0.04, 6.78)	- 4.39 (- 7.43, - 1.35)	1.76 (- 0.01, 3.52)	0.97 (0.50, 1.86)
Palmitic Acid	- 3.31 (- 4.40, - 2.21)	5.53 (2.87, 8.19)	- 2.58 (- 5.15, - 0.00)	2.05 (0.19, 3.91)	1.04 (0.56, 1.93)
Palmitoleic Acid	- 4.51 (- 6.28, - 2.75)	2.93 (- 1.15, 7.00)	- 6.29 (- 10.15, -0.43)	-	2.14 (1.19, 3.86)
Pentadecanoic Acid	- 3.66 (- 5.00, - 2.33)	-1.08 (- 1.59, - 0.56)	-	2.69 (0.60, 4.78)	1.10 (0.55, 2.18)
Sebacic Acid	- 4.69 (- 6.00, - 0.37)	0.55 (- 0.03, 1.14)	-	2.60 (0.75, 4.46)	0.91 (0.43, 1.95)
Stearic Acid	- 2.17 (- 2.77, - 1.58)	-	-	1.92 (1.13, 2.71)	-
Stigmasterol	- 0.22 (- 0.54, 0.10)	-	-	-	-
Tetracosanoic Acid	- 2.34 (- 3.31, - 1.37)	- 0.60 (- 1.06, - 0.15)	-	2.52 (1.10, 3.94)	0.68 (0.29, 1.59)
Tricosanoic Acid	- 1.08 (- 1.77, -0.39)	- 1.02 (- 1.52, - 0.52)	-	1.85 (1.04, 2.66)	-
Tridecanoic Acid	- 1.49 (- 2.04, - 0.92)	-7.20 (- 10.95, - 3.46)	6.00 (2.40, 9.60)	1.13 (0.42, 1.84)	-
25-hydroxycholesterol	- 0.89 (- 1.64, - 0.15)	- 3.05 (- 7.31, 1.20)	- 6.85 (-11.07, - 2.63)	-	0.76 (0.35, 1.66)

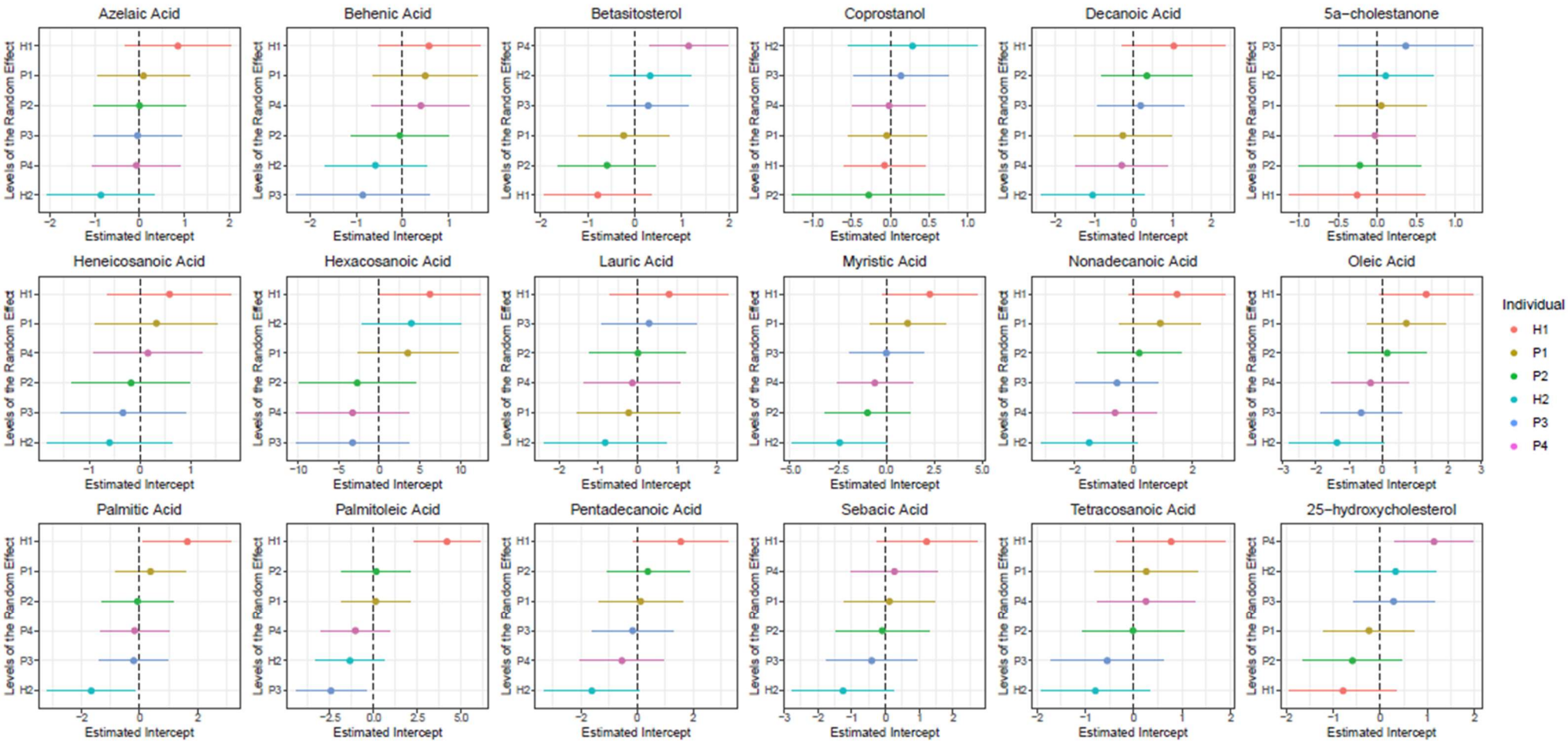

Figure 5. S. 8 Random effects plots for selected models demonstrating the levels of the random effects (y-axis), over the estimated intercept (x-axis), colour coded by individual.

Table 5. S. 3 Summary of residual diagnostics for hierarchical mixed regression models obtained using the DHARMa package. Cells highlighted in yellow indicate statistically significant results ($p < 0.05$). Non-significant results denoted by 'n.s.'

	KS test p =	Deviation	Disperion test p =	Deviation	Outlier test p =	Deviation
25-hydroxycholesterol	0.77	n.s.	0.86	n.s.	1.00	n.s.
5α-cholestanol	0.39	n.s.	0.55	n.s.	1.00	n.s.
5α-cholestanone	0.53	n.s.	0.86	n.s.	1.00	n.s.
Arachidic Acid	0.53	n.s.	0.00	significant	0.15	n.s.
Azelaic Acid	0.87	n.s.	0.15	n.s.	1.00	n.s.
Behenic Acid	0.99	n.s.	0.98	n.s.	1.00	n.s.
Cholesterol	0.76	n.s.	0.62	n.s.	0.15	n.s.
Coprostanol	0.53	n.s.	0.67	n.s.	0.15	n.s.
Decanoic Acid	0.94	n.s.	0.34	n.s.	0.50	n.s.
Deoxycholic Acid	0.06	n.s.	0.23	n.s.	1.00	n.s.
Ergosterol	0.32	n.s.	0.35	n.s.	1.00	n.s.
Heneicosanoic Acid	0.19	n.s.	0.82	n.s.	1.00	n.s.
Heptadecanoic Acid	0.88	n.s.	0.40	n.s.	1.00	n.s.
Hexacosanoic Acid	0.93	n.s.	0.97	n.s.	0.50	n.s.
Lauric Acid	0.85	n.s.	0.72	n.s.	0.50	n.s.
Linoleic Acid	0.71	n.s.	0.52	n.s.	1.00	n.s.
Lithocholic Acid	0.00	significant	0.01	significant	1.00	n.s.
Myristic Acid	0.89	n.s.	0.18	n.s.	1.00	n.s.
Nonadecanoic Acid	0.44	n.s.	0.28	n.s.	1.00	n.s.
Oleic Acid	0.35	n.s.	0.20	n.s.	0.50	n.s.
Palmitic Acid	0.85	n.s.	0.28	n.s.	1.00	n.s.
Palmitoleic Acid	0.01	significant	0.14	n.s.	0.50	n.s.
Pentadecanoic Acid	0.64	n.s.	0.10	n.s.	0.15	n.s.
Sebacic Acid	0.79	n.s.	0.18	n.s.	0.50	n.s.
Stearic Acid	0.36	n.s.	0.15	n.s.	1.00	n.s.
Stigmasterol	0.25	n.s.	0.34	n.s.	0.50	n.s.
Tetracosanoic Acid	0.80	n.s.	0.46	n.s.	1.00	n.s.
Tricosanoic Acid	0.48	n.s.	0.90	n.s.	1.00	n.s.
Tridecanoic Acid	0.48	n.s.	0.90	n.s.	1.00	n.s.
β-sitosterol	0.77	n.s.	0.86	n.s.	1.00	n.s.

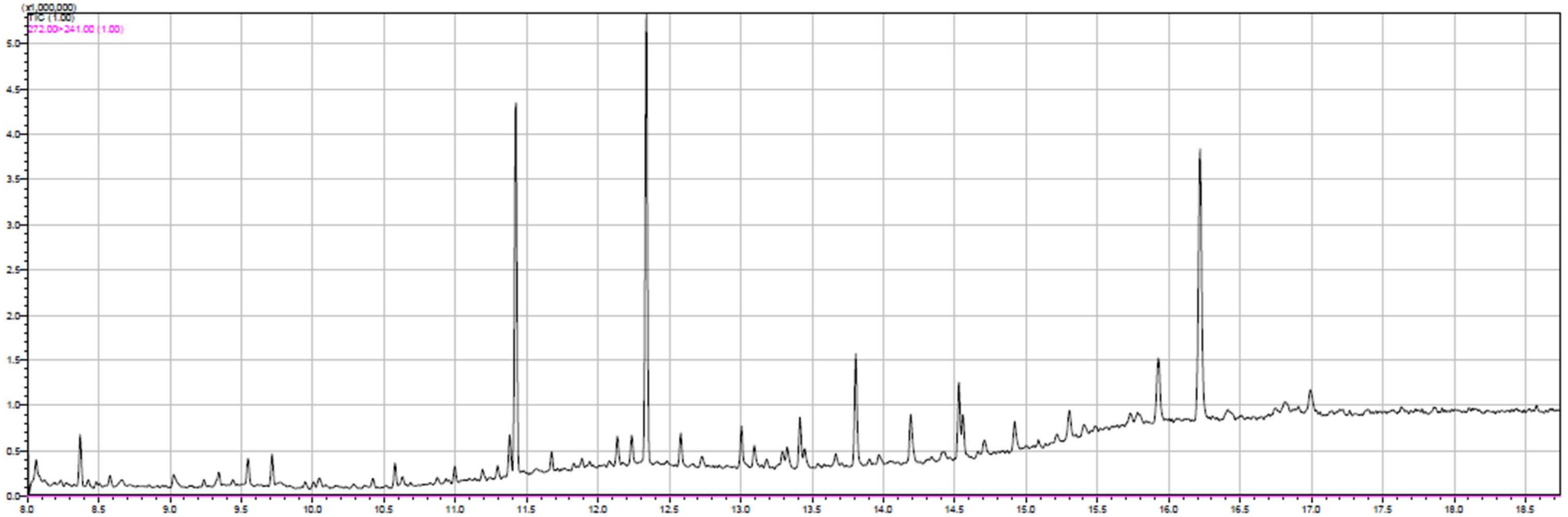

Figure 5. S. 9 Representative Total Ion Chromatogram (TIC) showing H1 Day 13.